

# Preliminary Assessment of Earthquake-Induced Liquefaction Susceptibility at Five San Francisco Bay Area Airports

Prepared for:

Association of Bay Area Governments  
c/o: Danielle Hutchings Mieler  
P.O. Box 2050  
Oakland, California 94604-2050

Prepared by:

Fugro Consultants, Inc.  
1777 Botelho Drive, Suite 262  
Walnut Creek, CA 94596

May 31, 2013

*Oakland airport, 1939*



## EXECUTIVE SUMMARY

The Association of Bay Area Governments (ABAG), under a grant issued by the California Department of Transportation (CalTrans), is revising and updating their 1999 earthquake-induced liquefaction susceptibility assessments of San Francisco International Airport (SFO) and Oakland International Airport (OAK), as well as performing new assessments at three smaller general aviation regional airports; Moffett Federal Airfield (Moffett), located in Sunnyvale; Buchanan Field Airport (Buchanan), located in Concord; and Livermore Municipal Airport (Livermore), located in Livermore. These assessments are part of a larger planning study to evaluate the use of and access to these facilities following a hypothetical large-magnitude earthquake. Fugro Consultants, Inc. (FCL) is collaborating with ABAG to assess the susceptibility to liquefaction at each of these five airports.

Liquefaction is the transformation of a granular material from a solid state into a liquefied state as a consequence of increased pore pressure and decreased effective stress (Youd, 1973). Increased pore pressures in unconsolidated sediment, especially in west-central California, are typically earthquake-induced (co-seismic). Liquefaction related ground failure can result in settlement, foundation (bearing) failure, lateral movement (lateral spread), and general ground cracking. Airport runway surfaces are susceptible to damage and closure following liquefaction-related ground failure. In this study, FCL develops earthquake-induced liquefaction hazard maps following the general liquefaction susceptibility hazard analyses and mapping approach of the California Geological Survey and based on current and recent research studies performed by FCL and former William Lettis and Associates (WLA) in California.

Earthquake-induced liquefaction-related ground failures historically have caused extensive structural and lifeline damage in urbanized areas around the world. Recent examples of these effects include damage produced during the 1994 Northridge (California), 1995 Kobe (Japan), 1999 Izmit (Turkey), 2001 India earthquakes, and also the 2010-2011 Christchurch earthquake sequence (New Zealand). Damaging liquefaction occurred in the San Francisco Bay Area during the 1868 Hayward earthquake, the 1906 San Francisco earthquake, the 1957 Daly City earthquake, and the 1989 Loma Prieta earthquake (Youd and Hoose, 1978; Holzer, 1998).

Studies of historical earthquakes show that the areal distribution of liquefaction-related damage is generally restricted to alluviated basins and filled land areas that contain shallow layers of low density, saturated, granular sediment (e.g. Youd and Hoose, 1978; Holzer, 1998; Tinsley et al., 1985). In the areas around San Francisco Bay, the geologic materials with a history of liquefaction include Holocene-aged estuarine deposits, Holocene stream and alluvial fan deposits, Holocene and Pleistocene eolian deposits, and artificially emplaced fill materials. Understanding the distribution and extent of these materials is critical to understanding the potential hazard posed by co-seismically induced liquefaction.

All five of the subject airports are sited on young unconsolidated sediments and artificial fill, materials considered to have moderate to very high susceptibility to liquefaction (Knudsen et al.,



2000, Witter et al., 2006). The San Francisco and Oakland airports sit on artificial fill placed over tidal marsh deposits and bay mud. Most of the fill is non-engineered, emplaced before 1970, and may include loose sandy material highly susceptible to liquefaction. Moffett, Buchanan, and Livermore airports are built over young alluvial fan sediments, considered to have moderate susceptibility to liquefaction.

There are numerous faults in the San Francisco Bay Area that are capable of producing large-magnitude earthquakes and strong ground shaking that can induce liquefaction. Ground shaking from an earthquake is measured in units of gravitational acceleration (g), and one "g" is about 9.8 m/sec<sup>2</sup>, or 32 ft/sec<sup>2</sup>. For a given location and earthquake scenario, the strongest acceleration anticipated to occur is called peak ground acceleration (PGA). Each earthquake scenario, deterministic or probabilistic, generates a grid of PGA values that spans the area of influence.

For this study, we consider ground motions from three likely earthquake scenarios (deterministic), and for two different probability levels (probabilistic) based on the United States National Seismic Hazard Maps working group (Petersen et al., 2008). Earthquakes on the following fault segments are considered for the deterministic events: 1) 1906 San Andreas Fault scenario, 2) Hayward-Rodgers Creek Fault scenario, and 3) Concord-Green Valley Fault scenario (Figure 1). The two probabilistic ground motions consider the contribution of all the faults in the Bay Area, and use the compiled probabilities assigned by the Working Group on California Earthquake Probabilities (WGCEP, 2008). For this study, we considered the 2% chance of exceedance in 50 years scenario, and the 10% chance of exceedance in 50 years scenario.

Fugro compiled existing borehole and cone penetration test (CPT) data for each airport to perform quantitative liquefaction potential assessments. A liquefaction analysis using the Simplified Procedure was performed for San Francisco, Oakland, Moffett, and Buchanan airports, and yield ranges of settlement values between 0 and 4 inches, 2 and 9 inches, less than one to 3 inches, and 1 to 4 inches, respectively. A liquefaction analysis was not performed for Livermore because the available subsurface data did not extend below the historical high water table. The geologic units found to be most susceptible to liquefaction include coarse-grained artificial fill, artificial fill over estuarine mud, the Merritt Sand and coarse grained lenses within the Young Bay Mud, Old Bay Mud, and Holocene alluvial fan deposits.

Given the limitation in data density and extent, we recommend that a liquefaction specific investigation be conducted for Buchanan and Livermore airports to better characterize the liquefaction hazard. To address the gaps in subsurface data coverage at Moffett and Oakland, we recommend additional subsurface studies. A comprehensive investigation to determine the characteristics of different fill types (type, distribution, and thickness), and the potential for differential settlement should be performed at Moffett, Oakland, and San Francisco. In addition, we recommend future evaluations should specifically address perimeter dikes and levees at



San Francisco and Oakland airports to assess the potential for slope instability and seepage resulting from co-seismic liquefaction.

## TABLE OF CONTENTS

---

Executive Summary .....	ii
1.0 introduction .....	1
1.1 Purpose.....	2
2.0 Background.....	2
2.1 Liquefaction during the 1989 Loma Prieta Earthquake .....	3
2.2 Fill Emplacement around San Francisco Bay .....	3
3.0 Scope and Methodology.....	4
3.1 Project Scope.....	4
3.2 Methodology.....	5
3.2.1 Data Compilation and Review.....	5
3.2.2 Development of a Geologic Map and Model .....	5
3.2.3 Liquefaction Susceptibility Analysis .....	6
3.2.4 Preparation of Settlement Maps .....	7
4.0 Geologic Setting.....	8
4.1 San Francisco International Airport (SFO).....	9
4.2 Oakland International Airport (OAK) .....	10
4.3 Buchanan Field Airport (CCR).....	11
4.4 Livermore Municipal Airport (LVK).....	12
4.5 Moffett Federal Airfield (NUQ) .....	13
5.0 Liquefaction Hazard Assessment .....	14
5.1 Methodology.....	14
5.1.1 Ground Motion Parameters .....	15
5.1.2 Groundwater.....	17
5.1.3 Quality of Available Subsurface Data.....	18
5.2 Results .....	18
5.2.1 San Francisco International Airport.....	20
5.2.2 Oakland International Airport .....	20
5.2.3 Buchanan Field Airport .....	21



5.2.4	Livermore Municipal Airport .....	21
5.2.5	Moffett Federal Airfield .....	21
6.0	Conclusions .....	22
6.1	Liquefaction Hazards.....	23
6.1.1	San Francisco International Airport.....	23
6.1.2	Oakland International Airport .....	24
6.1.3	Buchanan Field Airport.....	25
6.1.4	Livermore Municipal Airport.....	26
6.1.5	Moffett Federal Airfield .....	26
6.2	Recommendations .....	27
6.2.1	Liquefaction Investigations .....	27
6.2.2	Additional Site Studies.....	27
6.2.3	Mitigation.....	27
7.0	References.....	29

## LIST OF FIGURES

---

Figure 1	Airport and Fault Location Map
Figure 2	A and B. Photographs of Liquefaction Features at Oakland International Airport Following the October 17, 1989 Loma Prieta Earthquake
Figure 3A	Quaternary Geologic Map, San Francisco International Airport
Figure 3B	Historical Bay Environments Map, San Francisco International Airport
Figure 3C	Geologic Cross Section AA-AA', San Francisco International Airport, San Francisco, California
Figure 3D	Historical Aerial Views of San Francisco International Airport
Figure 3E	Approximate Extent of Developed Land in 1943, 1956, 1968, 1973, 1974, and Circa 1850 Bay Margin, San Francisco International Airport
Figure 4A	Quaternary Geologic Map, Oakland International Airport
Figure 4B	Historical Bay Environments Map, Oakland International Airport
Figure 4C	Geologic Cross Section BB-BB', Oakland International Airport, Oakland, California
Figure 4D	Historical Aerial View of Oakland International Airport, 1939



Figure 4E	Approximate Extent of Developed Land in 1939, 1958, 1959, 1968, 1999, and Circa 1850 Bay Margin, Oakland International Airport
Figure 5A	Quaternary Geologic Map, Buchanan Field Airport
Figure 5B	Historical Bay Environments Map, Buchanan Field Airport
Figure 5C	Geologic Cross Section CC-CC', Buchanan Field Airport, Concord, California
Figure 5D	Historical Aerial Photograph, 1939, Buchanan Field
Figure 5E	Buchanan – Aerial Photo from NAIP 2009
Figure 6A	Quaternary Geologic Map of Livermore Municipal Airport
Figure 6B	Geologic Cross Section DD-DD', Livermore Municipal Airport, Livermore, California
Figure 6C	Historical Aerial Photograph, 1949, Livermore
Figure 6D	Livermore – Aerial Photo from NAIP 2009
Figure 7A	Quaternary Geologic Map, Moffett Federal Airfield
Figure 7B	Historical Bay Environments Map, Moffett Federal Airfield
Figure 7C	Geologic Cross Section EE-EE', Moffett Federal Airfield, Mountain View, CA
Figure 7D	Historical Aerial Photograph, 1939, Moffett Field
Figure 7E	Moffett Field – Aerial Photo from NAIP 2009
Figure 8	Liquefaction Settlement Map, San Francisco International Airport, San Francisco, California
Figure 9	Liquefaction Settlement Map, Oakland International Airport, Oakland, California
Figure 10	Liquefaction Settlement Map, Buchanan Field Airport, Concord, California
Figure 11	Liquefaction Settlement Map, Moffett Federal Airfield, Mountain View, California
Figure 12	Preliminary Liquefaction Hazard Map, San Francisco International Airport
Figure 13	Preliminary Liquefaction Hazard Map, Oakland International Airport
Figure 14	Regional Liquefaction Susceptibility, Buchanan Field Airport
Figure 15	Regional Liquefaction Susceptibility, Livermore Municipal Airport
Figure 16	Regional Liquefaction Susceptibility, Moffett Federal Airfield



---

## **LIST OF TABLES**

---

Table 1 Ground Motion Parameters for Liquefaction Assessment

Table 2 Summary of Subsurface Explorations Analyzed for Liquefaction Susceptibility

Table 3 Calculated Liquefaction Settlement Summary

---

## **LIST OF APPENDICES**

---

Appendix A Reports Reviewed as Part of this Study

Appendix B Description of Geologic Units

Appendix C Subsurface Data Used in Liquefaction Analyses

Appendix D Liquefaction Analyses

## 1.0 INTRODUCTION

---

The Association of Bay Area Governments (ABAG), under a grant issued by the California Department of Transportation (CalTrans), is revising and updating the earthquake-induced liquefaction susceptibility assessments conducted in 1999 for San Francisco International Airport (San Francisco; SFO) and Oakland International Airport (Oakland; OAK) (WLA, 1999), and is performing new assessments at three smaller General Aviation (GA) airports; Moffett Federal Airfield (Moffett; NUQ), located in Sunnyvale; Buchanan Field Airport (Buchanan; CCR), located in Concord; and Livermore Municipal Airport (Livermore; LVK), located in Livermore (Figure 1). The Moffett, Buchanan, and Livermore airports have been identified by ABAG as airports that could provide emergency relief or could temporarily accommodate increased air traffic or serve as a back-up for certain airport functions in the event that the one of the major commercial airports (SFO, OAK, and SJC) suffer severe damage from an earthquake. The San Jose International airport is not included in this assessment because a detailed susceptibility analysis was recently conducted.

Major faults capable of producing large earthquakes that can result in strong ground shaking at the airports include the San Andreas, Hayward-Rogers Creek, and Concord-Green Valley faults. Other faults associated with the San Andreas fault system may also have the potential to generate large earthquakes (Figure 1). For this study we use earthquake scenarios considered 'likely' by the 2007 Working Group on California Earthquake Probabilities (WGCEP, 2008) for the San Andreas, Hayward-Rogers Creek, and Concord-Green Valley faults. Earthquakes on these three faults would expose the airports to long-duration ground motions with peak ground accelerations in excess of 0.2 g (20 percent of the acceleration due to gravity). The distance between an earthquake epicenter and the farthest effects of liquefaction is directly related to the magnitude of the event (Tinsley et al., 1985), the presence of susceptible geologic and shallow hydrologic conditions, and the amplification of ground motion at lower frequencies. In addition, empirical correlations between ground shaking intensity and geology show that the distribution of amplified ground shaking is correlated with geologic conditions, and is most severe in alluviated basins that contain thick deposits of unconsolidated sediments.

Previous damaging liquefaction occurred in the San Francisco Bay Area during the 1868 Hayward earthquake, the 1906 San Francisco earthquake, the 1957 Daly City earthquake, the 1983 Coalinga earthquake, and the 1989 Loma Prieta earthquake. Studies of the distribution of liquefaction features from these and other historical earthquakes demonstrate that liquefaction-related damage is generally restricted to alluviated basins that contain shallow layers of low-density, saturated, granular sediment (i.e., sand) (Youd and Hoose, 1978; Tinsley et al., 1985, Holzer, 1998; Cetin et al., 2004a; Cubrinovski et al., 2011).

## 1.1 Purpose

The purpose of this study is to evaluate the susceptibility to liquefaction at five San Francisco Bay area airports. The findings of this study provide input to ABAG's Airport and Infrastructure Resilience Project which evaluates the role of airports in regional disaster response and recovery. In this study we evaluate earthquake-induced liquefaction susceptibility at San Francisco and Oakland airports and conduct preliminary assessments at Buchanan, Moffett and Livermore airports. Examination of liquefaction susceptibility in the vicinity of these airports is important because they are developed on land underlain by saturated Holocene deposits and artificial fill. In the San Francisco Bay area, these types of geologic deposits are historically associated with earthquake-induced liquefaction ground failure (Youd and Hoose, 1978; Holzer, 1999). Delineating the extent of liquefaction-susceptible deposits and estimating the magnitude of deformation along runways provides awareness of damage-potential and helps start the conversation for mitigation and planning for the eventualities of the next large earthquake.

## 2.0 BACKGROUND

Earthquake-induced liquefaction has historically caused loss of life and damage to property and infrastructure. Observations show that the distribution of liquefaction phenomena is not random; liquefaction is typically restricted to areas underlain by saturated, loose, cohesionless sand, and silt. Areas susceptible to liquefaction can be delineated on the basis of geologic, geomorphic, geotechnical and hydrologic mapping, and purposed subsurface analyses (e.g., Youd and Perkins, 1987; Tinsley and Holzer, 1990; Witter et al., 2006). Based on a comparison of historical occurrences of liquefaction in the San Francisco Bay Area to geologic and geomorphic mapping, Knudsen and others (2000) found that Holocene estuarine deposits, Holocene stream and alluvial fan deposits, Holocene and Pleistocene eolian deposits, and artificial fill are the geologic materials most susceptible to liquefaction.

Liquefaction is the transformation of a granular material from a solid state into a liquefied state as a consequence of increased pore pressure and decreased effective stress (Youd, 1973). Increased pore pressures in unconsolidated sediment, especially in west-central California, are most typically seismically induced (co-seismic). Observed types of ground failure resulting from liquefaction can include sand boils, lateral spreads, ground settlement, ground cracking, and ground warping (Youd and Hoose, 1978).

Earthquake-induced liquefaction is of special concern in the San Francisco Bay Area. Mountains on either side have shed thick alluvial sediments that mantle the bay and form a gently sloping apron on which the bay cities are founded. The toe of the alluvial apron grades into estuarine deposits lining the margins of the bay. Many of these alluvial and estuarine deposits are young, unconsolidated, granular, saturated, and thus, susceptible to liquefaction.

Another characteristic of the bay margin areas is the presence of artificial fill. Fill has a long history in and around San Francisco Bay; fill placement has been ongoing for more than a hundred years, and much of the emplaced fill is susceptible to liquefaction. All five of the airports studied are founded on Holocene alluvium, estuarine deposits, or on fill overlying these Holocene deposits, and liquefaction is a hazard that needs to be evaluated when assessing the integrity of the infrastructure at these important facilities.

## **2.1 Liquefaction during the 1989 Loma Prieta Earthquake**

During the 1989 Loma Prieta earthquake, soil liquefaction at Oakland International Airport caused considerable damage to the 3,000 meter-long main jet runway, located along the southwest edge of the airport. This runway was built entirely on fill in the early 1960s. Sand boils, settlement, and lateral spreads were documented within wide areas of airport fill to the north, south, and east of the damaged runway section (Holzer, 1998; Figures 2A and 2B).

Extensive soil liquefaction was documented within the western section of the airport fill, where sand boils and cracks were observed and approximately the northwestern 900 meters of the runway was damaged (Figure 2A). In addition, the adjacent taxiway pavement sustained heavy damage, with cracks as wide as 30 centimeters and vertical displacement up to 15 centimeters (Figure 2B, photo A). The perimeter dikes at the west end of the runway experienced settlement and lateral spreading of approximately 0.5 to 0.7 meters (Holzer, 1998).

Liquefaction damage was also documented in other locations on the airport property. Sand boils and large fissures caused by lateral spreading damaged an undeveloped area of fill to the north and northeast of the main runway. Liquefaction and settlements of as much as 8 cm were observed in several locations near the main terminal buildings, which are supported on deeper foundations and were not significantly damaged. In addition, a below-ground tramway, which allows service vehicles carrying passengers' luggage to pass under part of one of the main terminal buildings, was filled with sand and water released from the subsurface (Figure 2B, photo B) (Holzer, 1998).

## **2.2 Fill Emplacement around San Francisco Bay**

The historical placement of fill into and on the margins of San Francisco Bay began in the 1850s and accelerated through the mid-1900s as urbanization encroached on the Bay (Hitchcock et al., 2008). By 1970, the rapid filling of the Bay and its tidal marshes had virtually halted after the 1969 implementation of the San Francisco Bay Plan (SFBCDC, 1969), which included restrictions on Bay margin development and requirements that fill be engineered.

Four of the five airports evaluated in this report were partly or wholly constructed prior to 1965 on fill over estuarine deposits of the tidal marsh, tidal flats, or bay mud. Fill materials and emplacement methods evolved over the decades, resulting in a mosaic of fill types present within the Bay area today. Emplacement methods included 1) scooping of tidal marsh



sediments and piling the material to make dikes, 2) hydraulic pumping of sand and silt from the bay, 3) the dumping of waste debris, rubble, quarry rock or soil, and, in later years, 4) construction using engineered compacted fill (Hitchcock et al., 2008). Studies by Knudsen and others (2000) show that about 50 percent of historical occurrences of liquefaction in the San Francisco Bay area occurred in artificial fill placed over estuarine deposits (Bay Mud). Areas of the greatest settlement and number of sand boils strongly correlate with hydraulically emplaced sand fills; likely emplaced in the 1930s and 1940s.

### **3.0 SCOPE AND METHODOLOGY**

---

This assessment was performed to support ABAG in its performance of an earthquake-induced liquefaction susceptibility assessment of five major and regional San Francisco Bay Area airports under a grant issued by CalTrans. This work was authorized by ABAG on December 12, 2011.

#### **3.1 Project Scope**

Subsequent to the 1999 ABAG liquefaction susceptibility assessment for San Francisco and Oakland International airports (WLA, 1999), additional subsurface data were collected as part of airport expansion project studies. Using these recently collected data in combination with existing data and the updated ground motion data of Petersen and others (2008), Wald and others (2005), and the USGS (2013c), the liquefaction susceptibility of materials underlying these airports were re-evaluated and the liquefaction susceptibility and settlement maps were updated. New liquefaction susceptibility assessments were performed for Moffett, Buchanan, and Livermore airports, which were identified by ABAG as General Aviation (GA) airports that could provide emergency relief, could temporarily accommodate increased air traffic, or could serve as a back up for certain airport functions in the event that the major commercial airports suffer severe damage from an earthquake.

For each of the five airports, existing geotechnical, geologic, geomorphic, and groundwater data were obtained from airport authorities, ABAG, or public sources. The data were compiled for each site, and used to develop geologic maps and cross-sections. Following compilation of subsurface data, a quantitative analysis was performed for San Francisco, Oakland, Moffett, and Buchanan airports to determine the liquefaction potential of each geologic unit. The quantitative analysis was not performed for the Livermore airport due to insufficient data (please refer to Section 5.0 for more information). The liquefaction analysis for Moffett and Buchanan was originally slated to be performed by ABAG, however these analyses were performed by FCL. The results of the analyses and geologic maps were integrated to generate liquefaction susceptibility maps and potential settlement maps.



## 3.2 Methodology

Our assessment follows the general liquefaction susceptibility hazard analyses and mapping approach of the California Geological Survey, and also relies on state of practice techniques including recent research studies performed and developed by FCL and former WLA in California. In general, our characterization of liquefaction susceptibility involves four main tasks:

- Data compilation and review
- Development of a geologic map and model
- Liquefaction susceptibility analysis
- Preparation of settlement maps

### 3.2.1 Data Compilation and Review

To characterize the geologic and geomorphic environments of the airports, a compilation of available near-surface geologic, historical, and geotechnical data from published and unpublished sources was created. Published maps of Quaternary geology and geomorphology include liquefaction maps from Witter and others (2006), liquefaction-potential maps from previous ABAG collaborative efforts (WLA, 1999; ABAG, 2001), and maps developed by the San Francisco Estuary Institute (SFEI) of the San Francisco Bay environment (1998). In addition, geotechnical, environmental, and engineering geologic reports were provided by ABAG or airport authorities, obtained from archived previous FCL investigations, or reviewed from public sources. A full list of reviewed reports can be found in Appendix A.

### 3.2.2 Development of a Geologic Map and Model

Geologic units were delineated and described using subsurface data, the results from previous studies, existing Quaternary geologic mapping, mapping by SFEI, and our understanding of the late Quaternary evolution of San Francisco Bay region. The subsurface data were also used to delineate and characterize subunits within the artificial fill at Livermore and Buchanan. Descriptions and engineering properties of subsurface materials were extracted from available geotechnical, environmental, and engineering geologic reports and then reconciled with surficial geologic units and integrated to formulate a geologic model for each airport site. A more detailed discussion of geologic units identified at each airport is included in Appendix B, and a complete list reports and subsurface data sources can be found in Appendix C.

The subsurface data for each airport includes borehole and CPT data acquired from several sources. A total of 245 borehole and CPT exploration points were evaluated: 62 points for Buchanan; 8 for Livermore; 14 for Moffett; 48 for Oakland; and 113 for San Francisco. A complete list of boring and CPT exploration points is included in Appendix C.

### 3.2.3 Liquefaction Susceptibility Analysis

Geologic deposits were evaluated for susceptibility to liquefaction based on historical occurrence of liquefaction, geologic and geomorphic indicators, and based on the results of the quantitative Simplified Procedure liquefaction analysis. Near-surface groundwater data was compiled from CPT and borehole logs and published historical high ground water levels (CGS, 2006 and 2008).

These data were analyzed using three deterministic (1906 San Francisco earthquake scenario, Hayward-Rogers Creek fault earthquake scenario, Concord-Green Valley fault earthquake scenario) and two probabilistic scenarios (10% Probability of exceedance in 50-Years scenario, 2% Probability of exceedance in 50-Years scenario). For a more detailed discussion of the approach and methodology applied to the liquefaction analyses, please refer to Section 5.0 and Appendix D.

#### *Geologic and Geomorphic Indicators of Liquefaction Susceptibility*

Previous studies of liquefaction hazards within the San Francisco Bay region identify several geologic and hydrologic factors that influence the susceptibility of a deposit to liquefaction (e.g. Knudsen et al., 1997a, 1997b; Sowers et al., 1998; Knudsen et al., 2000, Witter et al., 2006). These factors include the age and depositional environment of the deposit; the relative consolidation of sands and silts; and the local depth to groundwater (Youd et al., 1973; Youd et al., 1975; Youd and Perkins, 1978; Tinsley et al., 1985). As a deposit ages, soil formation, weathering, diagenetic processes, and earthquake shaking lead to consolidation and cementation, resulting in a reduced susceptibility to liquefaction (e.g. Witter et al., 2006; Leon et al. 2006; Hayati et al., 2008). For this study, we evaluated the most recent regional-scale liquefaction evaluation performed for the San Francisco Bay region (Witter et al., 2006). At Moffett, Livermore, and Buchanan, we also compared mapped surficial deposits with subsurface data to assess the potential for liquefaction.

#### *Simplified Procedure*

The Simplified Procedure is an analysis method developed to estimate a geologic unit's resistance to liquefaction based on observations and empirical case histories. The analysis relates the soil's capacity to resist liquefaction (cyclic resistance ratio or CRR), to the seismic demand on a soil (cyclic stress ratio or CSR) as a factor of safety. The CSR is determined based on the tectonic setting and empirical physical conditions, while the CRR is determined by individual soil sample characteristics as determined from laboratory testing or in-situ testing. The factor of safety against liquefaction is calculated as a ratio of CRR and CSR (a more detailed discussion of the Simplified Procedure is included in section 5.0).

Since CRR is determined based on the characteristics of a soil, a number of tests are employed to measure the properties of soils, including: the Standard Penetration Test (SPT), and Cone Penetration Test (CPT). The SPT is an in-situ test typically performed in conjunction with a borehole exploration program. Boreholes can be advanced using a variety of techniques, but



generally advance samplers that extract materials for visual inspection and laboratory testing. One type of samples is the SPT and it is designed to measure of the resistance of soil under a set of controlled conditions; a soil sampler of a known diameter is driven into the ground using a 140 pound hammer that is dropped from a known height. The number of blows required to advance the sampler a total of 12 inches into the ground is recorded and is known as the standard penetration resistance, or the N-value. High N-values correspond to high consistency (fine grained) or high density (coarse grained) soils, while low N-values correspond to low consistency, or low density soils. The CPT is another in-situ test that measures a soil's response to an instrumented cone that is pushed into the subsurface. The test measures the friction and penetration resistance as the cone is advanced into the soil at a controlled rate. One advantage of the CPT method is that a continuous measure of the soil column is possible (conversely, SPT's have spacing in-between test intervals – typically 2.5 to 5 feet). Other types of tests can be used to estimate liquefaction susceptibility and include: shear wave velocity (e.g. Andrus and Stokoe, 1999, Andrus, 2000; Andrus et al., 2004), or dynamic laboratory testing of undisturbed soil samples. These alternative testing techniques area comparably expensive; as a result, the SPT and CPT techniques are the predominant testing method employed when collecting data for liquefaction susceptibility hazard analyses.

Because the Simplified Procedure has been extensively used and studied, the method has benefited from revisions and refinements that have improved the level of overall analysis (e.g. Seed et al., 1982, 1983, 1985; Robertson and Wride, 1997; Youd et al., 2001; Idriss and Boulanger, 2004, Cetin et al., 2004b). For this study, the 2001 NCEER recommendations for employing the Simplified Procedure are used to analyze liquefaction potential at San Francisco, Oakland, Moffett, and Buchanan airports.

#### 3.2.4 Preparation of Settlement Maps

In addition to calculating factor of safety against liquefaction, our assessment also includes evaluation of liquefaction-induced reconsolidation settlements. Liquefaction induced settlements were calculated using the recommendations of Ishihara and Yoshimine (1992). Settlement maps were developed for San Francisco, Oakland, Moffett, and Buchanan airports. It should be noted that many of the borings at each airport are relatively shallow, with depths of penetration as low as 5 to 10 feet below ground surface. Because liquefaction induced settlements can occur at depths up to 50 or 80 feet, we only calculate estimates of settlement for borings that exceed 30 feet penetration. The shallower borings are omitted because the analytical results could be misinterpreted and promote underestimation of the settlement hazard. A discussion of these results is included in Section 5.0.

## 4.0 GEOLOGIC SETTING

---

The San Francisco Bay region is located within the Coast Range geomorphic province. The Coast Ranges are structurally controlled north- to northwest-trending mountain ranges that rise 2,000 to 4,000 feet above sea level (with peaks up to 6,000 feet), and have intervening valleys that trend subparallel to the San Andreas fault system (Figure 1). The northeastern and southwestern ranges, composed primarily of Mesozoic and Cenozoic sedimentary strata, are separated by a structural depression containing the San Francisco Bay (California Geological Survey, 2002). San Francisco Bay is a northwest-trending basin within the Bay Block, a terrane bounded on the west by the San Andreas fault and on the east by the Hayward and Calaveras fault systems (Figure 1). The Bay Block is underlain by late Mesozoic rocks of the Franciscan Complex.

San Francisco Bay is filled with as much as 600 feet of Quaternary sedimentary deposits; the sediments are shed from the surrounding hills, transported by the Sacramento River, and have accumulated in the bedrock basin that is San Francisco Bay (Lajoie and Helley, 1975; Helley and Lajoie, 1979; Witter et al., 2006; Rogers and Figuers, 1991). During the last glacial period, when sea level was significantly lower (about 425 feet below current sea level), fluvial and eolian sediment covered valleys that occupied the San Francisco basin. These non-marine deposits experienced a sustained period of sub-aerial exposure, weathering, and consolidation (Helley and Lajoie, 1979). Subsequent melting and retreat of glacial ice at the end of the Pleistocene caused global sea level to rise and invade the valleys now occupied by the San Francisco Bay (Helley and Lajoie, 1979), and Atwater and others (1977) suggest that the water re-entered the Golden Gate around 10,000 years ago reached near-current water levels approximately 5,000 years ago. Above the non-marine Pleistocene sediment are accumulations of poorly consolidated Holocene deposits. Sea level fluctuations at the end of the Pleistocene and beginning of the Holocene, are caused the interfingering of marine and terrestrial sediment facies at the San Francisco Bay margins (WLA, 1999). By comparing the historical occurrence of liquefaction in the San Francisco Bay area to geologic and geomorphic mapping, Knudsen and others (2000) found that Holocene estuarine deposits, Holocene stream and alluvial fan deposits, Holocene and Pleistocene eolian deposits, and artificial fill are the geologic materials most susceptible to liquefaction.

The geologic deposits underlying each of the five airports are shown on Quaternary geologic maps developed by Witter and others (2006), and by Rogers and Figuers (1991) (Figures 3A, 4A, 5A, 6A, 7A). These maps emphasize the areal extent of the Quaternary aged surficial deposits within the San Francisco Bay region.

Development along the bay margins began in the mid-1800s and accelerated during the population boom following World War II. Lowlands including tidal marshes, tidal flats, and shallow portions of the bay were developed by the placement of artificial fill. Most of this fill was

placed directly on young Bay mud and Holocene fluvial deposits around the bay margins. A variety of techniques were used to place and compact the fills, including emplacement of fill via large-scale hydraulic pumping (pumping or sluicing of water sand and silt slurry, typically dredged from the bay). Sandy and silty hydraulic fills along the bay margins are particularly susceptible to liquefaction. Much of the hydraulic fill was placed prior to 1965, before the effects of strong ground motions on non-engineered fill were well understood. Since 1969, engineering design and review of proposed Bay fills has been required (Hitchcock and others, 2008).

In the following sections, we describe the geologic setting and present a geologic model for each site based on subsurface information, regional geologic and geomorphic maps, historical aerial photography, and maps of fill placement through time. The geologic units found at each airport are described in detail in Appendix A.

#### **4.1 San Francisco International Airport (SFO)**

San Francisco International Airport is located on the west shore of the San Francisco Bay in northern San Mateo County. The airport is built entirely on artificial fill overlying estuarine deposits (Figure 3A). Maps of the historical extent of bay environments based on 1800s US Coast Survey mapping, show that the airport property encompasses former tidal marsh, tidal flat, shell flat, and shallow bay environments (Figure 3B; SFEI, 2000). The estuarine deposits are collectively referred to as Bay Mud on Figure 3A and Young Bay Mud (YBM) on Figure 3C. Borehole and CPT data show that the stratigraphy underlying San Francisco International Airport generally consists of artificial fill, underlain Young Bay Mud (YBM) alluvium, Old Bay Mud (OBM), and Pleistocene alluvium (Figure 3C). These sediments are underlain at depth by Franciscan Complex bedrock.

Development of the SFO property began with the construction of a perimeter levee around the tidal marsh lands in 1880 (Figure 3D, photo A). The construction of the first airfield in 1927 involved the import and placement of fill inboard of the levee (URS, 2006). By 1938 the fill had extended beyond the original perimeter to add new runways (Figure 3D, photo B). Later expansions of the airport involved subsequent episodes of fill placement on at least ten different occasions (URS, 2006). WLA (1999) identified three distinct units (Fills A, B, and C) at SFO:

- Fill A: lean clay with fine gravel and fine to medium sand
- Fill B: loose to medium dense, poorly graded sand with minor clay and silt
- Fill C: brown to gray to black, granular, poorly graded gravel with rounded to subangular fine to coarse gravel and minor clay and sand

The borehole data reviewed by WLA (1999) indicate that artificial fill at the airport ranges from 5 to 25 feet in thickness, with an average thickness throughout most of the site of 10 to 15 feet. The thickest sections of fill are located along the northern, eastern, and southern margins of the airport (WLA, 1999; URS, 2006; Figure 3C).

Young Bay Mud underlies the artificial fill and consists of unconsolidated clay to silty clay with a few lenses of well sorted sand shelly layers and peat (WLA, 1999). The thickness of the YBM ranges from 20 to 70 feet across the airfield and varies abruptly over short distances, reflecting the ground surface topography prior to deposition of the Bay Mud (URS, 2006). The YBM is formed in marshlands and tidal mud flats of the San Francisco Bay and interfingers landward with distal alluvial fan deposits shed eastward from the hills west of SFO (WLA, 1999).

The YMB unconformably overlies OBM and Late Pleistocene alluvium. OBM deposits consist of sandy clay to clayey sand with some sandy and shelly horizons that represent an ancestral bay that occupied today's San Francisco Bay about 110,000 years ago. OBM interfingers with late Pleistocene alluvial material that originated in the hills located west of SFO and consists of moderately dense clay, silt, and sand with minor gravel. These deposits were laid down during a sea level lowstand when streams flowed farther out onto the Bay plain before meeting the Bay along the paleo-Bay margin. The Old Bay Mud and alluvial material range in thickness from 50 to 160 feet near the airport terminal (WLA, 1999).

#### **4.2 Oakland International Airport (OAK)**

Oakland International Airport is located on the eastern shore of the San Francisco Bay in western Alameda County. Similar to the San Francisco airport, it is built entirely on fill over estuarine deposits (Figure 4A). Maps of the historical extent of bay environments based on 1800s US Coast Survey mapping, show that the airport property encompasses former tidal marsh, tidal flat, and shallow bay environments (Figure 4B; SFEI, 2000). The major geologic units underlying the fill include Holocene estuarine deposits, and Holocene and Pleistocene alluvial deposits, and the late Pleistocene to early Holocene Merritt Sand (Lajoie and Helley, 1975; Helley and Lajoie, 1979, Witter et al., 2006; Figure 4A and 4C). The Holocene estuarine deposits are collectively referred to as Bay Mud (Qhbm) on Figure 4A, and Young Bay Mud (YBM) on Figure 4C.

The northeastern half of the airport property is located on former tidal marsh where deltaic and stream channel deposits of San Leandro Creek interfinger with the fine-grained marsh deposits. The historical (1850s) San Leandro Creek channel is shown on Figure 4B, the 1939 channel in Figure 4D, and its present-day engineered course in Figure 4A. The northeastern half of the airport, now known as North Field, comprised the original Oakland airport built in 1927 (Port of Oakland, 2013). The USDA aerial photograph taken in 1939 (Figure 4D) shows meandering tidal marsh sloughs in-between the runways.

The southwestern half of the property is built on fill over tidal flats and shallow bay. Its terminal and south runway opened in 1962 (Port of Oakland, 2013). The southwestern shoreline is bordered by a perimeter dike that encompasses fill emplaced in the 1950s and 1960s (URS, 2011). The dike was constructed in three phases. The south and southwest perimeter was the first phase of construction in the late 1950s and fill materials consist of dredged Bay Mud (the "clay dike"; URS, 2011). The second and third phases of construction took place in the 1960s

and 1970s and extended the dike to the northwest using hydraulically-placed dredged sand and gravel (the “sand and gravel dike”; URS, 2011). WLA (1999) identified at least four different episodes of fill placement and three distinct fill units:

- Fill A: cohesive fill
- Fill B: loose to medium dense granular fills typically derived from dredged Merritt Sand (identified as the primary liquefiable zone)
- Fill C: dense to very dense granular fills

The thickness of fill varies across the site inboard of the dike from roughly 8.5 to 13.5 feet in the south to between 1 and 7 feet in the north (AGS, 2008). The fill material generally consists of loose to dense sand, silty sand, medium stiff to stiff silt and clay, with variable amounts of gravel. The thickness of the clay dike fill, composed of shelly Bay Mud, ranges between 10 and 20 feet. The thickness of the sand and gravel dike fill, composed of loose to medium dense sand and gravel, ranges between 15 and 30 feet. The fill bodies typically thicken to the west (WLA, 1999; URS, 2011).

The dike and artificial fill are underlain by YBM, which consists of soft, sandy clay to silty clay with thin peat layers locally present. The thickness of YBM ranges from 0 to 25 feet (WLA, 1999). The YBM rests unconformably on late Pleistocene to early Holocene Merritt Sand and OBM. The Merritt Sand consists of well sorted eolian sand that interfingers landward with Pleistocene alluvial fan deposits that consist of silty and sandy clay with gravelly lenses. The Merritt Sand and Pleistocene alluvial fan deposits unconformably overlie OBM (Yerba Buena mud), which consists of gray marine mud (low to high plasticity clay) with some sandy and shelly horizons (WLA, 1999).

### **4.3 Buchanan Field Airport (CCR)**

Buchanan Field Airport is located near the margin of Suisun Bay and the mouth of Walnut Creek in northern Contra Costa County. The airport is built on a layer of artificial fill placed over alluvial fan and estuarine sediments. The airport property is located on the distal portion of the interfingering alluvial fans of Walnut Creek and Grayson Creek where they grade into the estuarine environment of the San Francisco Bay margin. The major geologic units in the area include Holocene and Pleistocene alluvial deposits, and Holocene estuarine deposits (Figure 5A; Lajoie and Helley, 1975; Helley and Lajoie, 1979, Witter et al., 2006). Maps of the historical ecology of the area show that the airport property encompasses former estuarine, moist grassland, and willow grove habitats (Figure 5B; SFEI, 2000). These habitats are characterized by tidal or shallow groundwater conditions.

Aerial photography taken in 1939 (Figure 5D) shows the future airport property as farm land. The already straightened channel of Walnut Creek and the winding channel of Grayson Creek pass to the west and east, respectively, of the property. Topographic contours from show that the land slopes gently to the north, underlain by the alluvial fan deposits of Walnut Creek, and to

a lesser degree from the smaller Grayson Creek. The estuarine deposits shown on Figure 5B (tidal marsh) at the north end of the property are drained and farmed, thus do not have a distinct appearance from the alluvial fan deposits. Alluvial fan and estuarine deposits are expected to interfinger in this area.

Site development began in 1942 with the purchase by Contra Costa County of over 400 acres of land to build an airport. In 1943, the United States Army expropriated the site, added more than 100 additional acres to the site, and named the new development the Concord Army Air Base. In 1947, the War Assets Administration returned the airport to the County for public use and the County renamed the airport after County Supervisor William J. Buchanan. Additional structures were built on the site in 1949, 1961, and 1992 (Contra Costa County Airport, 2013). A recent aerial photograph (Figure 5E) shows the airport in its present urban setting.

Borehole and other subsurface data show that the stratigraphy underlying Buchanan Field Airport consists of artificial fill over Holocene alluvial fan deposits and, at the north end of the property, artificial fill over estuarine deposits (Figure 5C). The thickness of fill ranges from 4 to 10 feet (Parikh, 2011; EBA Engineering, 2008). According to borehole data reviewed, the fill can be subdivided into four distinct units (Fill A, B, C, and D (Figure 5C)). Fill A generally consists of aggregate baserock of sandy gravel with minor amounts of clay. Fill B generally consists of well graded sand with varying amounts of gravel. Fill C generally consists of clayey fine sand with trace amounts of gravel. Fill D generally consists of clay with silt and fine to medium sand. The Holocene alluvial deposits consist of silty clay interbedded with silty sand and gravel (Parikh, 2010; EBA Engineering, 2008; Witter et al., 2006). The estuarine deposits consist of very soft to stiff silt and clay with interbedded fine to coarse grained sand and gravel lenses. These deposits become very stiff below a depth of 40 feet.

#### **4.4 Livermore Municipal Airport (LVK)**

Livermore Municipal Airport is located on the floor of the Livermore basin, an east-west trending syncline or synclorium (CGS, 2008). The basin floor is underlain in the near-surface by Holocene and Pleistocene alluvial deposits, and at depth by the Plio-Pleistocene Livermore Gravels (Witter et al, 2006; CGS, 2008) (Figure 6A). The airport property is located on the distal portions of the Arroyo Mocho alluvial fan (mapped as Qhfy) and Las Positas alluvial fan (mapped as Qhff). The more clay-rich deposits of Arroyo Las Positas are expected to interfinger across the property with the sands and silts of Arroyo Mocho. Subsurface data suggest that the stratigraphy underlying the Livermore Municipal Airport consists of artificial fill thickening downslope over Holocene alluvial fan deposits of varying texture (Figure 6B).

Aerial photography taken in 1949 (Figure 6C) shows the airport property before development as grazing and farm lands. Arroyo Las Positas winds along the north boundary. Arroyo Mocho, a relatively larger stream draining the Diablo Range, enters from the southeast corner of the map and distributes into multiple channels, building a large alluvial fan, mapped as Qhfy on Figure 6A, that slopes southwest through the airport area to meet the deposits of Arroyo Las Positas.

The recency of the Arroyo Mocho deposits is indicated by the presence of fresh distributary channels, mapped in blue dots on Figure 6C.

Site development began in the early 1960s and airport construction was completed in December 1965. The new airport encompassed 257 acres, a 4,000-foot asphalt runway with a parallel taxiway, an aircraft parking apron with 100 tie-downs, a beacon, a lighted wind cone and segmented circle, and 50 based aircraft. Additional structures were built on the site in 1970, 1973, and 1979, 1985, and 1987. A second 2,699-foot parallel runway was built in 1985 and an extension of the main runway to 5,255 feet followed in 1989. Today, the Livermore Municipal Airport encompasses 644 acres (City of Livermore, 2013). A recent aerial photograph (Figure 6D) shows the airport in its present urban setting.

Borehole data indicate that artificial fill at the airport is present on the western 3/4 of the property and ranges in thickness from 4.5 to 10 feet, thickening westward or downslope (Figure 6B; Cornerstone Earth Group, 2010). Due to the limits of data, it is possible (but unlikely) that fill extends below depths of 10 feet. No significant fill thickness is found at the upslope, or eastern, end of the property. The fill can be subdivided into two distinct units (Fill A and Fill B). Fill A generally consists of very stiff to hard lean clay with fine sand. Fill B generally consists of medium dense, clayey, fine to coarse sand with fine to coarse gravel.

Underlying the artificial fill are Holocene medial and distal alluvial fans deposits. These deposits consist of lean clay with sand, sandy lean clay, sandy silty clay, and silty clay interbedded with silty sand, clayey sand, and poorly graded sand with gravel (CGS, 2008).

#### **4.5 Moffett Federal Airfield (NUQ)**

Moffett Federal Airfield is located at the southern margin of San Francisco Bay in Santa Clara County. The airport is built over Holocene fine-grained alluvial fan deposits (Qhff) and Holocene estuarine deposits or Bay Mud (Qhbm; Figure 7A). Most of the airport property is located on the distal end of the Stevens Creek alluvial fan, derived from the Santa Cruz Mountains to the south of the site. Maps of the historical extent of bay environments based on 1800s US Coast Survey mapping, show that the north end of the airport property encompasses former tidal marsh and salt panne environments (Figure 7B; SFEI, 2000). The estuarine deposits are collectively referred to as San Francisco Bay Mud (Qhbm) on Figure 7A and Young Bay Mud (YBM) on Figure 7C.

Aerial photography taken in 1939 (Figure 7D) shows the airport property before construction of the runways. Some facilities, including Hangar One, are already in place. The historical bay shoreline shown in Figure 7B is still visible, running parallel to an east-west dike that separates the uplands from the tidal marsh lands. The grasslands on which the airport runways are to be built are visible in the photograph. Topographic contours from the USGS Mountain View 7.5-minute quadrangle (1991) show a northward sloping alluvial fan surface, decreasing in gradient as it approaches the estuary. The airport is on the gently sloping north end of this alluvial fan.

The jog in the contours as they cross the runways reflects the presence of artificial fill on which the runways are now built.

Development of this area began in 1933 with the construction of the Sunnyvale Naval Air Station, which was later renamed Moffett Federal Airfield. Construction involved the import and placement of fill along the northern edge of the property (NASA, 2013; Atchley and Dobbs, 1959), and beneath the runways.

CPT and other subsurface data suggest that the stratigraphy underlying Moffett Federal Airfield consists of artificial fill over Holocene alluvial fan deposits and, at the north end of the property, artificial fill over estuarine deposits, Old Bay Mud (OBM), and Pleistocene alluvial deposits (Figure 7C). These sediments are underlain at depth by the Santa Clara Formation.

Holocene alluvial fan deposits and YBM underlie the artificial fill and consists of unconsolidated clay, silty clay, silt, sand, and gravel (CH2MHill, 2011; Atchley and Dobbs, 1959). The YBM formed in marshlands and tidal mud flats of the San Francisco Bay and interfingers landward with the distal Holocene alluvial fan deposits shed eastward from the hills west and south of NUQ (Atchley and Dobbs, 1959). Drainage ditches and cuts north of the hangars expose gravelly clay alluvium near the surface, while adjacent areas show black humus-rich soil (Atchley and Dobbs, 1959).

The YMB and Holocene alluvial fan deposits unconformably overlie older alluvium and estuarine deposits. OBM deposits consist of firm to very stiff silty and sandy clays and loose to dense silty and gravelly sands that represent an ancestral bay that occupied today's San Francisco Bay about 110,000 years ago (Peter Kaldveer and Associates, Inc., 1980). OBM interfingers with late Pleistocene alluvial material that originated in the Santa Cruz mountains west and south of NUQ and consist of moderately dense clay, silt, and sand with minor gravel. These deposits were laid down during a sea level lowstand when streams flowed farther out onto the Bay plain before meeting the Bay along the paleo-Bay margin.

---

## 5.0 LIQUEFACTION HAZARD ASSESSMENT

### 5.1 Methodology

Liquefaction is typically defined as the loss of strength in saturated, loose, sandy, or low plasticity fine-grained soils resulting from strong shaking during earthquakes. The loose sandy soils have a tendency to contract (compress) during shaking, resulting in the development of increased pore pressures between the soil particles. If the intensity or duration of the shaking is great enough, the build-up of excess pressure can lead to a significant loss of strength in the

soils. Additionally, even if the soil does not fully liquefy, dissipation of excess pore pressure following the earthquake can result in soil compression and settlement.

The susceptibility of soil to liquefaction is a function of gradation, density, fines content, and plasticity of fines. Increases in grain size distribution, soil density, fines content, and plasticity index decreases the susceptibility of soils to liquefaction. In addition, the liquefaction susceptibility of soils also decreases with respect to the age of the deposit and effective overburden stress.

The liquefaction susceptibility of the soils was assessed following state of practice analysis methodology using simplified empirical SPT and CPT based procedures (e.g. the Simplified Procedure). Due to its widespread application, multiple revisions of these Simplified Procedures have been developed and reported over time (e.g. Seed et al., 1982, 1983, 1985; Robertson and Wride, 1997; Youd et al., 2001; Idriss and Boulanger, 2004, Cetin et al., 2004b). The approach recommended by Youd et al. (2001) is currently one of the predominant approaches adopted in the state of practice and has been selected for this study as it provides recommendations for both the SPT and CPT based liquefaction susceptibility approaches.

In order to perform the liquefaction assessment, two variables need to be estimated: cyclic stress ratio (CSR), which characterizes the seismic demand on the soil, and the cyclic resistance ratio (CRR), which characterizes the soil capacity in resisting liquefaction. A factor of safety against liquefaction is then calculated as a ratio of CRR and CSR.

CSR is estimated using input ground motion characteristics, peak ground acceleration (PGA) and earthquake magnitude (M). The selection of PGA and M values is discussed in the following section. CRR is calculated using SPT blow count values or CPT cone tip resistance corrected for overburden stress and fines content. The relationships between CRR and corrected SPT blow count or CPT tip resistance have been developed by Youd and others (2001) through a review of historical cases of liquefaction occurrence.

In addition to calculating a factor of safety against liquefaction, our assessment also includes evaluation of liquefaction-induced reconsolidation settlements. Liquefaction-induced settlements were calculated using Ishihara and Yoshimine (1992) recommendations. It should be noted that the soil above the groundwater can also settle due to dynamic compaction, however, we have not included dynamic compaction settlements as part of this study.

### 5.1.1 Ground Motion Parameters

Liquefaction susceptibility analyses were performed for five sets of ground motion parameters corresponding to the following deterministic and probabilistic scenarios:

- 1906 San Francisco Earthquake Scenario (Deterministic median)

- Hayward-Rodgers Creek Scenario (Deterministic median)
- Concord-Green Valley Scenario (Deterministic median)
- 10% Probability of Exceedance in 50 Years Scenario (Probabilistic)
- 2% Probability of Exceedance in 50 Years Scenario (Probabilistic)

For each ground motion scenario, a single set of PGA and M values was selected for the analyses. The selected values are summarized in Table 1. For the deterministic scenarios, the M value was defined by the earthquake magnitude of each source and the PGA value was selected based on the review of the PGA grid maps developed for each scenario (Petersen et al., 2008; USGS, 2013c, Wald et al., 2005). Multiple grid points with varying PGAs were available within the area of each analyzed airport and are presented on Figures DA-1 through DA-5 in Appendix D. The selected value is generally between the average and the maximum of the individual data points and was based on the review of data point locations and variability.

For the probabilistic scenarios, PGA and M values were selected by using the USGS online interactive deaggregation calculator (USGS, 2013). The calculations using the online USGS calculator were performed for several points within each airport footprint to evaluate possible variability in ground motions, and representative values were selected. Site conditions characterized by shear wave velocity in the upper 30 meters ( $V_{s30}$ ) below ground surface were assessed using USGS  $V_{s30}$  maps for California (USGS, 2013b). Because multiple data points for  $V_{s30}$  are available within the airports' footprint, an averaged value spanning the entire airport area was selected and is reported in Table 1.

In addition to summarizing the PGA and M values applied for our analyses, Table 1 also presents the PGA normalized to a 7.5 magnitude earthquake ( $PGA_{7.5}$ ). The  $PGA_{7.5}$  normalized value can be used to compare seismic intensity with respect to liquefaction triggering between earthquakes of different magnitudes. For example, an initial comparison of PGA values of 0.32g and 0.49g for the 1906 San Francisco earthquake scenario and 10% probability of exceedance in 50-year scenario, respectively, for the Oakland International Airport differ significantly; once adjusted for earthquake magnitude, the two scenarios have similar  $PGA_{7.5}$  values at 0.35g and 0.37g, respectively (i.e., a comparable level of liquefaction hazard and impact would be expected for both scenarios).

**Table 1. Ground Motion Parameters for Liquefaction Assessment**

Airport Location ( $V_{s30}$ ) <sup>3</sup>	Peak Ground Acceleration (PGA) / Moment Magnitude (M) ( $PGA_{7.5}$ )				
	1906 San Francisco Earthquake Scenario <sup>1</sup>	Hayward-Rodgers Creek Scenario <sup>1</sup>	Concord-Green Valley Scenario <sup>1</sup>	10% Probability of Exceedance in 50-Years Scenario <sup>2</sup>	2% Probability of Exceedance in 50-Years Scenario <sup>2</sup>
San Francisco International Airport (200 m/s)	0.48 / 7.8 (0.53)	0.27 / 7.26 (0.25)	0.15 / 6.71 (0.11)	0.48 / 8.0 (0.57)	0.75 / 8.0 (0.89)
Oakland International Airport (210 m/s)	0.32 / 7.8 (0.35)	0.35 / 7.26 (0.32)	0.20 / 6.71 (0.15)	0.49 / 6.7 (0.37)	0.73 / 6.7 (0.55)
Buchanan Field Airport (250 m/s)	0.15 / 7.8 (0.17)	0.24 / 7.26 (0.22)	0.53 / 6.71 (0.40)	0.54 / 6.6 (0.39)	0.87 / 6.6 (0.63)
Livermore Municipal Airport (330 m/s)	0.18 / 7.8 (0.20)	0.25 / 7.26 (0.23)	0.17 / 6.71 (0.13)	0.53 / 6.7 (0.40)	0.84 / 6.7 (0.63)
Moffett Federal Airfield (290 m/s)	0.31 / 7.8 (0.34)	0.32 / 7.26 (0.29)	0.10 / 6.71 (0.07)	0.49 / 6.7 (0.37)	0.75 / 6.7 (0.56)

Notes:

<sup>1</sup> Based on the PGA data points provided by USGS

<sup>2</sup> Based on USGS deaggregation calculator (2013)

<sup>3</sup> Based on USGS  $V_{s30}$  maps (2013)

### 5.1.2 Groundwater

Depth-to-groundwater (DTW) is an important variable in the assessment of liquefaction susceptibility since saturated soil conditions are required for liquefaction to occur. Saturation reduces the effective normal stress of near-surface sediment, increasing the likelihood of earthquake-induced liquefaction (Youd, 1973). DTW can vary daily, seasonally, and annually, as well as locally and regionally.

For this assessment, only near-surface groundwater (i.e., groundwater levels at depths less than 40 feet) was considered and applied. The DTW data was compiled from CPT and borehole logs, and historical high ground water levels published by the California Geological Survey (2006 and 2008).



### 5.1.3 Quality of Available Subsurface Data

Quality and quantity of available subsurface data varied greatly by airport location. Subsurface data coverage (provided by large number of CPTs performed as part of past Fugro projects) for the San Francisco International Airport is very high in terms of both areal coverage, penetration depth, and data quality.

For the Oakland International Airport, subsurface data is available in the form of borings, with relatively good aerial coverage, but with variable penetration depth. Shallow borings do not provide any insight into potentially liquefiable soil layers at deeper depths. Additionally, the available boring data provide limited information regarding soil fines content, which is an important characteristic for liquefaction triggering evaluation. Where fines content was not available, it was assumed based on soil description. The same approach to the interpretation of the fines content was applied for the other airports where liquefaction susceptibility was analyzed using boring data.

Subsurface data coverage for the Buchanan Field Airport and Moffett Federal Airfield is limited. While the available data does provide an insight into the level of liquefaction susceptibility, the areal coverage is not sufficient to develop a robust understanding of the liquefaction hazard. Finally, for the Livermore Municipal Airport, the limited available subsurface data made a quantitative assessment of liquefaction susceptibility not possible.

## **5.2 Results**

Liquefaction assessment results are developed in terms of factors of safety against liquefaction and liquefaction-induced settlements. The factor of safety can be used to determine the susceptibility to liquefaction of individual soil units, while liquefaction-induced settlements are a measure of the severity of the impact of liquefaction at the ground surface. Table 2 summarizes the number of borings and CPTs reviewed for this study and for which liquefaction analyses was performed. A complete list of CPT and borehole data analyzed can be found in Appendix C.



**Table 2. Summary of Subsurface Explorations Analyzed for Liquefaction Susceptibility**

Data Type	Location				
	San Francisco International Airport	Oakland International Airport	Buchanan Field Airport	Livermore Municipal Airport	Moffett Federal Airfield
Borings					
- total	- <sup>1</sup>	48 <sup>2</sup>	62	8	-
- greater than 30 feet depth	-	12	10	0	-
- 10 to 30 feet depth	-	32	21	1	-
- less than 10 feet depth	-	4	31	7	-
Cone Penetration Test (CPT)	86	-	-	-	14 <sup>3</sup>

Notes:

<sup>1</sup> Boring data was available for San Francisco Airport but was not reviewed because of the high quantity and area coverage of available CPT soundings.

<sup>2</sup> Additional borings were identified for Oakland Airport but were not included because of their limited depth.

<sup>3</sup> Seven out of fourteen CPTs were analyzed using partial data records because electronic data was not available.

Many of the available borehole logs are relatively shallow, with depths of penetration as low as 5 to 10 feet. The shallow explorations may be too shallow to capture deeper liquefiable soil layers. Accordingly, the liquefaction-induced settlement, which is a cumulative measure of the liquefaction impact on the ground surface, may be underestimated by shallow explorations. Occurrence of liquefaction as deep as 50 to 80 feet can contribute to total settlement. Therefore, data points presented in liquefaction settlement plots differentiate between borings with penetration exceeding 30 feet and borings with penetration depths between 10 and 30 feet. Borings that have a penetration depth of less than 10 feet were not included in the settlement analysis. Interpretation of settlement potential using shallower borings should be done with caution as they may underestimate liquefaction-induced settlements (i.e., layers of liquefiable soils may be present below the bottom of the boring). The number of borings and individual penetration depths categories are summarized in Table 2.

A summary of the liquefaction assessment results are presented in the following sections. Figures 8 through 11 present the liquefaction settlement maps for the 2% probability of exceedance in 50 years scenario for four out of five airports. This scenario has the highest normalized PGA values for each of the evaluated airports (Table 1). A settlement map was not developed for the Livermore Municipal Airport because the available borings were too shallow to penetrate the historically high groundwater levels for the area (e.g. total borehole depths did not exceed 11 feet below ground surface), making an assessment of liquefaction susceptibility unfeasible. Appendix D presents a more thorough discussion of the liquefaction assessments performed and presents additional data for each analyzed airport location, including:



- Site map showing the locations of analyzed borings or CPTs and cross section locations
- Geotechnical cross sections showing subsurface conditions along airport runways
- Liquefaction settlement maps, one for each of the five earthquake scenarios (no liquefaction assessment results provided for the Livermore Municipal Airport)
- Liquefaction cross sections showing soil types, liquefaction susceptibility and zones contributing to liquefaction settlements for the five earthquake scenarios (no liquefaction assessment results provided for the Livermore Municipal Airport)

### 5.2.1 San Francisco International Airport

The liquefaction assessment performed for San Francisco International Airport indicates that both coarse-grained fill and Holocene alluvium could be susceptible to liquefaction under the different earthquake scenarios evaluated (Figure 8, Appendix D). For the 2% probability of exceedance in 50 years scenario, calculated total liquefaction-induced settlements vary between about 1 and 4 inches across the site (Figure 8), with differential settlements between adjacent data points between 1 and 3 inches. As the result of the variable thickness and depth of the coarse-grained soils, the liquefaction induced total and differential settlements may vary across the site and between the exploration locations. For cases where closely spaced exploration points are not available to assess differential settlements, Martin and Lew (1999) suggests that differential settlements could be estimated on the order of one-half to two-thirds of the total settlements.

The calculated settlement values for the 2% probability of exceedance in 50 years scenario account for liquefaction in the top 80 feet of soil. Deeper soil was neglected because of the limitations of simplified liquefaction triggering method and relatively smaller surface manifestations of possible liquefaction at depth.

### 5.2.2 Oakland International Airport

The liquefaction assessment performed for Oakland indicates that both coarse-grained fill and Merritt Sand could be susceptible to liquefaction under any of the considered earthquake scenarios (Figure 9, Appendix D). For the 2% probability of exceedance in 50 years scenario, total liquefaction-induced settlements were calculated to vary from about 2 to 9 inches, with the higher values located under the main runway area where thicker deposits of artificial fill are present. However, high settlement values were also calculated in the eastern half of the site where deposits of artificial fill are thinner (Figure 9).

The calculation of differential settlement cannot be reliably assessed based on the existing data. Comparing adjacent data points that have different penetration depths can be misleading. Differential settlement approximations may be on the order of one-half to two-thirds of the total



settlements (Martin and Lew, 1999). Based on the calculated values of total settlement, differential settlements could be as high as 4 to 6 inches at OAK.

### 5.2.3 Buchanan Field Airport

The data available for analysis at Buchanan Field Airport is limited in extent and depth of penetration. The deeper subsurface data is generally clustered at the northwest end of the site. Data under the runway footprints are shallow in penetration, and do not provide much subsurface information.

Figure 10 presents the liquefaction settlement maps for the 2% probability of exceedance in 50 years scenario. Figures DD-1 through DD-8 present a complete set of liquefaction assessment results.

The results of the settlement calculations are included in Figure 11. The magnitude of settlement is generally less than 3 inches, with the exception of one location. Because of the limited subsurface data, no conclusions can be made about potential liquefaction settlement along the airport runways, but the results in adjacent areas suggest it is possible.

### 5.2.4 Livermore Municipal Airport

It was not possible to perform a quantitative assessment of liquefaction potential at Livermore Municipal Airport. The available subsurface data did not reach the historical high water table and thus it was not possible to assess the liquefaction potential. The available geotechnical data are presented in cross sections in Figures DE-1 through DE-2.

### 5.2.5 Moffett Federal Airfield

The liquefaction assessment performed for Moffett Federal Airfield indicates that coarse-grained lenses within the Young Bay Mud could be susceptible to liquefaction under certain earthquake scenarios (Figure 11, Appendix D). The density of the coarse-grained lenses as well as their liquefaction susceptibility varies laterally and with depth. For the 2% probability of exceedance in 50 years scenario, total calculated liquefaction-induced settlements vary between about less than 1 inch to about 3 inches along the runway, with differential settlements between adjacent data points between 1 and 2 inches along the airfield runway. However, because of the large spacing between adjacent exploration points, settlements between points could vary significantly from the calculated values, depending on the localized variations in subsurface conditions.

Settlements as high as 4 to 5 inches were calculated using CPT data concentrated on the western side of the property and along the main runway. The CPT data here, however, were collected less frequently with depth (i.e., one data point at one foot depth intervals compared to one data point every 2 inches for a typical CPT) and higher settlements might be an artifact of



the incomplete dataset. It should also be noted that the coverage of subsurface data available to assess liquefaction potential was limited, with CPT locations spaced 1,000 to 3,000 feet apart.

## 6.0 CONCLUSIONS

---

This assessment updates and revises the earthquake-induced liquefaction susceptibility assessments conducted in WLA (1999) for San Francisco and Oakland International airports. The evaluation utilizes the updated ground motion data of Petersen and others (2008) and uses the updated procedures outlined by Youd and others (2001) to make the analysis consistent with accepted state of practice methodology. Additionally, the settlement estimate methodology employed in this study is comparably more quantitative and consistent with updated state of practice methodologies.

The purpose of this assessment is to identify areas that may be susceptible to earthquake-induced liquefaction and related settlement at San Francisco, Oakland, Moffett, Buchanan, and Livermore airports. A summary of the calculated liquefaction settlements is presented in Table 3. The findings presented herein are based on available and existing geologic, geomorphic, and geotechnical data and should be considered preliminary and provisional.

**Table 3. Calculated Liquefaction Settlement Summary**

Airport Location	Calculated Liquefaction Induced Settlements Range (inches)				
	1906 San Francisco Earthquake Scenario <sup>1</sup>	Hayward-Rodgers Creek Scenario <sup>1</sup>	Concord-Green Valley Scenario <sup>1</sup>	10% Probability of Exceedance in 50-Years Scenario <sup>2</sup>	2% Probability of Exceedance in 50-Years Scenario <sup>2</sup>
San Francisco International Airport	1 to 4	1 to 3	0 to 2	1 to 4	1 to 4
Oakland International Airport	2 to 9	2 to 9	2 to 8	2 to 9	2 to 9
Buchanan Field Airport <sup>1</sup>	1 to 4	1 to 4	1 to 4	1 to 4	1 to 4
Livermore Municipal Airport <sup>2</sup>	N/A	N/A	N/A	N/A	N/A
Moffett Federal Airfield <sup>3</sup>	1 to 3	1 to 3	below 1	2 to 3	2 to 3

Notes:

<sup>1</sup> Based on limited number of data points. No data points available along the runways.

<sup>2</sup> Available borings to shallow to evaluate liquefaction induced settlements.

<sup>3</sup> Based on seven CPTs along the runway (USC-01 to USC-07). Seven CPTs located adjacent to the airport and analyzed using partial data not considered for this summary.

## 6.1 Liquefaction Hazards

### 6.1.1 San Francisco International Airport

The liquefaction analyses performed for San Francisco used data available from 86 CPT locations, representing the largest number of data locations used for analysis at any of the five airport locations. The CPT data used are well-distributed across the property and mostly exceed 30 feet in depth. The CPT data indicate that the surficial deposits at the airport are primarily composed of artificial fill and are underlain by Young and Old Bay Mud.

The analyses performed for each of the five scenarios results in a calculated settlement of between 0 and 4 inches (Table 3), and suggest that both coarse grained artificial fill and Holocene alluvium have the highest susceptibility to liquefaction. The range of settlement values calculated for the assessment are significantly lower than the range of settlement values of 12 inches to 30 inches calculated during the study performed by WLA in 1999. A number of factors could be responsible for the different settlement values, including:



- Data distribution: the data locations used in the WLA study were concentrated in the main terminal area and the northern end of the property. The data used in this study are more equally distributed across the site, and may be more representative of the site conditions.
- Data extent: of the approximately 230 boreholes evaluated as part of the WLA study, approximately 130 of the boreholes were shallower than 30 feet, with approximately 80 of those boreholes shallower than 10 feet.
- Sampling intervals: the number and spacing of sampling intervals using borehole data can be limited, where as CPT data locations contain more sampling intervals for better resolution of liquefiable materials thicknesses.
- Updated liquefaction procedures: the updated ground motion data of Petersen and others (2008) and procedures outlined by Youd and others (2001) applied during this study are different than those applied during the WLA (1999) study.

### 6.1.2 Oakland International Airport

The liquefaction analyses performed for Oakland used data available from 48 borehole locations. The borings analyzed were concentrated within the southwestern and northeastern edges of the property. Additional data is available, but it was either 1) in a format that was difficult to analyze, or 2) not provided before the analysis was completed. As a result of the data limitations, no subsurface data was analyzed in the main terminal area located in the center of the property. The borehole data indicates that the surficial deposits at the airport are primarily composed of artificial fill and are underlain by Young and Old Bay Mud and Merritt Sand.

The analyses performed for each of the five scenarios results in a calculated settlement of between 2 and 9 inches (Table 3). This settlement range is lower than the settlement range of 4 to 12 inches calculated during the initial study performed by WLA in 1999. A number of factors could be responsible for the different settlement values, including:

- Data distribution: The data locations used in the WLA study are located throughout the property, but are located in smaller clusters and widely spaced. The data used in this study are clustered along the western and northeastern portions of the property. No subsurface data was available or analyzed for the main terminal area for this study.
- Data extent: Of the approximately 180 boreholes evaluated as part of the WLA study, approximately 70 of the boreholes were shallower than 30 feet, with approximately 4 of those boreholes shallower than 10 feet. Liquefiable material may be present below the maximum depth achieved by the borings.
- Updated liquefaction procedures: the updated ground motion data of Petersen and others (2008) and procedures outlined by Youd and others (2001) during this study are different than those applied during the WLA (1999) study.



The liquefaction analyses performed generally calculated the highest settlement values along the perimeter levees and dike along the western edge of the property. The levees and dike are primarily composed of two distinct fill units: medium stiff Bay Mud fill, approximately 10 to 20 feet thick between stations 0+00 to 168+00; and loose to medium dense sand and gravel approximately 15 to 30 feet between stations 168+00 to 250+00 (URS, 2011; Figure 4A). The foundation materials underlying the levees and dikes are composed of soft to medium stiff silty clay (likely to be Young Bay Mud) along most of the alignment, with the exception of the northern end of the alignment, where it is underlain by predominantly clayey sand and silty sand. Of the levee and dike fill materials, the sand and gravel fill was calculated to be liquefiable in all 5 scenarios while the Bay Mud fill yielded varying results.

In addition to the levee and dike fill, coarse grained layers within the Young Bay Mud and the Merritt Sand were found to be liquefiable. Along the western portion of the property, the Merritt Sand is located approximately 10 to 40 feet below ground surface. Along the eastern and northern portions of the property, the borings suggest the presence of Merritt Sand, however the deepest boring analyzed (36.5 feet below ground surface) does not fully penetrate through the sand, leaving the thickness of the Merritt Sand in this portion of the property unknown. It is also unclear what the nature, extent, and thickness of the Merritt Sand is below the main airport terminals, where no subsurface data was evaluated.

### 6.1.3 Buchanan Field Airport

The liquefaction analyses performed for each of the five scenarios results in a calculated settlement of between 1 and 4 inches (Table 3). The analyses used data available from 62 borings. Of the borings analyzed, only 10 were deeper than 30 feet and 31 were drilled to a total depth of less than 10 feet (Table 2). The borings analyzed were concentrated within the northern half of the property and outside of the property along the western property boundary. No subsurface data was available for the southern half of the property.

Borehole data indicates that the surficial deposits at the airport are primarily composed of artificial fill (subdivided into four distinct units; Fills A, B, C, and D), underlain by estuarine mud in the northern portion of the property, and Holocene medial and distal alluvial fans deposits in the southern portion of the property. Due to the sparse data available below 30 feet and absence of subsurface borehole data for the southern half of the property, the nature and extent of the contact between the estuarine mud and Holocene alluvial fan deposits is poorly constrained.

Based on geologic and geomorphic mapping, Witter and others (2006) characterize Quaternary deposits at Buchanan as having a moderate susceptibility to liquefaction, with a small cluster of deposits at the north end having a very high susceptibility to liquefaction. These deposits likely correspond to areas of mapped artificial fill over estuarine mud deposits. Given the relative ages, densities, and textures of these deposits, Fill A (aggregate baserock composed of sandy gravel with minor amounts of fill), Fill B (well graded sand with varying amounts of gravel), Fill C



(clayey fine sand with trace amounts of gravel), and the coarse-grained layers within the estuarine mud and Holocene alluvial fan deposits may have the highest potential for liquefaction.

#### 6.1.4 Livermore Municipal Airport

A liquefaction analysis was not performed at Livermore due to the shallow total depths of the limited number of boreholes available for analysis. Logs for eight boreholes were reviewed for the site, extending to a maximum total depth of 11 feet below ground surface. Groundwater was not encountered in any of the borings and the total depth of these borings is shallower than the historical high groundwater range of 15 to 25 feet below ground surface anticipated for the site (CGS, 2008).

Based on geologic and geomorphic mapping, Witter and others (2006) characterize Quaternary deposits at Livermore as having a moderate to high susceptibility to liquefaction. A small cluster of deposits with a very high susceptibility to liquefaction mapped along the northern property boundary, correspond to former channels of the Arroyo Mocho fluvial system.

Borehole data indicates that the surficial deposits at the airport are primarily composed of artificial fill and are underlain by Holocene medial and distal alluvial fans deposits composed of lean clay with sand, sandy lean clay, sandy silty clay, and silty clay interbedded with silty sand, clayey sand, and poorly graded sand with gravel. The fill can be subdivided into two distinct units: a very stiff to hard lean clay with fine sand (Fill A), and medium dense, clayey, fine to coarse sand with fine to coarse gravel (Fill B). Given the relative ages, densities, and textures of these deposits, Fill B and the coarse-grained layers within the Holocene alluvial fan deposits may have the highest liquefaction potential.

#### 6.1.5 Moffett Federal Airfield

A liquefaction analysis was performed for the Moffett Federal airport using data available from 14 CPT locations. The CPT data used are concentrated on the western side of the property and along the main runway, with the runway locations spaced 1,000 to 3,000 feet apart. The CPT data indicate that the surficial deposits at the airport are primarily composed of artificial fill underlain by fine-grained alluvial and estuarine deposits. Due to the relatively low density of CPT data points throughout the property, the nature and thickness of these deposits are poorly constrained.

Based on geologic and geomorphic mapping, Witter and others (2006) characterize Quaternary deposits at Moffett as having a moderate susceptibility to liquefaction, with a small cluster of deposits at the north end having a very high susceptibility to liquefaction. These deposits correspond to areas of mapped artificial fill over estuarine mud deposits. Given the relative ages, densities, and textures of these deposits, the coarse-grained layers within the deposits may have the highest potential for liquefaction.

## 6.2 Recommendations

### 6.2.1 Liquefaction Investigations

Liquefaction investigations are necessary for Buchanan and Livermore to more fully characterize the potential aerial extent and amount of liquefaction-related deformation. Those investigations should include a review of all available subsurface data, the collection of both CPT and soil boring data and samples, geotechnical laboratory analyses that would include, at a minimum, grain size analysis and Atterberg limits, aerial photographic analysis of site development and fill placement history, and the construction of geologic cross sections across the site showing the lateral extent and thickness of fill.

### 6.2.2 Additional Site Studies

Additional site studies are necessary at Moffett and Oakland to address the gaps in subsurface data coverage across these properties. All available geotechnical and engineering geologic reports for these airports should be obtained and reviewed to identify any data suitable for liquefaction analysis and to identify areas with gaps in data coverage. Where significant coverage gaps occur, a subsurface investigation should be developed in order to collect the additional data.

A more comprehensive evaluation of fill thickness and character is recommended at Moffett, Oakland, and San Francisco to address differential settlement potential and identify areas with a higher susceptibility to liquefaction. This evaluation should include a review of all available subsurface data, aerial photographic analysis of fill placement history, and the construction of geologic cross sections across the site showing the lateral extent and thickness of both fill and, specifically at Oakland, the Merritt Sand.

This evaluation should also include a review of all perimeter dikes and levees at San Francisco and Oakland to assess the potential for slope stability and seepage that may result from earthquake-induced liquefaction (it should be acknowledged that OAK is currently making improvements to their dikes and levees to meet the FEMA recommendations and requirements). The borings analyzed along the perimeter levees and dikes at Oakland do not cover the first 80 feet and the last 30 feet of the alignment, resulting in the liquefaction susceptibility of fill materials in these locations poorly constrained. In addition, evidence for seepage was documented by URS (2011) along the Oakland levees and dikes between stations 168+00 and 188+00 and stations 193+00 to 220+00 that should be further evaluated.

### 6.2.3 Mitigation

Various methods have been used to mitigate liquefaction hazards within the San Francisco Bay Area. Some of the most commonly used and effective techniques suggested by Martin and Lew (1999) include:



- Densification (e.g. vibrocompaction, vibro-replacement or vibro-stone columns, deep dynamic compaction, compaction or pressure grouting)
- Drainage and dewatering
- Reinforcement
- Mixing (e.g. permeation grouting, soil mixing, or jet grouting)
- Materials replacement
- Structural mitigation

Factors that need to be considered when selecting the appropriate mitigation strategy include cost, disruption to operations/facilities, subsurface and groundwater conditions, depth and lateral extent of liquefiable layers, accessibility and staging requirements, and changes in foundation response between treated and untreated areas. A site study should be performed to evaluate and select the technique best suited for the local site conditions.



## 7.0 REFERENCES

---

- 2007 Working Group on California Earthquake Probabilities (WGCEP), 2008, The Uniform California Earthquake Rupture Forecast, Version 2 (UCERF 2): U.S. Geological Survey Open-File Report 2007-1437 and California Geological Survey Special Report 203.
- Association of Bay Area Governments (ABAG), 2001, The REAL Dirt on Liquefaction: A Guide to the Liquefaction Hazard in Future Earthquakes Affecting the San Francisco Bay Area.
- AGS, 2008, Technical Memorandum No. 2: Geotechnical Study for Runway Safety Areas, Oakland International Airport.
- Andrus, R.D., and Stokoe, K.H., 1999, A liquefaction Evaluation Procedure Based on Shear Wave Velocity: U.S./Japan Natural Resources Development Program, 31st Joint Meeting Proceedings, May 11 – 14, Japan, p. 71-78.
- Andrus, R.D., Stokoe II, K.H., and Juang, C.H., 2004, Guide for Shear-Wave-Based Liquefaction Potential Evaluation, *Earthquake Spectra*, v. 20, no. 2, p. 285-308.
- Atchley, F. W., & Dobbs, R. O., 1959, Engineering Geology of Moffett Field and Coyote Hills, Santa Clara and Alameda Counties, California: Prepared for John Blume & Associates. Atchley.
- Atwater, B.F., Hedel, C.W., and Helley, E.J., 1977, Late Quaternary depositional history, Holocene sea-level changes, and vertical crustal movement, southern San Francisco Bay, California: U.S. Geological Survey Professional Paper 1014, 15p.
- California Geological Survey (CGS), 2002, California Geomorphic Provinces Note 36.
- California Geological Survey (CGS), 2006, Seismic Hazard Zone Report for the Mountain View 7.5-Minute Quadrangle, Santa Clara, Alameda, and San Mateo Counties, California, 64 p.
- California Geological Survey (CGS), 2008, Seismic Hazard Zone Report for the Livermore 7.5-Minute Quadrangle, Alameda County, California, 66 p.
- Cetin, K. O., Youd, T. L., Seed, R. B., Bray, J. D., Stewart, J. P., Durgunoglu, H. T., & Yilmaz, M. T., 2004a, Liquefaction-induced lateral spreading at Izmit Bay during the Kocaeli (Izmit)-Turkey earthquake: *Journal of geotechnical and geoenvironmental engineering*, 130(12), 1300-1313.
- Cetin, K.O, Seed, R.B., Kiureghian, A.D., Tokimatsu, K., Harder, L.F. Jr., Kayen, R.E., and Moss, R.E.S., 2004b, Standard penetration test-based probabilistic and deterministic assessment of seismic soil liquefaction potential: *Journal of Geotechnical and Geoenvironmental Engineering*, v. 12, p. 1314-1340.

- CH2M Hill, 2011, Condition Assessment and Rehabilitation Plan, Hangar One, for NASA Headquarters and Ames Research Center, California, Volume 1 Condition Assessment.
- City of Livermore, 2013, The History of Livermore Municipal Airport: <http://www.cityoflivermore.net/civicax/filebank/documents/5727/> (Accessed March 2013).
- Contra Costa County Airport, 2013, The History of Contra Costa County Airports: <http://ca-contracostacounty.civicplus.com/static/depart/airport/TheHistoryofContraCostaCountyAirports.htm> (accessed March 2013).
- Cornerstone Earth Group, 2010, Livermore Municipal Airport, Geotechnical Investigation Report.
- Cubrinovski, M., Bradley, B., Wotherspoon, L., Green, R., Bray, J., Wood, C., Pender, M., Allen, J., Bradshaw, A., Rix, G., Taylor, M., Robinson, K., Henderson, D., Giorgini, S., Ma, K., Winkley, A., Zupan, J., O'Rourke, T., DePascale, G., Wells, D., 2011, Geotechnical Aspects of the 22 February 2011 Christchurch earthquake: Bulletin of the New Zealand Society of Earthquake Engineering, 44(4), pp. 205-226.
- EBA Engineering, 2008, Report of Subsurface Investigation, Apex Aviation, Buchanan Field Airport, 1450 Sally Ride Drive, Concord, California.
- Fugro West, 1999, Airfield Development Program, Preliminary Report No. 2A (Task B1), Preliminary (Phase 1) Geotechnical Site Characterization, Volume 1-Main Text, Figures & Maps.
- Fugro West, 1999, Airfield Development Program, Preliminary Report No. 2, Conditions Assessment.
- Fugro West, 1999, Airfield Development Program, Preliminary Report No. 2C (Task 3B), Reconnaissance Sand Search Investigation.
- Fugro West, 2000, Preliminary Report No. 3D (Task D–Partial Submittal), Preliminary (Phase 1) Geotechnical Analyses, Volume 1-Main text & Figures.
- Helley, E. J. and K. R. Lajoie, 1979, Flatland deposits of the San Francisco Bay region, California: their geology and engineering properties, and their importance to comprehensive planning, U. S. Geological Survey Professional Paper. 943, 88 pp.
- Hitchcock, C., Givler, R., De Pascale, G., & Dulberg, R., 2008, Detailed Mapping of Artificial Fills, San Francisco Bay Area, California, National Earthquake Hazards Reduction Program, U.S. Geological Survey Award Number 07HQGR0078
- Holzer, T.L., 1998, The Loma Prieta, California, Earthquake of October 17, 1989 - Liquefaction: U.S. Geological Survey Professional Paper 1551-B, 314 p.
- Holzer, T.L., 1999, Extensive research on Loma Prieta improves understanding of earthquakes: Transactions, American Geophysical Union, Eos, v. 80, no. 41, p. 482-483.



- Holzer, T. L., Noce, T. E., and Bennett, M. J., 2010, Maps and documentation of seismic CPT soundings in the central, eastern, and western United States: U.S. Geological Survey Open-File Report 2010-1136, 80 p. and 3 data tables.
- Hossein, H., Andrus, R.D., Gassman, S.L., Hasek, M., Camp, W.M., Talwani, P., 2008, Characterizing the Liquefaction Resistance of Aged Soils (Abs.), Geotechnical Earthquake Engineering and Soil Dynamics IV, ASCE.
- Idriss, I.M., and Boulanger, R.W., 2004, Semi-empirical procedures for evaluating liquefaction potential during earthquakes: Invited Paper to the 11th SDEE and 3rd ICEGE conferences, University of California, Berkeley.
- Ishihara, K. and Yoshimine, M., 1992, Evaluation of Settlements in Sand Deposits Following Liquefaction during Earthquakes, Soils and Foundations, Vol. 32, No. 1, pp. 173-188.
- Knudsen, K.L., and Lettis, W.R., 1997a, Preliminary maps showing Quaternary geology of twenty 7.5-minute quadrangles, eastern Stockton, California, 1:100,000 quadrangle: National Earthquake Hazards Reduction Program, U.S. Geological Survey, Final Technical Report , Award #1434-94-G-2499.
- Knudsen, K.L., Noller, J.S., Sowers, J.M., Lettis, W.R., Graham, S.E., Randolph, C.E., and May, T.E., 1997b, Quaternary geology and liquefaction susceptibility, San Francisco, California 1:100,000 quadrangle: a digital database: U.S. Geological Survey Open-File Report 97-715, scale 1:100,000..
- Knudsen, K.L., J.M. Sowers, R.C. Witter, C.M. Wentworth, and E.J. Helley, 2000, Preliminary Maps of Quaternary Deposits and Liquefaction Susceptibility, Nine-County San Francisco Bay Region, California: A Digital Database, U.S. Geological Survey Open-File Report 00-444. Digital Database by Wentworth, C.M., Nicholson, R.S., Wright, H.M., and Brown, K.H. Online Version 1.0.
- Lajoie, K. R., & Helley, E. J., 1975, Differentiation of sedimentary deposits for purposes of seismic zonation. Studies for seismic zonation of the San Francisco Bay region: US Geological Survey Professional Paper, A39-A51.
- Leon, E., Gassman, S.L., and Talwani, P., 2006, Accounting for Soil Aging When Assessing Liquefaction Potential, *Journal of Geotechnical and Geoenvironmental Engineering*, 363-377.
- Martin, G. R., & Lew, M., 1999. Recommended Procedures for Implementation of DMG Special Publication 117, Guidelines for Analyzing and Mitigating Liquefaction Hazards in California. Southern California Earthquake Center (SCEC), University of Southern California
- National Aeronautics and Space Administration (NASA), 2013, Moffett Field History: <http://history.arc.nasa.gov/moffett.htm> (Accessed March 2013).
- Parikh Consultants, Inc. 2011, Geotechnical Engineering Investigation Report, Buchanan Field Airport, Runway Rehabilitation Project

Peter Kaldveer and Associates, Inc., 1980, Foundation Investigation, Proposed Locker And Exercise Facility, Moffett Field, California.

Petersen, Mark D., Frankel, Arthur D., Harmsen, Stephen C., Mueller, Charles S., Haller, Kathleen M., Wheeler, Russell L., Wesson, Robert L., Zeng, Yuehua, Boyd, Oliver S., Perkins, David M., Luco, Nicolas, Field, Edward H., Wills, Chris J., and Rukstales, Kenneth S., 2008, Documentation for the 2008 Update of the United States National Seismic Hazard Maps: U.S. Geological Survey Open-File Report 2008–1128, 61 p.

Port of Oakland, 2013, A History of Aviation Excellence and Importance to the Community, [http://www.oaklandairport.com/media\\_backgrounder.shtml](http://www.oaklandairport.com/media_backgrounder.shtml), accessed March 15, 2013.

Robertson, P.K., and Wride, C.E., 1997, Cyclic liquefaction and its evaluation based on SPT and CPT: Seismic Short Course on Evaluation and Mitigation of Earthquake Induced Liquefaction Hazards, NCEER Workshop, San Francisco, CA, March, 1997.

Rogers, A. M., and S. H. Figures, 1991, Engineering geologic site characterization of the greater Oakland-Alameda area, Alameda and San Francisco Counties, California: Final Report to the National Science Foundation, Grant no. BCS –9003785.

San Francisco Bay Conservation and Development Commission (SFBCDC), 1969, San Francisco Bay Plan, approved by the California State Legislature in 1969.

San Francisco Estuary Institute (SFEI). 1998. San Francisco Bay Area EcoAtlas Geographic Information System, version 1.50b4.

Seed, H.B., and Idriss, I.M., 1982, Ground motions and soil liquefaction during earthquakes: Earthquake Engineering Research Institute, Engineering Monograph volume 5, 134 p.

Seed, H.B., Idriss, I.M., and Arango, I., 1983, Evaluation of liquefaction potential using field performance data: American Society of Civil Engineers, Journal of Geotechnical Engineering, v. 109, no. 3, p. 458-482.

Seed, H. B., Tokimatsu, K., Harder, L. F., and Chung, R. M., 1985, Influence of SPT procedures in soil liquefaction resistance evaluations: Journal of Geotechnical Engineering, ASCE, v. 111, no. 12, p. 1425-1445.

Sowers, J.M., Noller, J.S., and Lettis, W.R., 1998, Quaternary geology and liquefaction susceptibility, Napa, California 1:100,000 quadrangle: a digital database: U.S. Geological Survey Open-File Report 98-460.

Tinsley, J.C., Youd, T.L., Perkins, D.M., and Chen, A.T.F, 1985, Evaluating Liquefaction Potential, in Ziony, J.I., ed., Evaluating earthquake hazards in the Los Angeles Region - an earth-science perspective: U.S. Geological Survey Professional Paper 1360, p. 263-316.

Tinsley, J.C., and Holzer, T.L., 1990, Liquefaction in the Monterey Bay region: U.S. Geological Survey Open-File Report 90-334, p. 642-643.

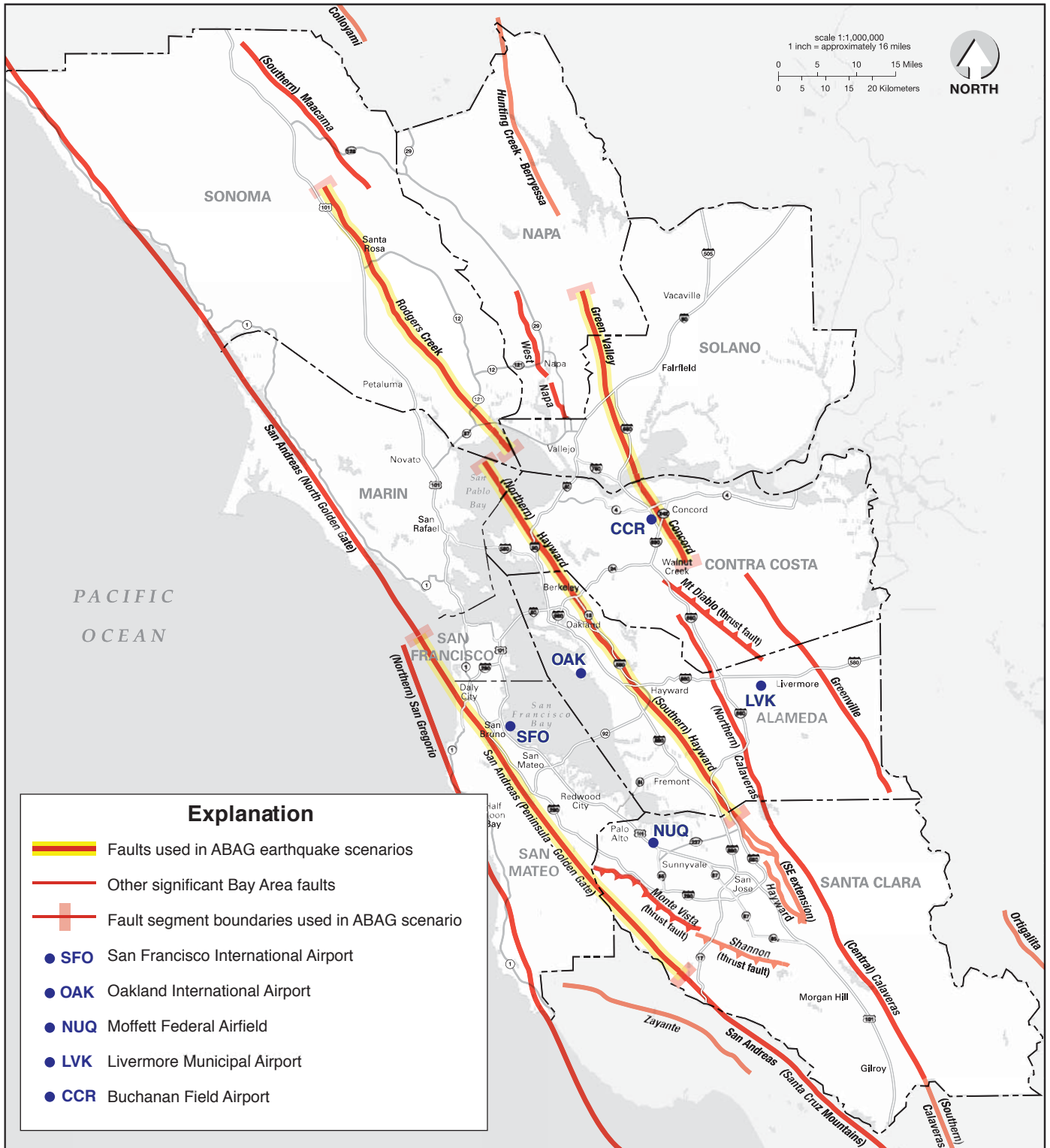
- URS Corporation, 2006, San Francisco International Airport, Airfield Seismic Stabilization and Realignment, Phase A Engineering Report, Volumes 1 and 2.
- URS Corporation, 2011, Geotechnical Data and Coastal Conditions Report for Perimeter Dike, Oakland International Airport, Oakland, California.
- U. S. Department of Agriculture (USDA), 1939, Black and white aerial photography, 1:20,000 scale, frame BUT-289.
- U.S. Geological Survey (USGS), 2013a, 2008 Interactive Deaggregations (Beta): <https://geohazards.usgs.gov/deaggint/2008/> (Accessed March 2013).
- U.S. Geological Survey (USGS), 2013b, Predefined Vs30 Mapping: <http://earthquake.usgs.gov/hazards/apps/vs30/predefined.php> (Accessed March 2013).
- U.S. Geological Survey (USGS), 2013c, Scenario Shake Maps: <http://earthquake.usgs.gov/eqcenter/shakemap>, (Released Scenarios "HaywardRC\_se", "ConcordGV\_se", "1906\_se") publication in progress.
- Wald, D. J., B. C. Worden, K. Lin, and K. Pankow (2005). "ShakeMap manual: technical manual, user's guide, and software guide." U. S. Geological Survey, Techniques and Methods 12-A1, 132 pp.
- William Lettis & Associates, Inc. (WLA), 1999, Evaluation of earthquake-induced liquefaction hazards at San Francisco Bay Area commercial airports, report prepared for the Association of Bay Area Governments, 37 p.
- Witter, R.C., Knudsen, K.L, Sowers, J.M., Wentworth, C.M., Koehler, R.D., Randolph, C.E., Brooks, S.K., and Gans, K.D., 2006, Maps of Quaternary deposits and liquefaction susceptibility in the central San Francisco Bay region, California: U.S. Geological Survey Open-File Report 2006-1037, scale 1:100,000.
- Youd, T.L., 1973, Liquefaction, flow, and associated ground failure: U.S. Geological Survey Circular 688, 12 p.
- Youd, T.L., Nichols, D.R., Helley, E.J., and Lajoie, K.R., 1975, Liquefaction potential, in Studies for seismic zonation of the San Francisco Bay region: U.S. Geological Survey Prof Paper 941-A, p. 68-74. Youd, T.L., and Idriss, I.M., 1997, editors, Proceedings of the NCEER workshop on evaluation of liquefaction resistance of soils: Nation Center for Earthquake Engineering Research Technical Report NCEER-97-0022, 276 p.
- Youd, T.L., and Hoose, S.N., 1978, Historic ground failures in Northern California triggered by earthquakes: United States Geological Survey Professional Paper 993.
- Youd, T.L., and Perkins, J.B., 1987, Map showing liquefaction susceptibility of San Mateo County, California: United States Geological Survey Miscellaneous Investigations Map I-1257-G.



Youd, T. L.; Idriss, I. M., 2001, "Liquefaction Resistance of Soils: Summary Report from the 1996 NCEER and 1998 NCEER/NSF Workshops on Evaluation of Liquefaction Resistance of Soils," Journal of Geotechnical and Geoenvironmental Engineering, Vol. 127(10), 817-833.



## Figures



Map from Association of Bay Area Governments, 2003.

79.221200 F01 Airport and Fault Location Map.ai Monday, March 11 2013 13:38:20



A) Northwest end of main runway (bottom) and adjacent taxiway (top) at Oakland International Airport. Photo source: Holzer (1998).

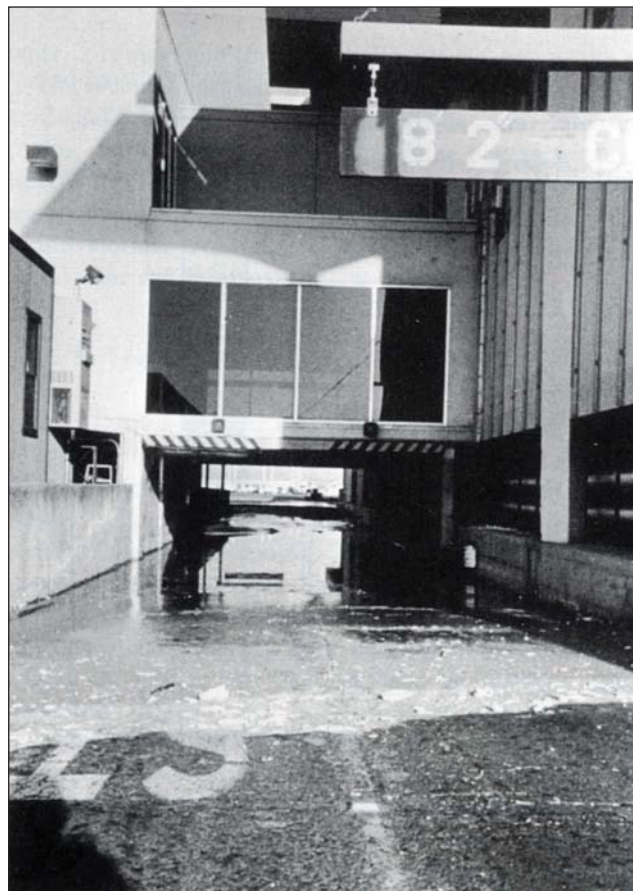


B) Large sand boil near north end of main runway at Oakland International Airport. Photo source: Holzer (1998).

**Photographs of Liquefaction Features at Oakland International Airport  
Following the October 17, 1989 Loma Prieta Earthquake**



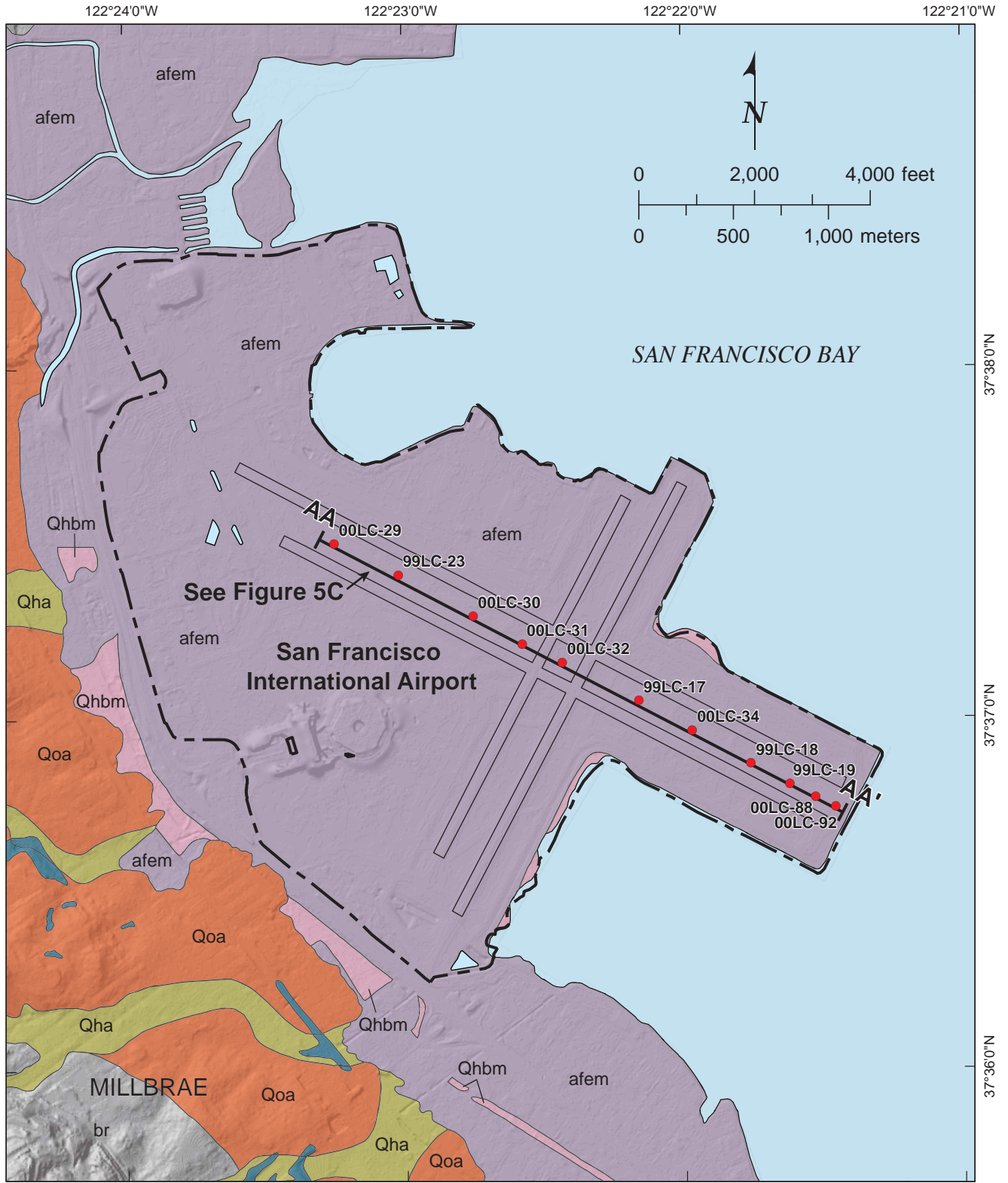
A) Fissures, sand boils, and grabens associated with lateral spreading near northwest end of main runway at Oakland International Airport. Photo source: Holzer (1998).



B) Below-grade tramway, filled with as much as 1.8 m of extruded sand, at Oakland International Airport Terminal Building. Photo source: Holzer (1998).

**Photographs of Liquefaction Features at Oakland International Airport  
Following the October 17, 1989 Loma Prieta Earthquake**

FIGURE 2B



Source: Witter et al., 2006; USGS OFR 06-1037.

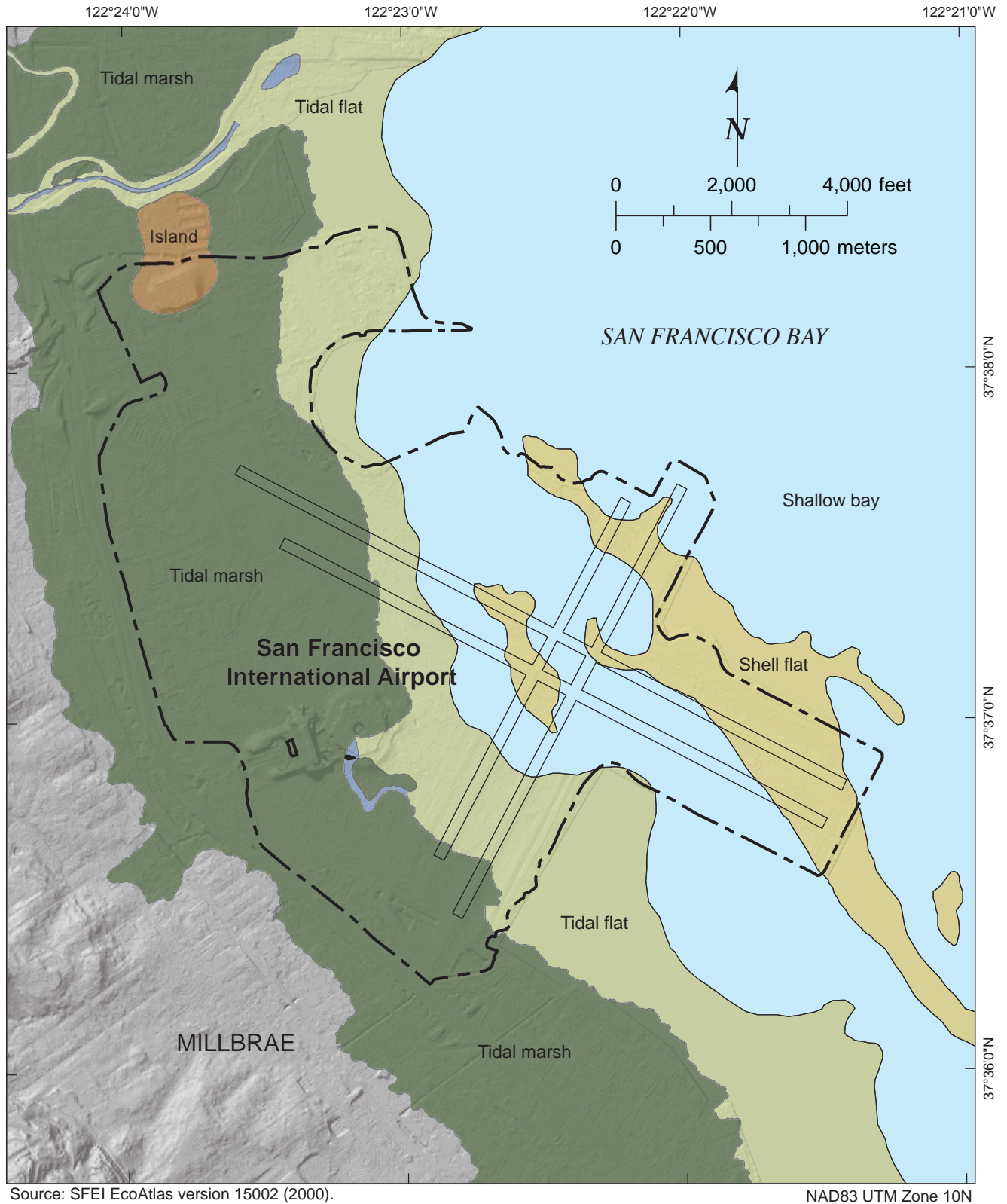
NAD83 UTM Zone 10N

**Explanation**

- |  |   |  |
|--|---|--|
| <span style="background-color: #4682b4; border: 1px solid black; padding: 2px;">af</span> Artificial fill                      | <span style="background-color: #f08080; border: 1px solid black; padding: 2px;">Qhbm</span> San Francisco Bay mud     | <span style="background-color: #ffa07a; border: 1px solid black; padding: 2px;">Qoa</span> Early to late Pleistocene alluvial deposits |
| <span style="background-color: #d8bfd8; border: 1px solid black; padding: 2px;">afem</span> Artificial fill over estuarine mud | <span style="background-color: #90ee90; border: 1px solid black; padding: 2px;">Qha</span> Holocene alluvial deposits | <span style="background-color: #a9a9a9; border: 1px solid black; padding: 2px;">br</span> Bedrock                                      |
| <span style="color: red;">●</span> USC-02 Borehole location  | <span style="background-color: #add8e6; border: 1px solid black; padding: 2px;"></span> Water                         |  |

**Quaternary Geologic Map, San Francisco International Airport**

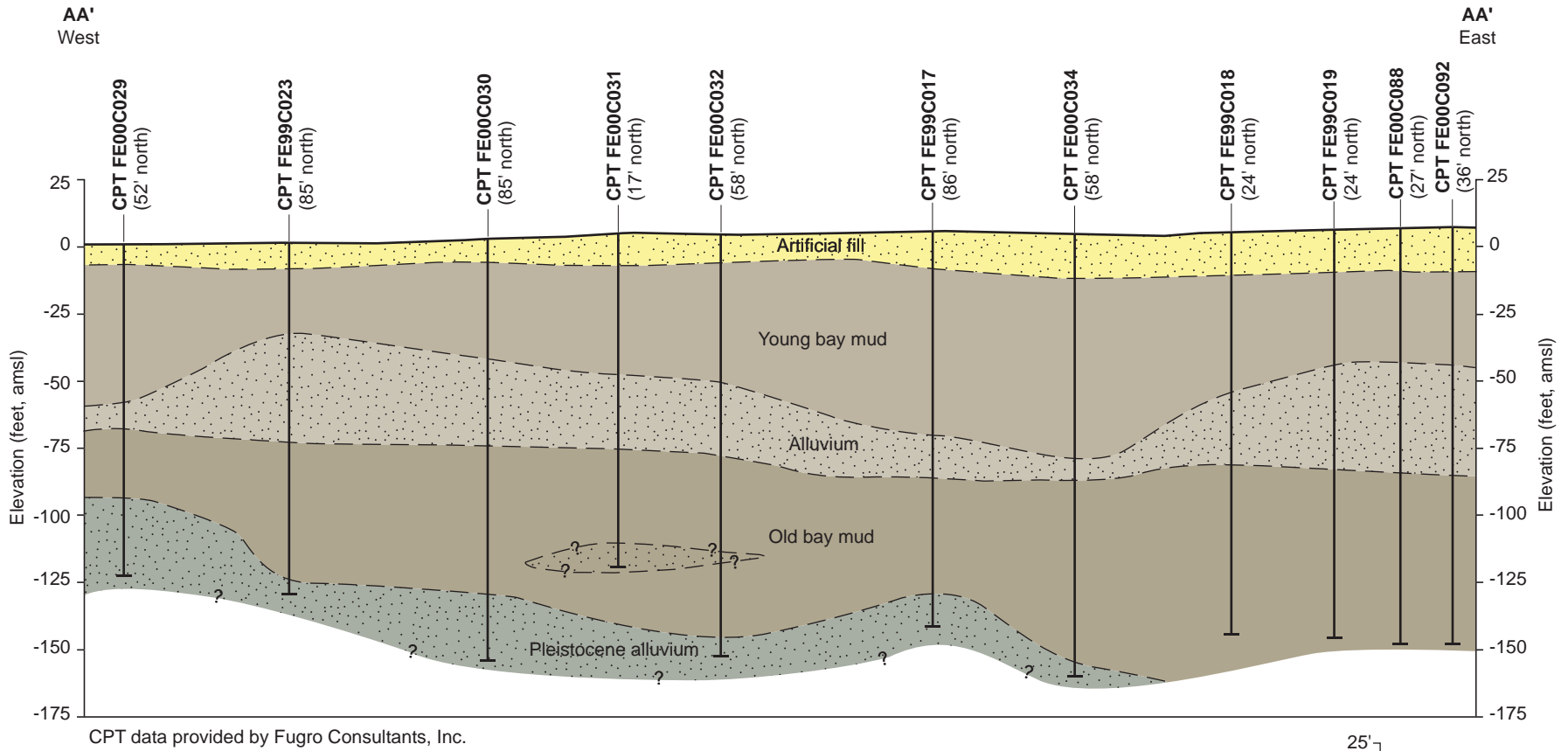
**FIGURE 3A**



**Explanation**

- Island
- Tidal flat
- Shallow bay/channel
- Tidal marsh
- Shell flat

**Historical Bay Environments Map, San Francisco International Airport** FIGURE 3B



**Explanation**

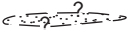
- |   |   |                              |
|---|---|------------------------------|
|  Artificial fill: loose to medium dense poorly graded sand with silt, clay, and gravel |  Old bay mud: sandy clay to clayey sand                                | Vertical exaggeration = 120X |
|  Young bay mud: unconsolidated clay to silty clay                                      |  Pleistocene alluvium: moderate dense clay, silt, and sand with gravel |                              |
|  Holocene alluvium: interbedded sand, silt, and clay                                   |  Coarse-grained lens, composed mainly of sand and gravel               |                              |

FIGURE 3C

**Geologic Cross Section AA-AA', San Francisco International Airport, San Francisco, California**

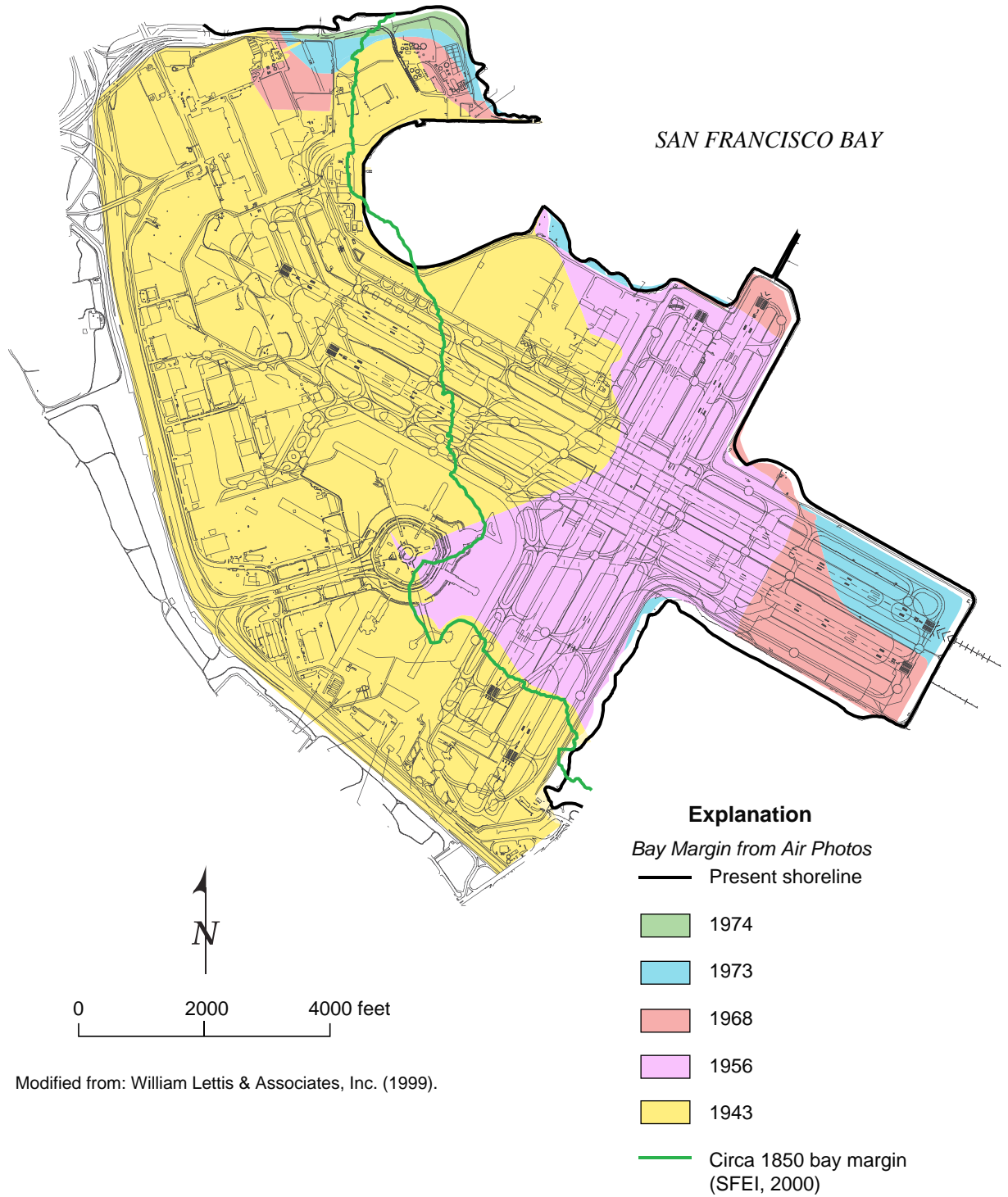




A) View looking north-northwest at airport site prior to construction (1927).

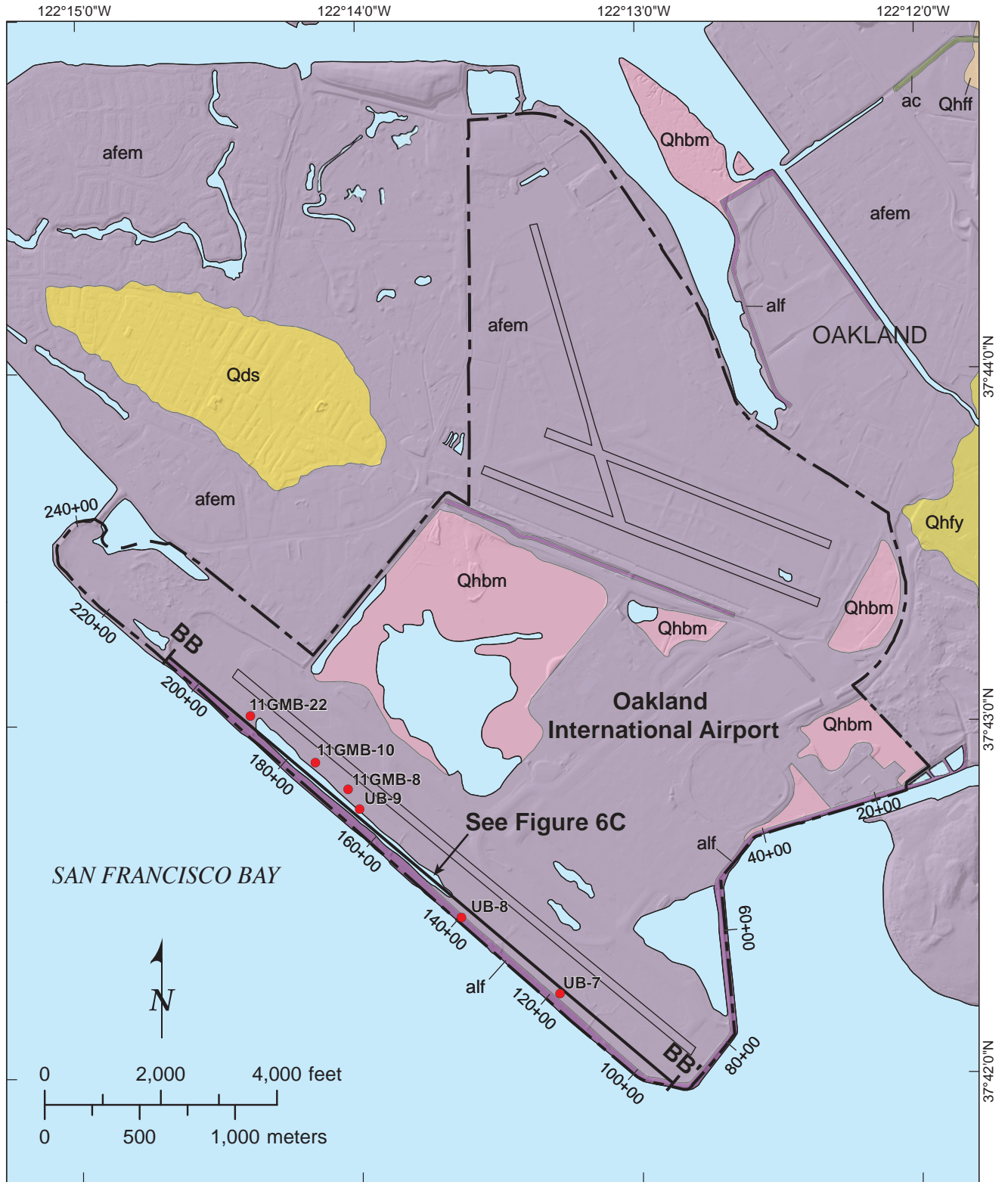


B) View looking north-northwest at airport site during construction (1938).



**Approximate Extent of Developed Land in 1943, 1956, 1968, 1973, 1974 and Circa 1850 Bay Margin, San Francisco International Airport**

**FIGURE 3E**



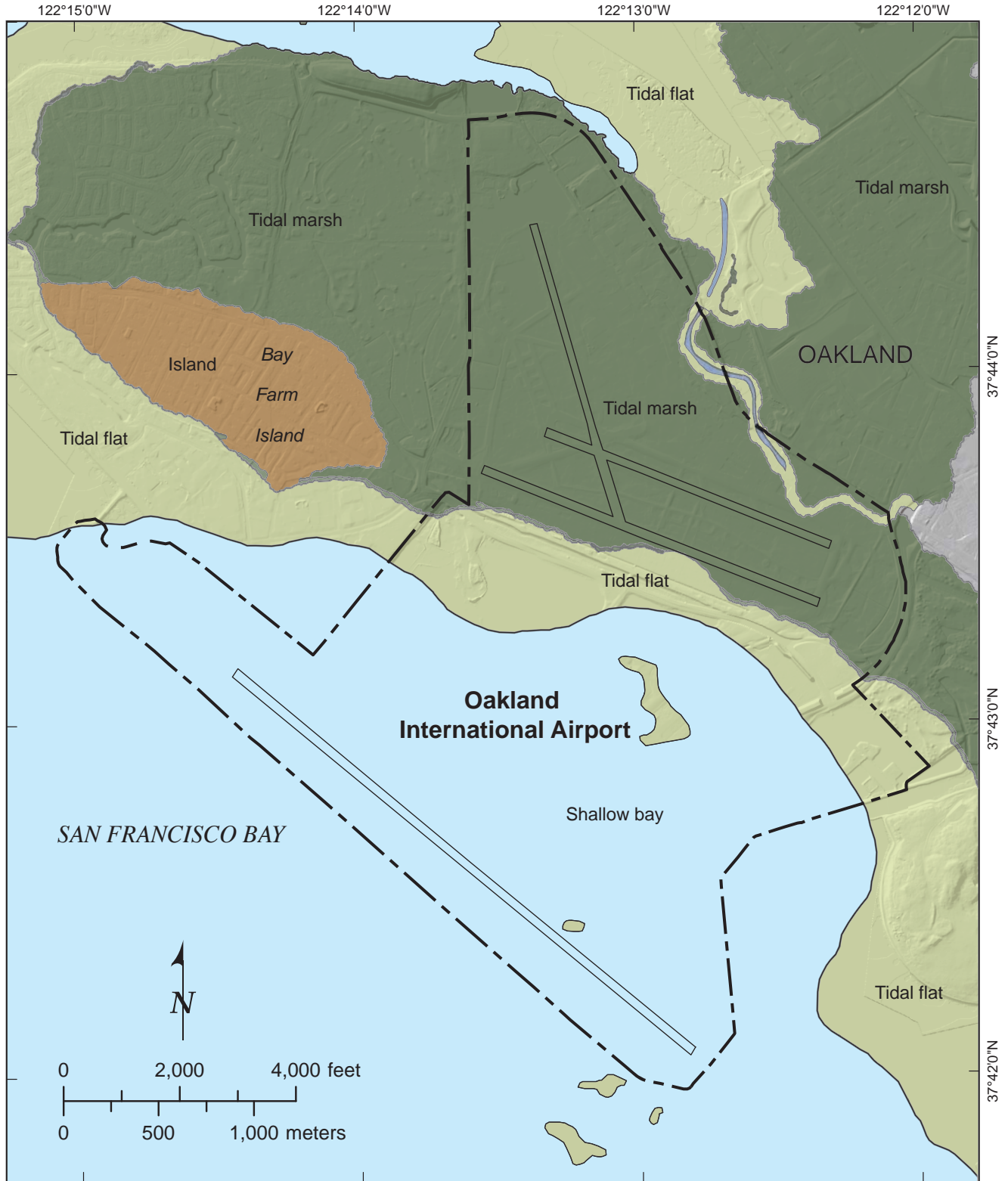
Source: Witter et al., 2006; USGS OFR 06-1037.  
Levee stations from URS (2011).

**Explanation**

afem	Artificial fill over estuarine mud	Qhfy	Latest Holocene alluvial fan deposits	Qds	Merritt Sand
alf	Artificial levee fill	Qhbm	San Francisco Bay mud		Water
ac	Artificial stream channel	Qhff	Holocene alluvial fan deposits, fine facies		Borehole location
					Station location and number

**Quaternary Geologic Map, Oakland International Airport**

**FIGURE 4A**



Source: SFEI EcoAtlas version 15002 (2000).

NAD83 UTM Zone 10N

**Explanation**

- Island
- Tidal flat
- Shallow bay/channel
- Tidal marsh

**Historical Bay Environments Map, Oakland International Airport**

**FIGURE 4B**

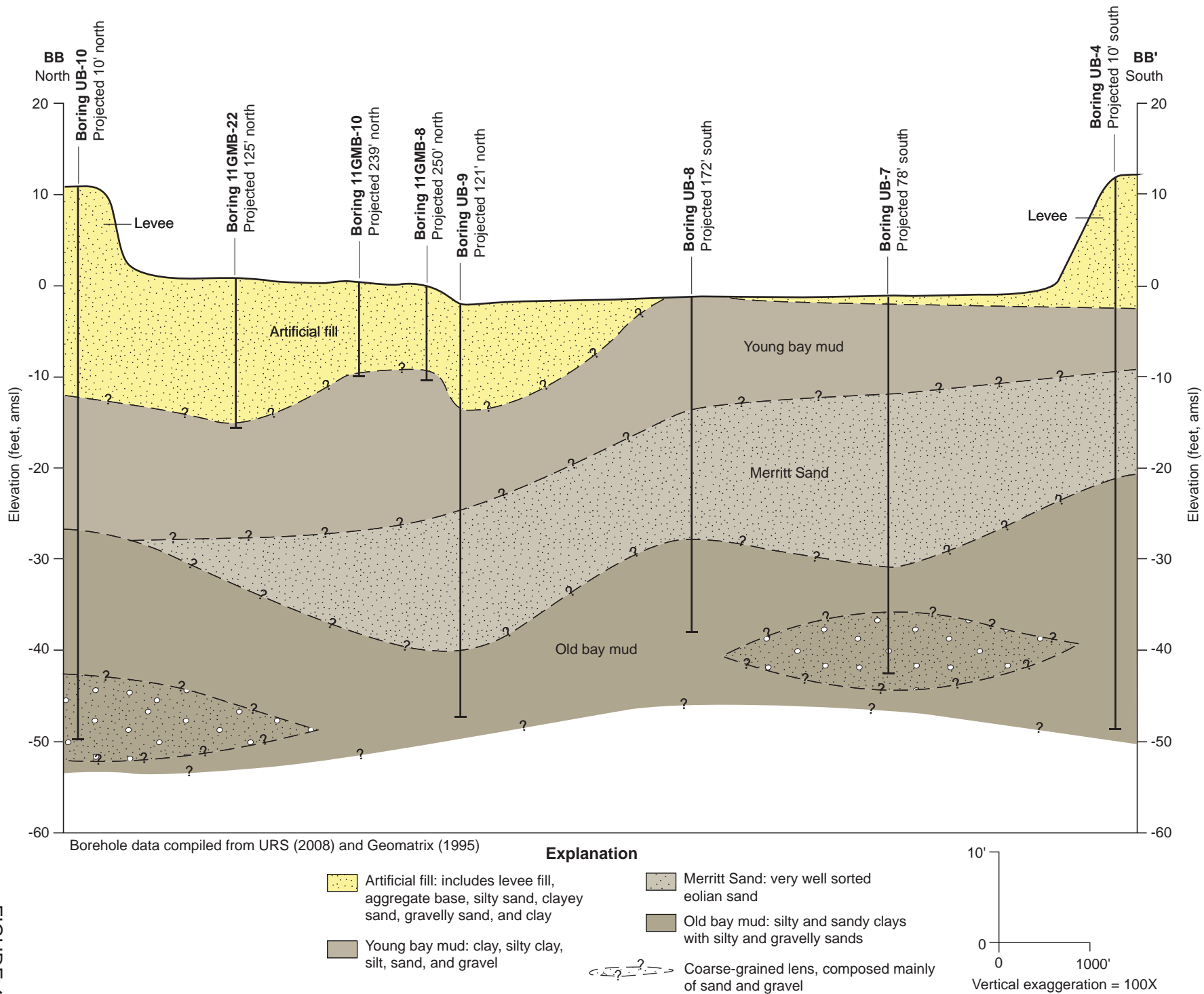
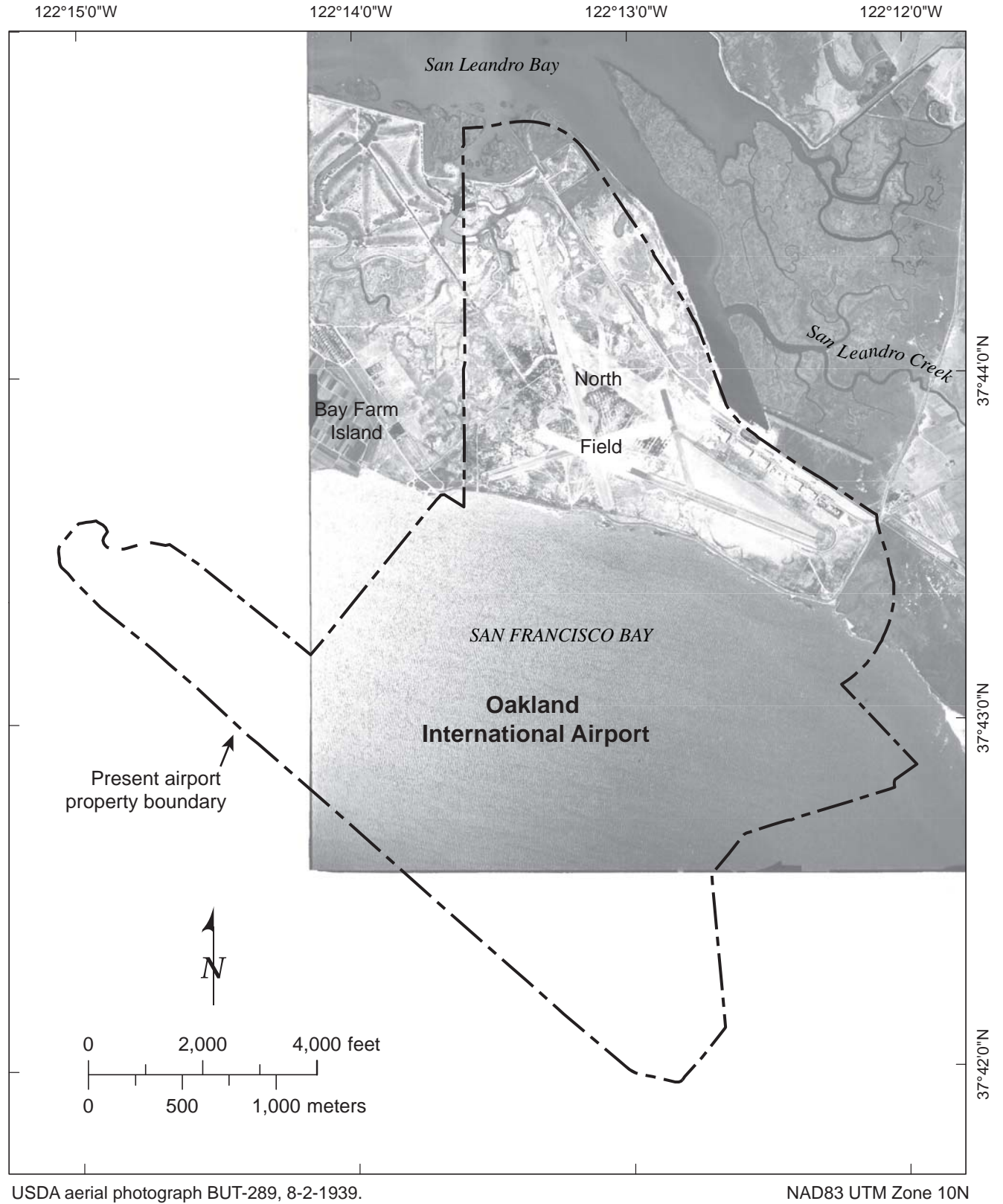


FIGURE 4C

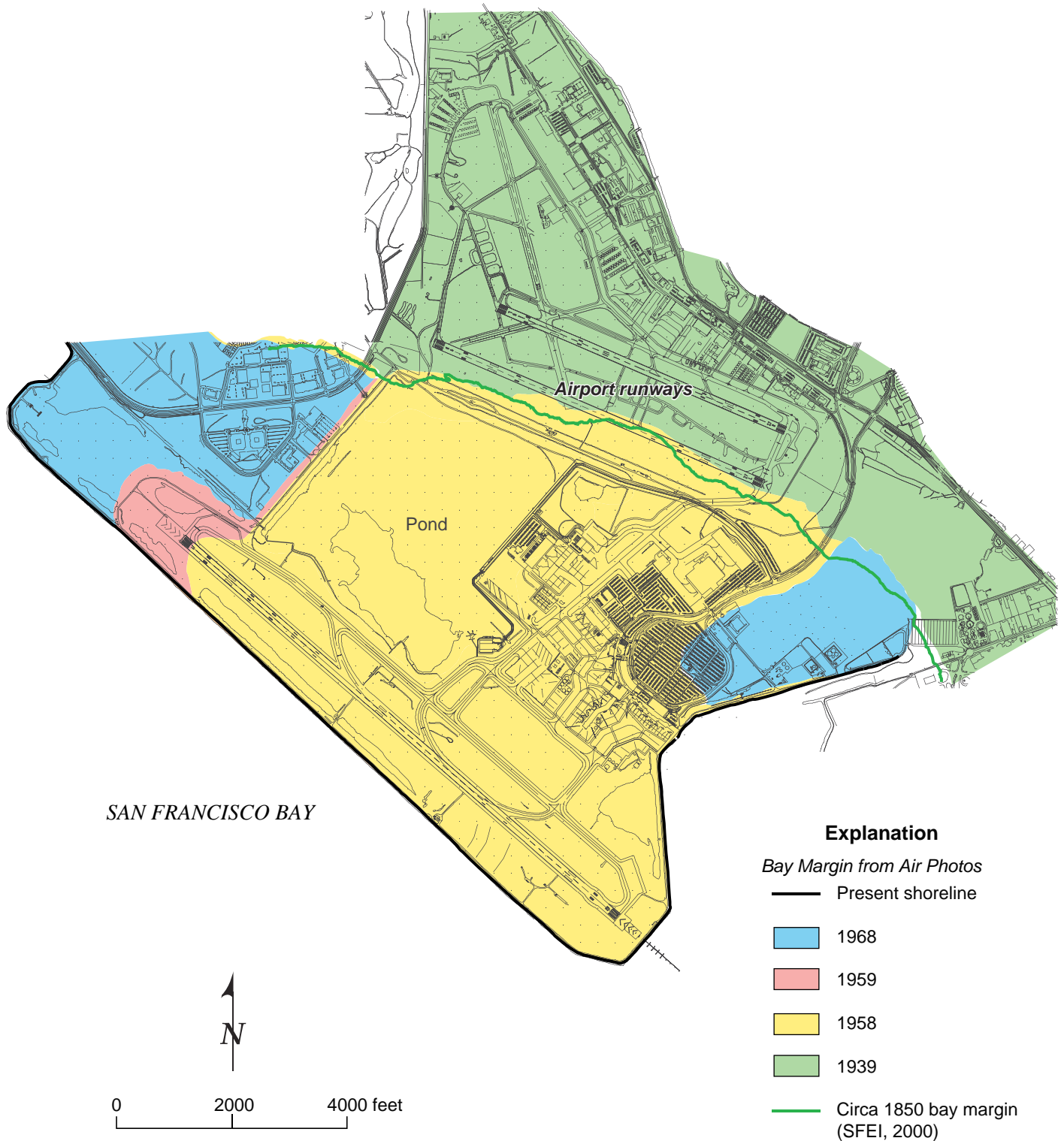
**Geologic Cross Section BB-BB', Oakland International Airport, Oakland, California**





Historical Aerial View of Oakland International Airport, 1939

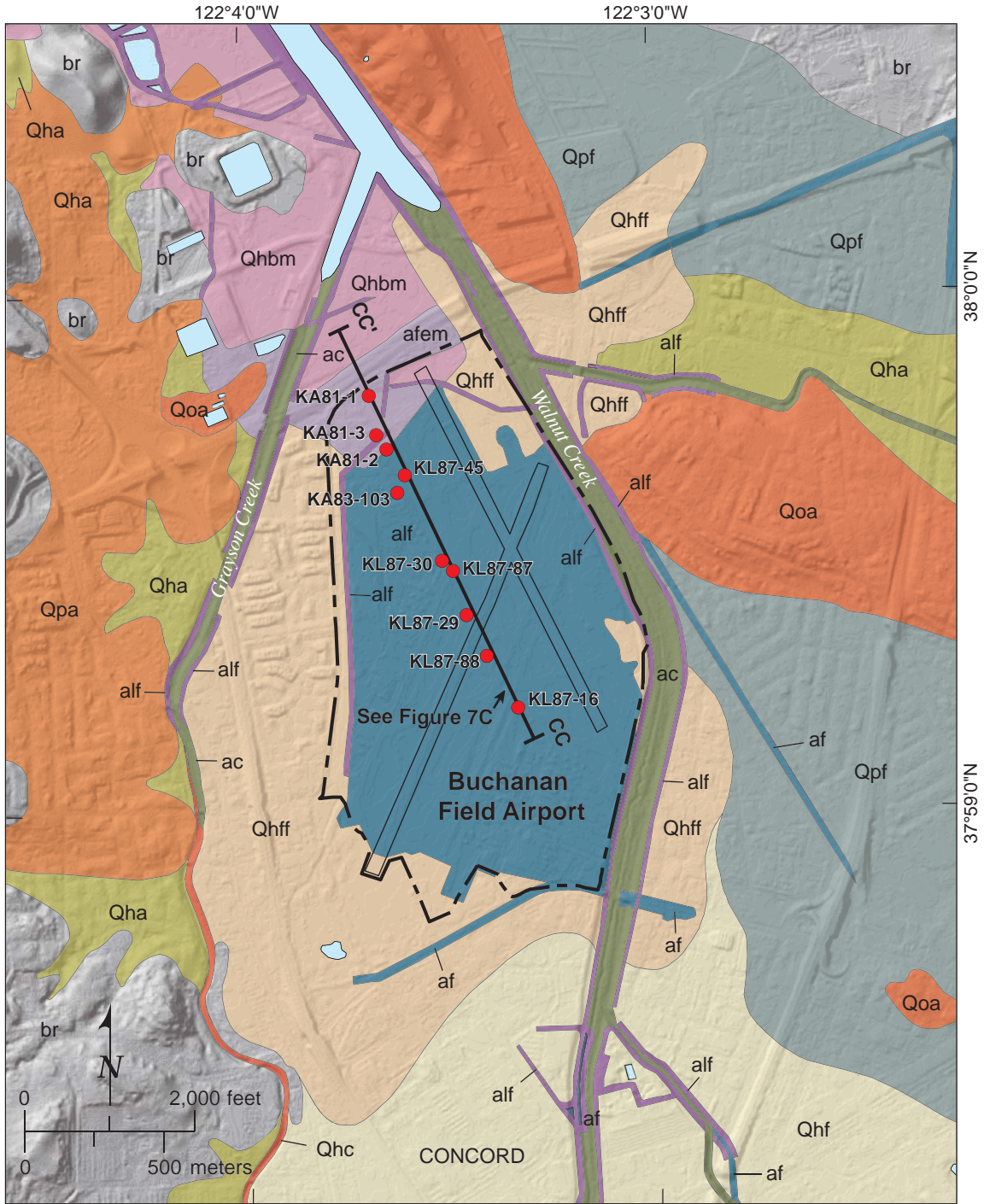
FIGURE 4D



Modified from: William Lettis & Associates, Inc. (1999).

**Approximate Extent of Developed Land in 1939, 1958, 1959, 1968, 1999, and Circa 1850 Bay Margin, Oakland International Airport**

**FIGURE 4E**



Source: Witter et al., 2006; USGS OFR 06-1037.

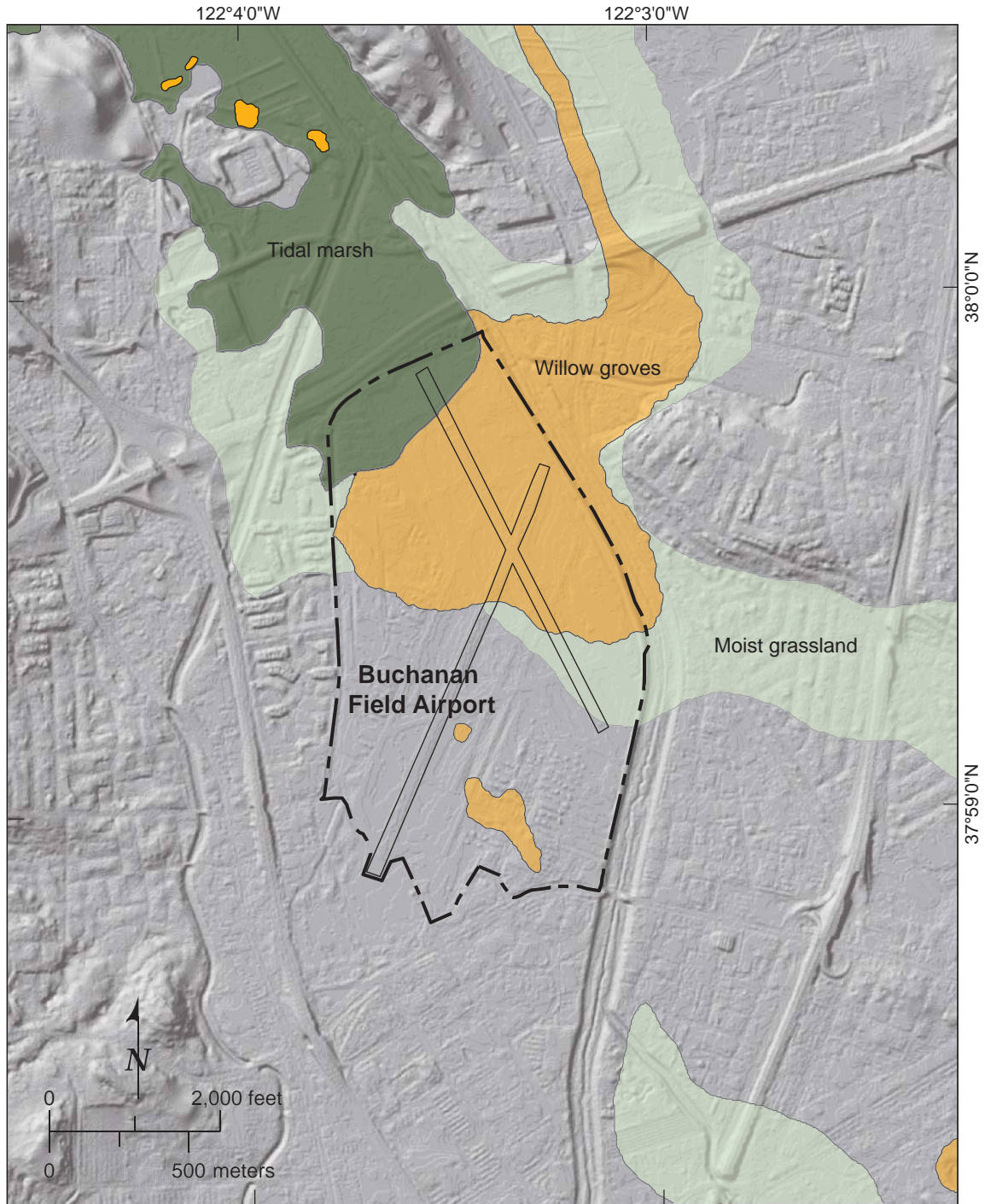
NAD83 UTM Zone 10N

**Explanation**

<span style="background-color: #4682b4; border: 1px solid black; padding: 2px;">af</span> Artificial fill	<span style="background-color: #c08080; border: 1px solid black; padding: 2px;">Qhbm</span> San Francisco Bay mud	<span style="background-color: #ffa07a; border: 1px solid black; padding: 2px;">Qpa</span> Latest Pleistocene alluvial deposits, undifferentiated
<span style="background-color: #9370db; border: 1px solid black; padding: 2px;">afem</span> Artificial fill over estuarine mud	<span style="background-color: #d2b48c; border: 1px solid black; padding: 2px;">Qhf</span> Holocene alluvial fan deposits	<span style="background-color: #ff8c00; border: 1px solid black; padding: 2px;">Qoa</span> Early to late Pleistocene alluvial deposits, undifferentiated
<span style="background-color: #9932cc; border: 1px solid black; padding: 2px;">alf</span> Artificial levee fill	<span style="background-color: #f5deb3; border: 1px solid black; padding: 2px;">Qhff</span> Holocene alluvial fan deposits, fine facies	<span style="background-color: #a9a9a9; border: 1px solid black; padding: 2px;">br</span> Bedrock
<span style="background-color: #6aa84f; border: 1px solid black; padding: 2px;">ac</span> Artificial stream channel	<span style="background-color: #90ee90; border: 1px solid black; padding: 2px;">Qha</span> Holocene alluvial deposits, undifferentiated	<span style="background-color: #add8e6; border: 1px solid black; padding: 2px;"></span> Water
<span style="background-color: #ff4500; border: 1px solid black; padding: 2px;">Qhc</span> Historical stream channel deposits	<span style="background-color: #4682b4; border: 1px solid black; padding: 2px;">Qpf</span> Latest Pleistocene alluvial fan deposits	<span style="color: red;">●</span> KL87-16 Borehole

**Quaternary Geologic Map, Buchanan Field Airport**

**FIGURE 5A**

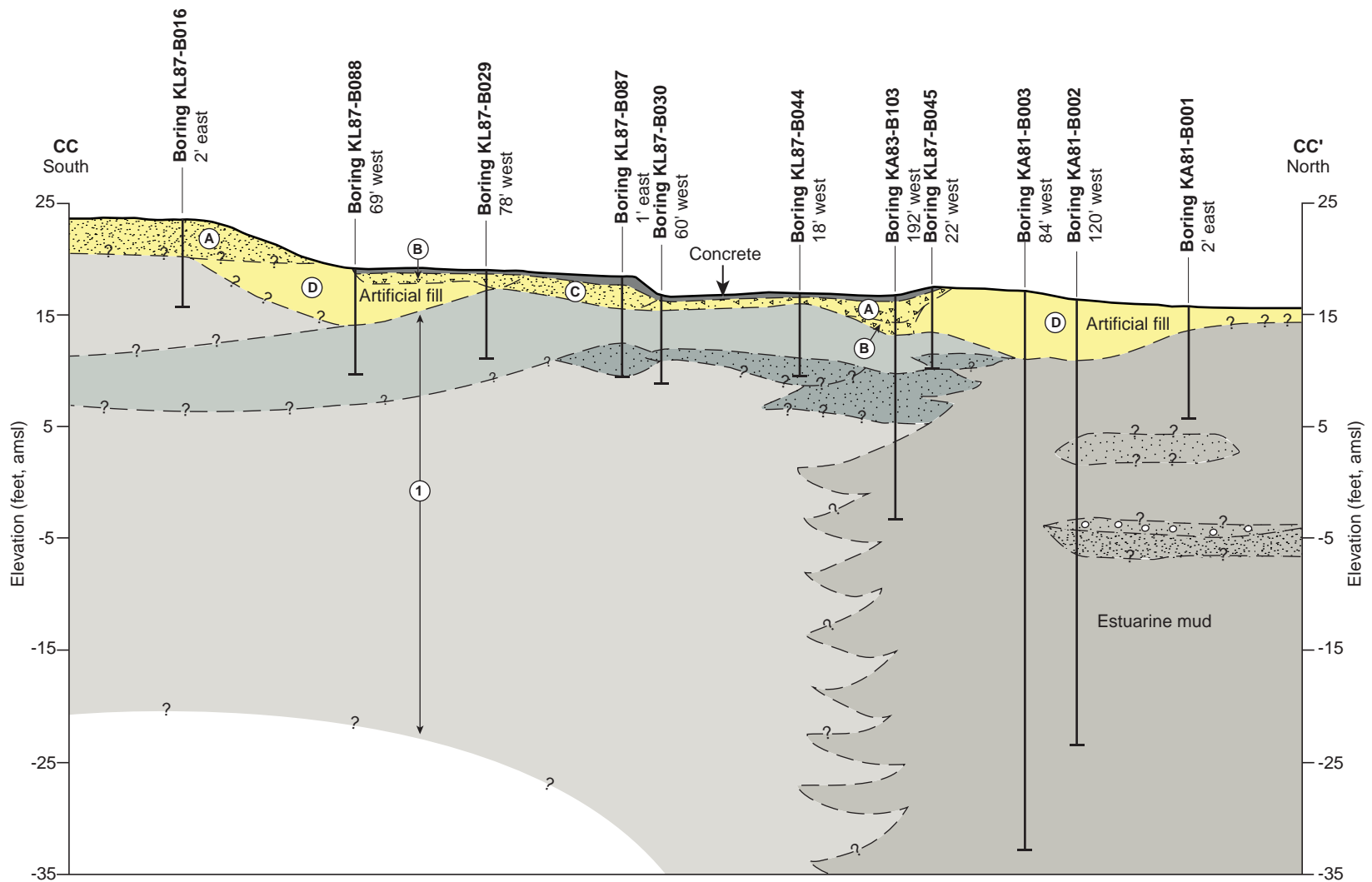


Source: SFEI EcoAtlas version 15002 (2000).

NAD83 UTM Zone 10N

**Explanation**

-  Tidal marsh
-  Willow groves
-  Moist grassland



Borehole data compiled from Peter Kaldveer and Associates (1981 and 1983) and J.H. Kleinfelder and Associates (1987).

**Explanation**

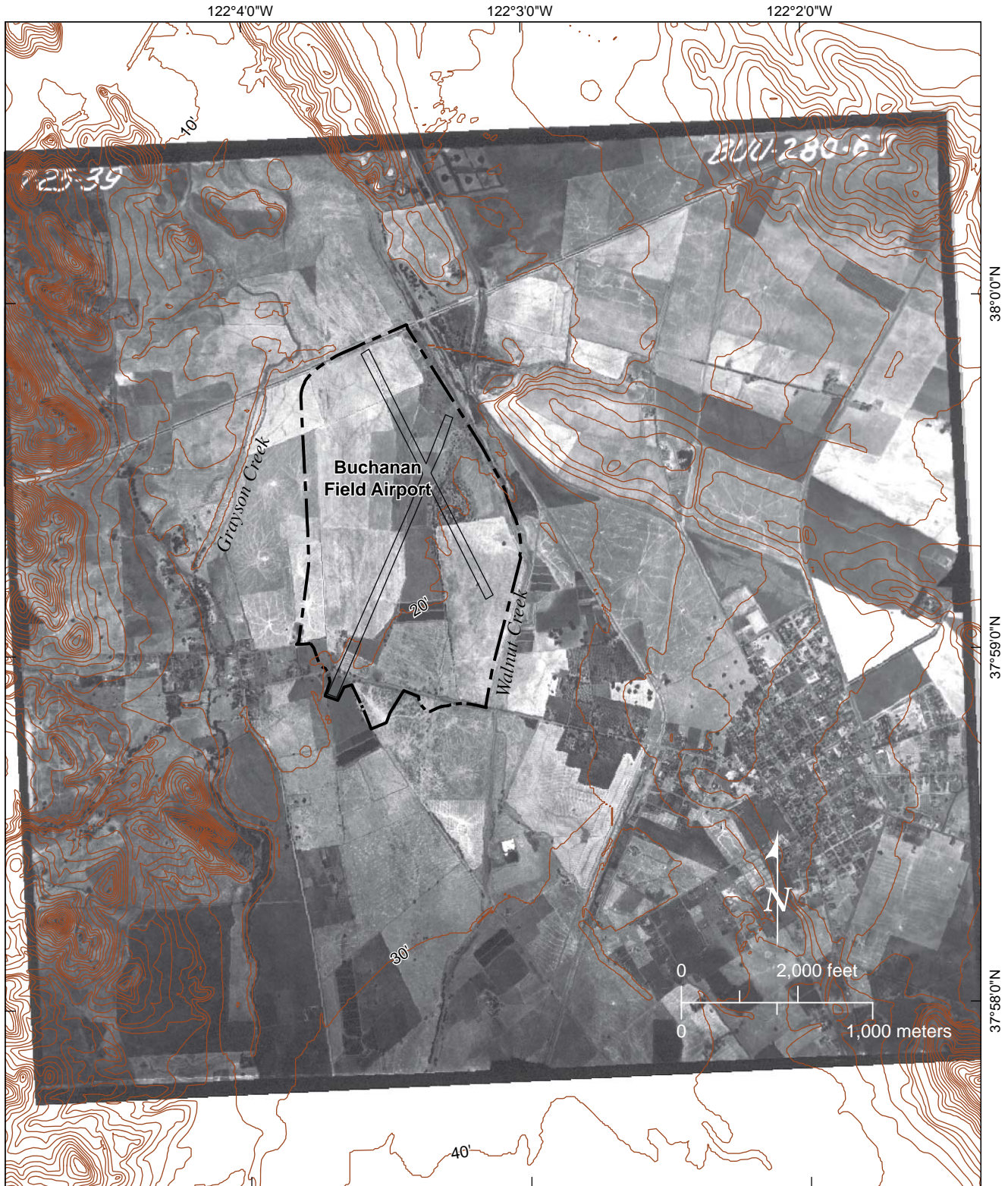
- Concrete
- Artificial fill: aggregate base, consisting of sandy gravel with minor amounts of clay
- Artificial fill: well graded sand with varying amounts of gravel
- Artificial fill: clayey fine sand with trace amounts of gravel
- Artificial fill: clay with silt and fine to medium sand
- Estuarine mud: silt and clay with interbedded fine to coarse-grained sand
- Holocene alluvial fan deposits: interbedded sand, silt, and clay
- Coarse-grained lens, composed mainly of sand and gravel

10'  
0 400'  
Vertical exaggeration = 40X

FIGURE 5C

**Geologic Cross Section CC-CC', Buchanan Field Airport, Concord, California**



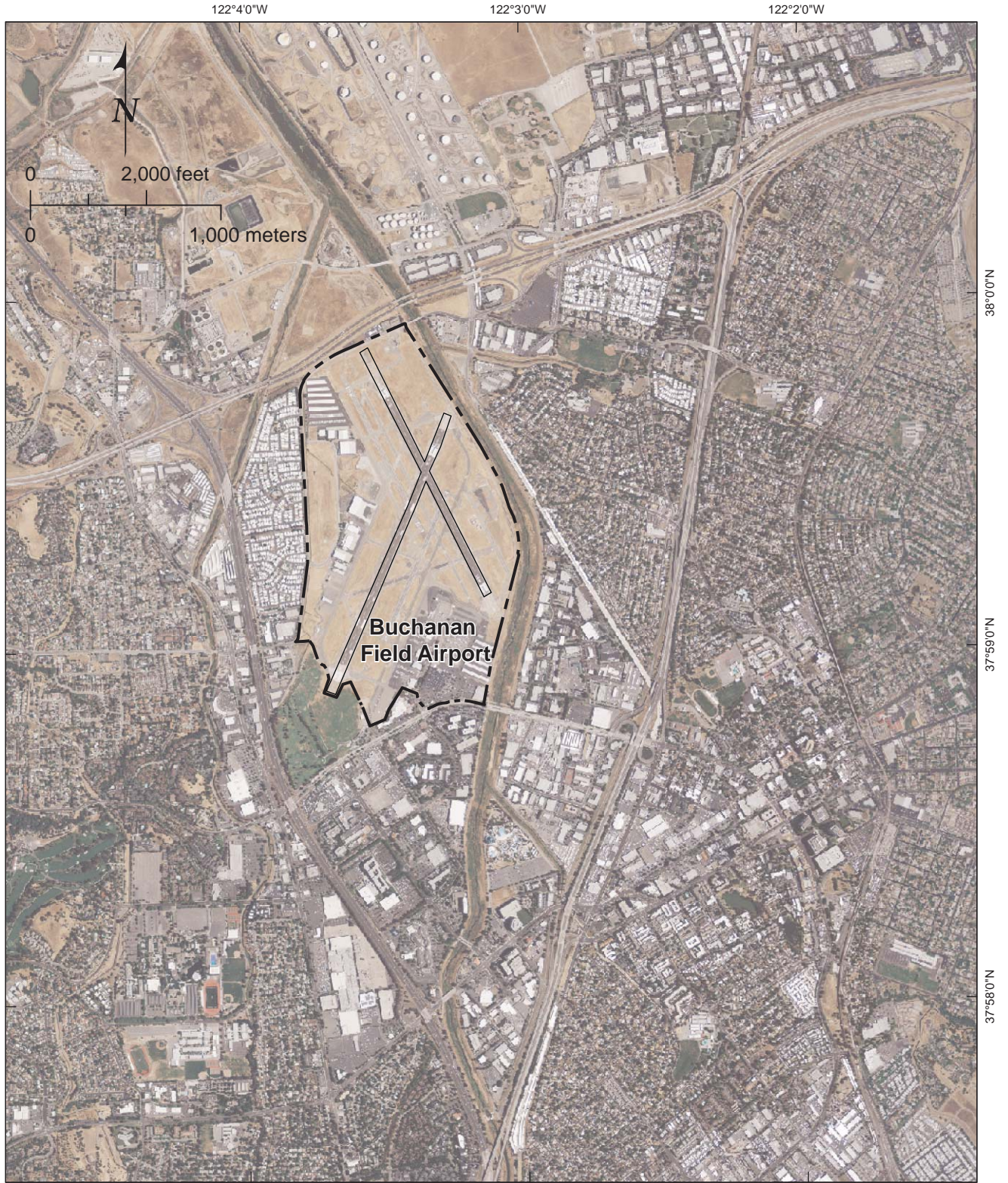


Photograph BUU-280-67, 1939.

Topographic contours from USGS

**Explanation**

— Contour line (10-foot interval)

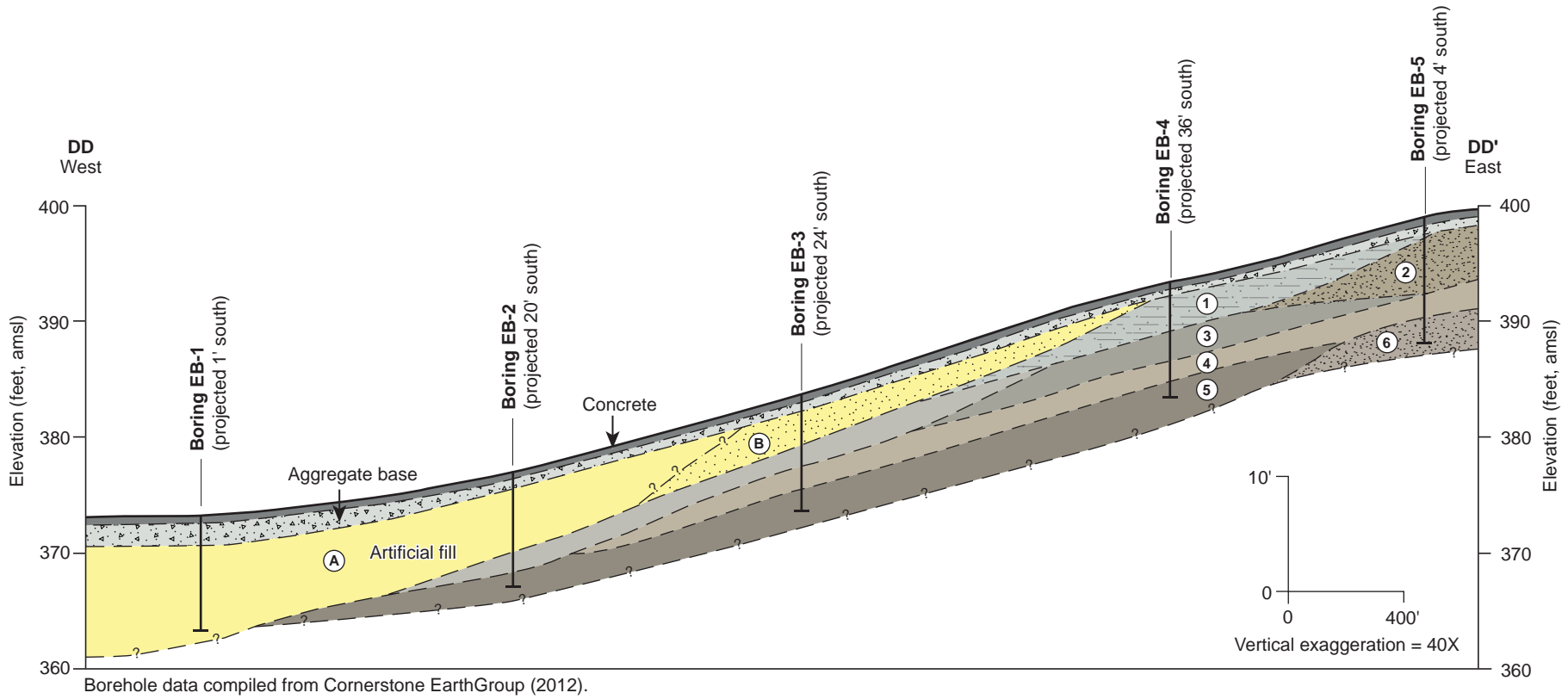


79.221200 F5E Buchanan\_Aerial\_Figure\_2009.ai Friday, March 22 2013 13:33:42

Buchanan - Aerial Photo from NAIP 2009

FIGURE 5E





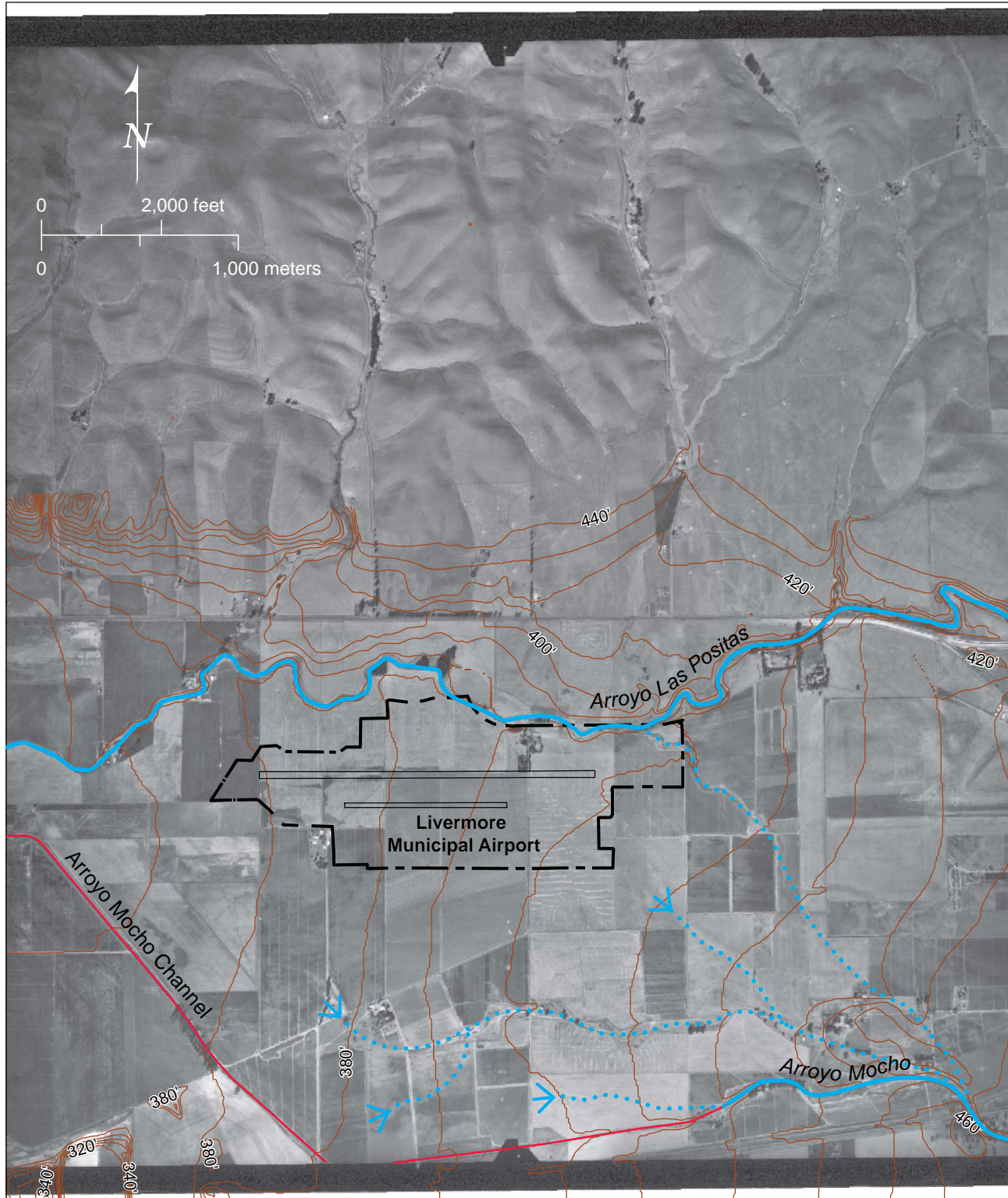
**Explanation**

- |  |  |
|--|--|
| <ul style="list-style-type: none"> <li> Concrete</li> <li> Aggregate base (artificial fill)</li> <li> Artificial fill: very stiff to hard lean clay with sand</li> <li> Artificial fill: medium dense clayey sand with gravel</li> <li> Coarse-grained lens, composed mainly of sand and gravel</li> </ul> | <p><b>Holocene alluvial fan deposits:</b> interbedded silt, clay, and sand with varying amounts of gravel</p> <ul style="list-style-type: none"> <li>① Silty clayey sand</li> <li>② Sandy silt</li> <li>③ Silty clay</li> <li>④ Lean clay with sand</li> <li>⑤ Sandy silty clay</li> <li>⑥ Clayey sand gravel</li> </ul> |
|--|--|

FIGURE 6B

**Geologic Cross Section DD-DD', Livermore Municipal Airport, Livermore, California**





Photograph GS-JL-2-31, 1949.

Topographic contours from USGS

**Explanation**

- Contour line (10-foot interval)
- Stream channel
- Artificial channel
- Former channel with distributary point

**Historical Aerial Photograph, 1949, Livermore**

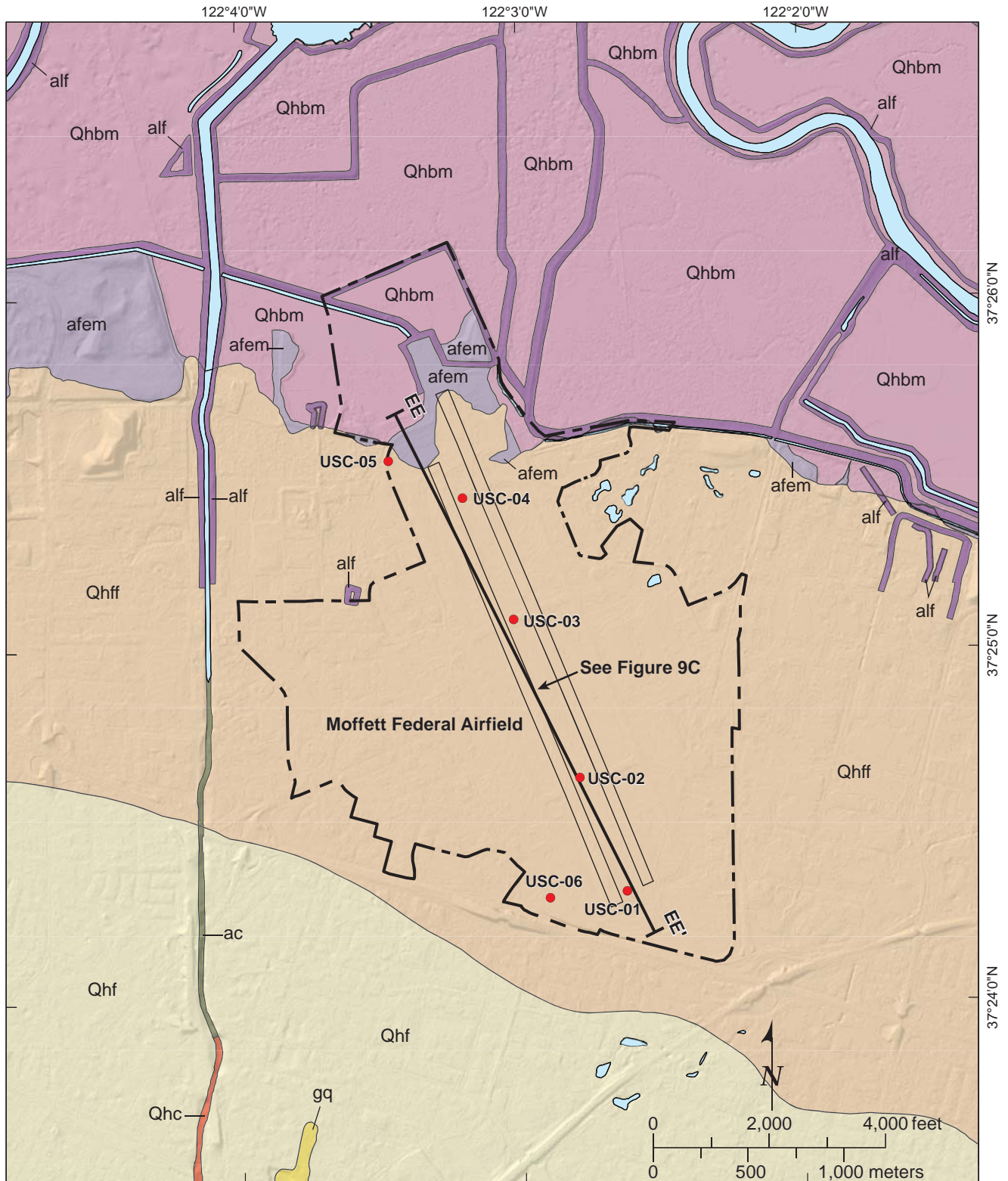
**FIGURE 6C**



79.221200 F07C Moffett\_Air Photo and Contours.ai Friday, March 22 2013 12:02:40

Livermore - Aerial Photograph from NAIP 2009

FIGURE 6D



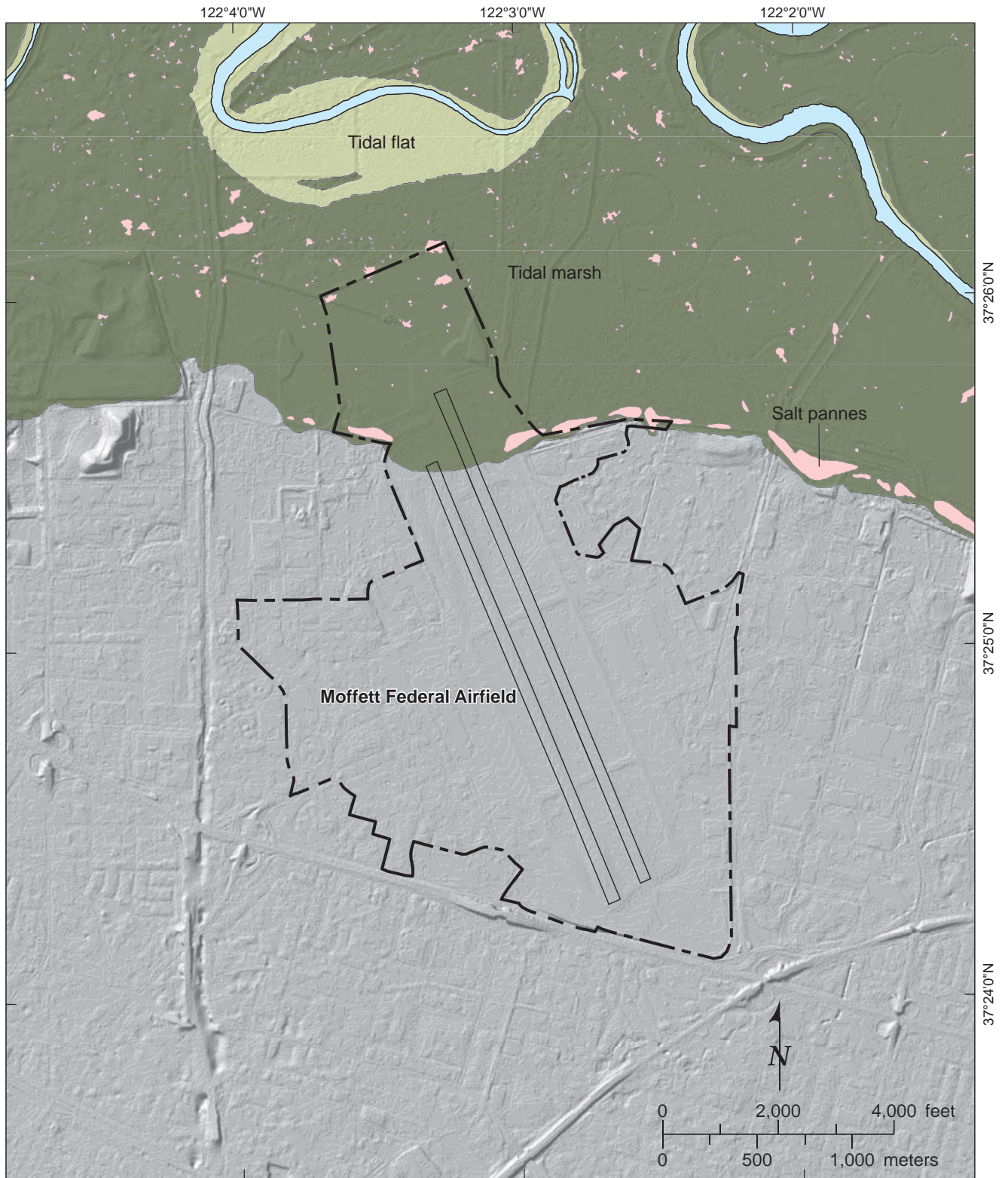
Source: Witter et al. 2006. USGS OFR 06-1037.

**Explanation**

- |          |                                       |      |   |
|----------|---------------------------------------|------|---|
| afem     | Artificial fill over estuarine mud    | Qhc  | Historical stream channel deposits          |
| alf      | Artificial levee fill                 | Qhbm | San Francisco Bay mud                       |
| gq       | Gravel quarries and percolation ponds | Qhf  | Qhf: Holocene alluvial fan deposits         |
| ac       | Artificial stream channel             | Qhff | Holocene alluvial fan deposits, fine facies |
| USC-02 ● | Borehole location                     |      | Water                                       |

**Quaternary Geologic Map, Moffett Federal Airfield**

**FIGURE 7A**



Source: SFEI EcoAtlas version 15002 (2000).

NAD83 UTM Zone 10N

**Explanation**

- |                     |             |
|---------------------|-------------|
| Shallow bay/channel | Tidal marsh |
| Tidal flat          | Salt pannes |

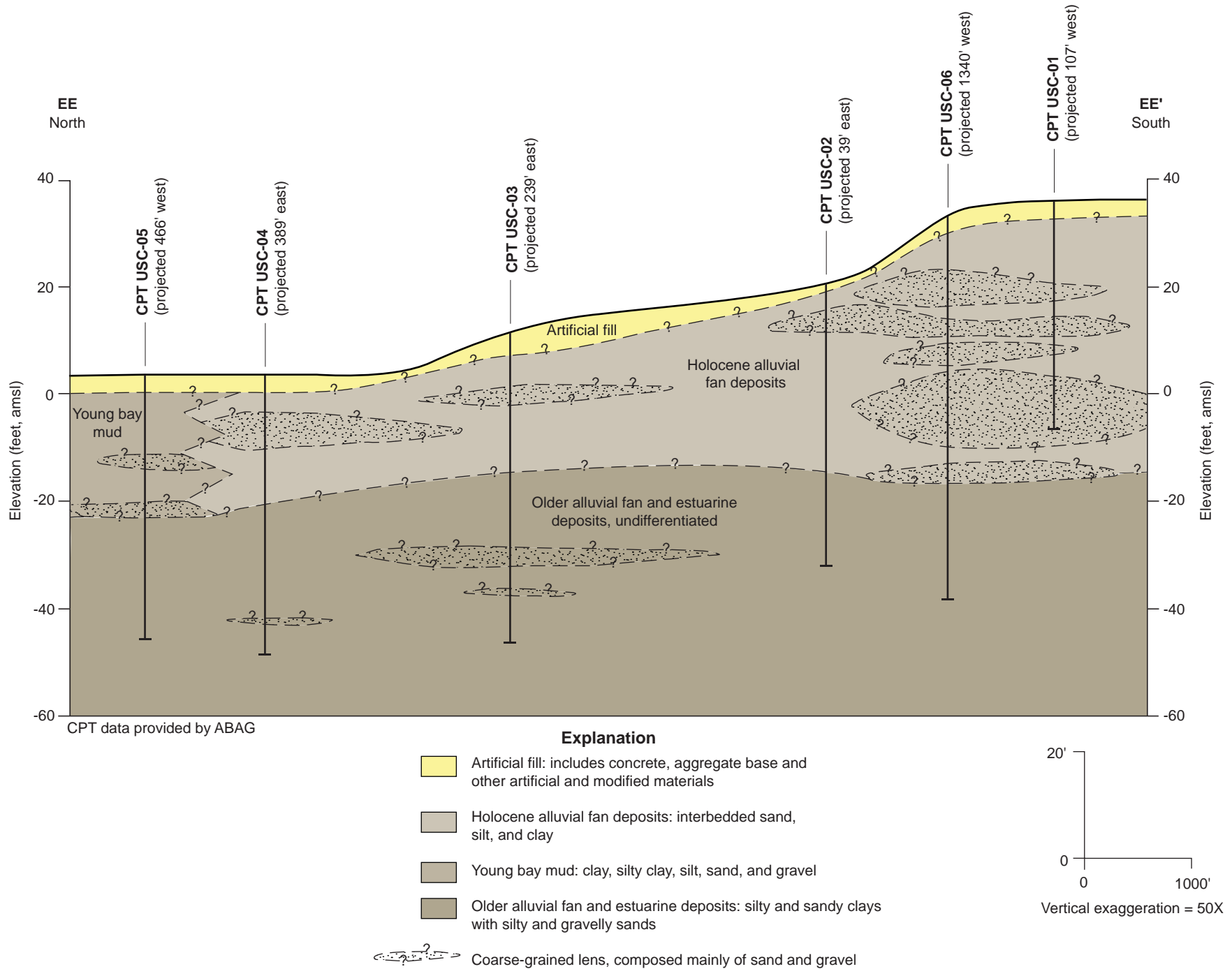
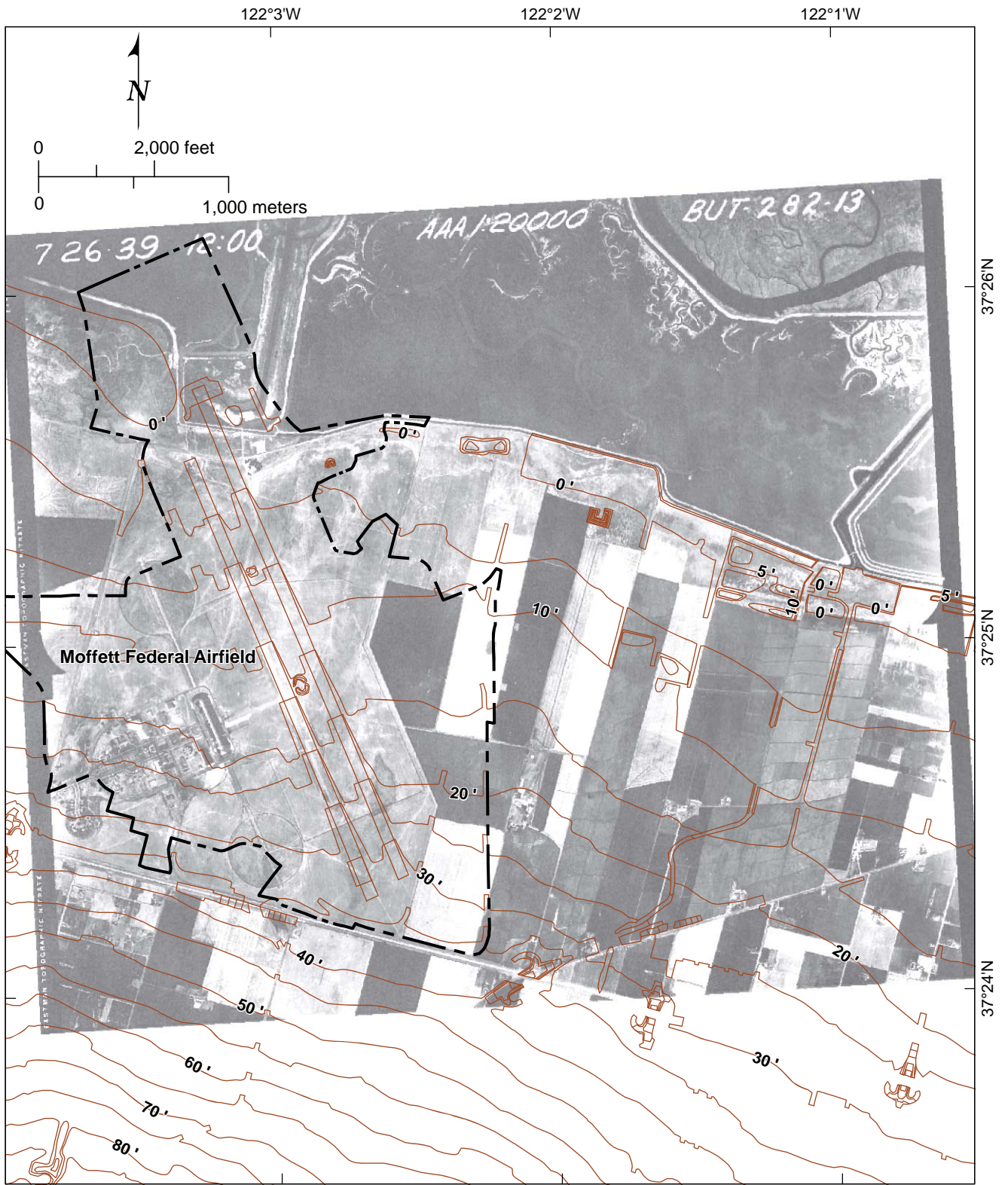


FIGURE 7C

Geologic Cross Section EE-EE', Moffett Federal Airfield, Mountain View, CA



Photograph BUT-282-13, 1939.

Topographic contours from USGS

**Explanation**

— Contour line (5-foot interval)

**Historical Aerial Photograph, 1939, Moffett Field**

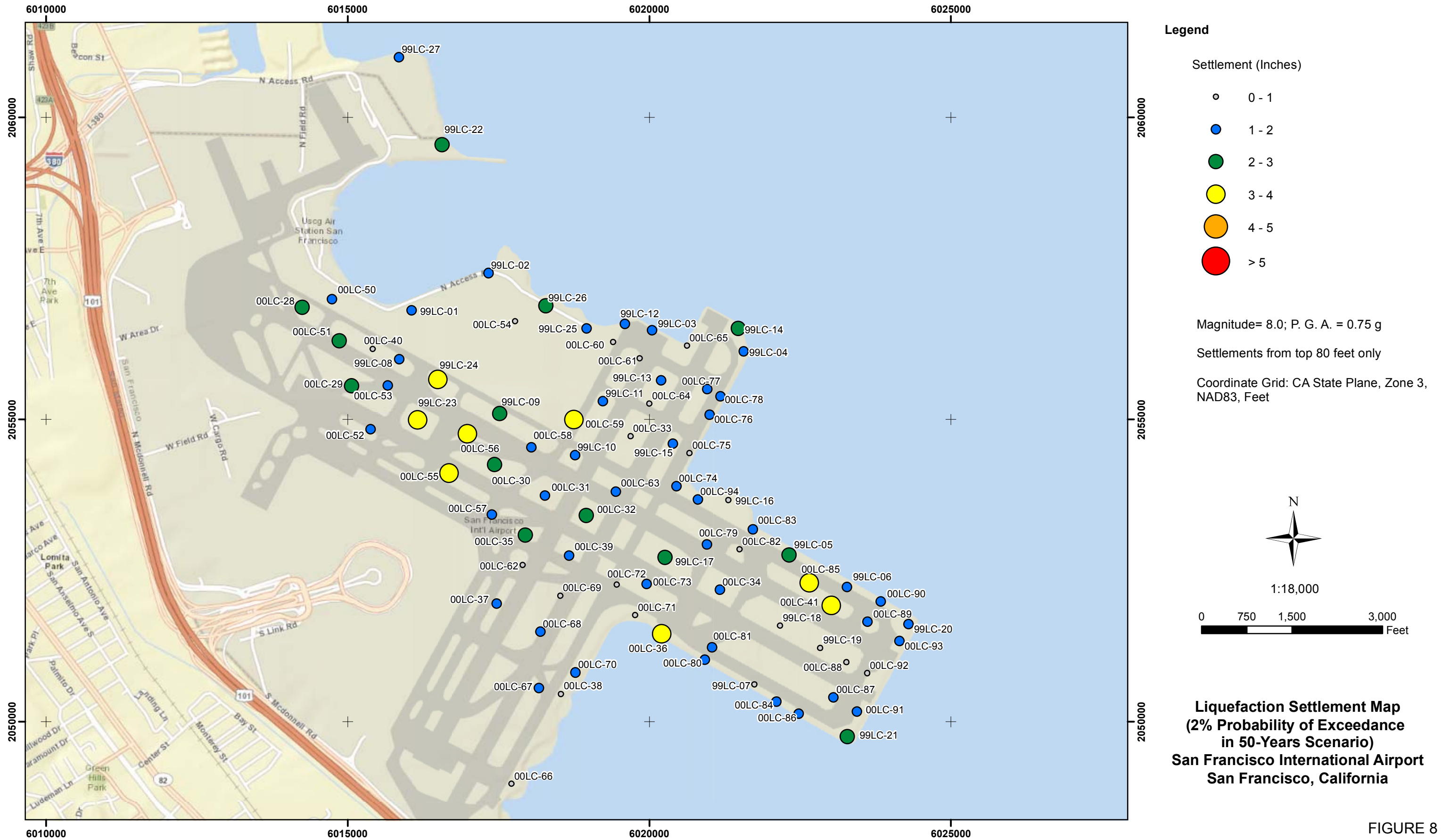
**FIGURE 7D**



79.221200 F16 ABAG\_Moffett\_Air Photo 2009.ai Friday, March 22 2013 13:20:58

Moffett Field - Aerial Photograph from NAIP 2009

FIGURE 7E



N:\Projects\04\_2012\04\_7922\_1200\_CaltransAirportRecon\Outputs\2013\_03\_05\_Report\mxd\Fig\_08\_SFO\_LiquSettl\_M8\_00\_a075\_2008USGS\_2Perc\_50Yrs\_1080Ft.mxd, 03/14/13, dpoliard

FIGURE 8

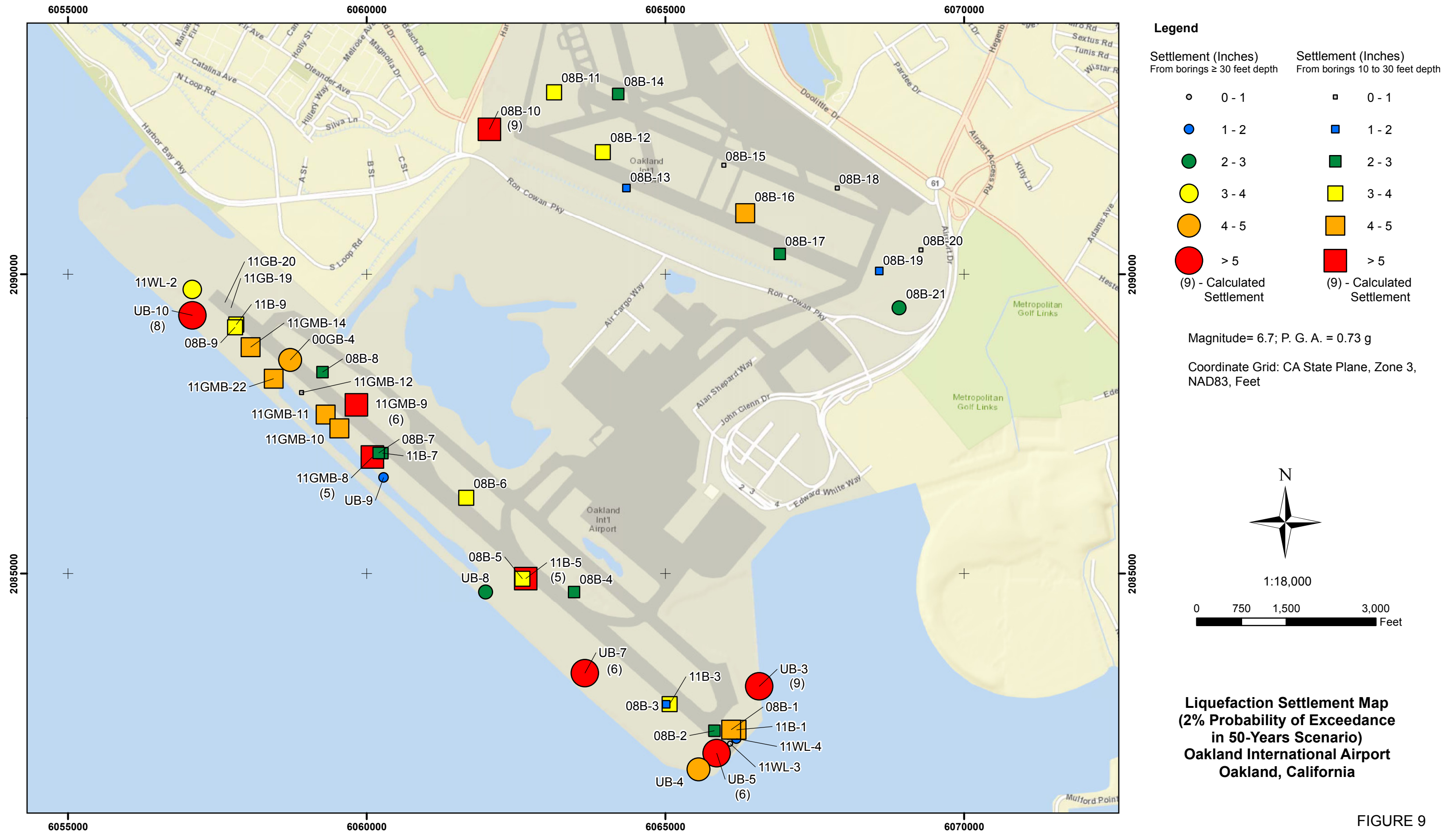


FIGURE 9

N:\Projects\04\_2012\04\_7922\_1200\_CaltransAirportRecov\Outputs\2013\_03\_05\_Report\mxd\Fig\_09\_OAK\_LiquSettl\_M6\_70\_a073\_2475Yr.mxd, 03/14/13, dpollard

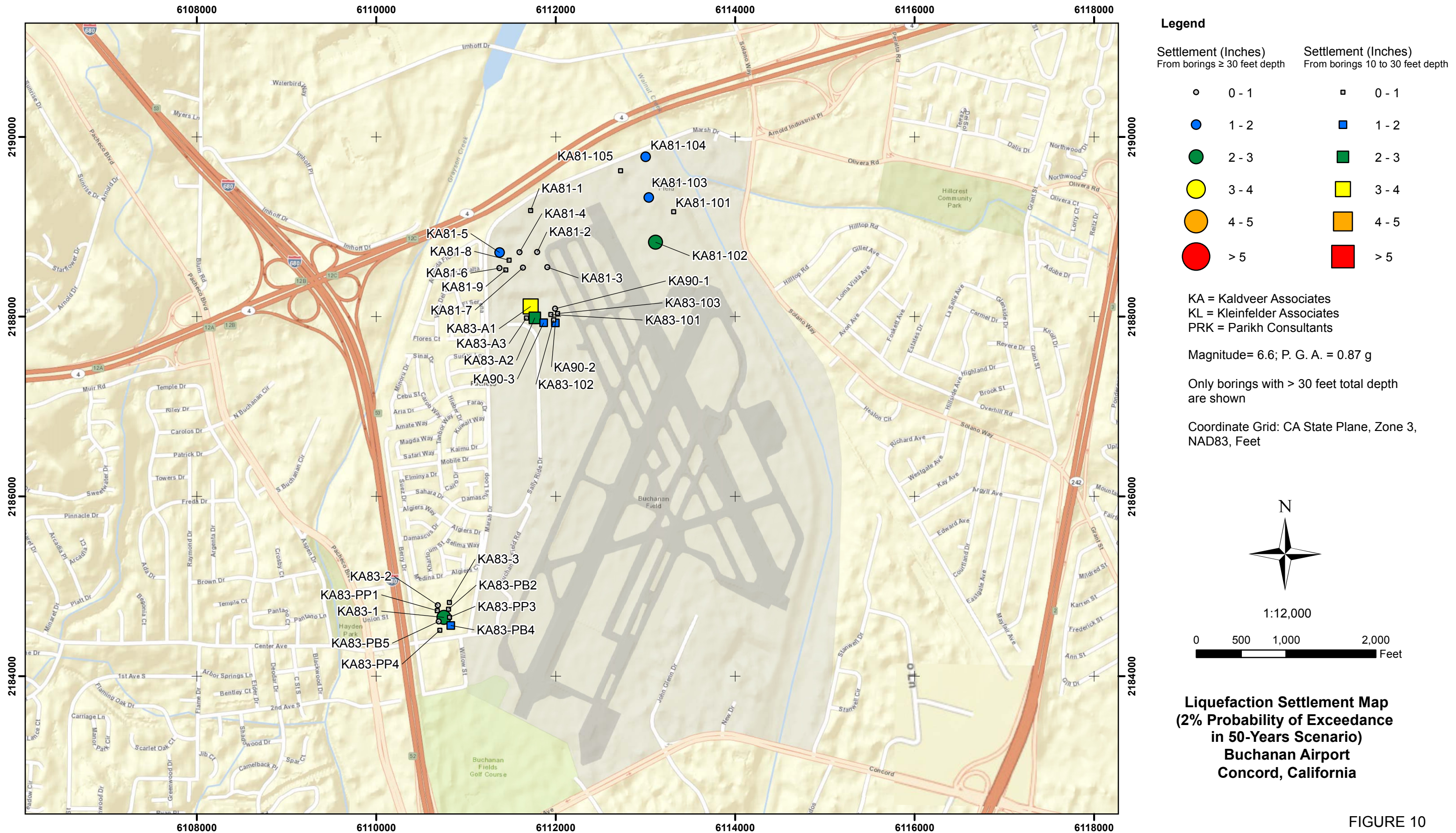
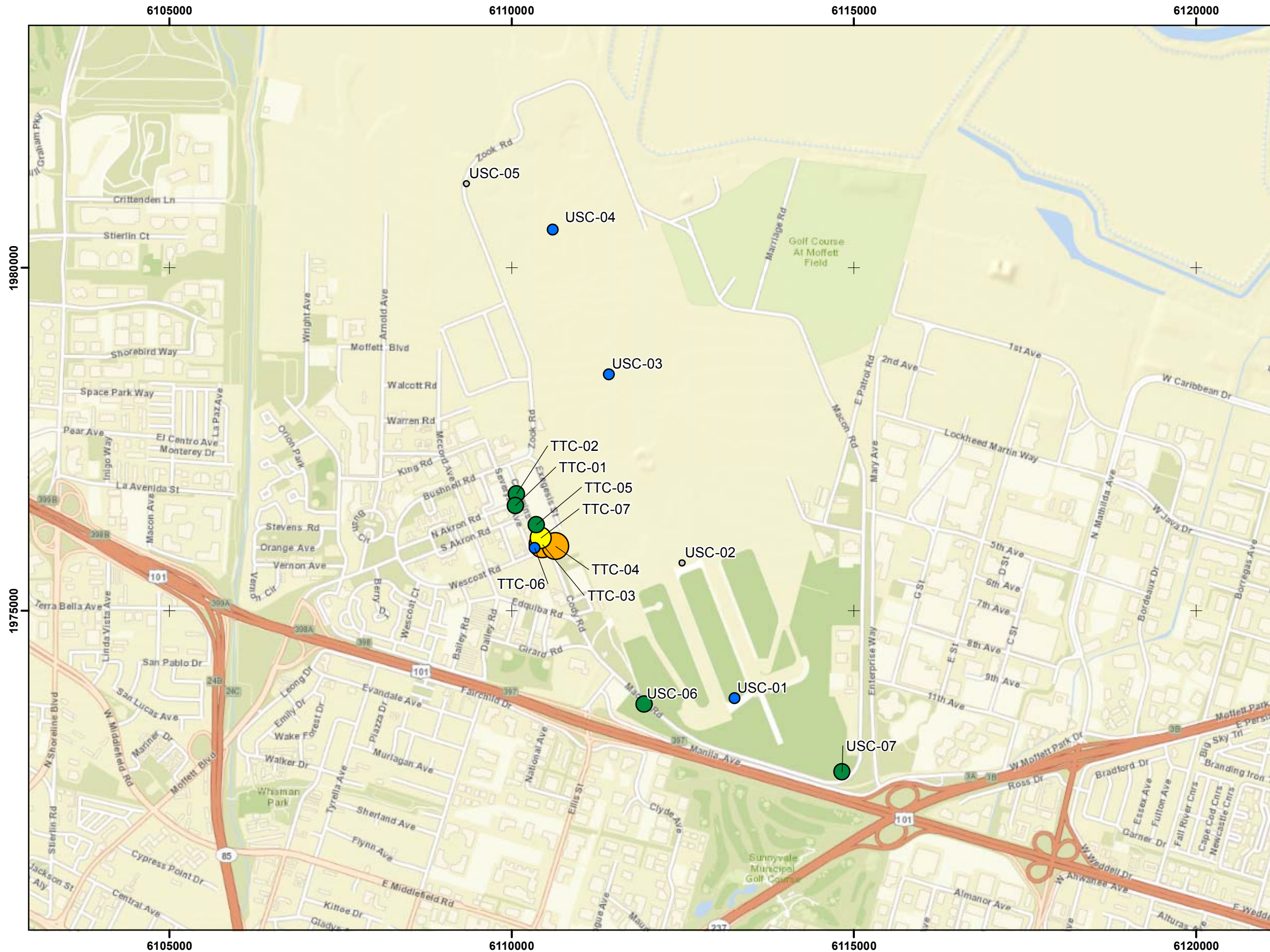


FIGURE 10

N:\Projects\04\_2012\04\_7922\_1200\_CaltransAirportRecov\Outputs\2013\_03\_05\_Report\mxd\Fig\_10\_BUC\_LiquSettl\_M6\_60\_a087\_2475Yr.mxd:03/14/13, dpoliard



**Legend**

Settlement (Inches)

- 0 - 1
- 1 - 2
- 2 - 3
- 3 - 4
- 4 - 5
- > 5

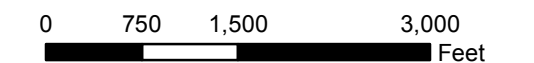
Magnitude= 6.7; P. G. A. = 0.75 g

Only borings with > 30 feet total depth are shown

Coordinate Grid: CA State Plane, Zone 3, NAD83, Feet



1:18,000



**Liquefaction Settlement Map  
 2% Probability of Exceedance  
 in 50-Years Scenario  
 Moffett Federal Airfield  
 Mountain View, California**



Source: William Lettis & Associates, Inc. (1999).

**Explanation**

- |   |  |
|---|--|
| <p>0.2  0.2 Estimated potential liquefaction related settlement (in feet, queried where uncertain)</p> <p>Bay margin, from air photos</p> <ul style="list-style-type: none"> <li> present</li> <li> 1974</li> <li> 1973</li> <li> 1968</li> <li> 1956</li> <li> 1943</li> </ul> | <p><b>Geotechnical Borings</b></p> <ul style="list-style-type: none"> <li> Geotechnical boring used to evaluate distribution and thickness of potentially liquefiable material</li> <li> Geotechnical boring used in assessing liquefaction susceptibility using Seed-Idriss approach (Appendix C)</li> <li> Areas with high potential for earthquake induced differential settlement</li> </ul> |
|---|--|

**Preliminary Liquefaction Hazard Map,  
 San Francisco International Airport**

FIGURE 12



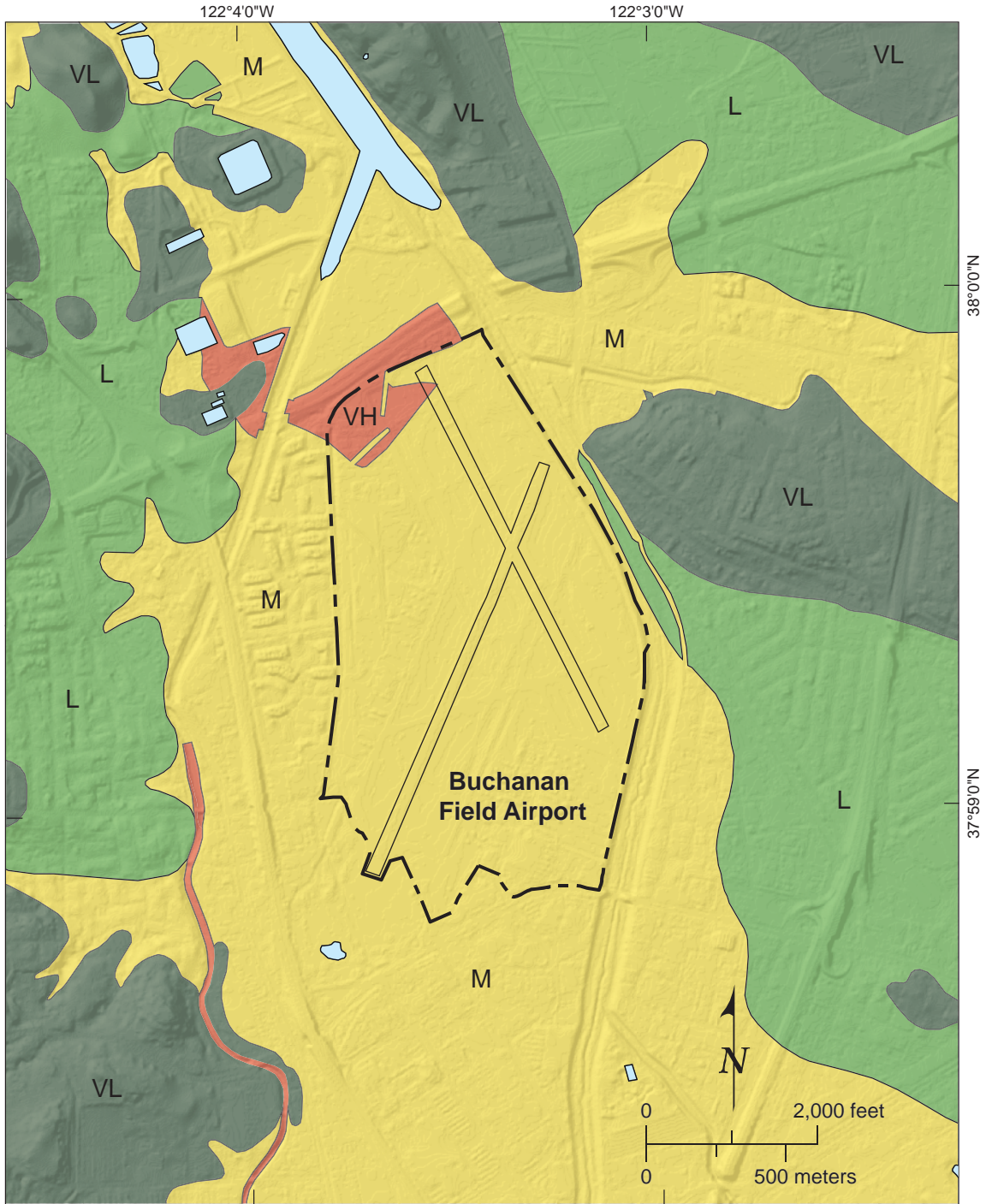
Source: William Lettis & Associates, Inc. (1999).

**Explanation**

- 0.2 Estimated potential liquefaction related settlement (in feet, queried where uncertain)
- Bay margin from air photos
  - present
  - 1959
  - 1958
  - 1939
- 1989 Loma Prieta ground cracks
- 1989 Loma Prieta liquefaction zones
- Geotechnical Borings
  - Sandy lenses in bay mud
  - Geotechnical boring also used to evaluate distribution and thickness of potentially liquefiable material
  - Geotechnical boring used in assessing liquefaction susceptibility using Seed-Idriss approach (Appendix C)
- Areas with high potential for earthquake induced differential settlement

**Preliminary Liquefaction Hazard Map, Oakland International Airport**

**FIGURE 13**



Source: Witter et al., 2006; USGS OFR 06-1037.

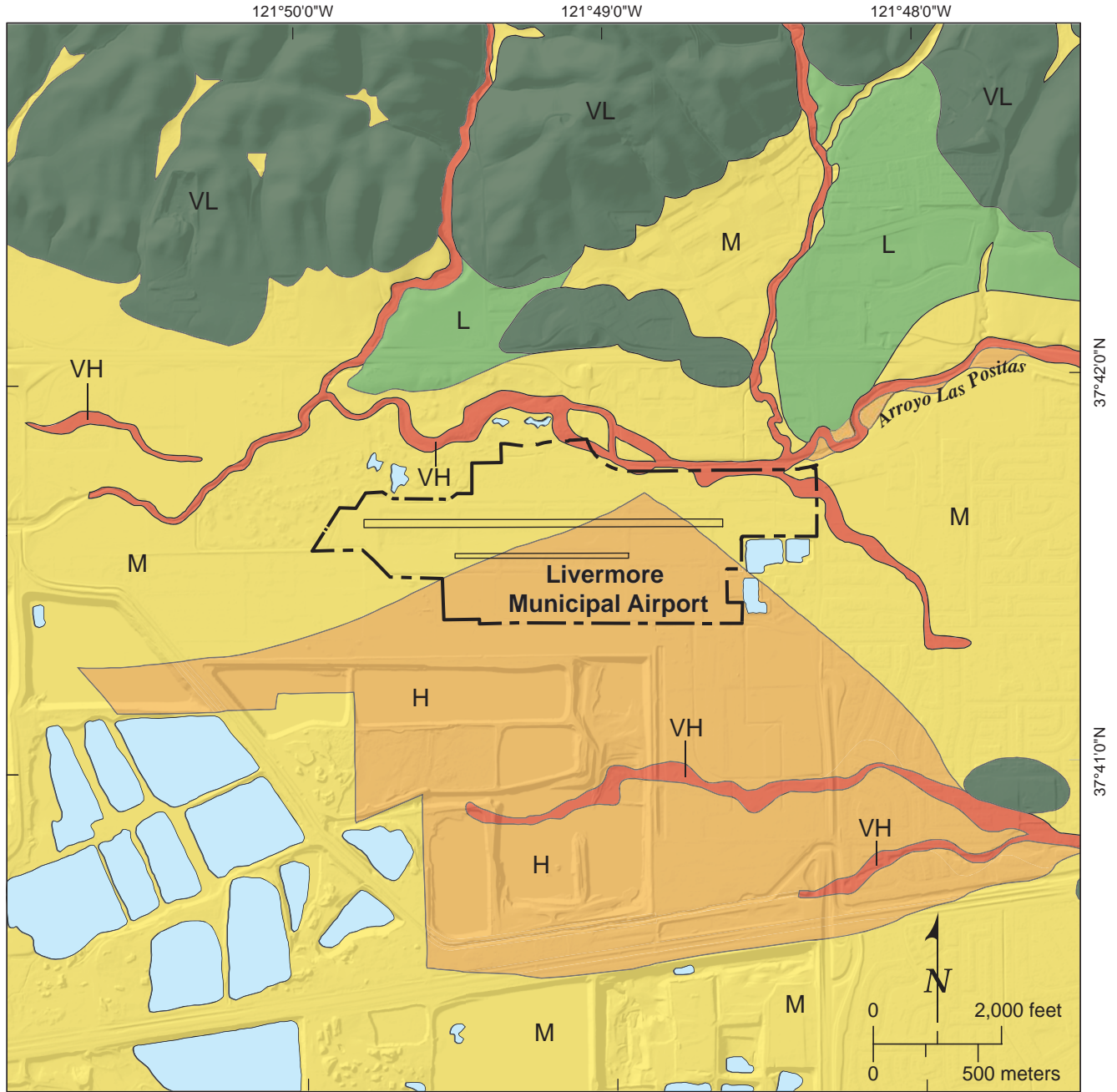
NAD83 UTM Zone 10N

**Explanation**  
*Liquefaction Susceptibility*

<span style="background-color: red; color: white; padding: 2px;">VH</span> Very high	<span style="background-color: darkgreen; color: white; padding: 2px;">VL</span> Very low
<span style="background-color: orange; color: white; padding: 2px;">H</span> High	<span style="background-color: lightblue; color: white; padding: 2px;">Water</span> Water
<span style="background-color: yellow; color: black; padding: 2px;">M</span> Medium	
<span style="background-color: green; color: black; padding: 2px;">L</span> Low	

**Regional Liquefaction Susceptibility, Buchanan Field Airport**

**FIGURE 14**



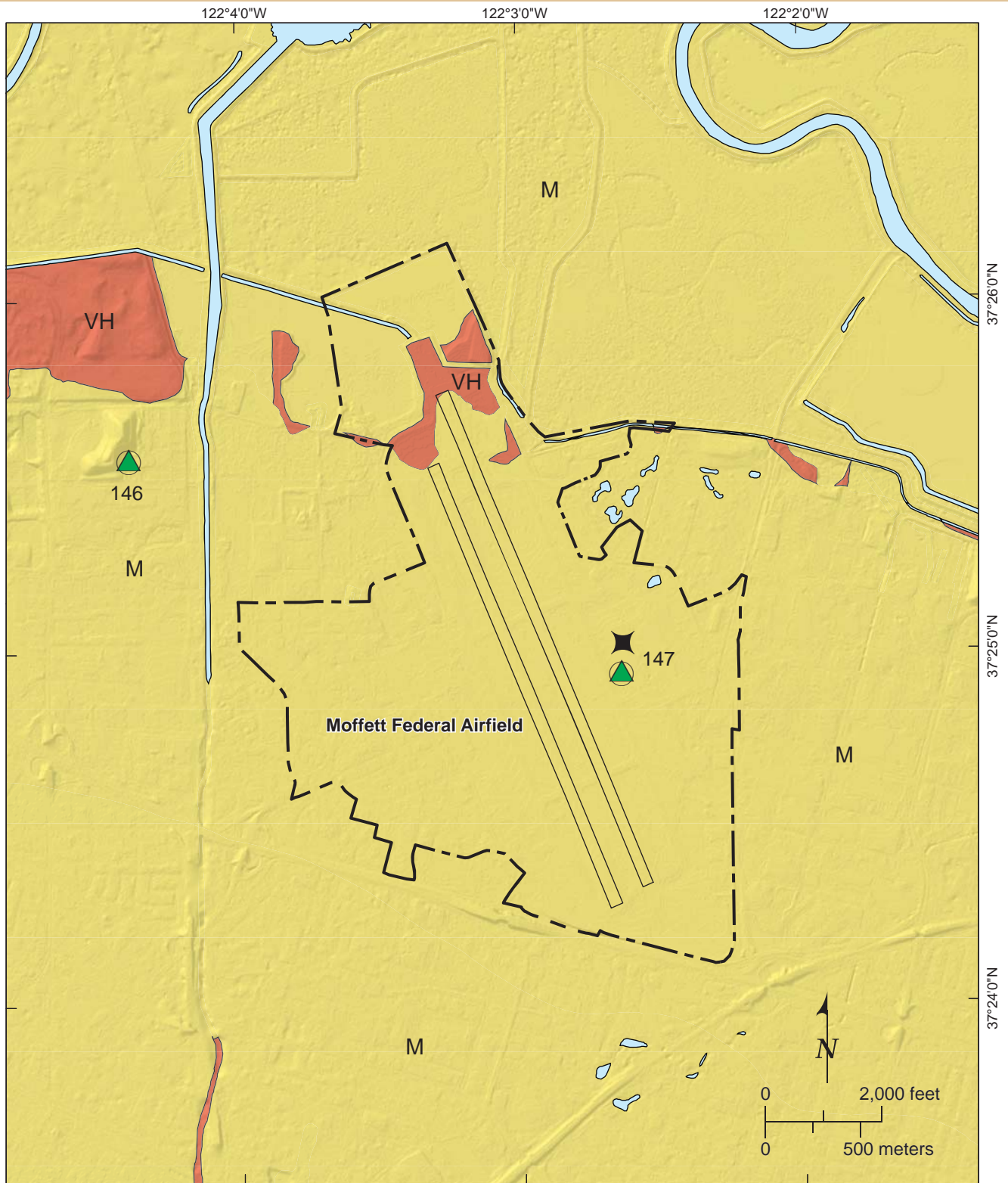
Source: Witter et al., 2006; USGS OFR 06-1037.

NAD83 UTM Zone 10N

**Explanation**

*Liquefaction Susceptibility*

<b>VH</b> Very high	<b>VL</b> Very low
<b>H</b> High	Water
<b>M</b> Medium	
<b>L</b> Low	



Source: Witter et al. 2006; USGS OFR 06-1037.

NAD83 UTM Zone 10N

Liquefaction Susceptibility		Liquefaction Effects of 1906 Earthquake (Youd and Hoose, 1978)	
<span style="background-color: red; border: 1px solid black; padding: 2px;">VH</span> Very high	<span style="background-color: darkgray; border: 1px solid black; padding: 2px;">VL</span> Very low	146  Disturbed well, approximate location	Ground settlement, approximate location
<span style="background-color: orange; border: 1px solid black; padding: 2px;">H</span> High	Water		
<span style="background-color: yellow; border: 1px solid black; padding: 2px;">M</span> Medium			
<span style="background-color: green; border: 1px solid black; padding: 2px;">L</span> Low			

**Regional Liquefaction Susceptibility, Moffett Federal Airfield**

**FIGURE 16**



**Appendix A**  
**Reports Reviewed as Part of this Study**



Airport	Report Name	Report Preparer	Report Date
CCR	Foundation Investigation for Federal Express Building; Pacheco, CA (K199 - 35)	Peter Kaldveer and Associates, Inc.	November 1983
CCR	Geotechnical Investigation for Bedford Aviation Hangar Buchanan Field Concord, California (K199 - 99 - 107)	Kaldveer and Associates, Inc.	May 1990
CCR	Foundation Investigation for Proposed "T" Hangars Buchanan Field Concord, California (K403 - 16)	Peter Kaldveer and Associates, Inc.	May 1981
CCR	Feasibility Foundation Investigation and Fault Location Study for Buchanan Field Heliport; Concord, California (K403 - 17)	Peter Kaldveer and Associates, Inc.	June 1981
CCR	Foundation Investigation for Proposed Corporate Hangar; Concord, California (K431 - 68)	Peter Kaldveer and Associates, Inc.	March 1983
CCR	Supplemental Foundation Investigation Proposed Corporate Hanger; Concord, California (K431 - 68A)	Peter Kaldveer and Associates, Inc.	August 1983
CCR	Foundation Investigation for Undeveloped Property; Pacheco, California (K566 - 3)	Peter Kaldveer and Associates, Inc.	August 1978
CCR	Foundation Investigation for Concord Office Park; Concord, California (K566 - 9)	Peter Kaldveer and Associates, Inc.	August 1980
CCR	Feasibility Foundation Investigation for Airport Center Office Park; Concord, California (K566 - 11)	Peter Kaldveer and Associates, Inc.	July 1985
CCR	Updated Feasibility Foundation Investigation for Pace Membership Warehouse; Concord, California (K566 - 22 - 732)	Kaldveer and Associates, Inc.	May 1991
CCR	Geotechnical Investigation for Pace Membership Warehouse; Concord, California (K566 - 22A - 1075)	Kaldveer and Associates, Inc.	December 1991
CCR	Foundation Investigation for Micropump Building; Pacheco, California (K689 - 1)	Peter Kaldveer and Associates, Inc.	December 1981
CCR	Foundation Investigation for Wendy's Restaurant; Pacheco, California (K845 - 1)	Peter Kaldveer and Associates, Inc.	October 1984
CCR	Geotechnical Investigation for Improvements to Taxiways E and J	Kleinfelder and Associates, Inc.	June 1987
CCR	Geotechnical and Testing Services for Pavement Rehabilitation and Design of Taxiway E and Apron Construction	Geotecnica	August 1998
CCR	Geotechnical Engineering Investigation Report, Buchanan Field Airport, Runway Rehabilitation Project	Parikh Consultants, Inc.	March 2011
CCR	Soils Engineering and Nondestructive Pavement Testing	Kleinfelder and Associates, Inc.	March 1986



Airport	Report Name	Report Preparer	Report Date
CCR	Soil and Pavement Investigation for Pavement Improvements	Kleinfelder and Associates, Inc.	August 1986
LVK	Livermore Municipal Airport	Cornerstone Earth Group	May 2010
NUQ	Foundation Investigation for Proposed Locker and Exercise Facility Moffett Field, California (K215 - 14)	Peter Kaldveer and Associates, Inc.	January 1980
NUQ	Foundation Investigation for Proposed Two-Story Locker and Exercise Facility Moffett Field, California (K215 -14A)	Peter Kaldveer and Associates, Inc.	April 1980
NUQ	Foundation Investigation for Building 191 Addition; Sunnyvale, California (K609 - 2)	Peter Kaldveer and Associates, Inc.	July 1980
NUQ	Addition to Building N206; Moffett Field, California (K649 - 1)	Peter Kaldveer and Associates, Inc.	October 1980
NUQ	Earthquake Hazards Program	U.S. Geological Survey	June 2000
NUQ	Condition Assessment and Rehabilitation Plan, Hangar One, Volume 1, Conditional Assessment	CH2M Hill	November 2011
OAK	Maps and documentation of seismic CPT soundings in the central, eastern, and western United States	U.S. Geological Survey	2010
OAK	Geotechnical Data and Coastal Conditions Report for Perimeter Dike, Oakland International Airport, Oakland, California	URS Corporation	May 2011
OAK	Technical Memorandum No. 2: Geotechnical Study Geotechnical Study for Runway Safety Areas, Oakland International Airport	AGS	April 2008
OAK	RSA Improvements, Oakland International Airport, South Field, Oakland, California	URS Corporation	December 2012
OAK	Geotechnical Data and Coastal Conditions Report	URS Corporation	November 2008
OAK	Draft Geotechnical Investigation and Site Characterization Data Report	AGS	October 2012
SFO	Foundation Investigation Proposed Jet Engine Test Cell No. 5; San Francisco International Airport; For United Air Lines (San Francisco 196)	Dames and Moore	December 1974
SFO	Foundation Investigation and Pavement Design Studies Proposed Trash Compactor Facility; San Francisco International Airport; For United Airlines (San Francisco 197)	Brian, Kangas, Foulk, and Associates	April 1980
SFO	Airfield Seismic Stabilization and Realignment, Phase A Engineering Report	URS Corporation	July 2006

Notes:

SFO: San Francisco International Airport  
LVK: Livermore Municipal Airport

OAK: Oakland International Airport  
NUQ: Moffett Federal Airfield

CCR: Buchanan Field Airport



## Appendix B

### Description of Geologic Units

Descriptions modified from Witter et al. (2006)

#### **Artificial fill (historical)**

**Map units:** *af, afem, alf, ads, acf, adf, gq*

Material deposited by humans. Additional types of artificial fill are mapped as separate geologic map units, including: artificial fill over estuarine mud (*afem*), artificial levee fill (*alf*), dredge spoils (*ads*), artificial channel fill (*acf*), artificial dam fill (*adf*), and gravel quarries and percolation ponds (*gq*). Fill may be engineered and/or non-engineered material; each may occur within the same area on the map. Fill whose thickness is less than the contour interval (typically 5 to 10 ft) and fill emplaced after the topographic base maps were surveyed are not shown. Small bodies of fill, such as small road embankments and earthen dams for farm ponds, are not shown. Included within this unit are small areas of Holocene alluvial deposits that are too small to be mapped at this scale.

#### **Artificial stream channel (historical)**

Map unit: *ac*

Modified stream channels, including straightened or realigned channels, flood control channels, and concrete canals. Deposits within artificial channels can range from almost none in some concrete canals, to significant thicknesses of loose, unconsolidated sand, gravel and cobbles, similar to deposits of modern stream channel deposits (*Qhc*).

#### **Historical stream channel deposits**

Map unit; *Qhc*

Fluvial deposits within active, natural stream channels. Materials consist of loose, unconsolidated, poorly to well sorted sand, gravel and cobbles, with minor silt and clay. These deposits are reworked by frequent flooding and exhibit no soil development. These deposits, like most other alluvial deposits, become finer grained downstream (i.e., sediment is coarser upstream).

#### **Latest Holocene alluvial fan deposits**

Map unit: *Qhfy*

Alluvial fan sediment judged to be latest Holocene (<1,000 years) in age, based on records of historical inundation or the presence of youthful braid bars and distributary channels. Alluvial fan sediment is deposited by streams emanating from mountain canyons onto alluvial valley floors or alluvial plains. Most apices of the mapped latest Holocene alluvial fan deposits occur partway down older piedmont alluvial fan complexes. The stream channel typically is incised into older fan deposits near the fan apex, then gradually is less incised down fan, until the stream becomes unconfined and distributes young sediment across the toe of the fan. Sediment is



moderately too poorly sorted and bedded, and may be composed of gravel, sand, silt and clay. Grain size generally fines down slope.

### **Latest Holocene stream terrace deposits**

**Map unit:** *Qhty*

Stream terrace deposits judged to be latest Holocene (<1,000 years) in age based on records of historical inundation, the identification of youthful meander scars and braid bars on aerial photographs or orthophoto quadrangles, and/or geomorphic position (elevation) very close to the stream channel. Stream terrace sediment includes sand, gravel, silt, and minor clay, is moderately to well sorted, and is moderately to well bedded.

### **Holocene San Francisco Bay Mud**

**Map unit:** *Qhbm*

Sediment deposited at or near sea level in the San Francisco Bay estuary that is presently, or was historically tidal marsh, mud flat or bay bottom. Bay Mud sediment typically has low bulk density and silt, clay, peat, and fine sand. This unit is time-transgressive and generally occupies the area between the modern shoreline and the historical limits of tidal marsh. Bay Mud deposits near the mouths of larger streams likely contain more sand and silt than the deposits that are distant from stream and river mouths. Bay Mud is mainly late Holocene in age with many areas presently subject to deposition and flooding. Some areas have been diked for farming, salt evaporators, or other purposes. Bay Mud deposits thin landward and may be as thick as 40 meters along the bay margin.

### **Holocene alluvial fan deposits**

**Map unit:** *Qhf*

Sediment deposited by streams emanating from mountain canyons onto alluvial valley floors or alluvial plains, including debris flow, hyperconcentrated mudflow, and braided stream deposits. Alluvial fan sediment includes sand, gravel, silt, and clay, and is moderately to poorly sorted, and moderately to poorly bedded. Sediment clast size and general particle size typically decreases down slope from the fan apex. Many Holocene alluvial fans exhibit levee/interlevee topography, particularly the fans associated with creeks flowing west from the East Bay hills. Alluvial fan surfaces are steepest near their apex at the valley mouth, and slope gently basin ward, typically with gradually decreasing gradient. Holocene alluvial fans are relatively undissected when compared to older alluvial fans. In places, Holocene deposits may be only a thin veneer over Pleistocene deposits.

### **Holocene alluvial fan deposits, fine facies**

**Map unit:** *Qhff*

Fine-grained alluvial fan and flood plain overbank deposits laid down in very gently sloping portions of the alluvial fan or valley floor. Slopes in these distal alluvial fan areas are generally less than or equal to 0.5 degrees, soils are clay rich, and ground water is within 3 meters of the surface. Deposits are dominated by clay and silt, with interbedded lobes of coarser alluvium

(sand and occasional gravel). Deposits of coarse material within these fine-grained materials are elongated in the down fan or down valley direction. These lobes are potential conduits for groundwater flow.

### **Holocene alluvial fan levee deposits**

Map unit: *Qhl*

Natural levee deposits of alluvial fans are formed by streams that overtop their banks and deposit sediment adjacent to the channel. Levees are identified as long, low ridges oriented down fan. They contain coarser material than adjoining interlevee areas, especially adjacent to creek banks where the coarsest material is deposited during floods. Levee deposits are loose, moderately to well sorted sand, silt and clay.

### **Holocene stream terrace deposits**

Map unit: *Qht*

Stream terrace deposits that were deposited in point bar and overbank settings. Terrace deposits include sand, gravel, silt, and minor clay, and are moderately to well-sorted, and moderately to well bedded. This unit is mapped where relatively smooth, undissected terraces are less than 25 to thirty feet above the active channel.

### **Holocene alluvial deposits, undifferentiated**

Map unit: *Qha*

Alluvium deposited in fan, terrace, or basin environments. This unit is mapped where separate types of alluvial deposits could not be delineated either due to complex interfingering of depositional environments or the small size of the area. Typically, undifferentiated alluvial deposits are mapped in relatively flat, smooth valley bottoms along small- to medium-sized streams. The planar and smooth geomorphic surfaces, with little to no dissection, indicate that there has been little post-stabilization modification/dissection of the surface; thus, deposits with smooth surfaces are interpreted to be Holocene in age. Undifferentiated Holocene alluvial deposits probably are intercalated sand, silt, and gravel that are poorly to moderately sorted.

### **Latest Pleistocene to Holocene dune sand**

Map Unit: *Qds*

Very well sorted fine to medium grained eolian sand (<30,000 years). Holocene sand may discontinuously overlie latest Pleistocene sand, both of which may form a mantle of varying thickness over older materials. Most of these deposits are thought to be associated with latest Pleistocene to early Holocene low sea level stands and subsequent transgression, during which large volumes of fluvial and glacially derived sediment from the Sierra Nevada via the Sacramento and San Joaquin Rivers were blown into dunes. The deposits include the Merritt Sand in the Oakland area and the sand dunes that cover much of the northern San Francisco Peninsula. These dunes consist of fine to medium sand that is semi-consolidated and weakly cemented.

---

### **Latest Pleistocene to Holocene alluvial fan deposits**

Map Unit: *Qf*

This unit is mapped on gently sloping, fan-shaped, relatively undissected alluvial surfaces where the age of deposits is not known (either latest Pleistocene or Holocene in age) or where the deposits consist of thin patches of Holocene sediment overlying latest Pleistocene alluvial fan sediment. Fan sediment includes sand, gravel, silt, and clay, and is moderately to poorly sorted, and moderately to poorly bedded.

### **Latest Pleistocene to Holocene stream terrace deposits**

Map Unit: *Qt*

This unit is mapped on relatively flat, undissected stream terraces where deposit age is uncertain. Terrace deposits include sand, gravel, and silt, with minor clay, and are moderately to well sorted, and moderately to well bedded.

### **Latest Pleistocene to Holocene alluvial deposits, undifferentiated**

Map Unit: *Qa*

This unit is mapped in small valleys where separate fan, basin, and terrace units could not be delineated at the scale of this mapping, and where deposits might be of either latest Pleistocene or Holocene age. The unit includes flat, relatively undissected fan, terrace, and basin deposits, and small active stream channels.

### **Latest Pleistocene alluvial fan deposits**

Map Unit: *Qpf*

This unit is mapped on alluvial fans where latest Pleistocene age is indicated by greater dissection than is present on Holocene fans, and/or the development of alfisols. Latest Pleistocene alluvial fan sediment was deposited by streams emanating from mountain canyons onto alluvial valley floors or alluvial plains and includes debris flow, hyperconcentrated mudflow, and braided stream deposits. Alluvial fan sediment typically includes sand, gravel, silt, and clay, and is moderately to poorly sorted, and moderately to poorly bedded. Sediment clast size and general particle size decreases down slope from the fan apex. Latest Pleistocene alluvial fan sediment is approximately 10% denser than Holocene alluvial fan sediment and has penetration resistance values about 50% greater than values for Holocene alluvial fan sediment. Latest Pleistocene alluvial fans may be overlain by thin unmapped Holocene alluvial fan deposits. Where multiple alluvial fans are identified, the younger deposits (*Qpf1*) are distinguished from older deposits (*Qpf2*). Along the west-facing hills of Oakland and Berkeley, where the latest Pleistocene alluvial fan deposits are mapped, the age of these deposits is not well constrained and the deposits may actually be a combination of early to middle Pleistocene alluvial fan and thin pediment deposits, and latest Pleistocene alluvial fan deposits.

### **Latest Pleistocene alluvial deposits, undifferentiated**

Map Unit: *Qpa*

---



This unit is mapped on gently sloping to level alluvial fan or terrace surfaces where latest Pleistocene age is indicated by depth of stream incision, development of alfisols, and lack of historical flooding. Undifferentiated latest Pleistocene alluvial deposits are mapped in small valleys where separate fan, basin, and terrace units could not be delineated at the mapping scale of this project. These undifferentiated latest Pleistocene alluvial deposits probably are intercalated sand, silt, and gravel that are poorly to moderately sorted.

**Early to late Pleistocene alluvial deposits, undifferentiated**

**Map unit:** *Qoa*

Moderately to deeply dissected alluvial deposits capped by alfisols, ultisols, or soils containing a silicic or calcic hardpan. Topography often consists of gently rolling hills with little or none of the original planar alluvial surface preserved.

**Early Quaternary and older (>1.4 Ma) deposits and bedrock, undifferentiated.**

**Map unit:** *br*

Primarily Jurassic to Pliocene sedimentary, metamorphic, volcanic and plutonic rocks, and poorly consolidated Tertiary sediment. Also includes some Pliocene to Pleistocene sedimentary units such as the Glen Ellen Formation, Santa Clara Formation, Livermore gravels, and Merced Formations.

---



**Appendix C**  
**Subsurface Data Used in Liquefaction Analyses**



Airport <sup>1</sup>	Report Preparer	Exploration Year	Borehole or CPT ID	Total Depth (feet)	Northing (UTM, meters)	Easting (UTM, meters)	Exploration Method <sup>2</sup>
OAK	URS	2000	00GB-4	46.00	2088565.74	6058721.55	HSA
OAK	URS	2008	UB-3	60.00	2083113.20	6066571.78	HSA
OAK	URS	2008	UB-4	60.50	2081726.06	6065556.79	HSA
OAK	URS	2008	UB-5	40.00	2081997.28	6065859.80	HSA
OAK	URS	2008	UB-7	41.50	2083334.25	6063653.42	HSA
OAK	URS	2008	UB-8	40.00	2084690.49	6061991.56	HSA
OAK	URS	2008	UB-9	45.00	2086604.85	6060285.24	HSA
OAK	URS	2008	UB-10	60.50	2089311.94	6057083.82	HSA
OAK	URS	2011	11WL-2	41.50	2089744.07	6057080.88	HSA
OAK	URS	2011	11B-1	11.50	2082387.00	6066191.00	HSA
OAK	URS	2011	11B-3	19.00	2082816.82	6065070.88	HSA
OAK	URS	2011	11B-5	12.00	2084913.79	6062661.31	HSA
OAK	URS	2011	11B-7	12.00	2087010.77	6060264.77	HSA
OAK	URS	2011	11B-9	20.00	2089159.84	6057816.13	HSA
OAK	URS	2011	11GMB-10	10.50	2087424.08	6059544.45	HSA
OAK	URS	2011	11GMB-11	10.50	2087653.52	6059315.54	HSA
OAK	URS	2011	11GMB-12	10.50	2088022.22	6058911.53	HSA
OAK	URS	2011	11GMB-13	5.00	2088391.62	6058278.93	HSA
OAK	URS	2011	11GMB-14	13.50	2088781.06	6058055.66	HSA
OAK	URS	2011	11GMB-21	7.50	2088326.60	6058381.83	HSA
OAK	URS	2011	11GMB-22	16.50	2088253.96	6058443.56	HSA
OAK	URS	2011	11GMB-8	10.50	2086945.62	6060097.21	HSA



Airport <sup>1</sup>	Report Preparer	Exploration Year	Borehole or CPT ID	Total Depth (feet)	Northing (UTM, meters)	Easting (UTM, meters)	Exploration Method <sup>2</sup>
OAK	URS	2011	11GMB-9	13.50	2087817.23	6059828.35	HSA
OAK	URS	2011	11GB-19	6.50	2089438.03	6057729.31	HSA
OAK	URS	2011	11GB-20	6.50	2089526.58	6057627.40	HSA
OAK	URS	2011	11WL-3	31.50	2082153.66	6066084.19	HSA
OAK	URS	2011	11WL-4	35.50	2082239.64	6066189.96	HSA
OAK	URS	2008	08B-1	11.50	2082390.00	6066103.00	HSA
OAK	URS	2008	08B-2	14.00	2082372.00	6065822.00	HSA
OAK	URS	2008	08B-3	19.00	2082814.00	6065015.00	HSA
OAK	URS	2008	08B-4	11.50	2084689.00	6063473.00	HSA
OAK	URS	2008	08B-5	12.00	2084913.00	6062608.00	HSA
OAK	URS	2008	08B-6	14.00	2086264.00	6061667.00	HSA
OAK	URS	2008	08B-7	12.00	2087014.00	6060201.00	HSA
OAK	URS	2008	08B-8	11.50	2088364.00	6059261.00	HSA
OAK	URS	2008	08B-9	20.00	2089115.00	6057797.00	HSA
OAK	URS	2008	08B-10	26.50	2092422.00	6062055.00	HSA
OAK	URS	2008	08B-11	11.50	2093040.00	6063137.00	HSA
OAK	URS	2008	08B-12	26.50	2092040.00	6063955.00	HSA
OAK	URS	2008	08B-13	11.50	2091439.00	6064349.00	HSA
OAK	URS	2008	08B-14	11.50	2093012.00	6064213.00	HSA
OAK	URS	2008	08B-15	13.35	2091822.00	6065979.00	HSA
OAK	URS	2008	08B-16	26.50	2091019.00	6066338.00	HSA
OAK	URS	2008	08B-17	11.50	2090339.00	6066914.00	HSA
OAK	URS	2008	08B-18	16.50	2091440.00	6067878.00	HSA



Airport <sup>1</sup>	Report Preparer	Exploration Year	Borehole or CPT ID	Total Depth (feet)	Northing (UTM, meters)	Easting (UTM, meters)	Exploration Method <sup>2</sup>
OAK	URS	2008	08B-19	26.50	2090055.00	6068583.00	HSA
OAK	URS	2008	08B-20	16.50	2090407.00	6069279.00	HSA
OAK	URS	2008	08B-21	36.50	2089436.00	6068914.00	HSA
SFO	Fugro West	1999	99LB-01	242.00	2057196.00	6016704.00	RSB
SFO	Fugro West	1999	99LB-02	303.10	2056758.00	6021005.00	RSB
SFO	Fugro West	1999	99LB-03	227.00	2052496.00	6022797.00	RSB
SFO	Fugro West	1999	99LB-04	289.50	2050805.00	6021387.00	RSB
SFO	Fugro West	1999	99LB-05	287.00	2050741.00	6023834.00	RSB
SFO	Fugro West	1999	99LC-01	115.72	2056806.00	6016059.00	CPT
SFO	Fugro West	1999	99LC-02	130.00	2057417.00	6017334.00	CPT
SFO	Fugro West	1999	99LC-03	141.96	2056474.00	6020046.00	CPT
SFO	Fugro West	1999	99LC-04	116.00	2056121.00	6021567.00	CPT
SFO	Fugro West	1999	99LC-05	152.50	2052752.00	6022324.00	CPT
SFO	Fugro West	1999	99LC-06	125.40	2052223.00	6023284.00	CPT
SFO	Fugro West	1999	99LC-07	155.80	2050610.00	6021749.00	CPT
SFO	Fugro West	1999	99LC-08	144.30	2055992.00	6015855.00	CPT
SFO	Fugro West	1999	99LC-09	128.60	2055091.00	6017521.00	CPT
SFO	Fugro West	1999	99LC-10	150.90	2054404.00	6018771.00	CPT
SFO	Fugro West	1999	99LC-11	145.50	2055298.00	6019233.00	CPT
SFO	Fugro West	1999	99LC-12	150.75	2056578.00	6019596.00	CPT
SFO	Fugro West	1999	99LC-13	166.90	2055645.00	6020198.00	CPT
SFO	Fugro West	1999	99LC-14	172.00	2056506.00	6021477.00	CPT
SFO	Fugro West	1999	99LC-15	139.90	2054593.00	6020393.00	CPT



Airport <sup>1</sup>	Report Preparer	Exploration Year	Borehole or CPT ID	Total Depth (feet)	Northing (UTM, meters)	Easting (UTM, meters)	Exploration Method <sup>2</sup>
SFO	Fugro West	1999	99LC-16	146.35	2053663.00	6021311.00	CPT
SFO	Fugro West	1999	99LC-17	147.80	2052715.00	6020259.00	CPT
SFO	Fugro West	1999	99LC-18	150.10	2051584.00	6022172.00	CPT
SFO	Fugro West	1999	99LC-19	152.00	2051214.00	6022839.00	CPT
SFO	Fugro West	1999	99LC-20	159.67	2051609.00	6024300.00	CPT
SFO	Fugro West	1999	99LC-21	134.40	2049749.00	6023289.00	CPT
SFO	Fugro West	1999	99LC-22	125.00	2059543.00	6016564.00	CPT
SFO	Fugro West	1999	99LC-23	131.70	2054987.00	6016158.00	CPT
SFO	Fugro West	1999	99LC-24	129.20	2055660.00	6016495.00	CPT
SFO	Fugro West	1999	99LC-25	144.80	2056504.00	6018959.00	CPT
SFO	Fugro West	1999	99LC-26	154.20	2056879.00	6018285.00	CPT
SFO	Fugro West	1999	99LC-27	134.00	2060991.00	6015852.00	CPT
SFO	Fugro West	2000	00LB-06	297.00	2057063.00	6017952.00	RSB
SFO	Fugro West	2000	00LB-07	280.00	2055884.00	6016648.00	RSB
SFO	Fugro West	2000	00LB-08	170.00	2053501.00	6021194.00	RSB
SFO	Fugro West	2000	00LB-09	256.00	2051433.00	6019113.00	RSB
SFO	Fugro West	2000	00LB-10	20.20	2056507.00	6018955.00	RSB
SFO	Fugro West	2000	00LB-11	19.50	2056876.00	6018290.00	RSB
SFO	Fugro West	2000	00LB-12	12.00	2056806.00	6015509.00	RSB
SFO	Fugro West	2000	00LB-13	253.00	2056228.00	6018691.00	RSB
SFO	Fugro West	2000	00LB-14	22.00	2056433.00	6021472.00	RSB
SFO	Fugro West	2000	00LB-15	222.50	2055775.00	6021418.00	RSB
SFO	Fugro West	2000	00LB-16	43.50	2055075.00	6021004.00	RSB



Airport <sup>1</sup>	Report Preparer	Exploration Year	Borehole or CPT ID	Total Depth (feet)	Northing (UTM, meters)	Easting (UTM, meters)	Exploration Method <sup>2</sup>
SFO	Fugro West	2000	00LB-17	188.00	2053208.00	6019559.00	RSB
SFO	Fugro West	2000	00LB-18	25.50	2052710.00	6020260.00	RSB
SFO	Fugro West	2000	00LB-19	260.00	2049700.00	6018120.00	RSB
SFO	Fugro West	2000	00LB-20	19.50	2051470.00	6020240.00	RSB
SFO	Fugro West	2000	00LB-21	323.10	2051260.00	6020580.00	RSB
SFO	Fugro West	2000	00LB-22	252.50	2051911.00	6021767.00	RSB
SFO	Fugro West	2000	00LB-23	15.50	2052740.00	6022320.00	RSB
SFO	Fugro West	2000	00LB-24	280.00	2049920.00	6022890.00	RSB
SFO	Fugro West	2000	00LB-25	29.50	0.00	6020340.00	RSB
SFO	Fugro West	2000	00LB-26	24.50	0.00	6018650.00	RSB
SFO	Fugro West	2000	00LB-27	30.00	0.00	6018850.00	RSB
SFO	Fugro West	2000	00LC-28	104.80	2056855.00	6014245.00	CPT
SFO	Fugro West	2000	00LC-29	124.60	2055554.00	6015067.00	CPT
SFO	Fugro West	2000	00LC-30	157.80	2054249.00	6017437.00	CPT
SFO	Fugro West	2000	00LC-31	125.10	2053739.00	6018270.00	CPT
SFO	Fugro West	2000	00LC-32	157.10	2053406.00	6018955.00	CPT
SFO	Fugro West	2000	00LC-33	152.60	2054719.00	6019691.00	CPT
SFO	Fugro West	2000	00LC-34	164.80	2052178.00	6021171.00	CPT
SFO	Fugro West	2000	00LC-35	122.00	2053085.00	6017944.00	CPT
SFO	Fugro West	2000	00LC-36	91.30	2051449.00	6020207.00	CPT
SFO	Fugro West	2000	00LC-37	164.30	2051946.00	6017470.00	CPT
SFO	Fugro West	2000	00LC-38	121.80	2050453.00	6018537.00	CPT
SFO	Fugro West	2000	00LC-39	166.10	2052745.00	6018669.00	CPT



Airport <sup>1</sup>	Report Preparer	Exploration Year	Borehole or CPT ID	Total Depth (feet)	Northing (UTM, meters)	Easting (UTM, meters)	Exploration Method <sup>2</sup>
SFO	Fugro West	2000	00LC-40	101.30	2056164.00	6015416.00	CPT
SFO	Fugro West	2000	00LC-41	165.80	2051916.00	6023021.00	CPT
SFO	Fugro West	2000	00LC-50	106.60	2056991.00	6014741.00	CPT
SFO	Fugro West	2000	00LC-51	96.10	2056299.10	6014858.80	CPT
SFO	Fugro West	2000	00LC-52	116.90	2054831.90	6015380.40	CPT
SFO	Fugro West	2000	00LC-53	145.10	2055557.00	6015667.80	CPT
SFO	Fugro West	2000	00LC-54	112.20	2056623.80	6017774.80	CPT
SFO	Fugro West	2000	00LC-55	138.30	2054109.70	6016681.50	CPT
SFO	Fugro West	2000	00LC-56	156.60	2054758.80	6016984.00	CPT
SFO	Fugro West	2000	00LC-57	134.10	2053420.70	6017391.70	CPT
SFO	Fugro West	2000	00LC-58	128.20	2054535.50	6018047.00	CPT
SFO	Fugro West	2000	00LC-59	142.00	2054992.60	6018751.70	CPT
SFO	Fugro West	2000	00LC-60	150.90	2056277.20	6019402.10	CPT
SFO	Fugro West	2000	00LC-61	157.70	2056009.90	6019840.70	CPT
SFO	Fugro West	2000	00LC-62	129.50	2052585.50	6017902.40	CPT
SFO	Fugro West	2000	00LC-63	135.80	2053802.90	6019447.90	CPT
SFO	Fugro West	2000	00LC-64	122.30	2055259.00	6020003.40	CPT
SFO	Fugro West	2000	00LC-65	132.80	2056217.60	6020626.00	CPT
SFO	Fugro West	2000	00LC-66	116.70	2048967.30	6017717.70	CPT
SFO	Fugro West	2000	00LC-67	134.70	2050552.10	6018170.40	CPT
SFO	Fugro West	2000	00LC-68	145.10	2051483.30	6018195.10	CPT
SFO	Fugro West	2000	00LC-69	121.60	2052078.50	6018524.20	CPT
SFO	Fugro West	2000	00LC-70	127.90	2050809.20	6018778.40	CPT



Airport <sup>1</sup>	Report Preparer	Exploration Year	Borehole or CPT ID	Total Depth (feet)	Northing (UTM, meters)	Easting (UTM, meters)	Exploration Method <sup>2</sup>
SFO	Fugro West	2000	00LC-71	142.60	2051756.80	6019767.80	CPT
SFO	Fugro West	2000	00LC-72	158.30	2052260.70	6019463.50	CPT
SFO	Fugro West	2000	00LC-73	155.60	2052272.80	6019955.20	CPT
SFO	Fugro West	2000	00LC-74	150.30	2053894.40	6020453.30	CPT
SFO	Fugro West	2000	00LC-75	127.50	2054440.10	6020668.30	CPT
SFO	Fugro West	2000	00LC-76	128.20	2055074.20	6021001.40	CPT
SFO	Fugro West	2000	00LC-77	127.30	2055499.40	6020963.90	CPT
SFO	Fugro West	2000	00LC-78	158.30	2055376.10	6021179.80	CPT
SFO	Fugro West	2000	00LC-79	158.20	2052926.50	6020956.70	CPT
SFO	Fugro West	2000	00LC-80	157.90	2051019.60	6020923.10	CPT
SFO	Fugro West	2000	00LC-81	158.50	2051221.30	6021040.30	CPT
SFO	Fugro West	2000	00LC-82	158.60	2052845.40	6021497.80	CPT
SFO	Fugro West	2000	00LC-83	158.20	2053176.80	6021720.40	CPT
SFO	Fugro West	2000	00LC-84	131.50	2050328.60	6022113.10	CPT
SFO	Fugro West	2000	00LC-85	83.20	2052290.50	6022659.50	CPT
SFO	Fugro West	2000	00LC-86	126.00	2050126.50	6022484.20	CPT
SFO	Fugro West	2000	00LC-87	126.20	2050395.10	6023058.50	CPT
SFO	Fugro West	2000	00LC-88	154.90	2050976.40	6023273.50	CPT
SFO	Fugro West	2000	00LC-89	83.40	2051648.40	6023623.30	CPT
SFO	Fugro West	2000	00LC-90	151.20	2051982.00	6023843.30	CPT
SFO	Fugro West	2000	00LC-91	145.30	2050160.50	6023446.30	CPT
SFO	Fugro West	2000	00LC-92	155.30	2050796.20	6023617.70	CPT
SFO	Fugro West	2000	00LC-93	128.70	2051327.70	6024152.20	CPT



Airport <sup>1</sup>	Report Preparer	Exploration Year	Borehole or CPT ID	Total Depth (feet)	Northing (UTM, meters)	Easting (UTM, meters)	Exploration Method <sup>2</sup>
SFO	Fugro West	2000	00LC-94	158.10	2053673.50	6020804.20	CPT
NUQ	USGS	2000	USC-01	42.98	1973719.09	6113257.49	CPT
NUQ	USGS	2000	USC-02	56.10	1975692.76	6112492.65	CPT
NUQ	USGS	2000	USC-03	59.55	1978442.74	6111423.49	CPT
NUQ	USGS	2000	USC-04	52.49	1980552.58	6110599.92	CPT
NUQ	USGS	2000	USC-05	49.54	1981223.01	6109340.75	CPT
NUQ	USGS	2000	USC-06	73.65	1973632.85	6111935.48	CPT
NUQ	USGS	2000	USC-07	52.00	1972649.71	6114827.75	CPT
NUQ	TetraTech	2005	TTC-01	61.00	1976530.08	6110055.58	CPT
NUQ	TetraTech	2005	TTC-02	61.00	1976700.85	6110072.11	CPT
NUQ	TetraTech	2005	TTC-03	61.00	1975962.65	6110452.22	CPT
NUQ	TetraTech	2005	TTC-04	61.00	1975937.86	6110642.28	CPT
NUQ	TetraTech	2005	TTC-05	61.00	1976249.12	6110361.33	CPT
NUQ	TetraTech	2005	TTC-06	61.00	1975915.83	6110336.54	CPT
NUQ	TetraTech	2005	TTC-07	61.00	1976059.06	6110427.43	CPT
LVK	Cornerstone Earth Group	2010	EB-1	10.00	2077874.00	6177354.00	HSA
LVK	Cornerstone Earth Group	2010	EB-2	10.00	2077828.00	6178562.00	HSA
LVK	Cornerstone Earth Group	2010	EB-3	10.00	2077846.00	6179690.00	HSA
LVK	Cornerstone Earth Group	2010	EB-4	10.00	2077755.00	6181112.00	HSA
LVK	Cornerstone Earth Group	2010	EB-5	11.00	2077765.00	6182100.00	HSA
LVK	Cornerstone Earth Group	2010	EB-6	10.00	2078213.00	6182291.00	HSA
LVK	Cornerstone Earth Group	2010	EB-7	10.00	2078176.00	6182047.00	HSA
LVK	Cornerstone Earth Group	2010	EB-8	10.00	2078186.00	6181776.00	HSA



Airport <sup>1</sup>	Report Preparer	Exploration Year	Borehole or CPT ID	Total Depth (feet)	Northing (UTM, meters)	Easting (UTM, meters)	Exploration Method <sup>2</sup>
CCR	Kleinfelder and Associates, Inc.	1987	KL87-16	8.00	2185492.00	6113366.00	HSA
CCR	Kleinfelder and Associates, Inc.	1987	KL87-20	8.00	2184109.00	6111533.00	HSA
CCR	Kleinfelder and Associates, Inc.	1987	KL87-21	6.00	2184684.00	6111555.00	HSA
CCR	Kleinfelder and Associates, Inc.	1987	KL87-22	8.00	2185226.00	6111831.00	HSA
CCR	Kleinfelder and Associates, Inc.	1987	KL87-25	6.50	2185702.00	6112018.00	HSA
CCR	Kleinfelder and Associates, Inc.	1987	KL87-26	8.00	2186241.00	6112266.00	HSA
CCR	Kleinfelder and Associates, Inc.	1987	KL87-28	6.00	2186743.00	6112504.00	HSA
CCR	Kleinfelder and Associates, Inc.	1987	KL87-29	8.00	2186582.00	6112793.00	HSA
CCR	Kleinfelder and Associates, Inc.	1987	KL87-30	8.00	2187224.00	6112526.00	HSA
CCR	Kleinfelder and Associates, Inc.	1987	KL87-44	7.50	2187746.00	6112339.00	HSA
CCR	Kleinfelder and Associates, Inc.	1987	KL87-45	7.50	2188239.00	6112115.00	HSA
CCR	Kleinfelder and Associates, Inc.	1987	KL87-46	7.50	2188745.00	6111890.00	HSA
CCR	Kleinfelder and Associates, Inc.	1987	KL87-47	7.50	2188931.00	6112267.00	HSA
CCR	Kleinfelder and Associates, Inc.	1987	KL87-51	8.00	2188179.00	6112965.00	HSA
CCR	Kleinfelder and Associates, Inc.	1987	KL87-52	8.00	2187655.00	6113128.00	HSA
CCR	Kleinfelder and Associates, Inc.	1987	KL87-55	8.00	2187386.00	6112768.00	HSA
CCR	Kleinfelder and Associates, Inc.	1987	KL87-76	6.50	2187738.00	6113549.00	HSA
CCR	Kleinfelder and Associates, Inc.	1987	KL87-87	9.00	2187104.00	6112646.00	HSA
CCR	Kleinfelder and Associates, Inc.	1987	KL87-88	9.50	2186101.00	6113017.00	HSA
CCR	Parikh Consultants, Inc.	2011	PRK11-1	7.00	2183956.00	6111815.00	HSA
CCR	Parikh Consultants, Inc.	2011	PRK11-2	7.00	2184733.00	6112081.00	HSA
CCR	Parikh Consultants, Inc.	2011	PRK11-3	7.00	2185397.00	6112506.00	HSA
CCR	Parikh Consultants, Inc.	2011	PRK11-4	7.50	2185967.00	6112643.00	HSA



Airport <sup>1</sup>	Report Preparer	Exploration Year	Borehole or CPT ID	Total Depth (feet)	Northing (UTM, meters)	Easting (UTM, meters)	Exploration Method <sup>2</sup>
CCR	Parikh Consultants, Inc.	2011	PRK11-5	7.00	2186629.00	6113022.00	HSA
CCR	Parikh Consultants, Inc.	2011	PRK11-6	7.00	2187326.00	6113282.00	HSA
CCR	Parikh Consultants, Inc.	2011	PRK11-7	7.00	2188052.00	6113640.00	HSA
CCR	Parikh Consultants, Inc.	2011	PRK11-8	7.00	2188245.00	6113680.00	HSA
CCR	Peter Kaldveer and Associates, Inc.	1990	KA90-1	31.50	2188088.00	6111994.00	HSA
CCR	Peter Kaldveer and Associates, Inc.	1990	KA90-2	21.50	2187932.00	6111995.00	HSA
CCR	Peter Kaldveer and Associates, Inc.	1990	KA90-3	23.50	2187934.00	6111866.00	HSA
CCR	Peter Kaldveer and Associates, Inc.	1990	KA90-4	5.00	2187877.00	6111891.00	HSA
CCR	Peter Kaldveer and Associates, Inc.	1990	KA90-5	5.00	2188017.00	6112044.00	HSA
CCR	Peter Kaldveer and Associates, Inc.	1990	KA90-6	6.00	2188136.00	6111923.00	HSA
CCR	Peter Kaldveer and Associates, Inc.	1983	KA83-1	30.00	2184653.00	6110756.00	HSA
CCR	Peter Kaldveer and Associates, Inc.	1983	KA83-2	30.00	2184789.00	6110688.00	HSA
CCR	Peter Kaldveer and Associates, Inc.	1983	KA83-3	23.50	2184820.00	6110816.00	HSA
CCR	Peter Kaldveer and Associates, Inc.	1983	KA83-PB2	25.00	2184745.00	6110806.00	HSA
CCR	Peter Kaldveer and Associates, Inc.	1983	KA83-PB4	25.00	2184563.00	6110830.00	HSA
CCR	Peter Kaldveer and Associates, Inc.	1983	KA83-PB5	30.00	2184609.00	6110698.00	HSA
CCR	Peter Kaldveer and Associates, Inc.	1983	KA83-PP1	20.00	2184728.00	6110680.00	HSA
CCR	Peter Kaldveer and Associates, Inc.	1983	KA83-PP3	20.00	2184656.00	6110817.00	HSA
CCR	Peter Kaldveer and Associates, Inc.	1983	KA83-PP4	20.00	2184510.00	6110709.00	HSA
CCR	Peter Kaldveer and Associates, Inc.	1981	KA81-1	10.00	2189182.00	6111721.00	HSA
CCR	Peter Kaldveer and Associates, Inc.	1981	KA81-2	40.00	2188718.00	6111794.00	HSA
CCR	Peter Kaldveer and Associates, Inc.	1981	KA81-3	50.00	2188550.00	6111908.00	HSA
CCR	Peter Kaldveer and Associates, Inc.	1981	KA81-4	38.00	2188717.00	6111597.00	HSA



Airport <sup>1</sup>	Report Preparer	Exploration Year	Borehole or CPT ID	Total Depth (feet)	Northing (UTM, meters)	Easting (UTM, meters)	Exploration Method <sup>2</sup>
CCR	Peter Kaldveer and Associates, Inc.	1981	KA81-5	50.00	2188713.00	6111375.00	HSA
CCR	Peter Kaldveer and Associates, Inc.	1981	KA81-6	40.00	2188540.00	6111374.00	HSA
CCR	Peter Kaldveer and Associates, Inc.	1981	KA81-7	30.50	2188545.00	6111636.00	HSA
CCR	Peter Kaldveer and Associates, Inc.	1981	KA81-8	20.00	2188628.00	6111481.00	HSA
CCR	Peter Kaldveer and Associates, Inc.	1981	KA81-9	20.00	2188520.00	6111444.00	HSA
CCR	Peter Kaldveer and Associates, Inc.	1981	KA81-101	25.00	2189169.00	6113316.00	HSA
CCR	Peter Kaldveer and Associates, Inc.	1981	KA81-102	50.00	2188829.00	6113114.00	HSA
CCR	Peter Kaldveer and Associates, Inc.	1981	KA81-103	50.00	2189325.00	6113039.00	HSA
CCR	Peter Kaldveer and Associates, Inc.	1981	KA81-104	48.50	2189778.00	6113005.00	HSA
CCR	Peter Kaldveer and Associates, Inc.	1981	KA81-105	25.00	2189623.00	6112724.00	HSA
CCR	Peter Kaldveer and Associates, Inc.	1983	KA83-101	25.00	2188023.00	6111946.00	HSA
CCR	Peter Kaldveer and Associates, Inc.	1983	KA83-102	20.00	2187964.00	6111978.00	HSA
CCR	Peter Kaldveer and Associates, Inc.	1983	KA83-103	20.00	2188033.00	6112021.00	HSA
CCR	Peter Kaldveer and Associates, Inc.	1983	KA83-A1	15.00	2188114.00	6111720.00	HSA
CCR	Peter Kaldveer and Associates, Inc.	1983	KA83-A2	20.00	2187987.00	6111767.00	HSA
CCR	Peter Kaldveer and Associates, Inc.	1983	KA83-A3	20.00	2187986.00	6111674.00	HSA

Notes:

- SFO: San Francisco International Airport  
OAK: Oakland International Airport  
CCR: Buchanan Field Airport  
LVK: Livermore Municipal Airport  
NUQ: Moffett Federal Airfield

- HAS: Hollow Stem Auger  
RSB: Rotary Sample Boring (Wet)  
CPT: Cone Penetrometer Test

## Appendix D

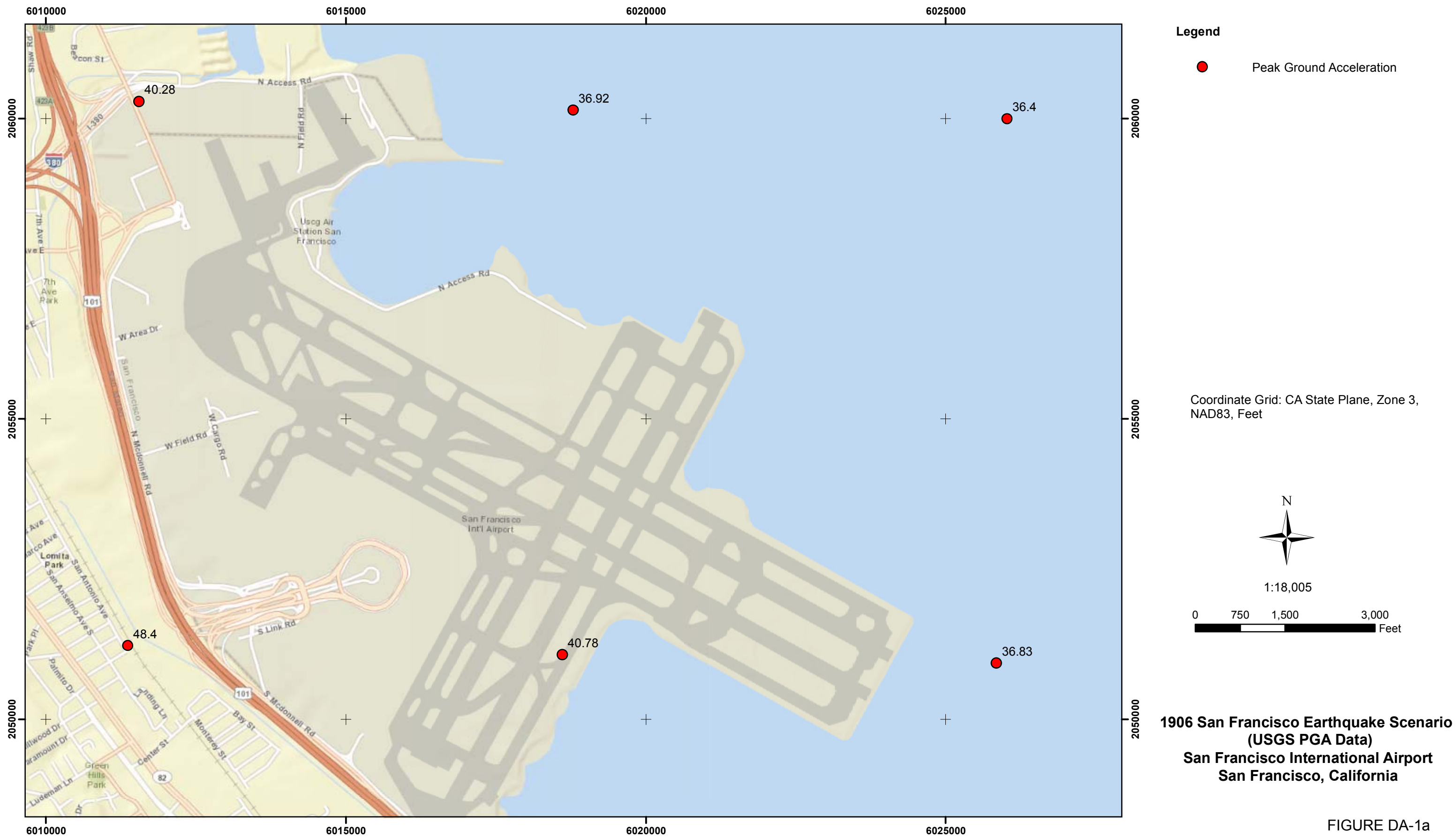
### Liquefaction Analyses

#### LIST OF FIGURES

---

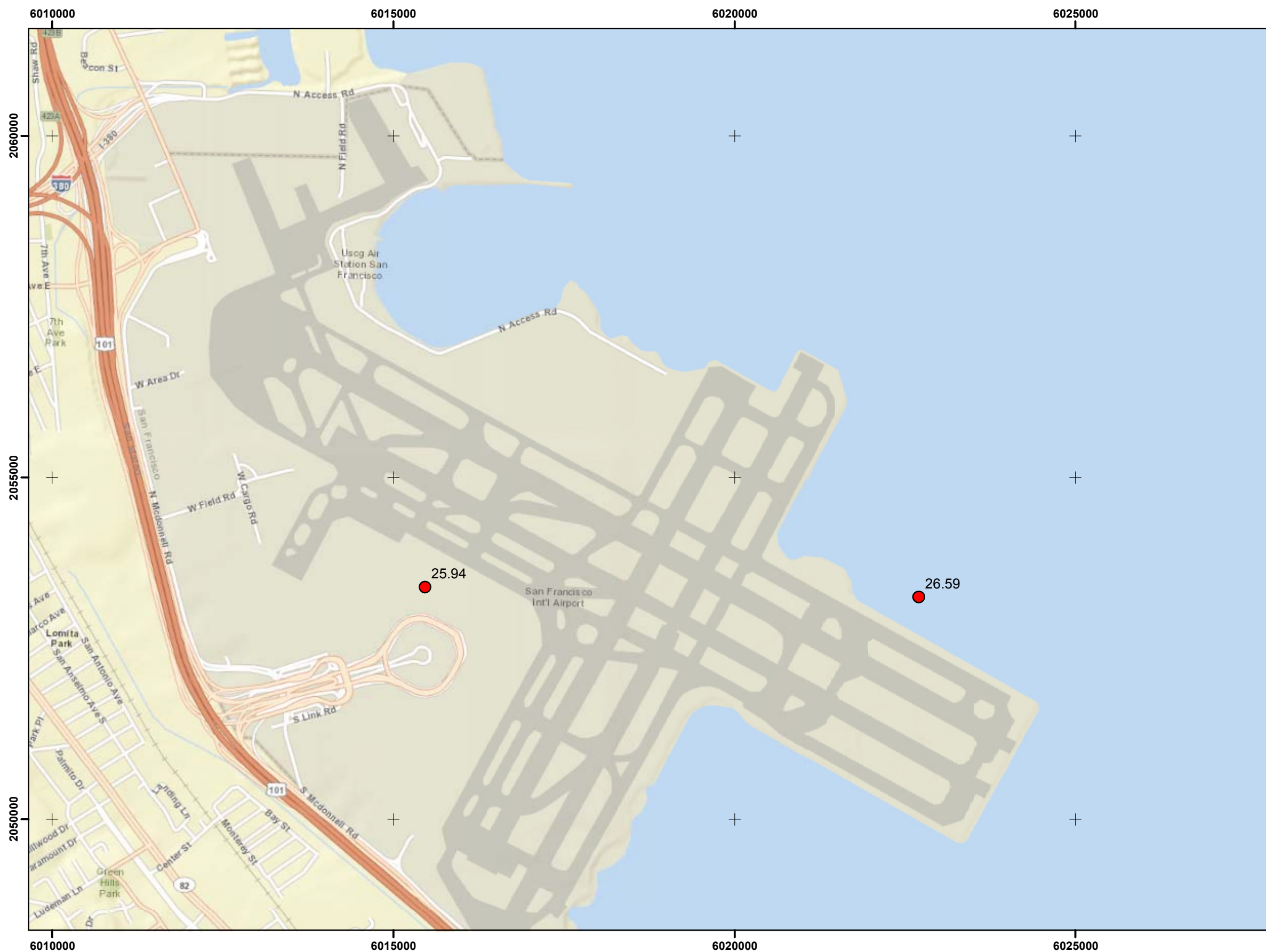
Figures DA-1 through DA-5	USGS PDA Data, All Airports
Figures DB-1 through DB-8	Geotechnical Data and Liquefaction Analysis Results, San Francisco International Airport
Figures DC-1 through DB-8	Geotechnical Data and Liquefaction Analysis Results, Oakland International Airport
Figures DD-1 through DB-8	Geotechnical Data and Liquefaction Analysis Results, Moffett Field Airport
Figures DE-1 through DB-2	Geotechnical Data, Livermore Municipal Airport
Figures DF-1 through DF-8	Geotechnical Data and Liquefaction Analysis Results, Moffett Federal Airfield

---



N:\Projects\04\_2012\04\_7922\_1200\_CaltransAirportRecov\Outputs\2013\_03\_05\_Report\mxd\Fig\_DA01a\_SFO\_PGA\_1906Scenario.mxd, 03/21/13, dpollard

FIGURE DA-1a



Legend

- Peak Ground Acceleration

Coordinate Grid: CA State Plane, Zone 3,  
NAD83, Feet



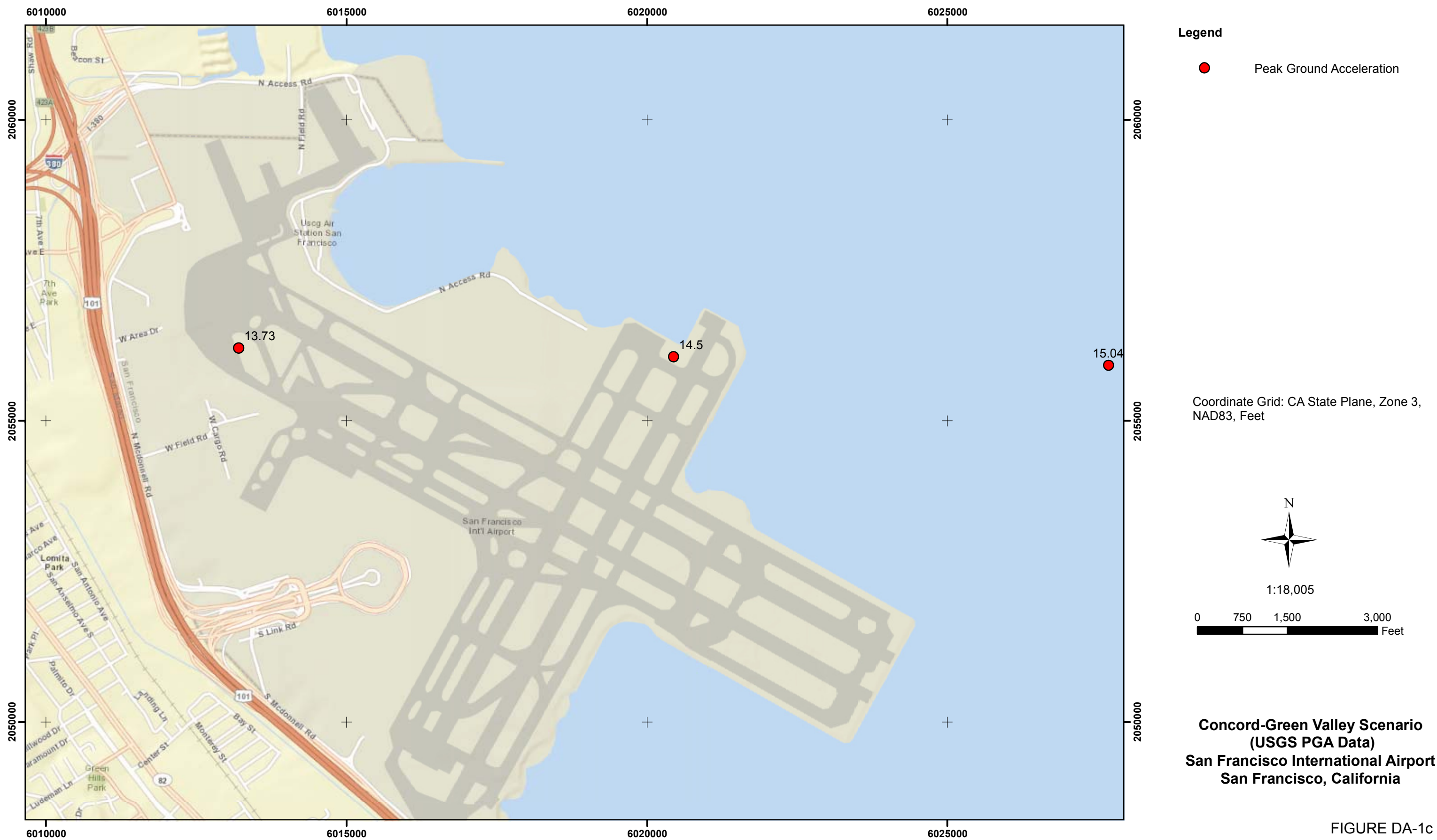
1:18,005



**Hayward-Rodgers Creek Scenario  
(USGS PGA Data)  
San Francisco International Airport  
San Francisco, California**

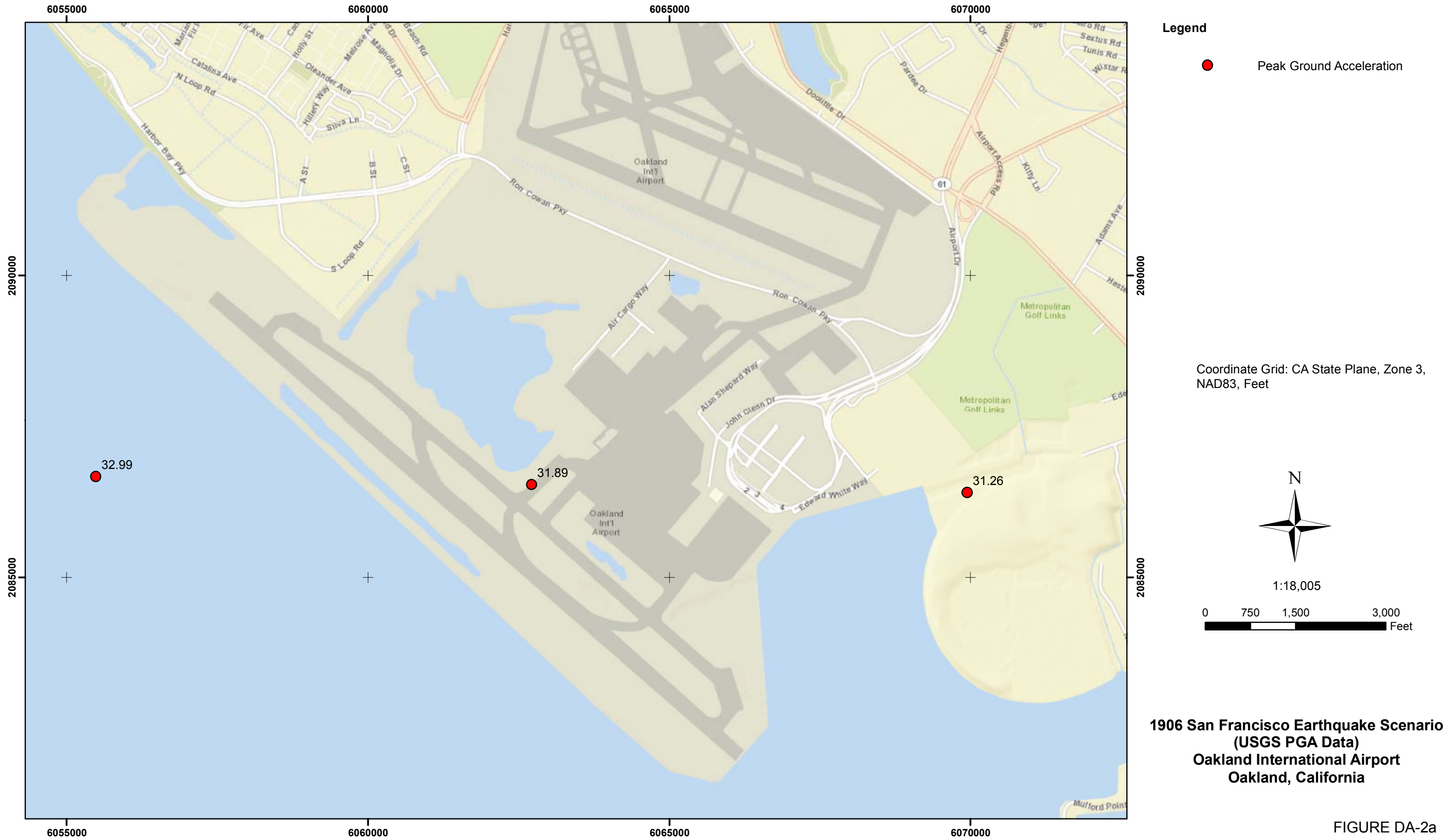
FIGURE DA-1b

N:\Projects\04\_2012\04\_7922\_1200\_CaltransAirportRecov\Outputs\2013\_03\_05\_Report\mxd\Fig\_DA01b\_SFO\_PGA\_HRCScenario.mxd, 03/21/13, dpollard



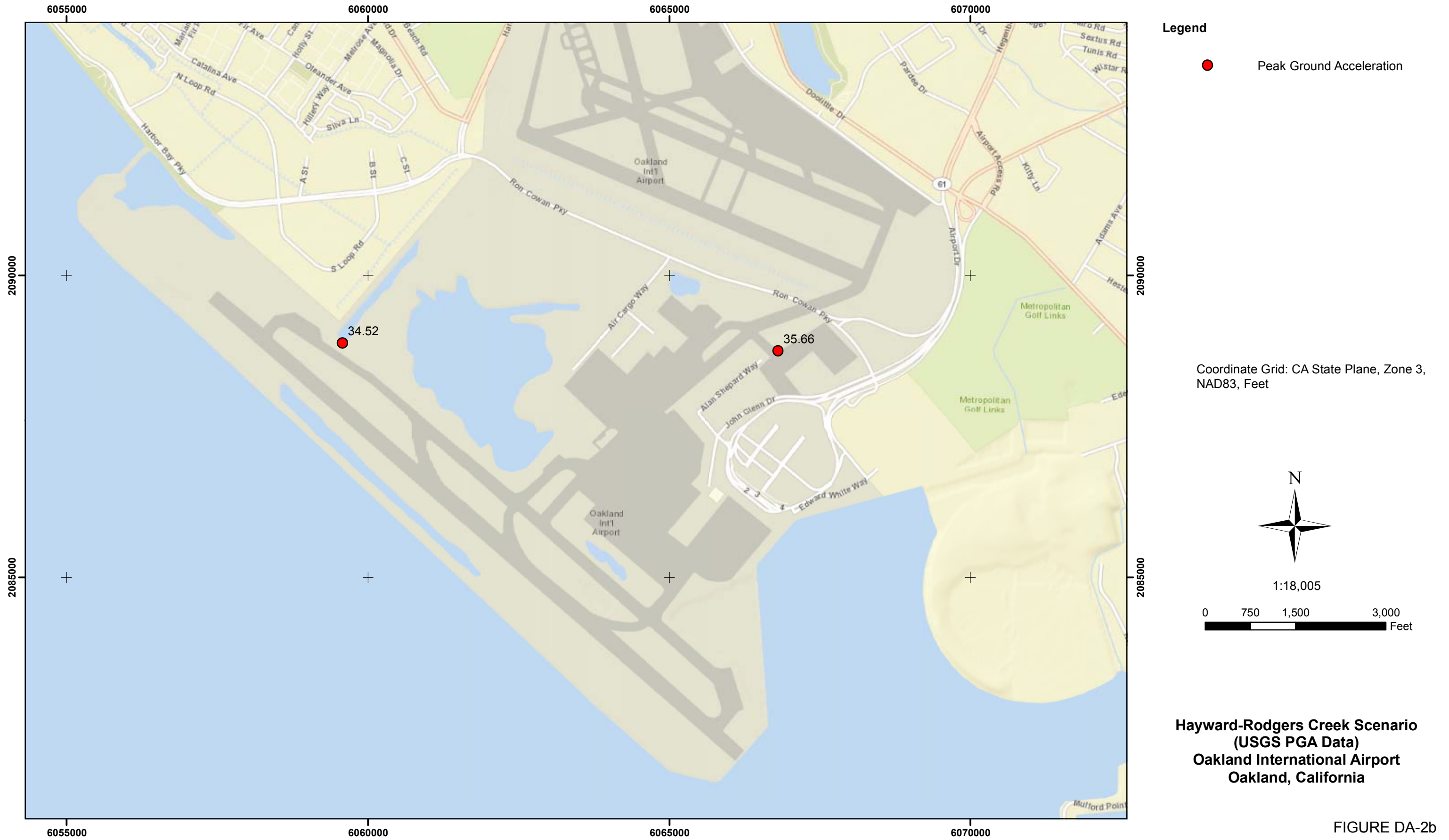
N:\Projects\04\_2012\04\_7922\_1200\_CaltransAirportRecov\Outputs\2013\_03\_05\_Report\mxd\Fig\_DA01c\_SFO\_PGA\_CGVScenario.mxd, 03/21/13, dpollard

FIGURE DA-1c



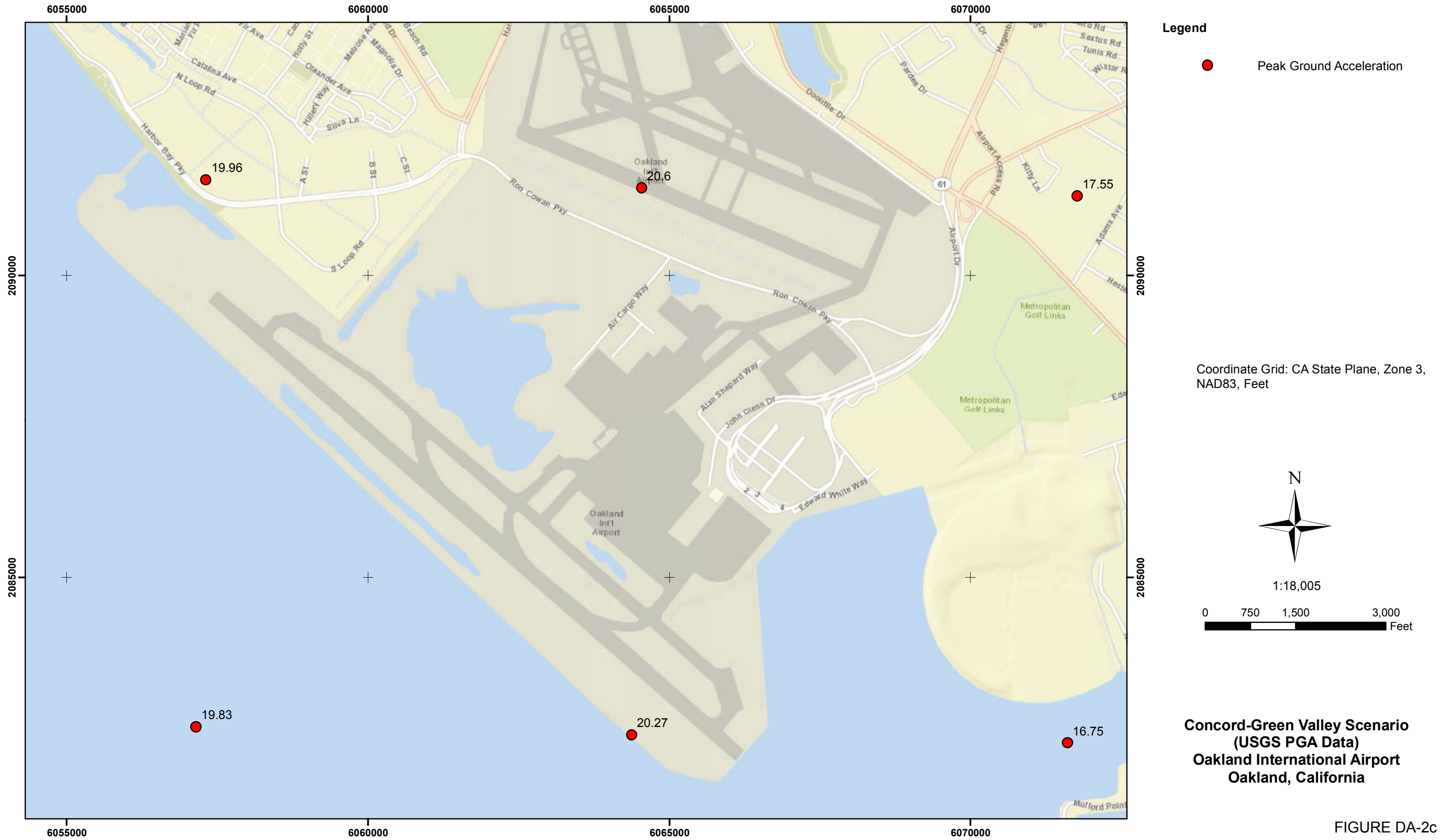
N:\Projects\04\_2012\04\_7922\_1200\_CaltransAirportRecov\Outputs\2013\_03\_05\_Report\mxd\Fig\_DA02a\_OAK\_PGA\_1906Scenario.mxd, 03/21/13, dpollard

FIGURE DA-2a



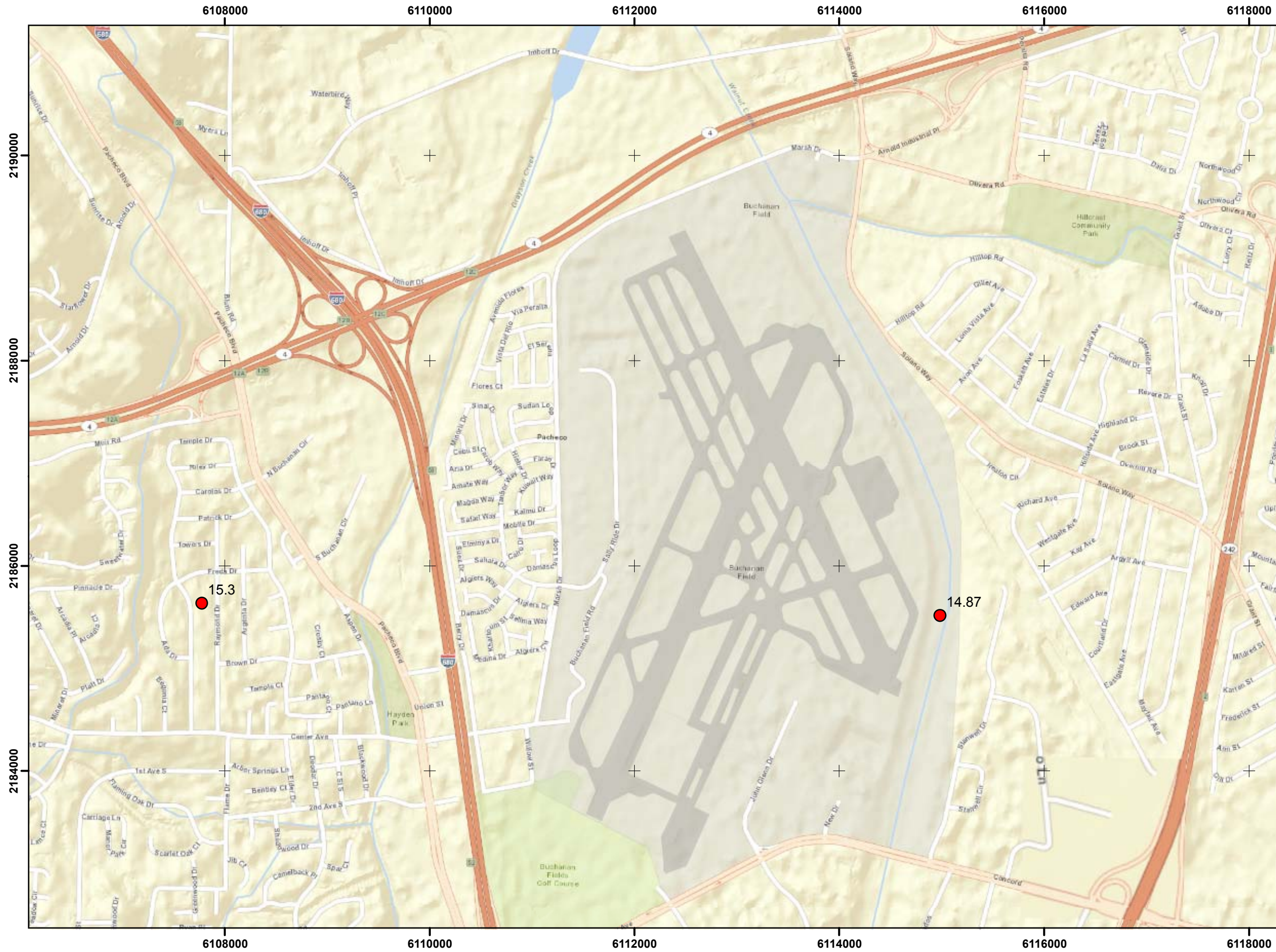
N:\Projects\04\_2012\04\_7922\_1200\_CaltransAirportRecov\Outputs\2013\_03\_05\_Report\mxd\Fig\_DA02b\_OAK\_PGA\_HRCScenario.mxd, 03/21/13, dpollard

FIGURE DA-2b



N:\Projects\04\_2012\04\_7922\_1200\_CaltransAirportRecov\Outputs\2013\_03\_05\_Report\mxd\Fig\_DA02c\_OAK\_PGA\_CGVScenario.mxd, 03/21/13, dpollard

FIGURE DA-2c



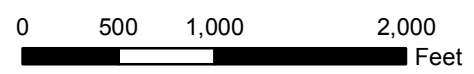
**Legend**

- Peak Ground Acceleration

Coordinate Grid: CA State Plane, Zone 3, NAD83, Feet



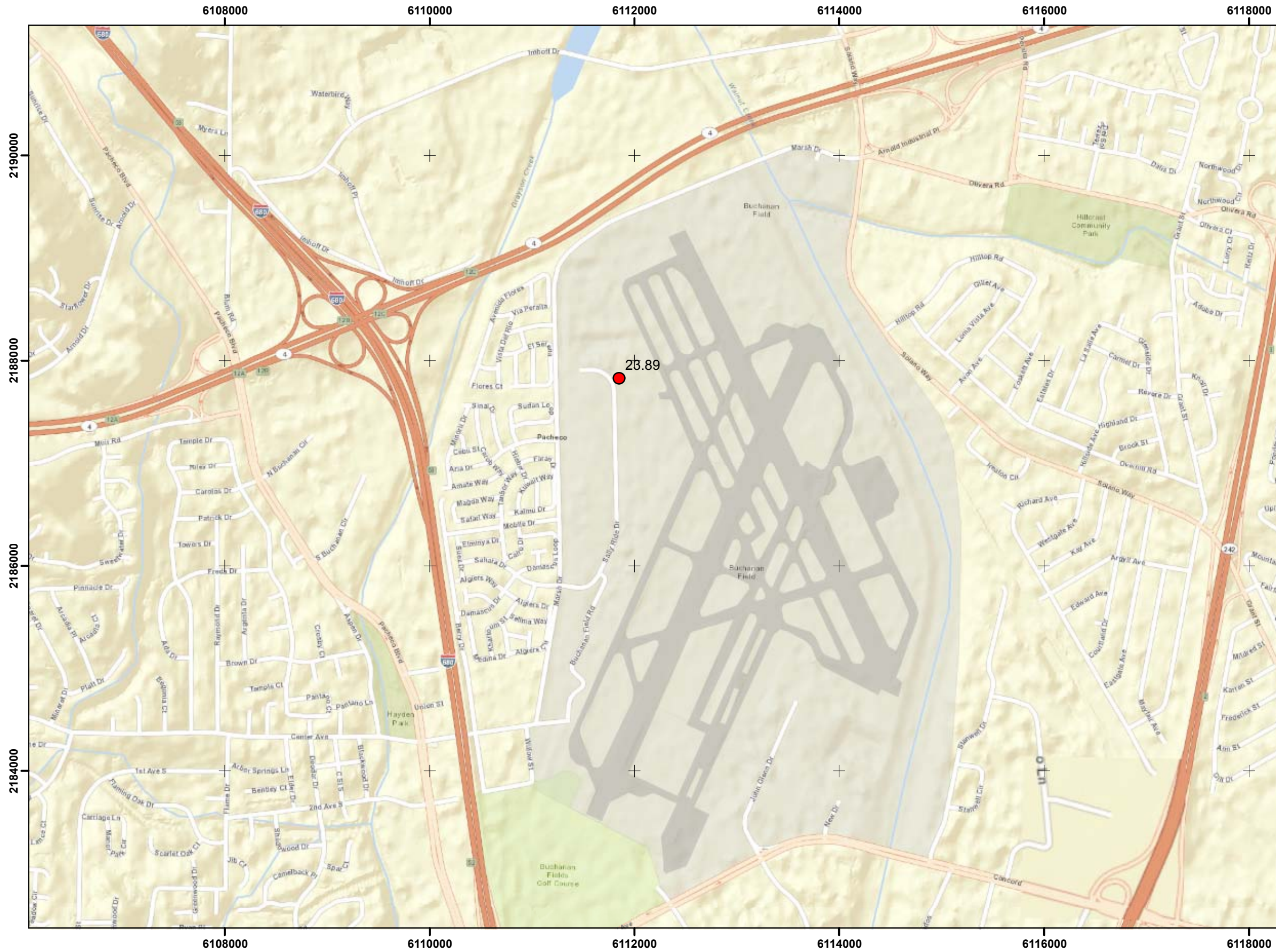
1:12,003



**1906 San Francisco Earthquake Scenario  
(USGS PGA Data)  
Buchanan Airport  
Concord, California**

FIGURE DA-3a

N:\Projects\04\_2012\04\_7922\_1200\_CaltransAirportRecon\Outputs\2013\_03\_05\_Report\mxd\Fig\_DA03a\_BUC\_PGA\_1906Scenario.mxd, 03/21/13, dpollard



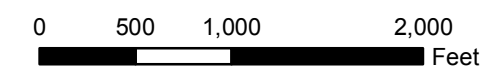
**Legend**

- Peak Ground Acceleration

Coordinate Grid: CA State Plane, Zone 3, NAD83, Feet



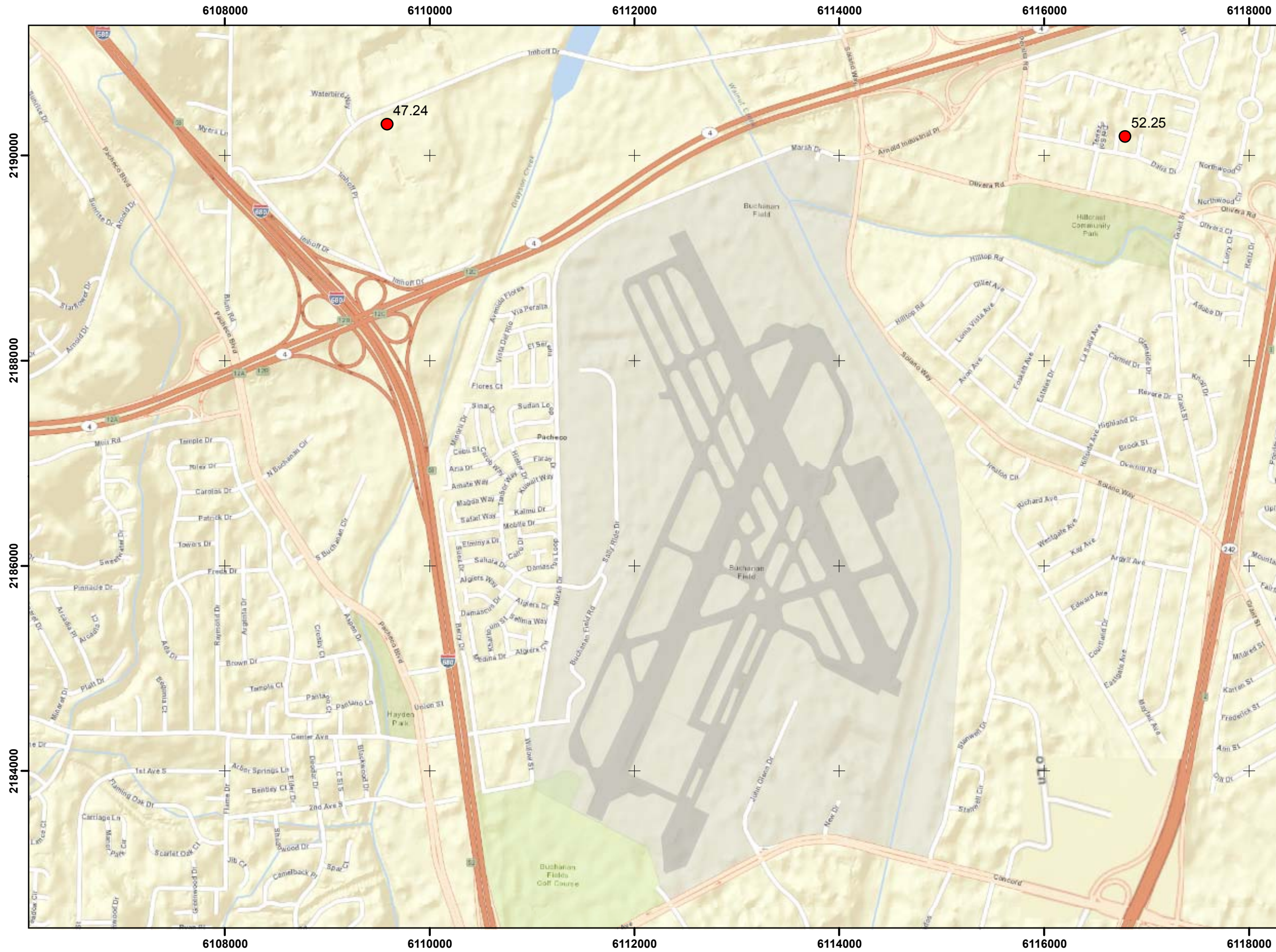
1:12,003



**Hayward-Rodgers Creek Scenario  
 (USGS PGA Data)  
 Buchanan Airport  
 Concord, California**

FIGURE DA-3b

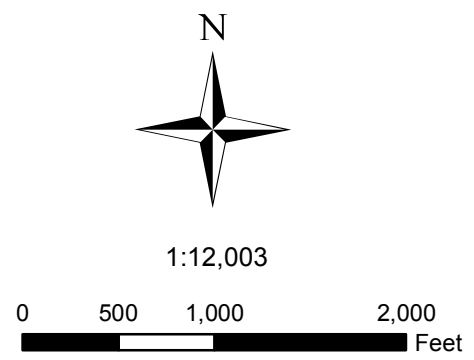
N:\Projects\04\_2012\04\_7922\_1200\_CaltransAirportRecon\Outputs\2013\_03\_05\_Report\mxd\Fig\_DA03b\_BUC\_PGA\_HRCScenario.mxd, 03/21/13, dpollard



**Legend**

- Peak Ground Acceleration

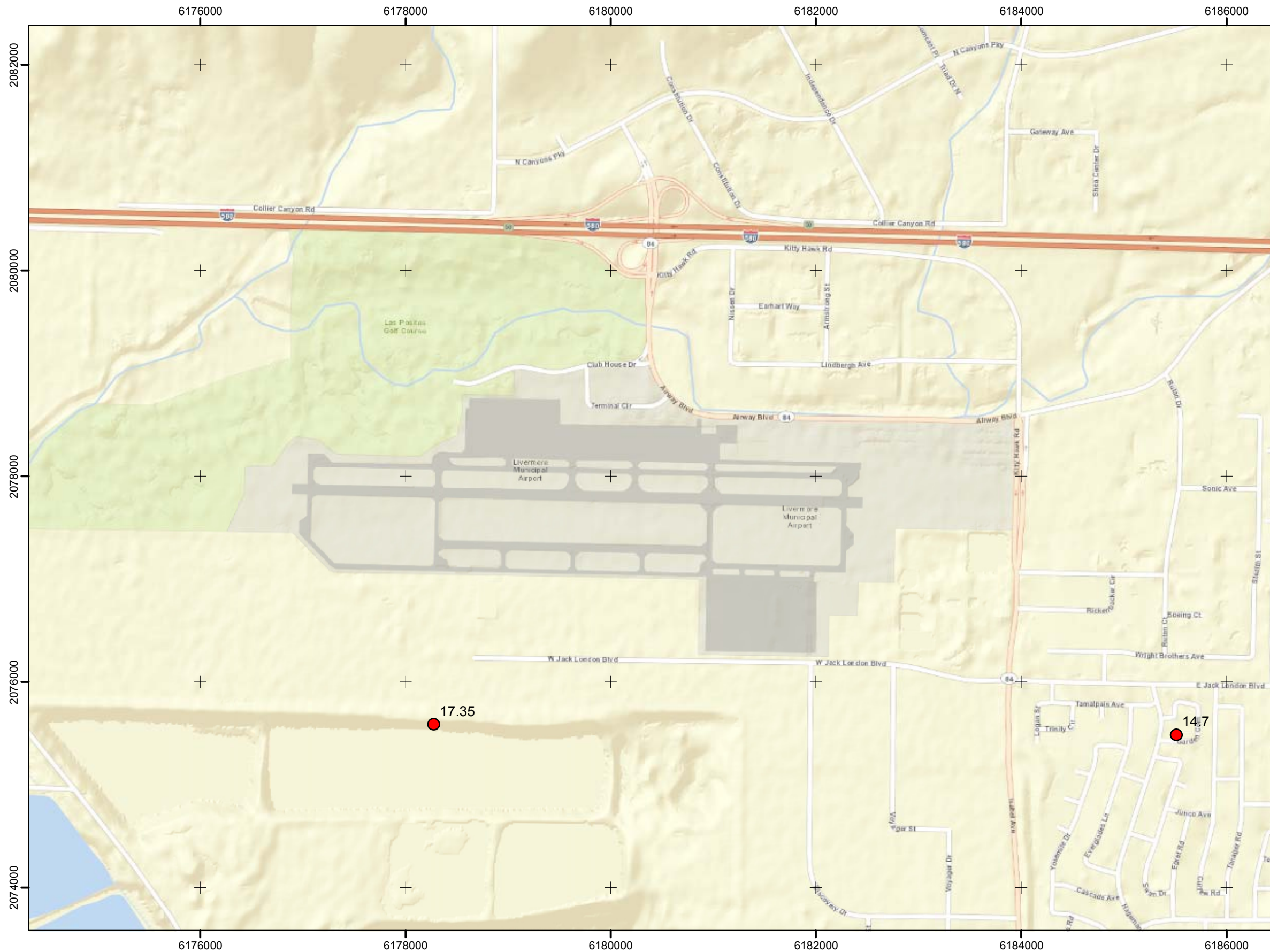
Coordinate Grid: CA State Plane, Zone 3, NAD83, Feet



**Concord-Green Valley Scenario  
 (USGS PGA Data)  
 Buchanan Airport  
 Concord, California**

FIGURE DA-3c

N:\Projects\04\_2012\04\_7922\_1200\_CaltransAirportRecov\Outputs\2013\_03\_05\_Report\mxd\Fig\_DA03c\_BUC\_PGA\_CGVScenario.mxd, 03/21/13, dpollard



**Legend**

- Peak Ground Acceleration

Coordinates System: CA State Plane,  
Zone 3, NAD83, Feet



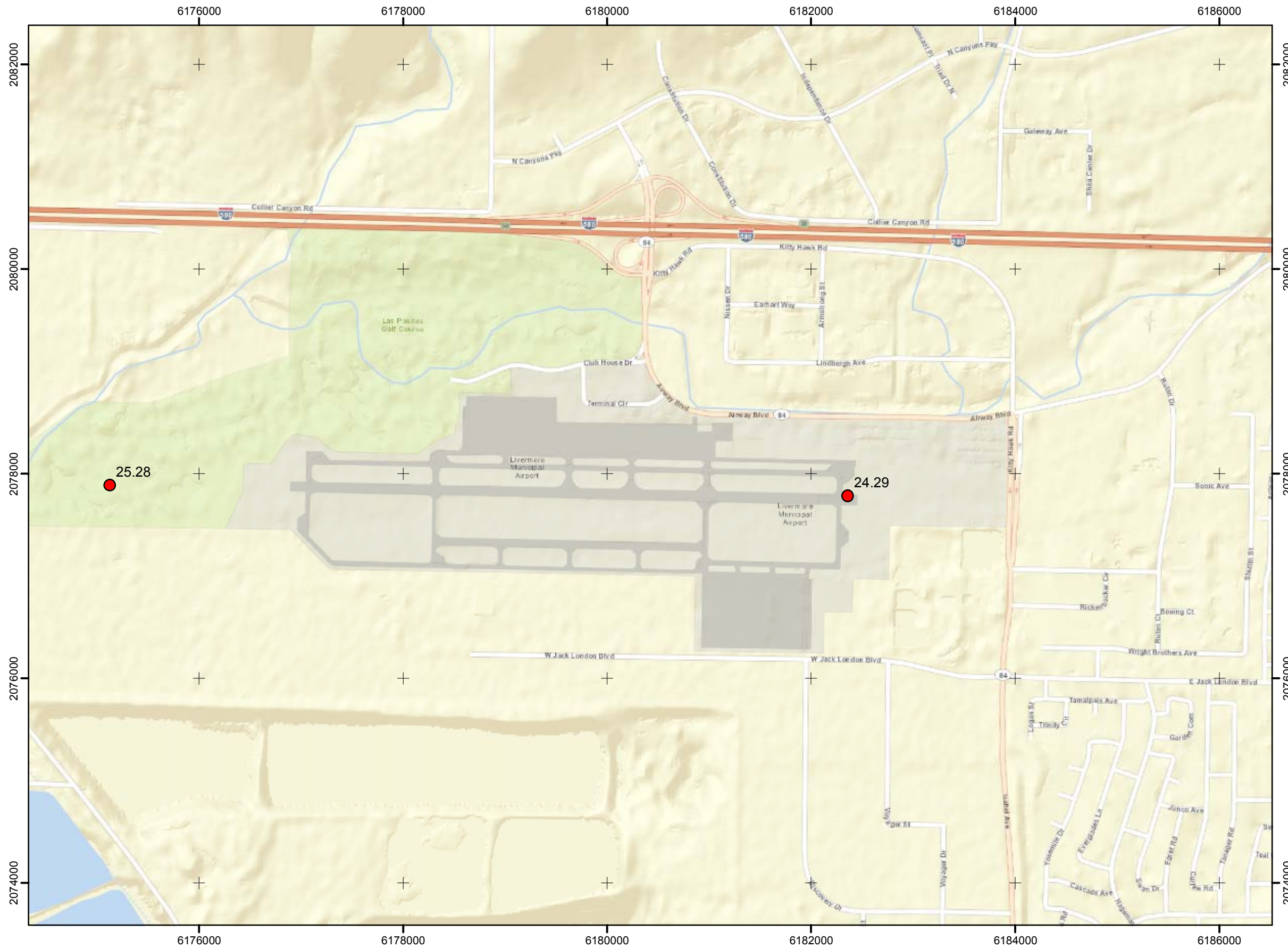
1:12,003



**1906 San Francisco Earthquake Scenario  
(USGS PGA Data)  
Livermore Airport  
Livermore, California**

FIGURE DA-4a

N:\Projects\04\_2012\04\_7922\_1200\_CaltransAirportRecov\Outputs\2013\_03\_05\_Report\mxd\Fig\_DA04a\_LIV\_PGA\_1906Scenario.mxd, 03/21/13, dpollard



**Legend**

- Peak Ground Acceleration

Coordinates System: CA State Plane,  
Zone 3, NAD83, Feet



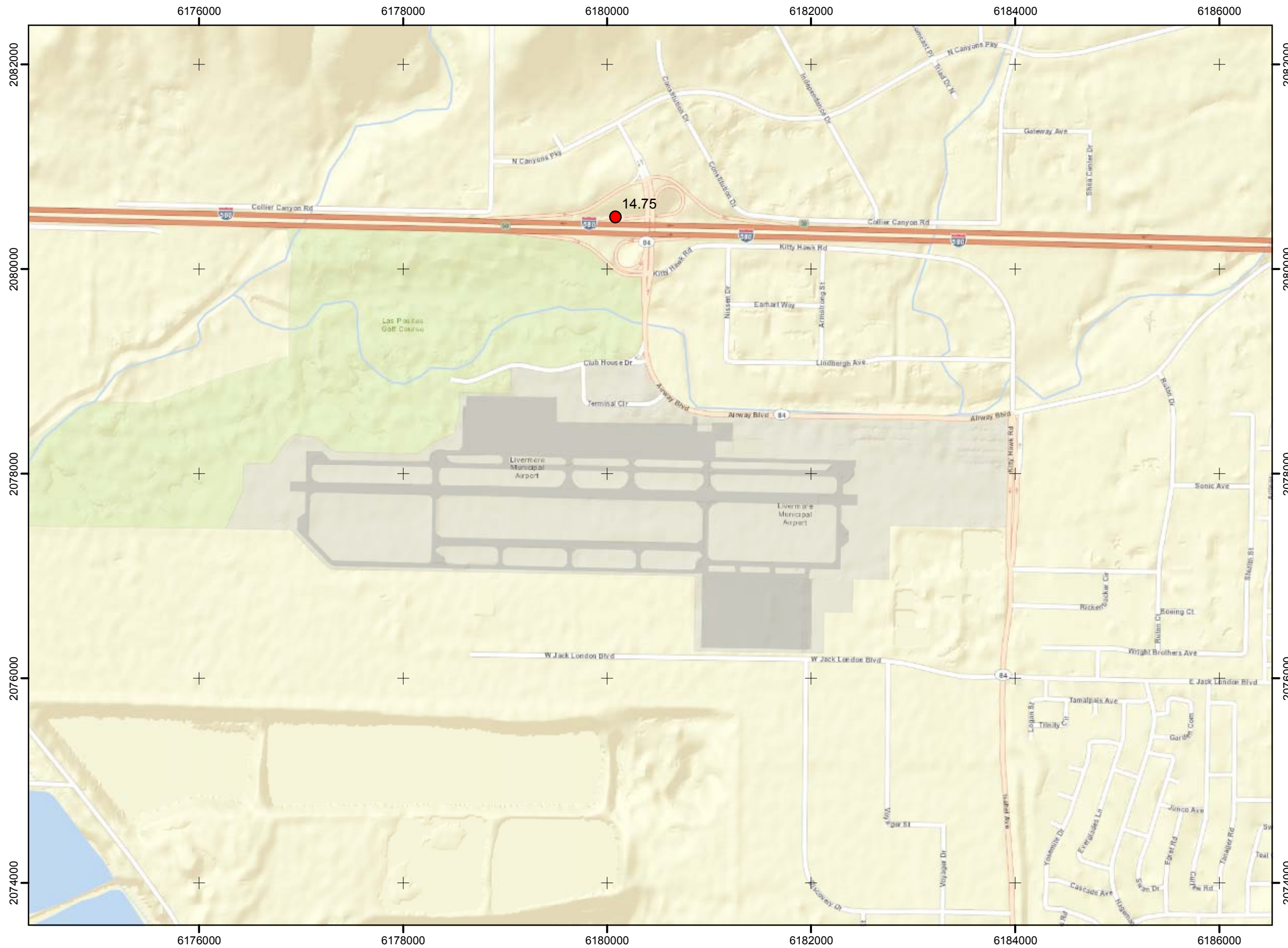
1:12,003



**Hayward-Rodgers Creek Scenario  
(USGS PGA Data)  
Livermore Airport  
Livermore, California**

FIGURE DA-4b

N:\Projects\04\_2012\04\_7922\_1200\_CaltransAirportRecov\Outputs\2013\_03\_05\_Report\mxd\Fig\_DA04b\_LIV\_PGA\_HRCScenario.mxd, 03/21/13, cpollard



**Legend**

-  Peak Ground Acceleration

Coordinates System: CA State Plane,  
Zone 3, NAD83, Feet

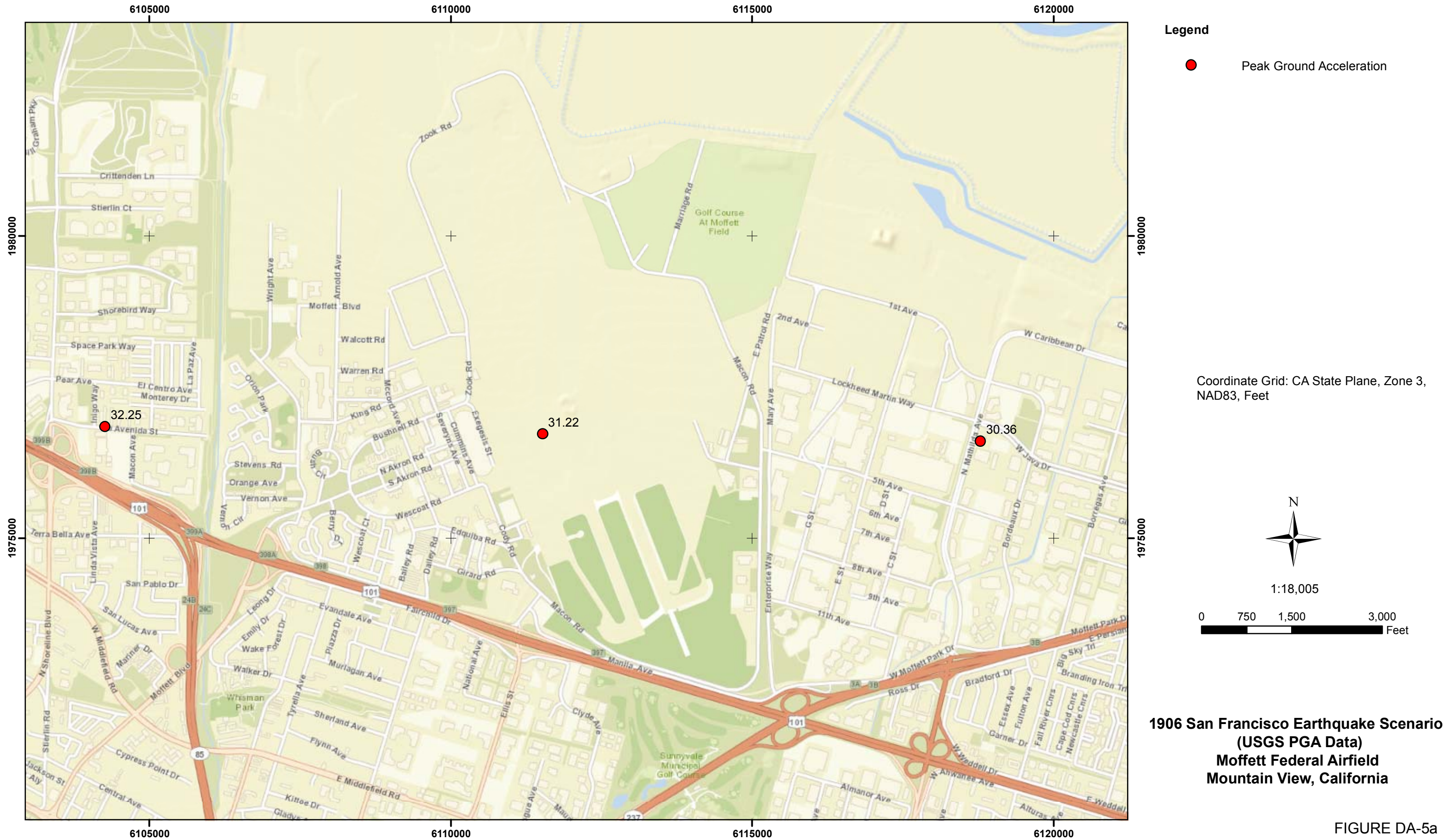


1:12,003



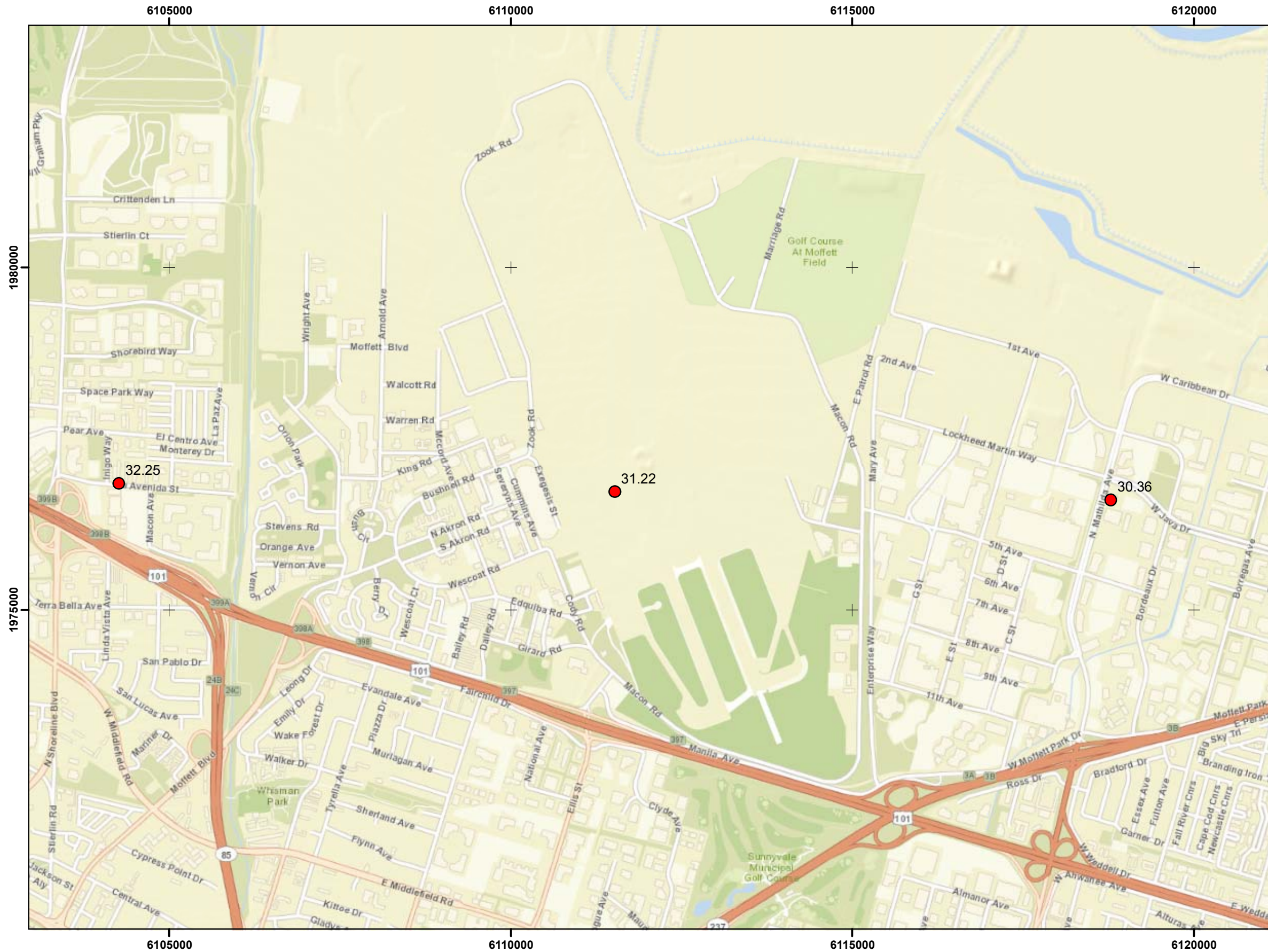
**Concord-Green Valley Scenario  
(USGS PGA Data)  
Livermore Airport  
Livermore, California**

FIGURE DA-4c



N:\Projects\04\_2012\04\_7922\_1200\_CaltransAirportRecov\Outputs\2013\_03\_05\_Report\mxd\Fig\_DA05a\_MOF\_PGA\_1906Scenario.mxd, 03/21/13, dpollard

FIGURE DA-5a



Legend

- Peak Ground Acceleration

Coordinate Grid: CA State Plane, Zone 3,  
NAD83, Feet

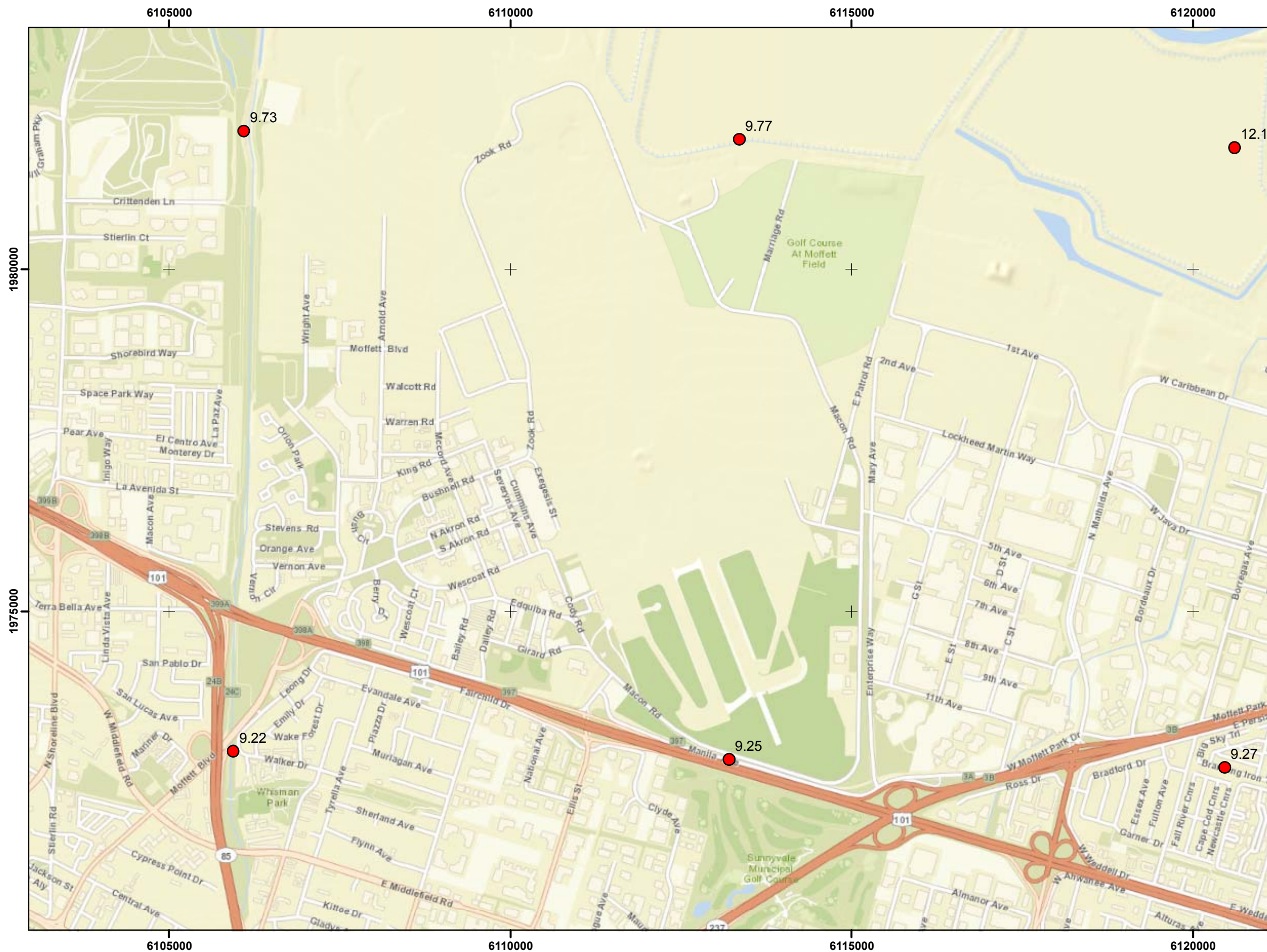


1:18,005



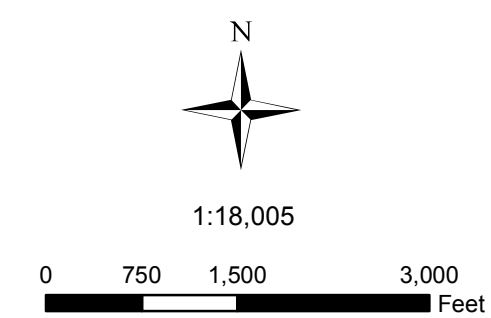
Hayward-Rodgers Creek Scenario  
(USGS PGA Data)  
Moffett Federal Airfield  
Mountain View, California

FIGURE DA-5b



**Legend**  
 Peak Ground Acceleration

Coordinate Grid: CA State Plane, Zone 3,  
 NAD83, Feet



**Concord-Green Valley Scenario  
 (USGS PGA Data)  
 Moffett Federal Airfield  
 Mountain View, California**

FIGURE DA-5c

N:\Projects\04\_2012\04\_7922\_1200\_CaltransAirportRecov\Outputs\2013\_03\_05\_Report\mxd\Fig\_DA05c\_MOF\_PGA\_CGVCScenario.mxd, 03/21/13, dpollard



**Legend**

- ▼ Fugro CPT, Phase 1, 1999
- ▼ Fugro CPT, 2000, Phase 2
- ▼ Fugro CPT, 2000, Phase 3
- Cross Section Location

Coordinates System: CA State Plane,  
 Zone 3, NAD83, Feet



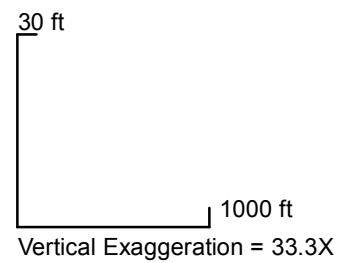
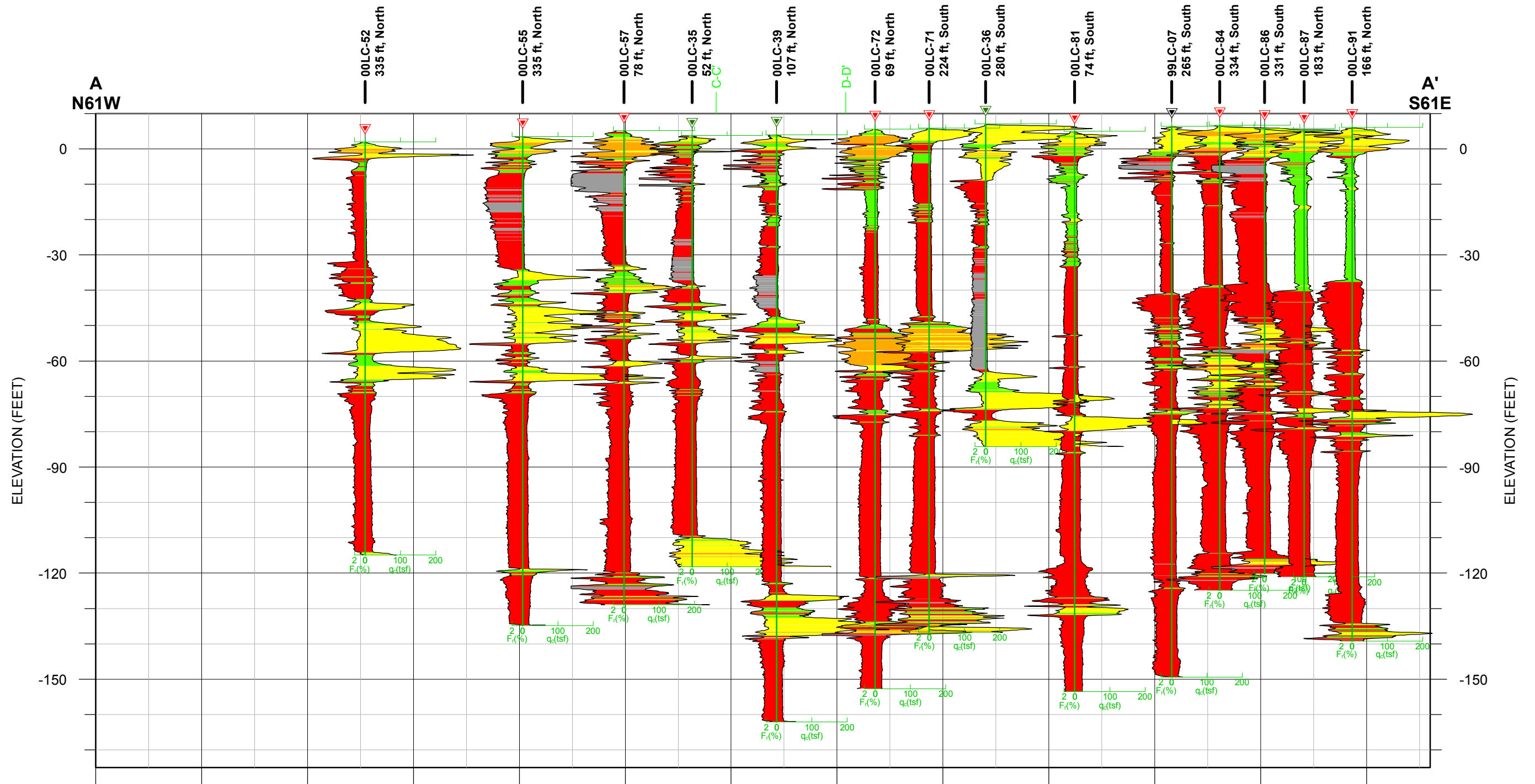
1:18,000



**PLAN VIEW**  
 San Francisco International Airport  
 San Francisco, California

FIGURE DB-1

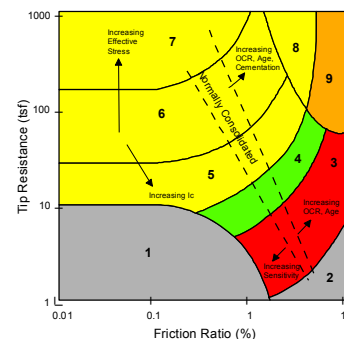
N:\Projects\04\_2012\04\_7922\_1200\_CaltransAirportRecov\Outputs\2013\_03\_05\_Report\mxd\Fig\_DB01\_SFO\_Exploration\LocationMap.mxd, 03/21/13, dpollard



**Legend**

- ▼ Fugro CPT, Phase 1, 1999
- ▼ Fugro CPT, 2000, Phase 2
- ▼ Fugro CPT, 2000, Phase 3
- $F_r$  = Friction Ratio
- $q_c$  = Tip Resistance

**CPT Correlation Chart**

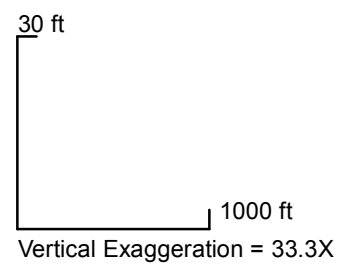
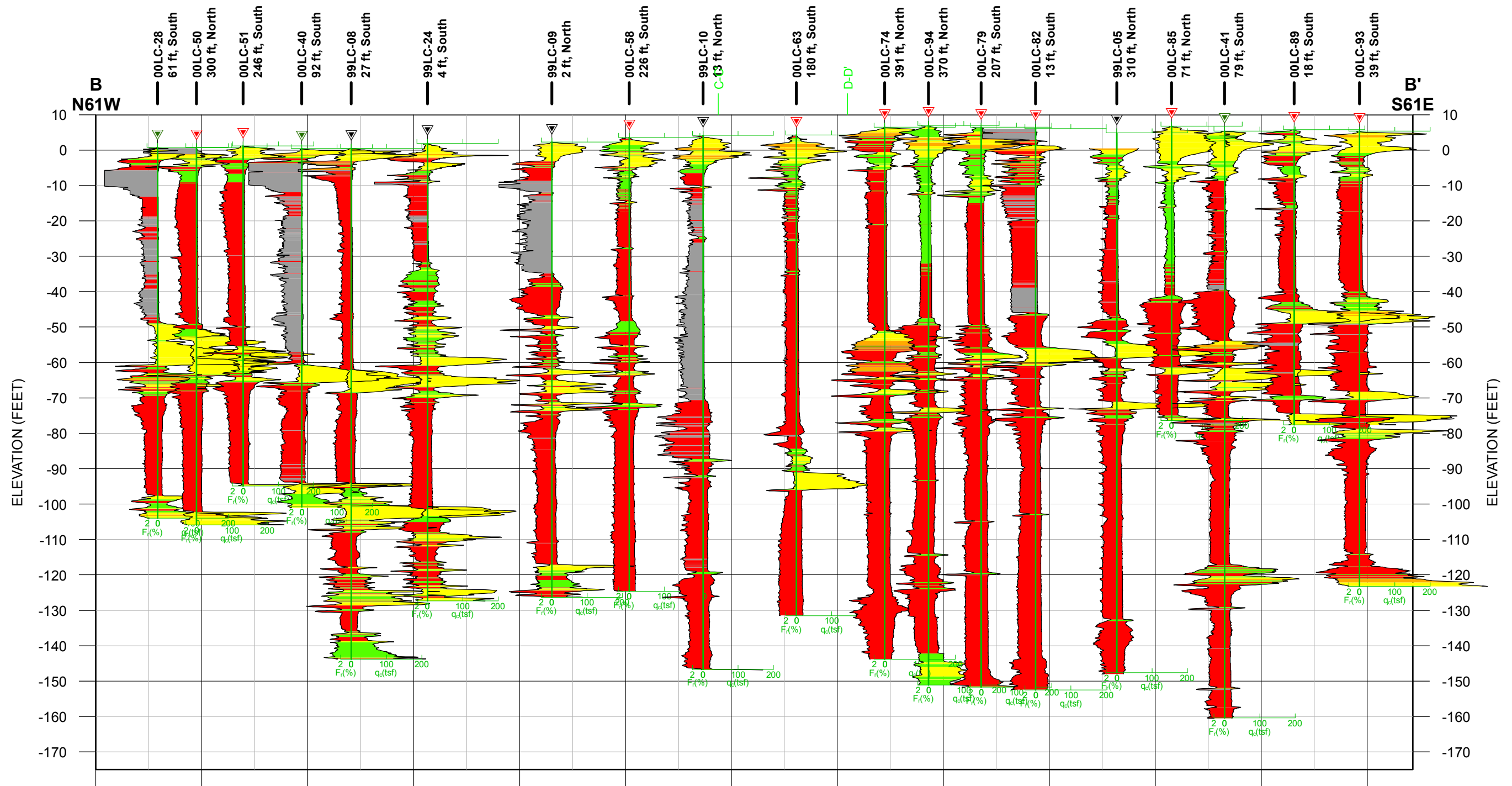


**Robertson and Wride, 1990**

Zone	Soil Behavior Type
1	Sensitive Fine-grained
2	Peats
3	Silty Clay to Clay
4	Clayey Silt to Silty Clay
5	Silty Sand to Sandy Silt
6	Clean Sand to Silty Sand
7	Gravelly Sand to Dense Sand
8	Very Stiff Sand to Clayey Sand*
9	Very Stiff Fine-Grained*

**GEOTECHNICAL CROSS SECTION A-A'**  
San Francisco International Airport  
San Francisco, California

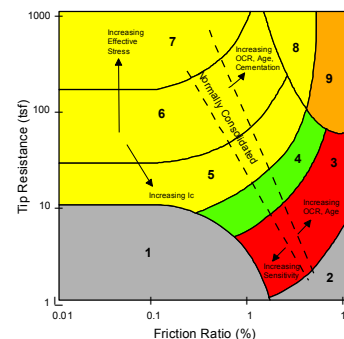
FIGURE DB-2a



**Legend**

- ▼ Fugro CPT, Phase 1, 1999
- ▼ Fugro CPT, 2000, Phase 2
- ▼ Fugro CPT, 2000, Phase 3
- $F_r$  = Friction Ratio
- $q_c$  = Tip Resistance

**CPT Correlation Chart**

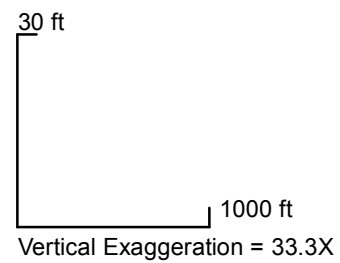
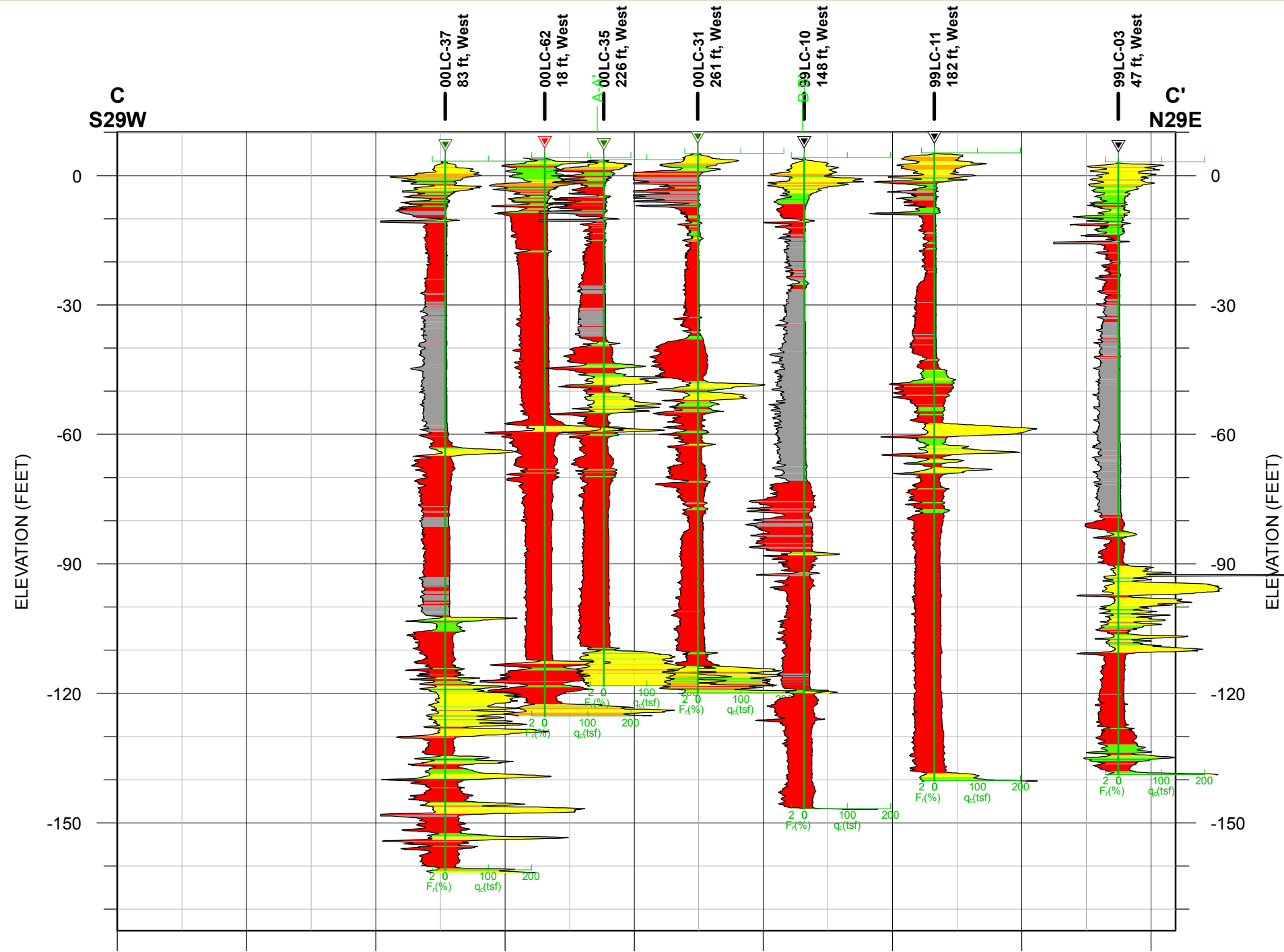


**Robertson and Wride, 1990**

Zone	Soil Behavior Type
1	Sensitive Fine-grained
2	Peats
3	Silty Clay to Clay
4	Clayey Silt to Silty Clay
5	Silty Sand to Sandy Silt
6	Clean Sand to Silty Sand
7	Gravelly Sand to Dense Sand
8	Very Stiff Sand to Clayey Sand*
9	Very Stiff Fine-Grained*

**GEOTECHNICAL CROSS SECTION B-B'**  
San Francisco International Airport  
San Francisco, California

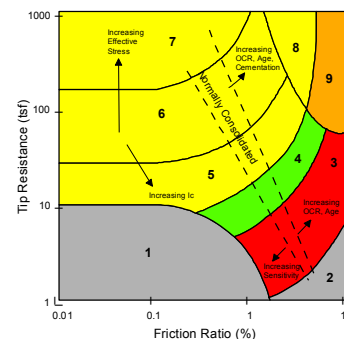
FIGURE DB-2b



**Legend**

- ▼ Fugro CPT, Phase 1, 1999
- ▼ Fugro CPT, 2000, Phase 2
- ▼ Fugro CPT, 2000, Phase 3
- $F_r$  = Friction Ratio
- $q_c$  = Tip Resistance

**CPT Correlation Chart**

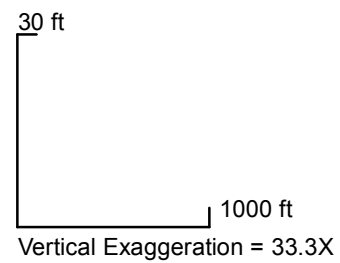
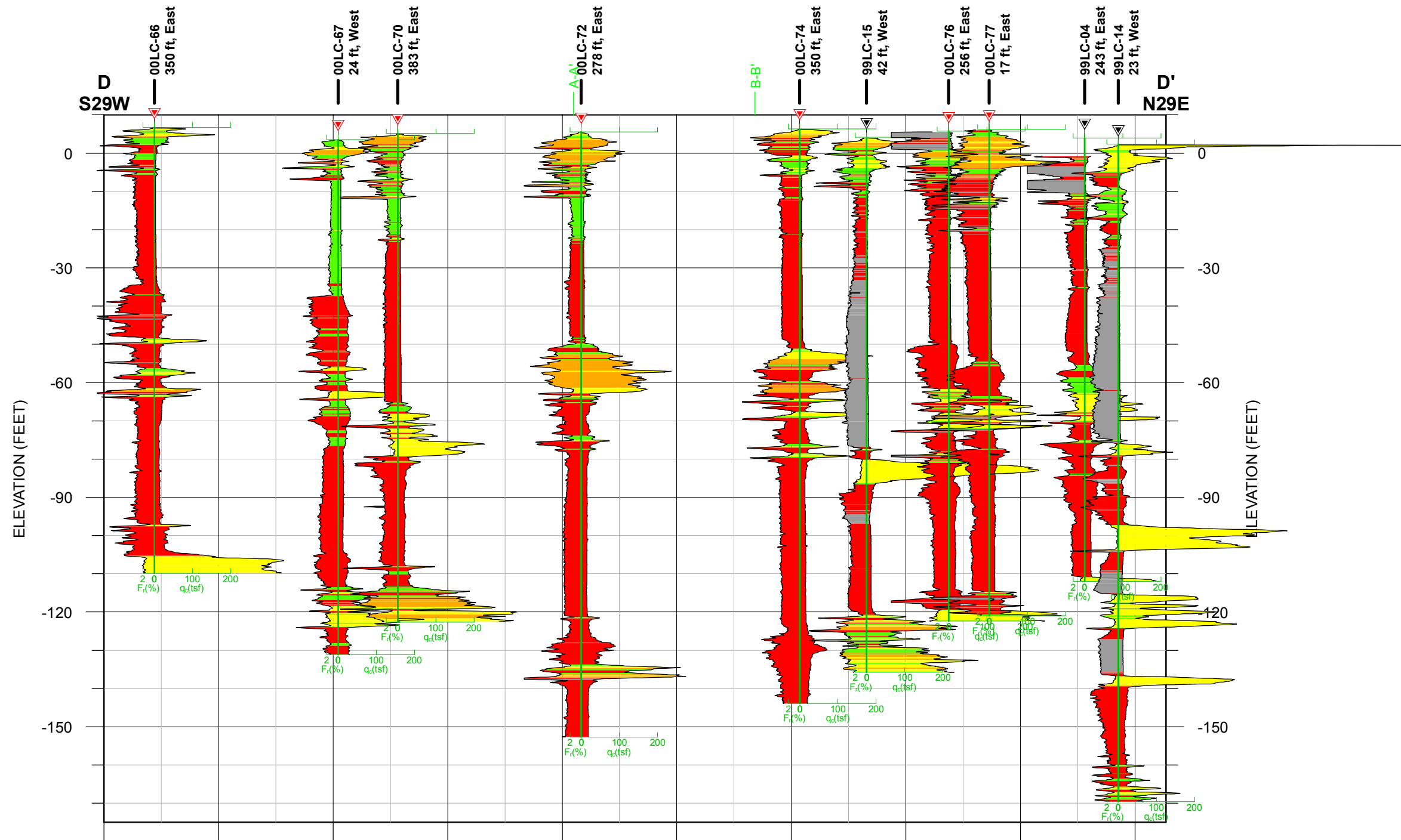


**Robertson and Wride, 1990**

Zone	Soil Behavior Type
1	Sensitive Fine-grained
2	Peats
3	Silty Clay to Clay
4	Clayey Silt to Silty Clay
5	Silty Sand to Sandy Silt
6	Clean Sand to Silty Sand
7	Gravelly Sand to Dense Sand
8	Very Stiff Sand to Clayey Sand*
9	Very Stiff Fine-Grained*

**GEOTECHNICAL CROSS SECTION C-C'**  
San Francisco International Airport  
San Francisco, California

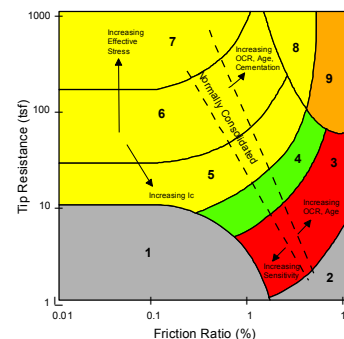
FIGURE DB-2c



**Legend**

- ▼ Fugro CPT, Phase 1, 1999
- ▼ Fugro CPT, 2000, Phase 2
- ▼ Fugro CPT, 2000, Phase 3
- $F_r$  = Friction Ratio
- $q_c$  = Tip Resistance

**CPT Correlation Chart**

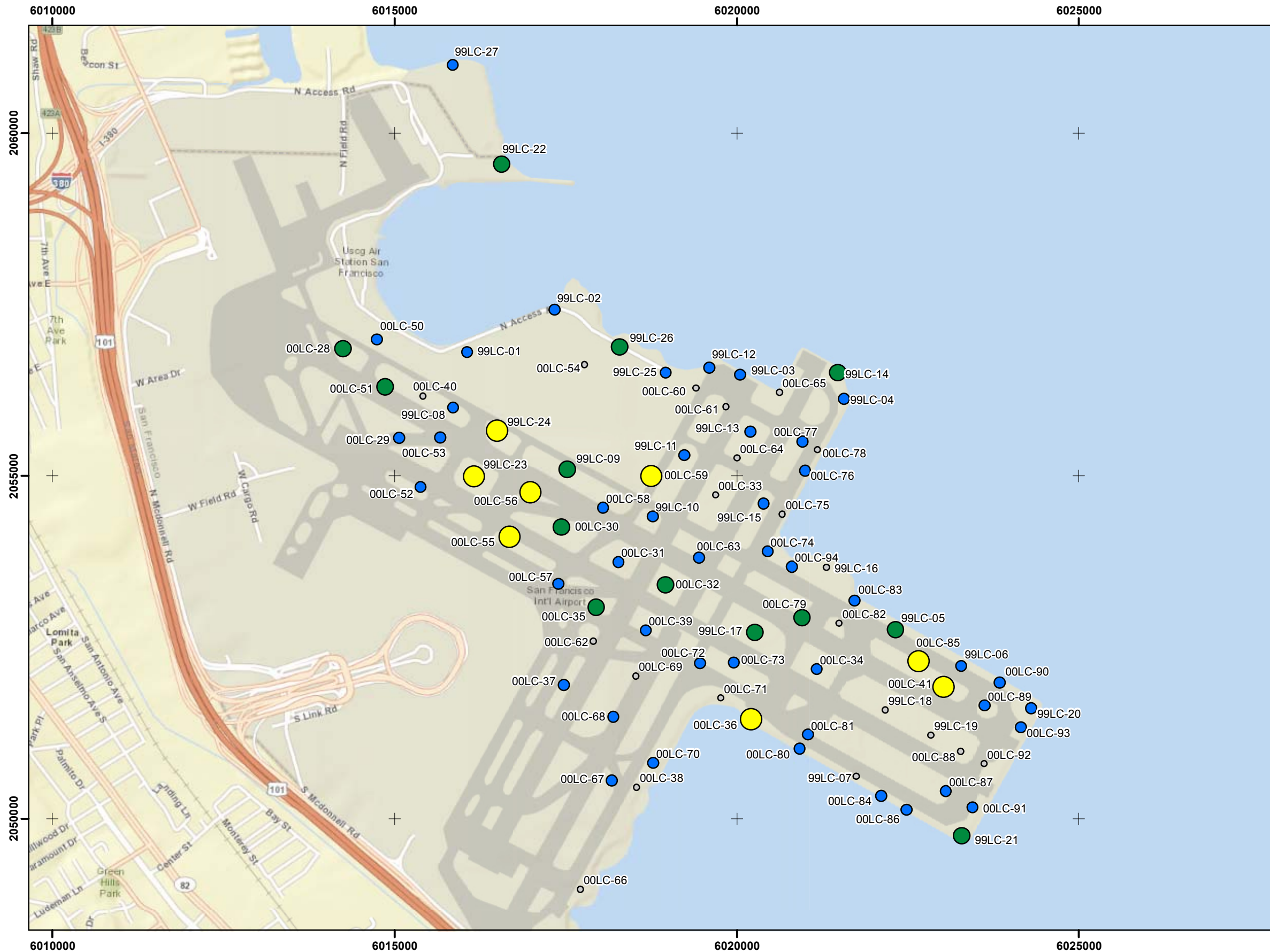


**Robertson and Wride, 1990**

Zone	Soil Behavior Type
1	Sensitive Fine-grained
2	Peats
3	Silty Clay to Clay
4	Clayey Silt to Silty Clay
5	Silty Sand to Sandy Silt
6	Clean Sand to Silty Sand
7	Gravelly Sand to Dense Sand
8	Very Stiff Sand to Clayey Sand*
9	Very Stiff Fine-Grained*

**GEOTECHNICAL CROSS SECTION D-D'**  
San Francisco International Airport  
San Francisco, California

FIGURE DB-2d



**Legend**

Settlement (Inches)

- 0 - 1
- 1 - 2
- 2 - 3
- 3 - 4
- 4 - 5
- > 5

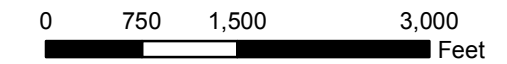
Magnitude= 7.8; P. G. A. = 0.48 g

Only CPTs with total depth >30 feet are shown

Coordinate Grid: CA State Plane, Zone 3, NAD83, Feet



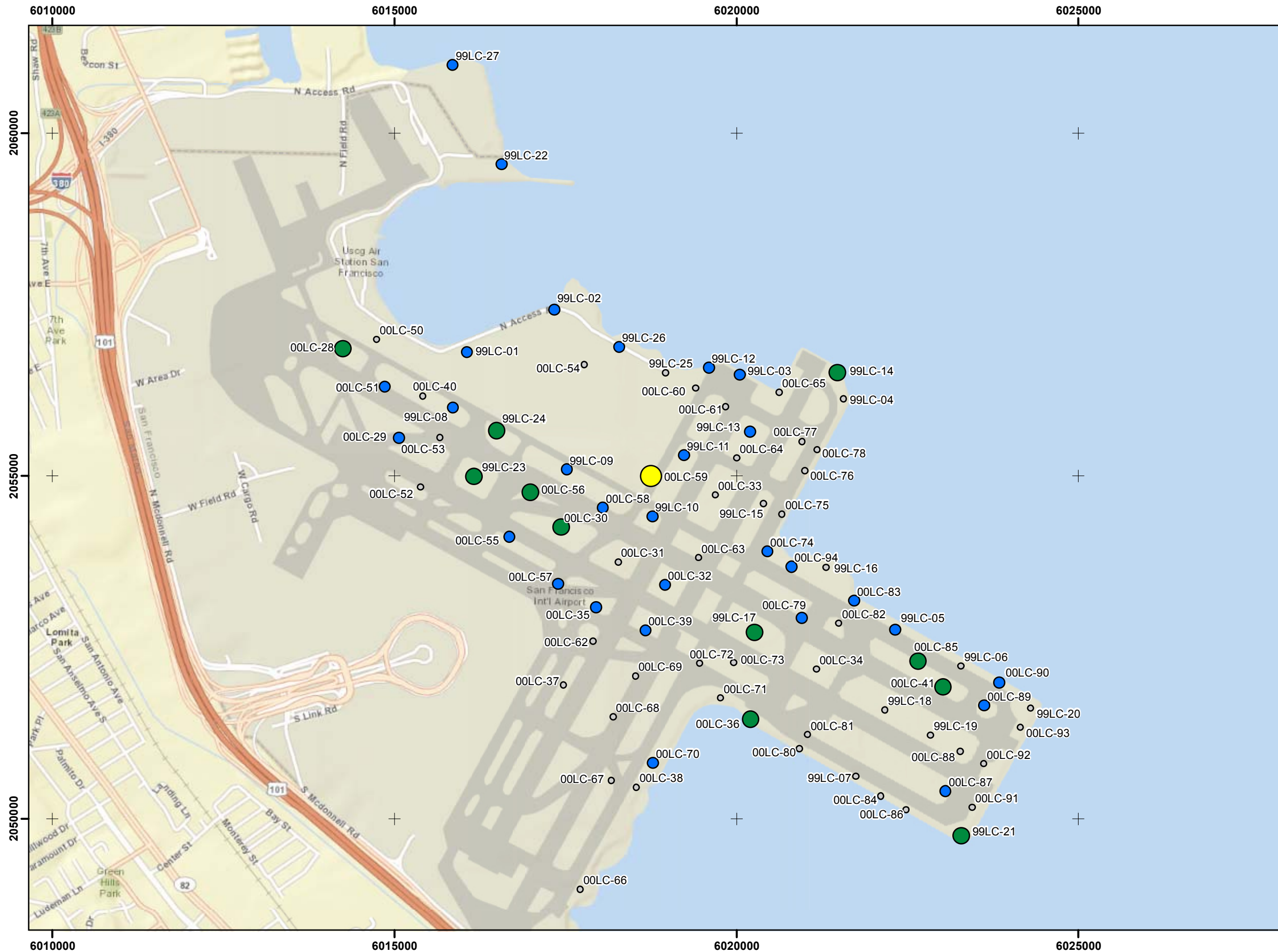
1:18,005



**LIQUEFACTION SETTLEMENT MAP  
 TOP 80 FEET  
 1906 San Francisco Earthquake Scenario  
 San Francisco International Airport  
 San Francisco, California**

N:\Projects\04\_2012\04\_7922\_1200\_CaltransAirportRecon\Outputs\2013\_03\_05\_Report\mxd\Fig\_DB03\_SFO\_LiquSettl\_M7\_80\_ac048\_SanAndreas\_1906\_io80Ft.mxd, 03/21/13, dpollard

FIGURE DB-3



**Legend**

Settlement (Inches)

- 0 - 1
- 1 - 2
- 2 - 3
- 3 - 4
- 4 - 5
- > 5

Magnitude= 7.26; P. G. A. = 0.27 g

Only CPTs with total depth >30 feet are shown

Coordinate Grid: CA State Plane, Zone 3, NAD83, Feet

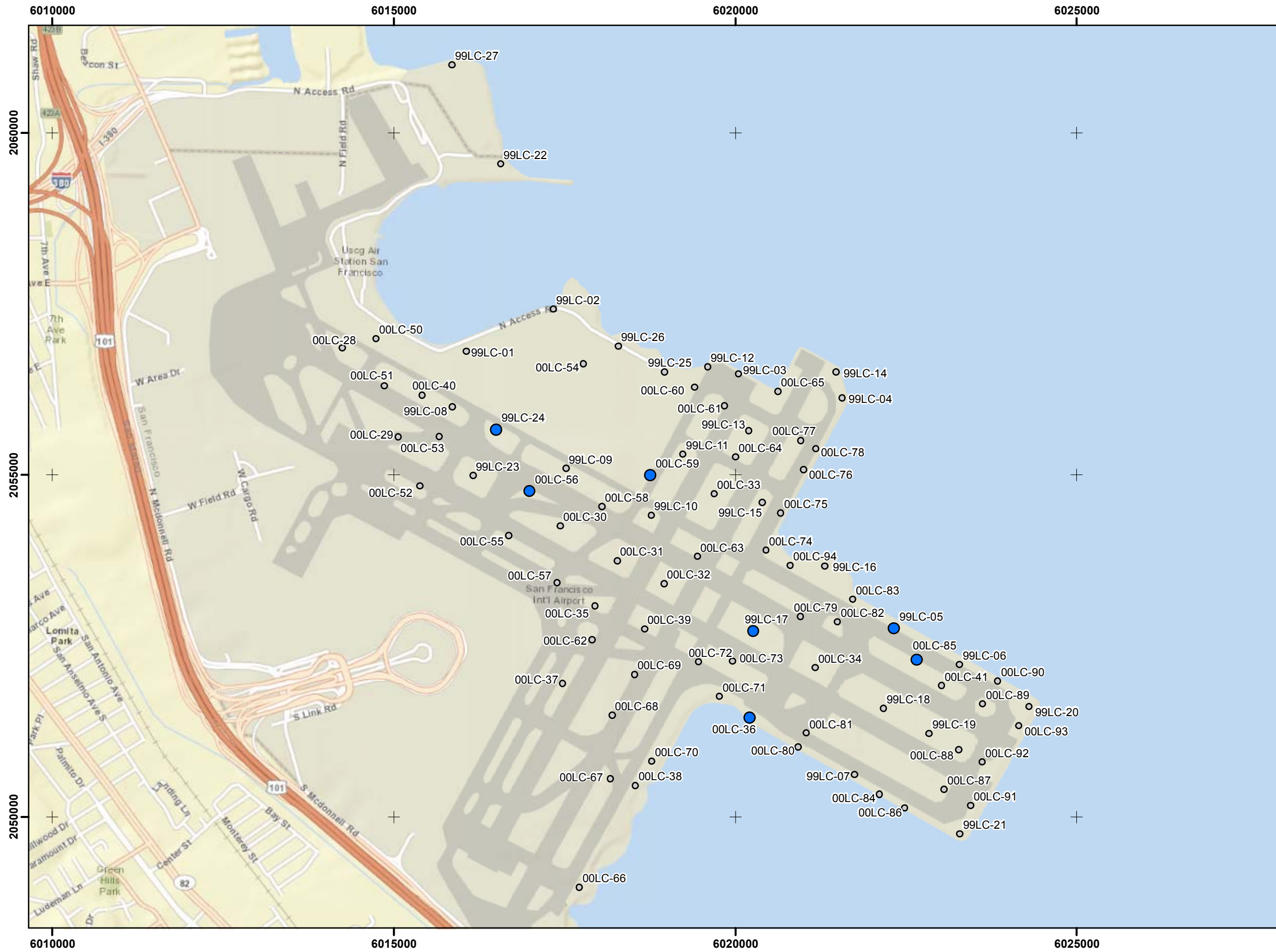


1:18,005



**LIQUEFACTION SETTLEMENT MAP  
 TOP 80 FEET  
 Hayward-Rodgers Creek Scenario  
 San Francisco International Airport  
 San Francisco, California**

FIGURE DB-4



**Legend**

Settlement (Inches)

- 0 - 1
- 1 - 2
- 2 - 3
- 3 - 4
- 4 - 5
- > 5

Magnitude= 6.71; P. G. A. = 0.15 g

Only CPTs with total depth >30 feet are shown

Coordinate Grid: CA State Plane, Zone 3, NAD83, Feet



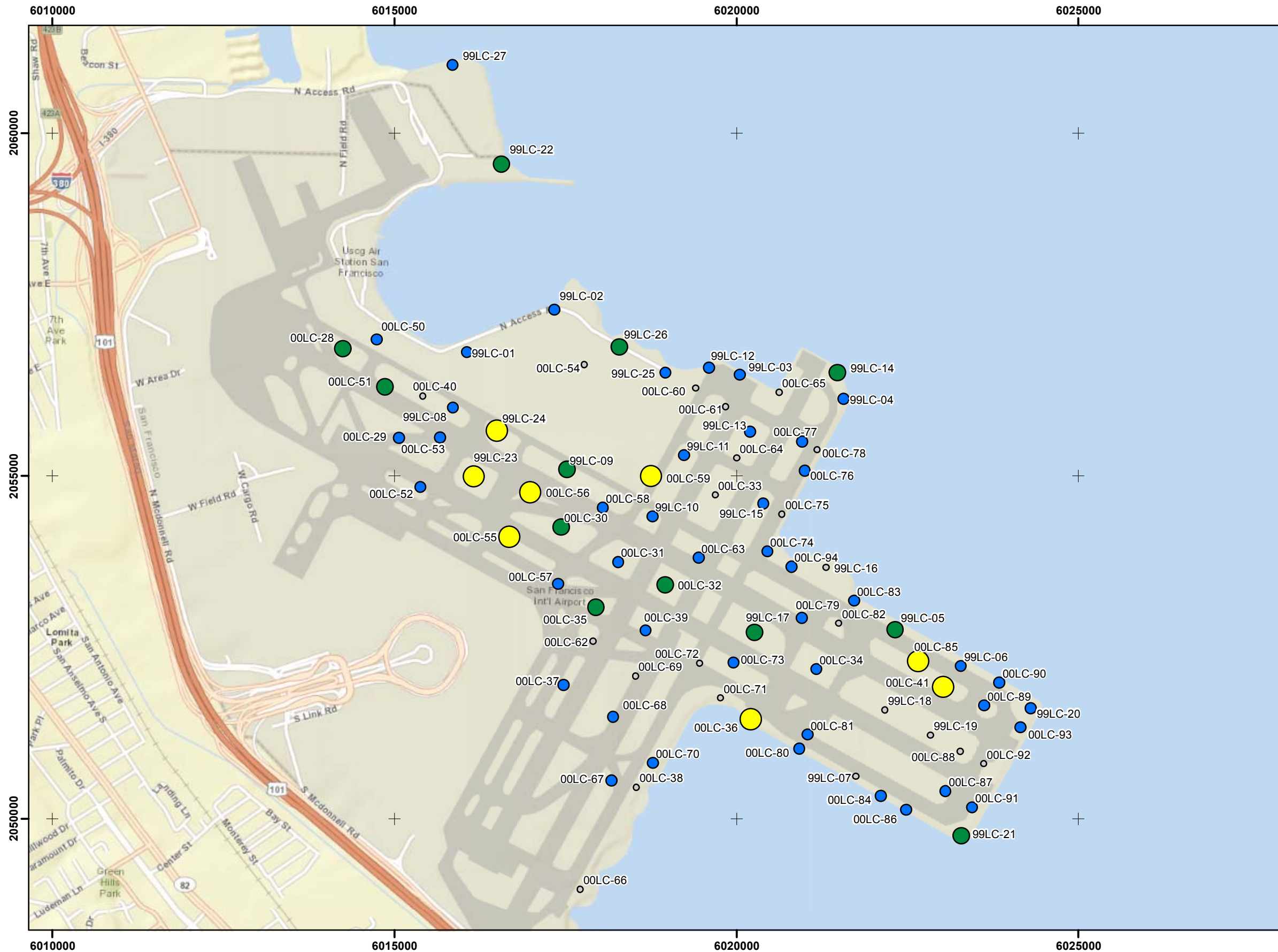
1:18,005



**LIQUEFACTION SETTLEMENT MAP  
 TOP 80 FEET  
 Concord-Green Valley Scenario  
 San Francisco International Airport  
 San Francisco, California**

FIGURE DB-5

N:\Projects\04\_2012\04\_7922\_1200\_CaltransAirportRecov\Outputs\2013\_03\_05\_Report\mxd\Fig\_DB05\_SFOLiquSettl\_M6\_71\_ac015\_CGV\_Faut\_to90Fmxd\_03/21/13\_dpollard



**Legend**

Settlement (Inches)

- 0 - 1
- 1 - 2
- 2 - 3
- 3 - 4
- 4 - 5
- > 5

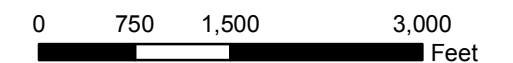
Magnitude= 8.0; P. G. A. = 0.48 g

Only CPTs with total depth >30 feet are shown

Coordinate Grid: CA State Plane, Zone 3, NAD83, Feet



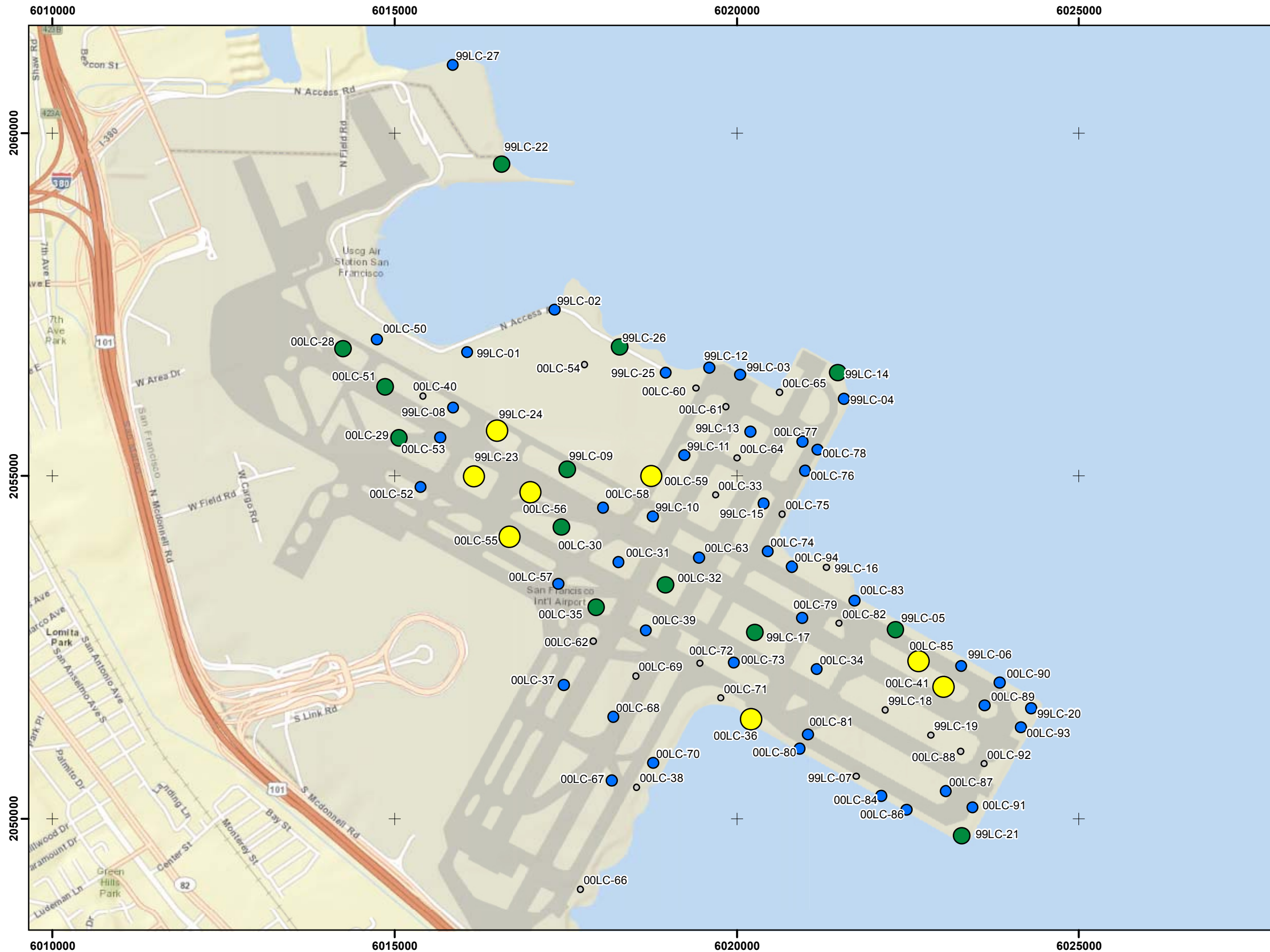
1:18,005



**LIQUEFACTION SETTLEMENT MAP  
 TOP 80 FEET  
 10% Probability of Exceedance  
 in 50-Years Scenario  
 San Francisco International Airport  
 San Francisco, California**

FIGURE DB-6

N:\Projects\04\_2012\04\_7922\_1200\_CaltransAirportRecov\Outputs\2013\_03\_05\_Report\mxd\Fig\_DB06\_SFOLiquSettl\_M8\_00\_ac48\_2008USGS\_10Perc\_50Yrs\_1080ft.mxd, 03/21/13, dpollard



**Legend**

Settlement (Inches)

- 0 - 1
- 1 - 2
- 2 - 3
- 3 - 4
- 4 - 5
- > 5

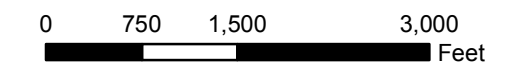
Magnitude= 8.0; P. G. A. = 0.75 g

Only CPTs with total depth >30 feet are shown

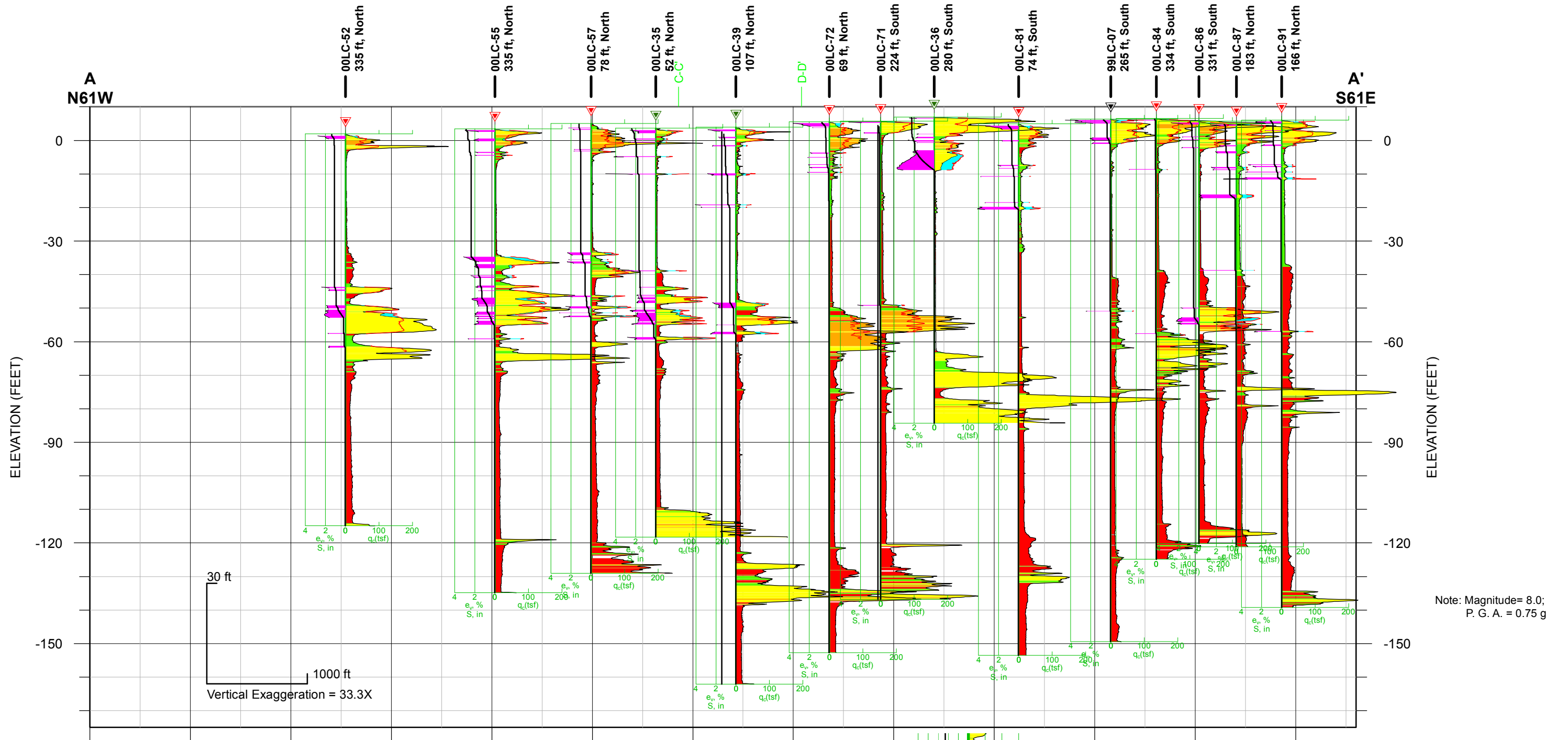
Coordinate Grid: CA State Plane, Zone 3, NAD83, Feet



1:18,005



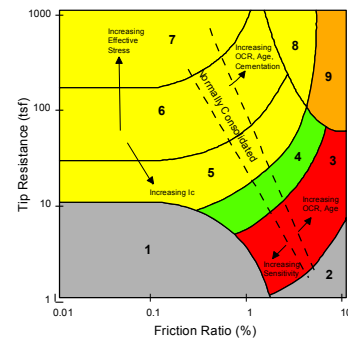
**LIQUEFACTION SETTLEMENT MAP  
 TOP 80 FEET  
 2% Probability of Exceedance  
 in 50-Years Scenario  
 San Francisco International Airport  
 San Francisco, California**



**Legend**

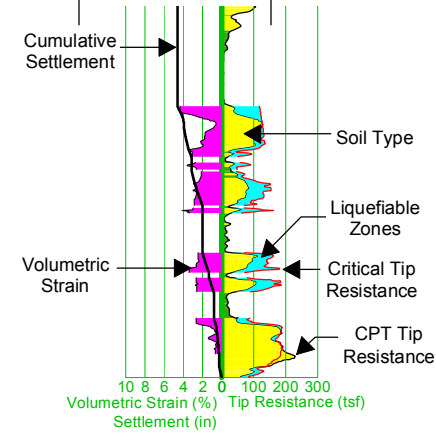
- ▽ Fugro CPT, Phase 1, 1999
- ▽ Fugro CPT, 2000, Phase 2
- ▽ Fugro CPT, 2000, Phase 3
- qc = Tip Resistance
- e = Volumetric Strain
- S = Settlement

**CPT Correlation Chart**



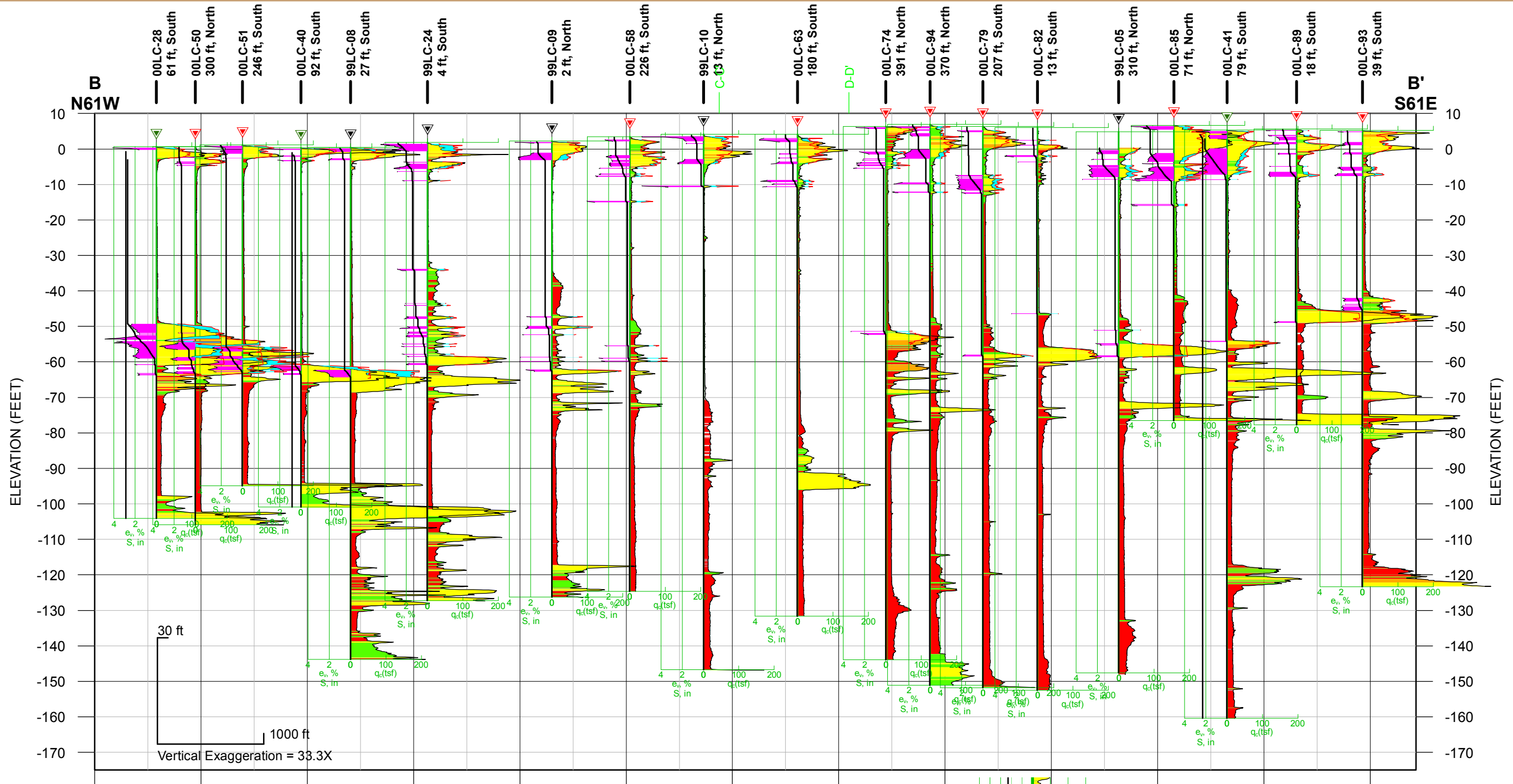
**Robertson and Wride, 1990**

Zone	Soil Behavior Type
1	Sensitive Fine-grained
2	Peats
3	Silty Clay to Clay
4	Clayey Silt to Silty Clay
5	Silty Sand to Sandy Silt
6	Clean Sand to Silty Sand
7	Gravelly Sand to Dense Sand
8	Very Stiff Sand to Clayey Sand*
9	Very Stiff Fine-Grained*



**LIQUEFACTION CROSS SECTION A-A'**  
**2% Probability of Exceedance**  
**in 50-Years Scenario**  
San Francisco International Airport  
San Francisco, California

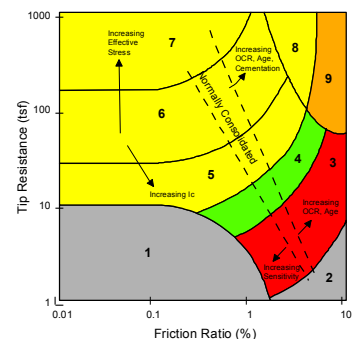
FIGURE DB-8a



**Legend**

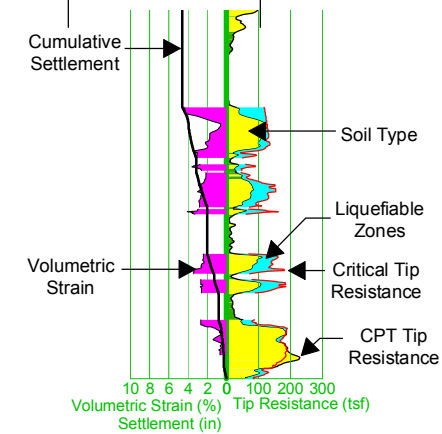
- ▼ Fugro CPT, Phase 1, 1999
- ▼ Fugro CPT, 2000, Phase 2
- ▼ Fugro CPT, 2000, Phase 3
- qc = Tip Resistance
- e = Volumetric Strain
- S = Settlement

**CPT Correlation Chart**



**Robertson and Wride, 1990**

Zone	Soil Behavior Type
1	Sensitive Fine-grained
2	Peats
3	Silty Clay to Clay
4	Clayey Silt to Silty Clay
5	Silty Sand to Sandy Silt
6	Clean Sand to Silty Sand
7	Gravelly Sand to Dense Sand
8	Very Stiff Sand to Clayey Sand*
9	Very Stiff Fine-Grained*

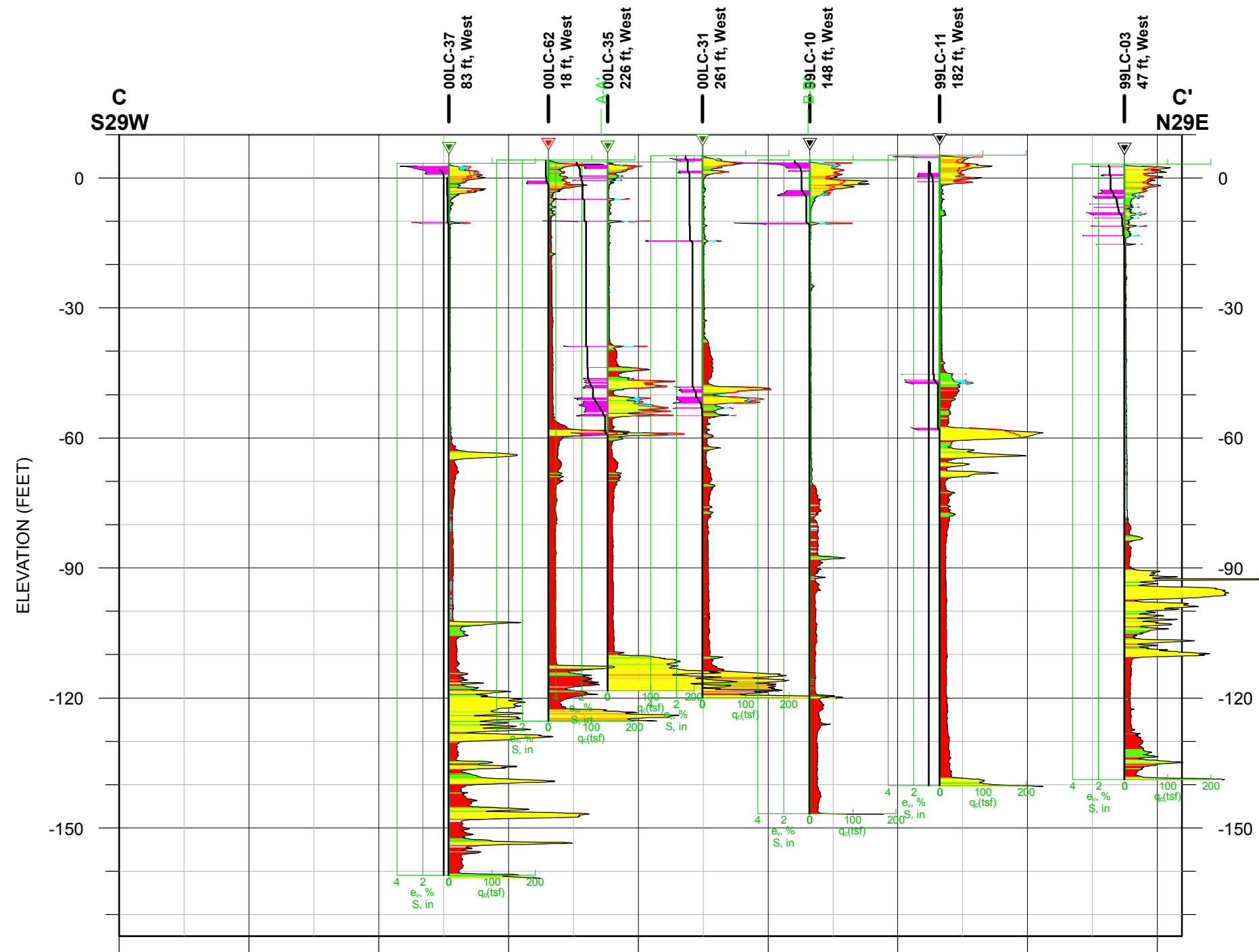


Note: Magnitude= 8.0; P. G. A. = 0.75 g

**LIQUEFACTION CROSS SECTION B-B'**  
**2% Probability of Exceedance**  
**in 50-Years Scenario**  
San Francisco International Airport  
San Francisco, California

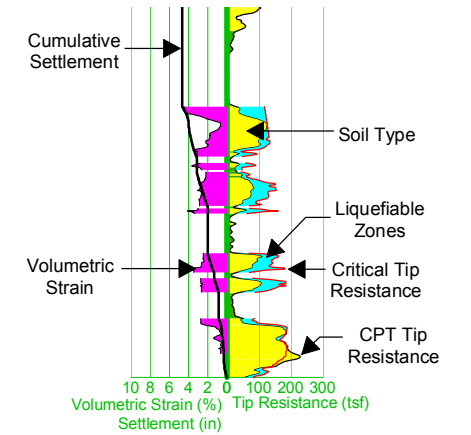
FIGURE DB-8b

N:\Projects\04\_2012\04\_7922\_1200\_CaltransAirportRecov\Outputs\2013\_03\_05\_Report\mxd\Fig\_DB08b\_SFO\_Profile\MB\_00\_a075\_2475Yr.mxd, 03/21/13, dpollard

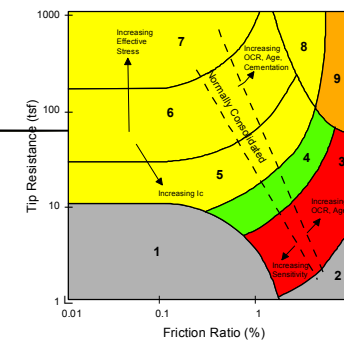


**Legend**

- ▼ Fugro CPT, Phase 1, 1999
- ▼ Fugro CPT, 2000, Phase 2
- ▼ Fugro CPT, 2000, Phase 3
- qc = Tip Resistance
- e = Volumetric Strain
- S = Settlement

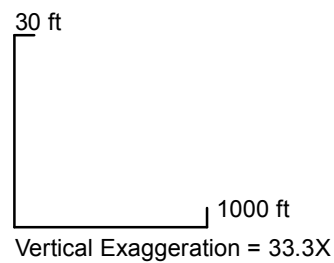


**CPT Correlation Chart**



**Robertson and Wride, 1990**

Zone	Soil Behavior Type
1	Sensitive Fine-grained
2	Peats
3	Silty Clay to Clay
4	Clayey Silt to Silty Clay
5	Silty Sand to Sandy Silt
6	Clean Sand to Silty Sand
7	Gravelly Sand to Dense Sand
8	Very Stiff Sand to Clayey Sand*
9	Very Stiff Fine-Grained*

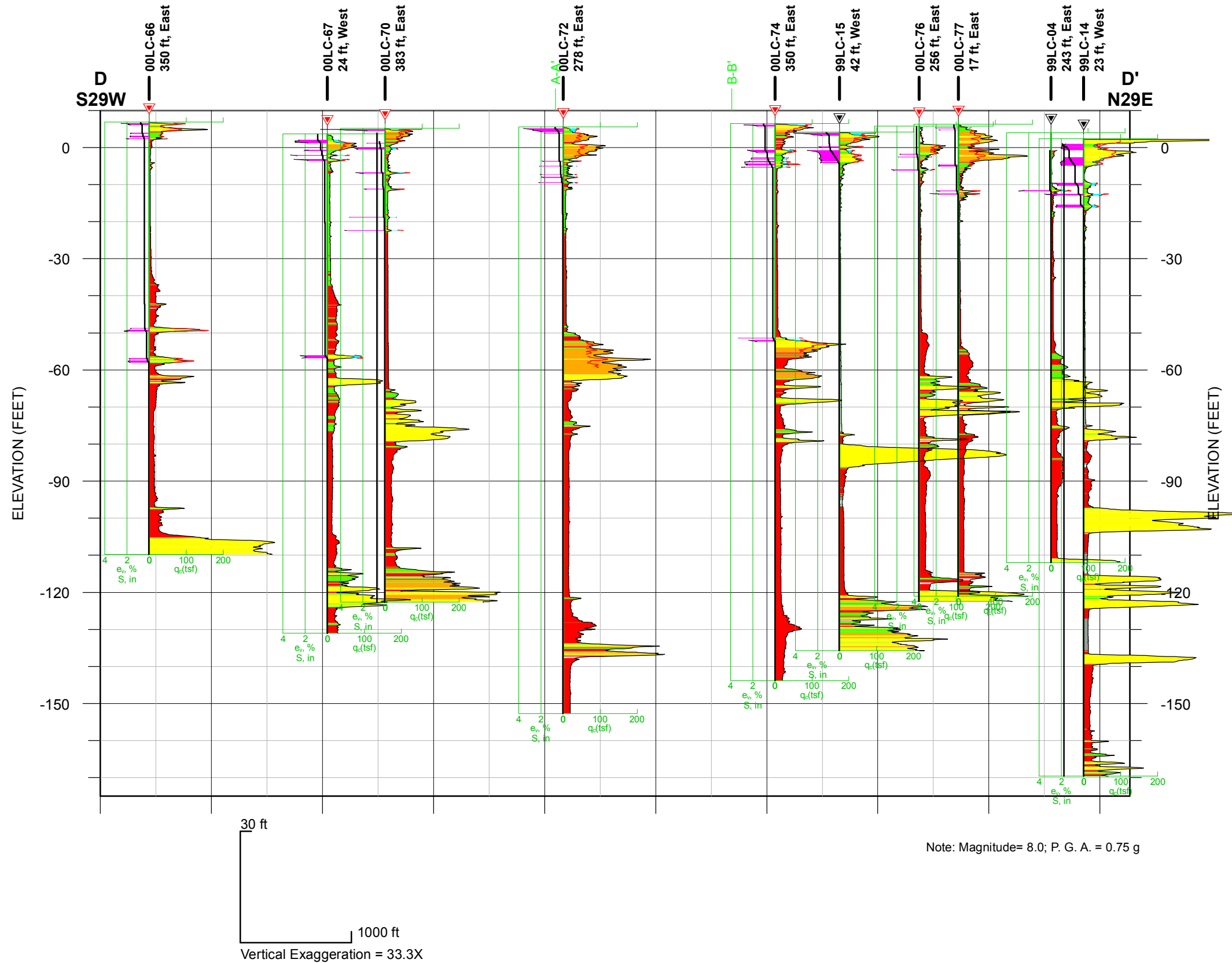


Note: Magnitude= 8.0; P. G. A. = 0.75 g

**LIQUEFACTION CROSS SECTION C-C'**  
**2% Probability of Exceedance**  
**in 50-Years Scenario**  
San Francisco International Airport  
San Francisco, California

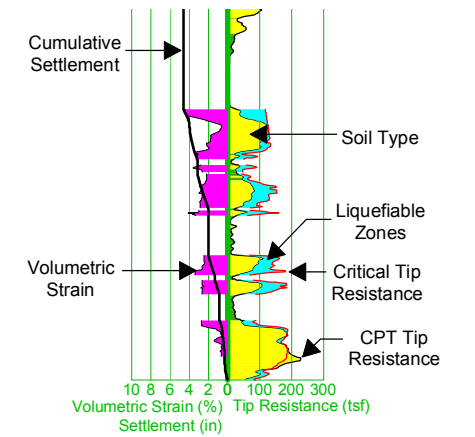
FIGURE DB-8c

N:\Projects\04\_2012\04\_7922\_1200\_CaltransAirportRecov\Outputs\2013\_03\_05\_Report\mxd\Fig\_DB08c\_SFO\_Profile\M8\_00\_a075\_2475Yr.mxd, 03/21/13, dpollard

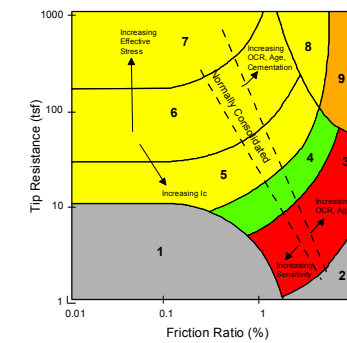


**Legend**

- ▼ Fugro CPT, Phase 1, 1999
- ▼ Fugro CPT, 2000, Phase 2
- ▼ Fugro CPT, 2000, Phase 3
- qc = Tip Resistance
- e = Volumetric Strain
- S = Settlement



**CPT Correlation Chart**

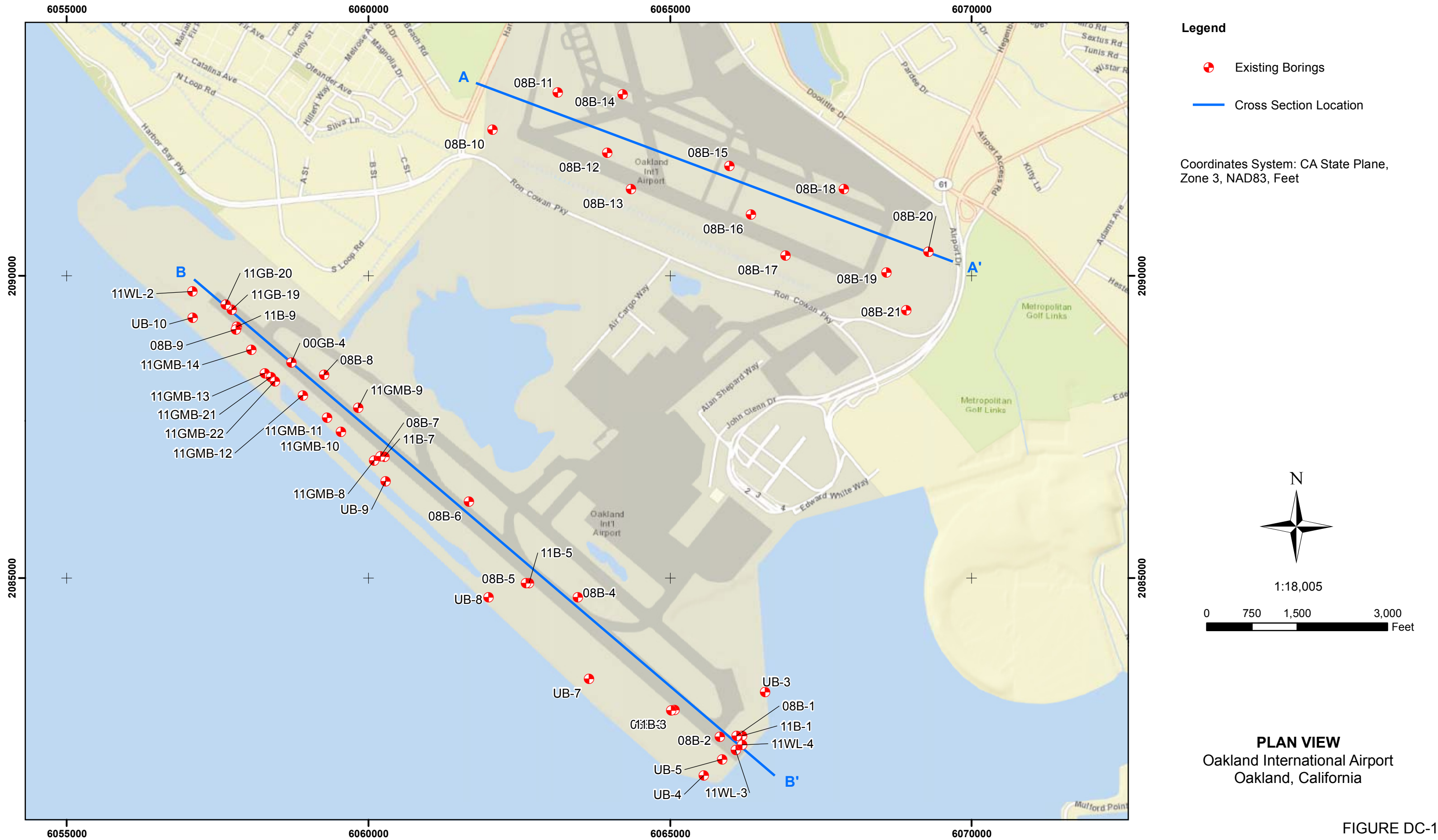


**Robertson and Wride, 1990**

Zone	Soil Behavior Type
1	Sensitive Fine-grained
2	Peats
3	Silty Clay to Clay
4	Clayey Silt to Silty Clay
5	Silty Sand to Sandy Silt
6	Clean Sand to Silty Sand
7	Gravelly Sand to Dense Sand
8	Very Stiff Sand to Clayey Sand*
9	Very Stiff Fine-Grained*

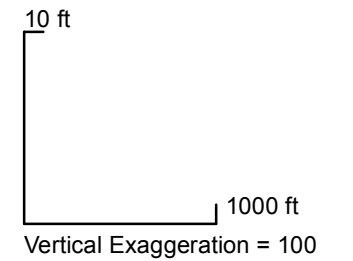
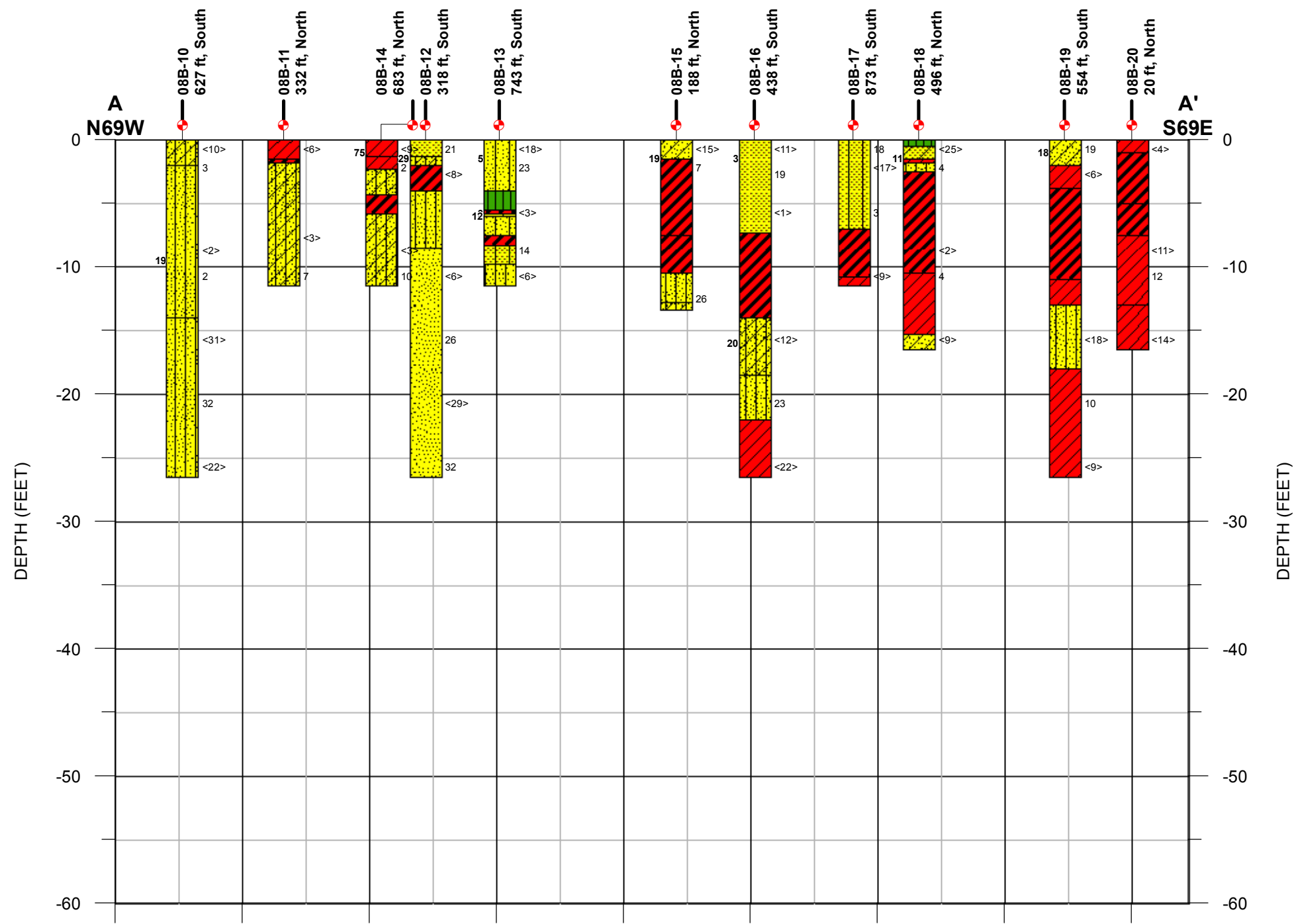
Note: Magnitude= 8.0; P. G. A. = 0.75 g

**LIQUEFACTION CROSS SECTION D-D'**  
**2% Probability of Exceedance**  
**in 50-Years Scenario**  
San Francisco International Airport  
San Francisco, California



N:\Projects\04\_2012\04\_7922\_1200\_CaltransAirportRecov\Outputs\2013\_03\_05\_Report\mxd\Fig\_DC01\_OAK\_ExplorationLocationMap.mxd, 03/21/13, dpcillard

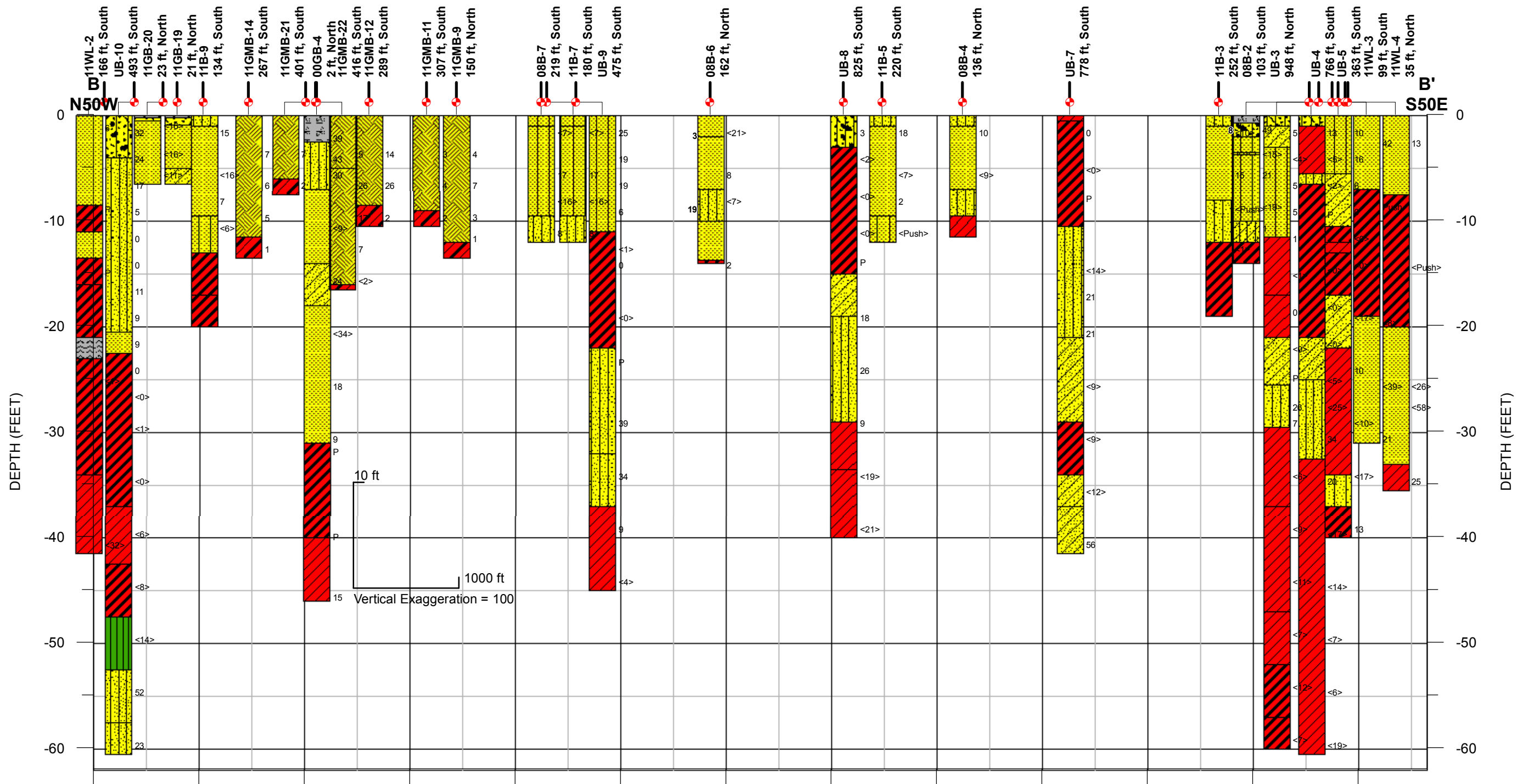
FIGURE DC-1



- |                                      |                                      |                                      |   |
|--------------------------------------|--------------------------------------|--------------------------------------|---|
| Lean CLAY (CL)                       | Poorly-Graded SAND with Silt (SP-SM) | Fill                                 | 10 SPT Blow Count                                 |
| Lean to Fat CLAY (CL-CH)             | Well-Graded SAND (SW)                | Well-Graded GRAVEL (GW)              | <20> Modified California Liner Sampler Blow Count |
| Fat CLAY (CH)                        | Well-Graded SAND with Silt (SW-SM)   | Well-Graded GRAVEL with Silt (GW-GM) | 75 Fines Content (% - plotted on left of boring)  |
| Silt (ML)                            | Clayey SAND (SC)                     | Silty Gravel (GM)                    |   |
| Poorly-Graded SAND (SP)              | Clayey to Silty SAND (SC-SM)         | Asphaltic Concrete                   |   |
| Poorly-Graded SAND with Clay (SP-SC) | Silty SAND (SM)                      |                                      |   |

**GEOTECHNICAL CROSS SECTION A-A'**  
Oakland International Airport  
Oakland, California

FIGURE DC-2a

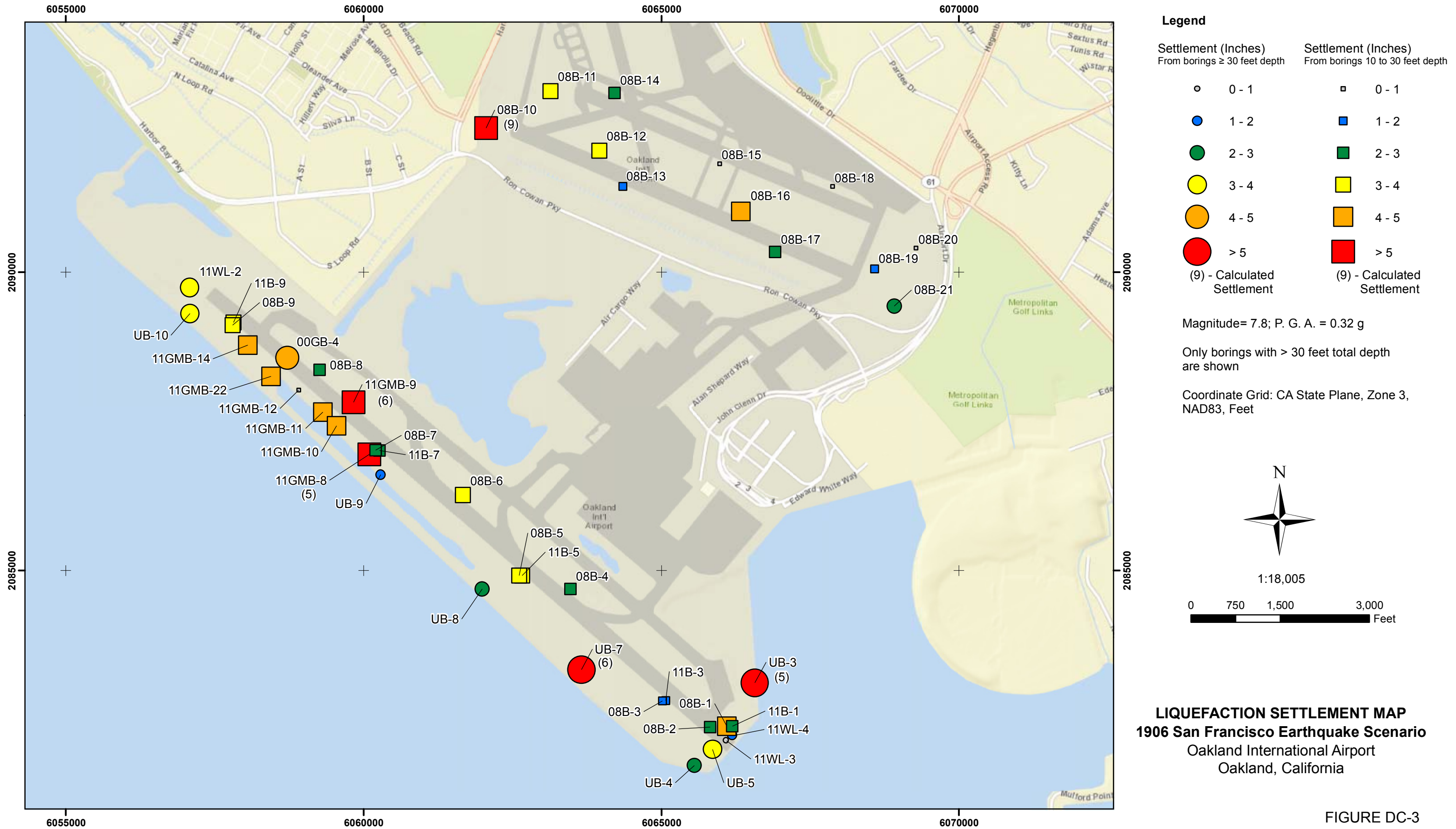


- |                                      |                                      |                                      |
|--------------------------------------|--------------------------------------|--------------------------------------|
| Lean CLAY (CL)                       | Poorly-Graded SAND with Silt (SP-SM) | Fill                                 |
| Lean to Fat CLAY (CL-CH)             | Well-Graded SAND (SW)                | Well-Graded GRAVEL (GW)              |
| Fat CLAY (CH)                        | Well-Graded SAND with Silt (SW-SM)   | Well-Graded GRAVEL with Silt (GW-GM) |
| Silt (ML)                            | Clayey SAND (SC)                     | Silty Gravel (GM)                    |
| Poorly-Graded SAND (SP)              | Clayey to Silty SAND (SC-SM)         | Asphaltic Concrete                   |
| Poorly-Graded SAND with Clay (SP-SC) | Silty SAND (SM)                      |                                      |

- |      |   |
|------|---|
| 10   | SPT Blow Count                                |
| <20> | Modified California Liner Sampler Blow Count  |
| 75   | Fines Content (% - plotted on left of boring) |

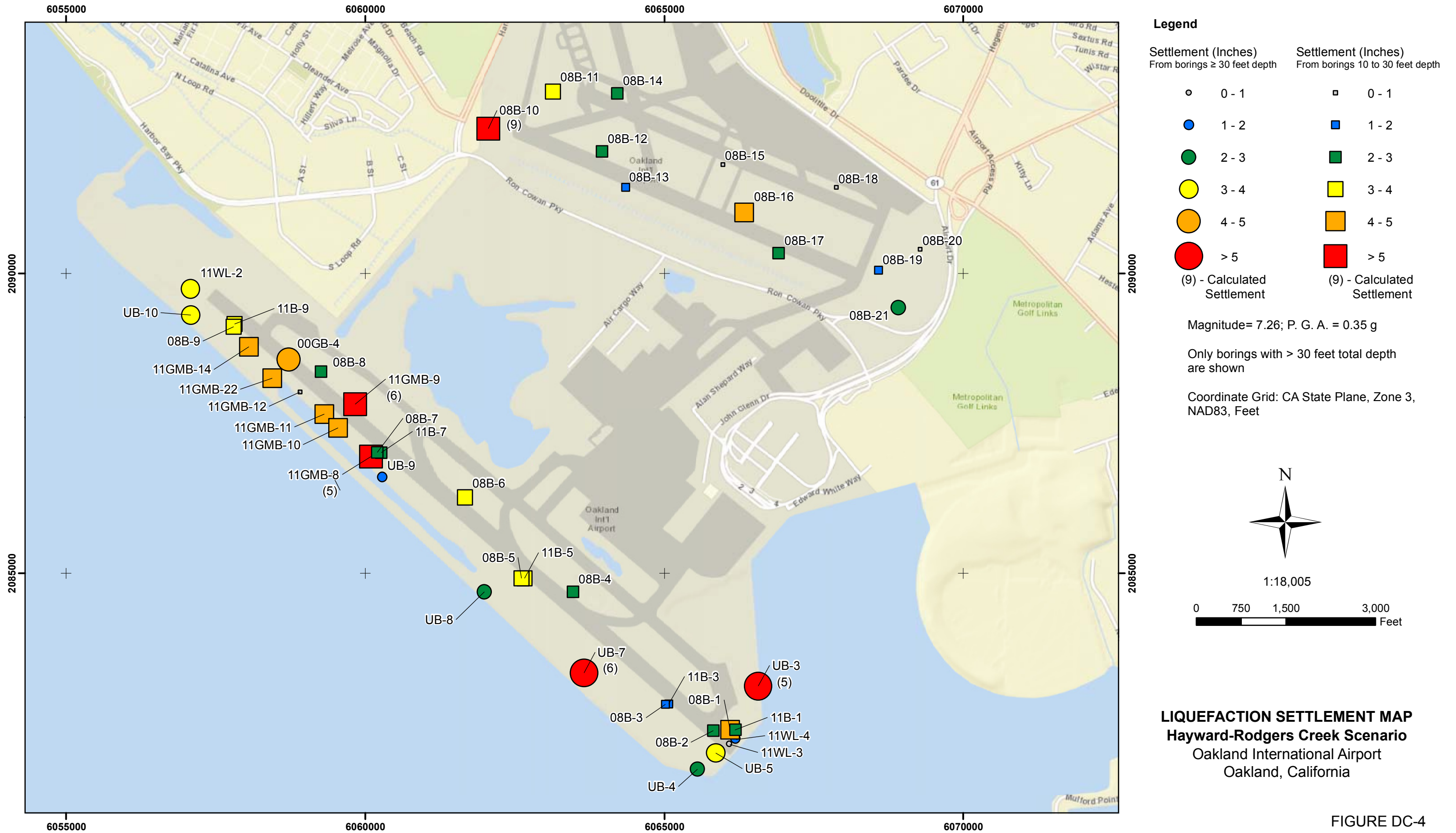
**GEOTECHNICAL CROSS SECTION B-B'**  
Oakland International Airport  
Oakland, California

FIGURE DC-2b



N:\Projects\04\_2012\04\_7922\_1200\_CaltransAirportRecov\Outputs\2013\_03\_05\_Report\mxd\Fig\_DC03\_OAK\_LiquSettl\_M7\_80\_a032\_1906SF.mxd, 03/21/13, dpollard

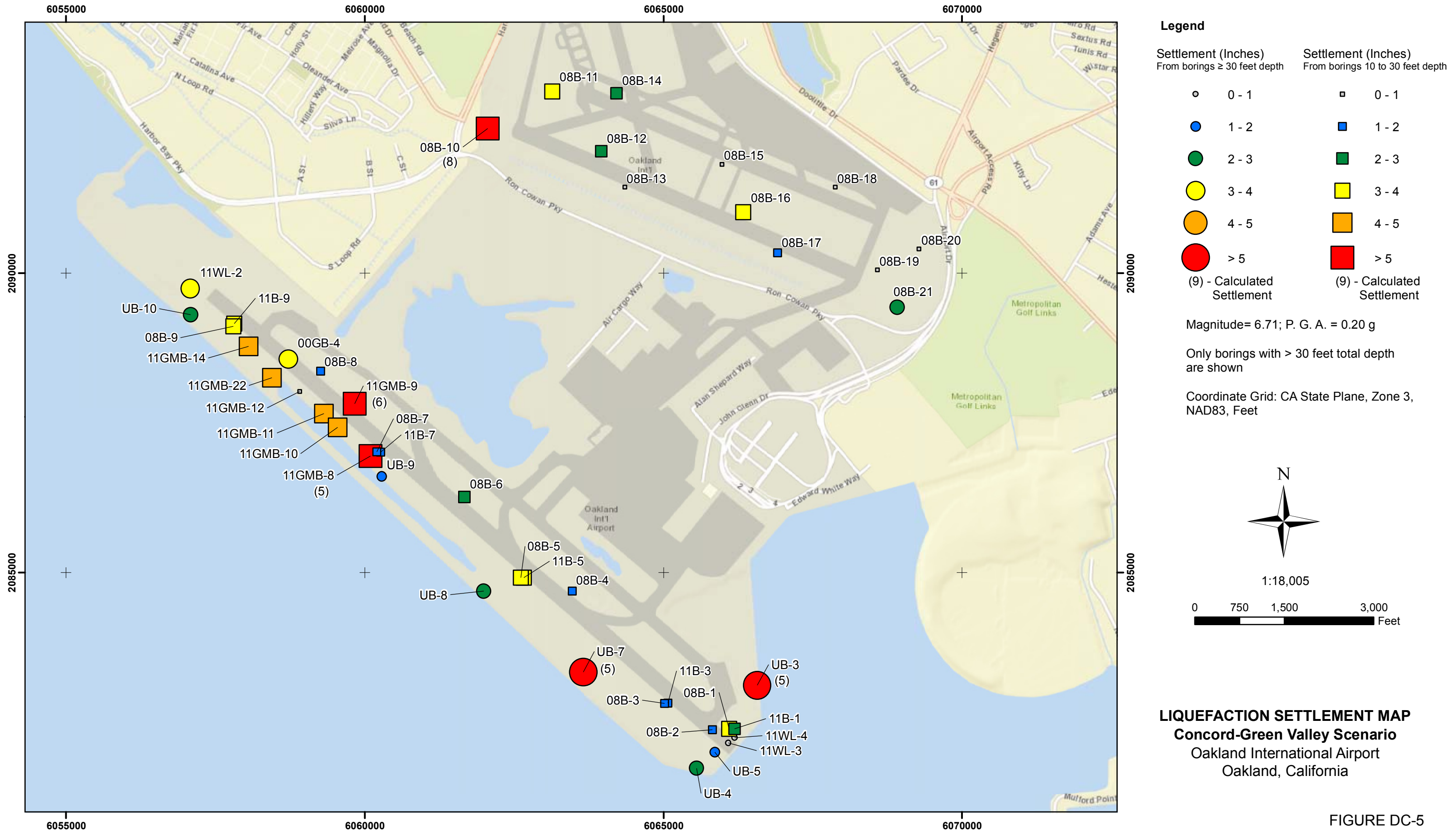
FIGURE DC-3



**LIQUEFACTION SETTLEMENT MAP**  
**Hayward-Rodgers Creek Scenario**  
Oakland International Airport  
Oakland, California

FIGURE DC-4

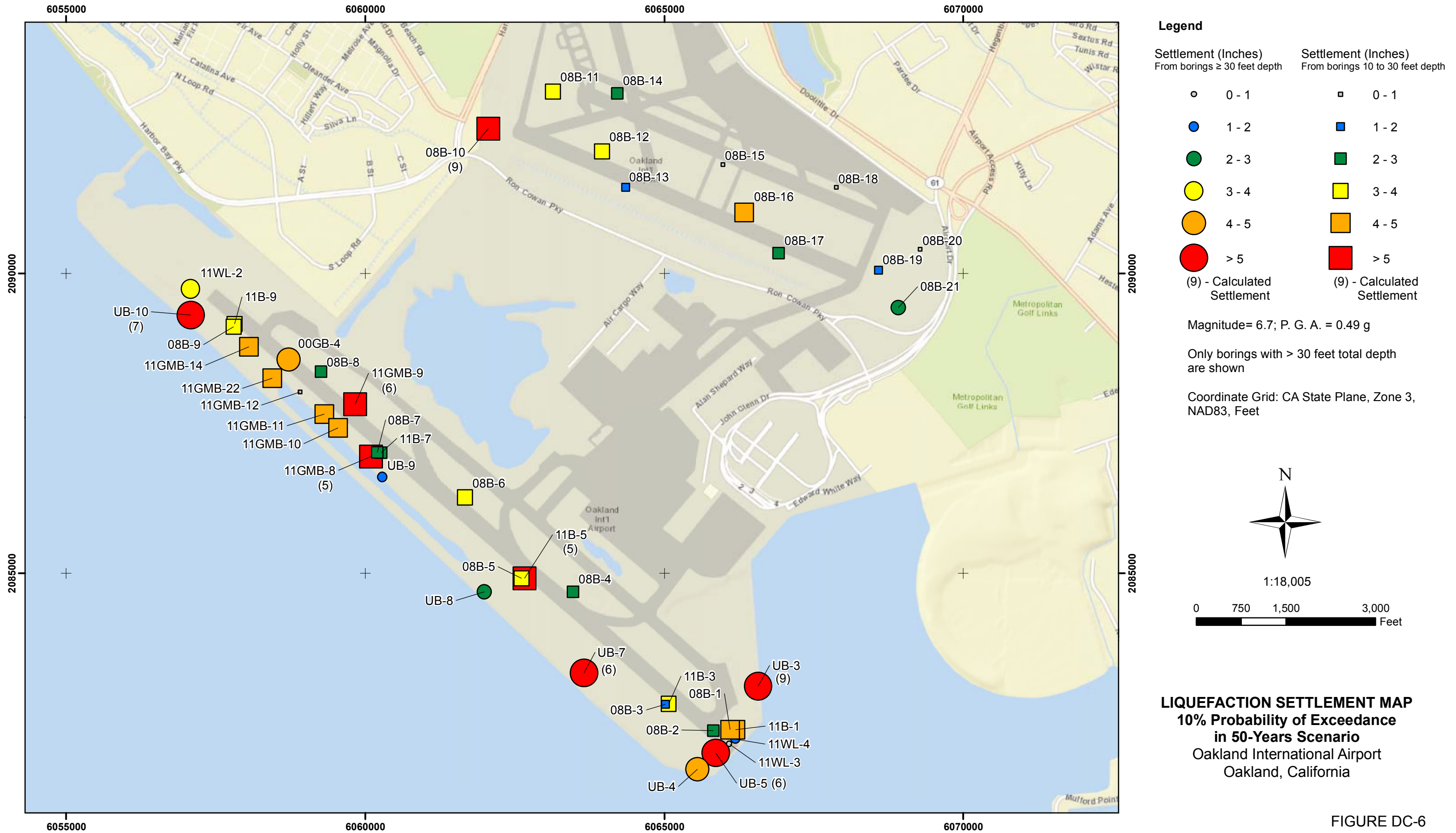
N:\Projects\04\_2012\04\_7922\_1200\_CaltransAirportRecov\Outputs\2013\_03\_05\_Report\mxd\Fig\_DC04\_OAK\_LiquSettl\_M7\_26\_a035\_HRC\_Fault.mxd\_03/21/13\_dpollard



**LIQUEFACTION SETTLEMENT MAP**  
**Concord-Green Valley Scenario**  
Oakland International Airport  
Oakland, California

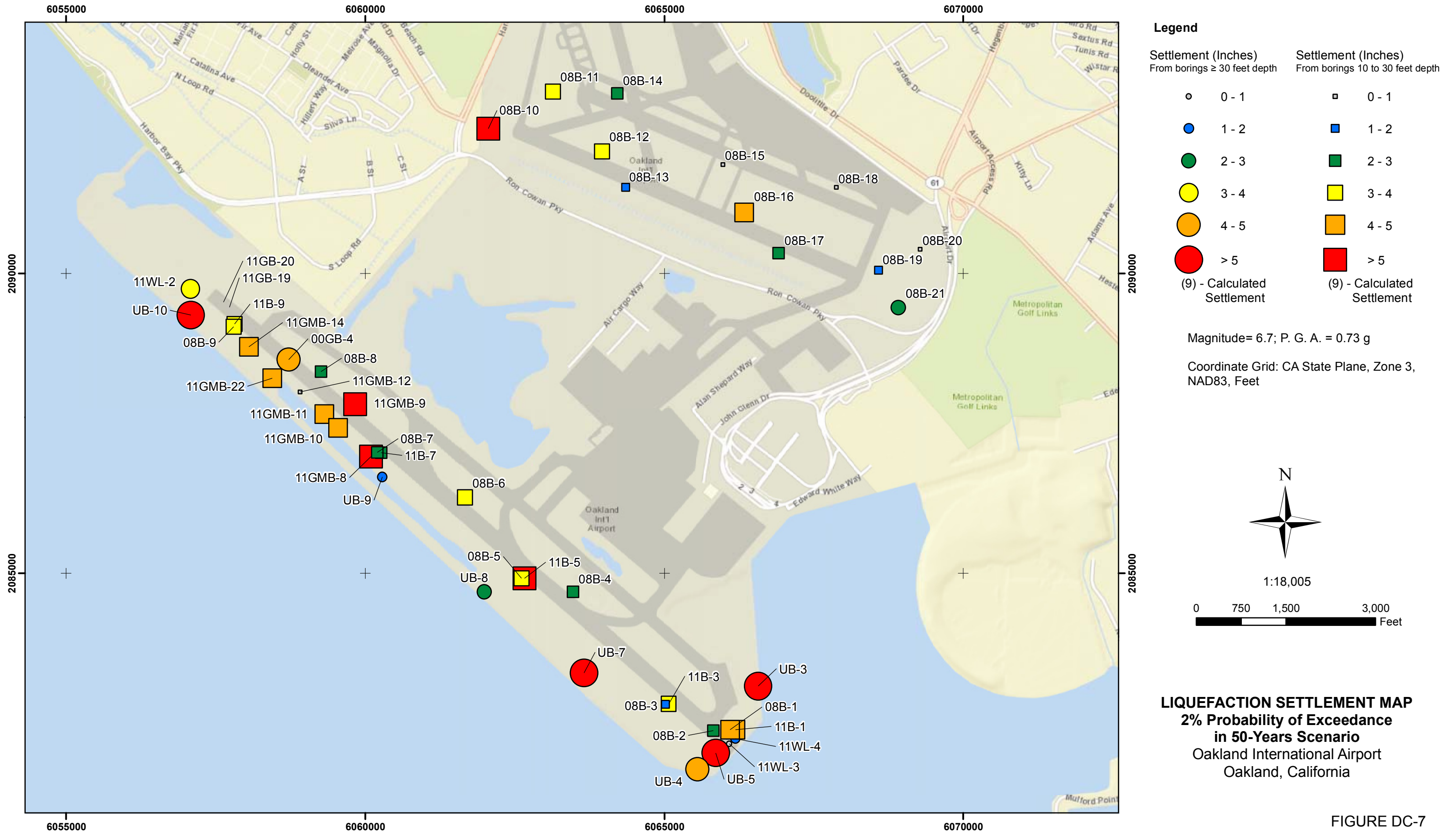
FIGURE DC-5

N:\Projects\04\_2012\04\_7922\_1200\_CaltransAirportRecov\Outputs\2013\_03\_05\_Report\mxd\Fig\_DC05\_OAK\_LiquSettl\_M6\_71\_a020\_CGV\_Fault.mxd\_03/21/13\_dpollard



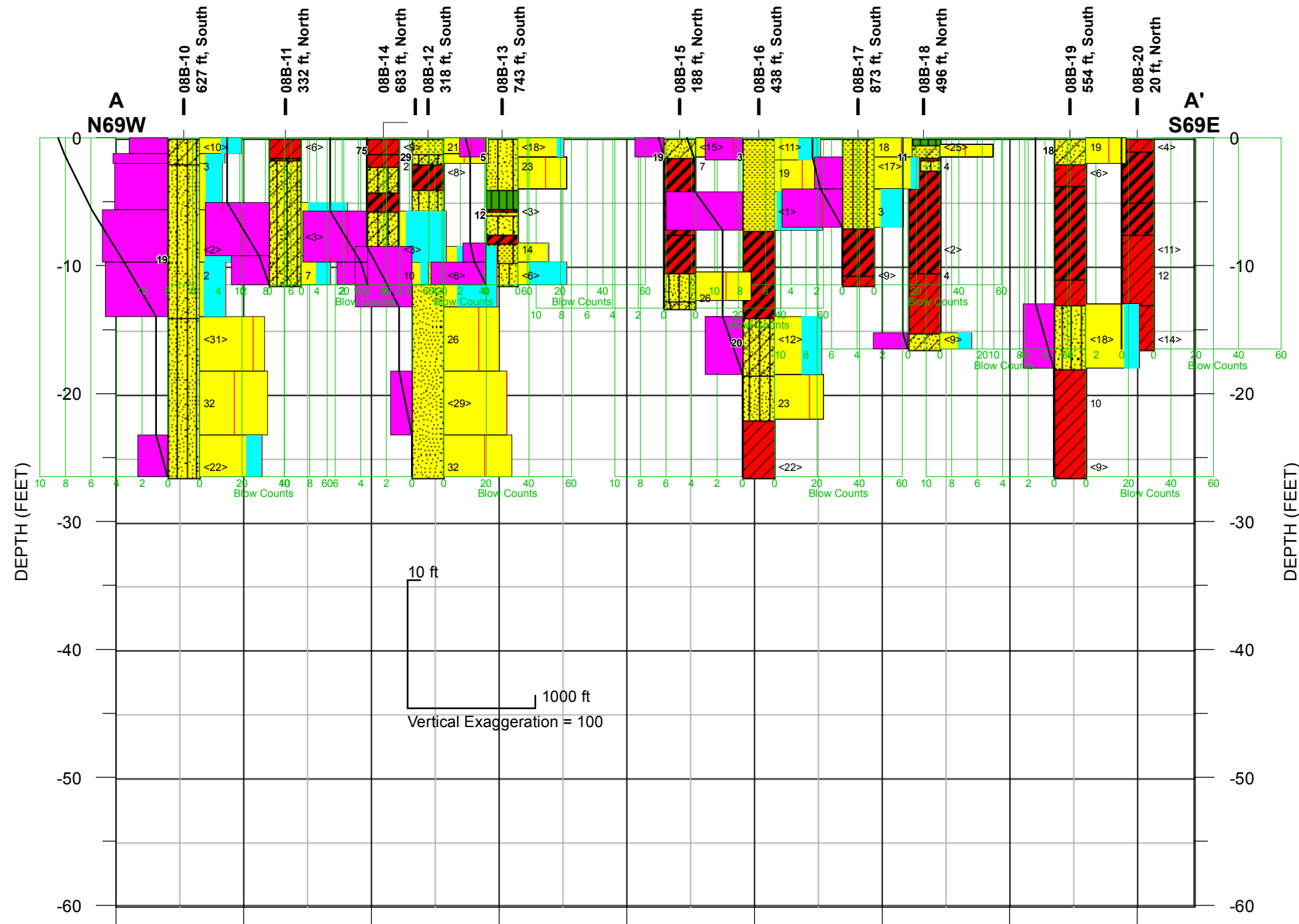
N:\Projects\04\_2012\04\_7922\_1200\_CaltransAirportRecov\Outputs\2013\_03\_05\_Report\mxd\Fig\_DC06\_OAK\_LiquSettl\_M6\_70\_a049\_475Yr.mxd, 03/21/13, dpollard

FIGURE DC-6

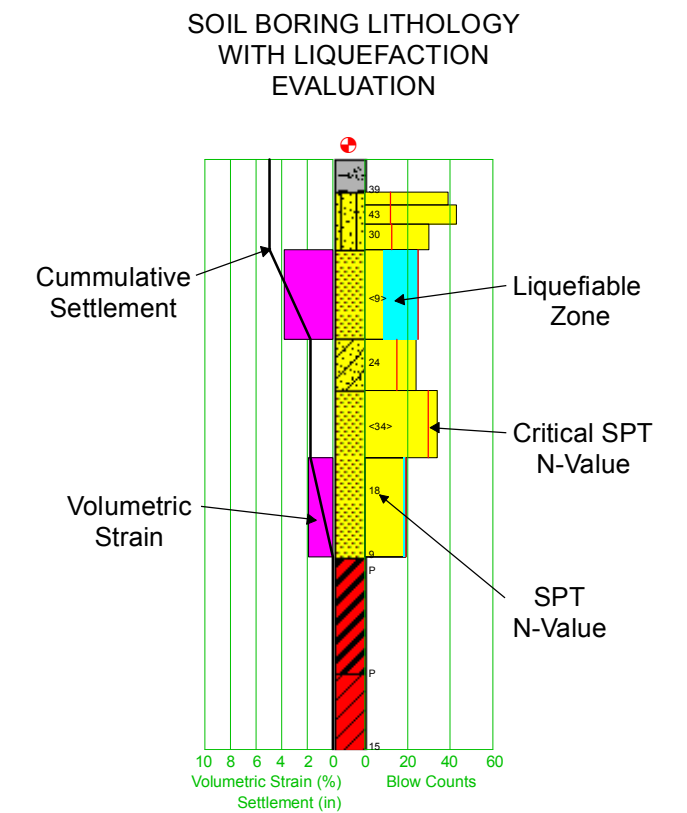


N:\Projects\04\_2012\04\_7922\_1200\_CaltransAirportRecov\Outputs\2013\_03\_05\_Report\mxd\Fig\_DC07\_OAK\_LiquSettl\_M6\_70\_a073\_2475Yr.mxd, 03/21/13, dpollard

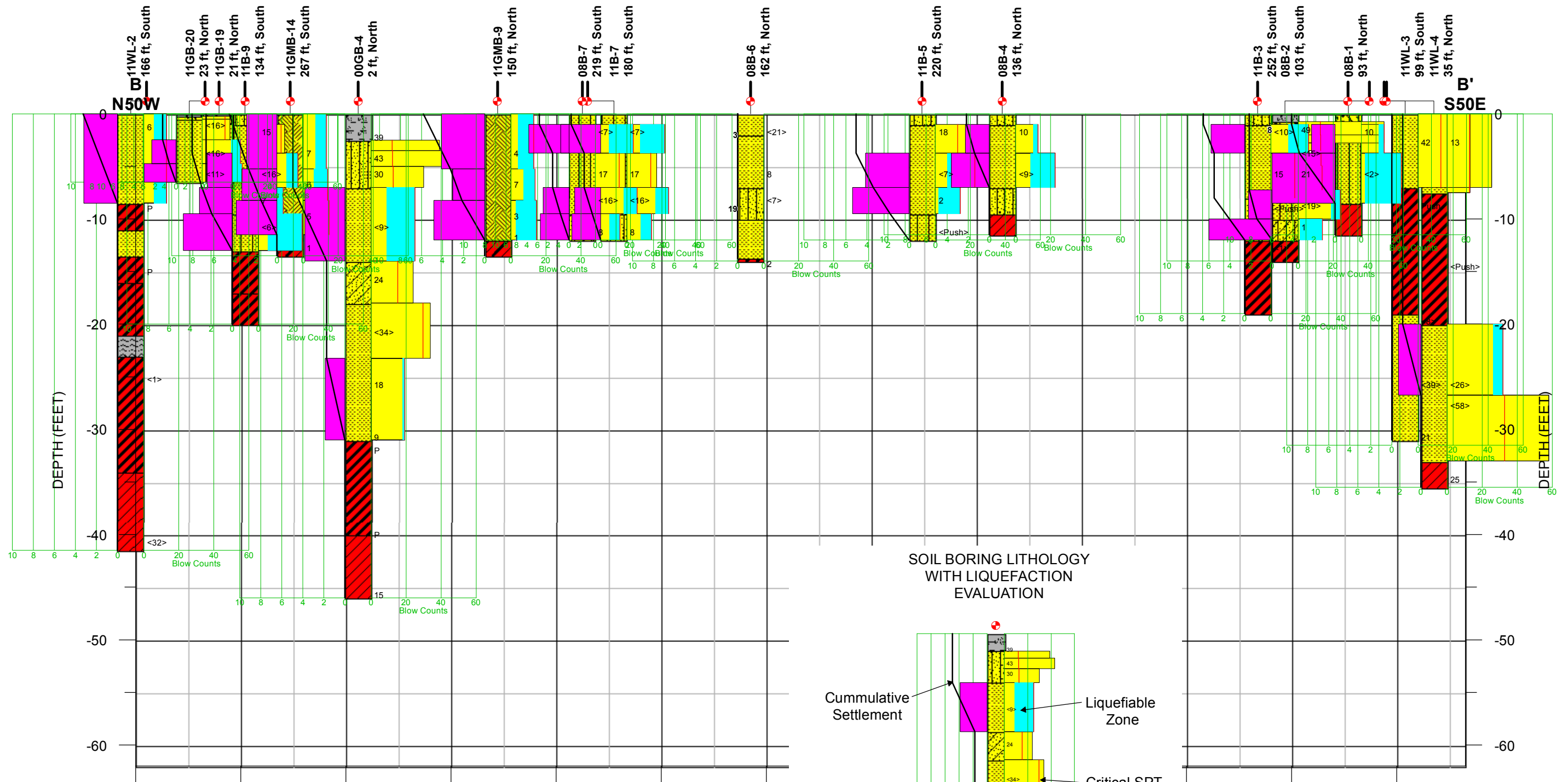
FIGURE DC-7



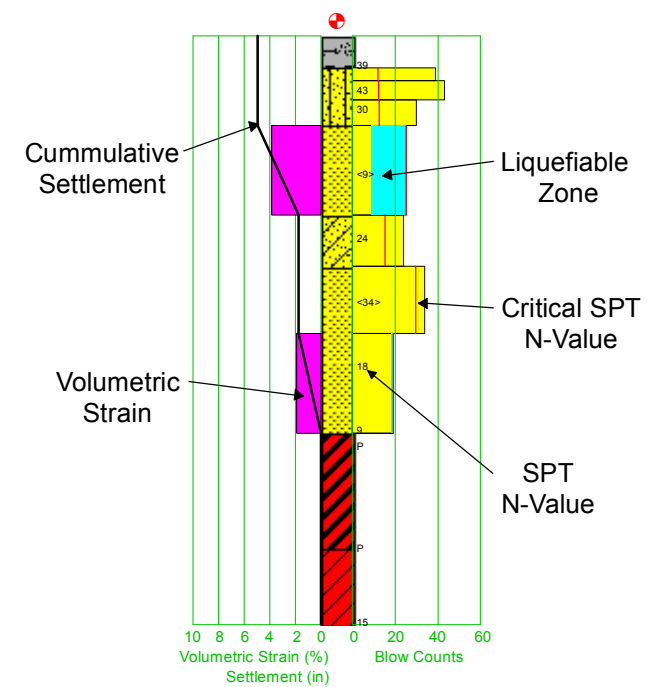
Note: Magnitude= 6.7; P. G. A. = 0.73 g



**LIQUEFACTION CROSS SECTION A-A'**  
**2% Probability of Exceedance**  
**in 50-Years Scenario**  
Oakland International Airport  
Oakland, California



SOIL BORING LITHOLOGY WITH LIQUEFACTION EVALUATION

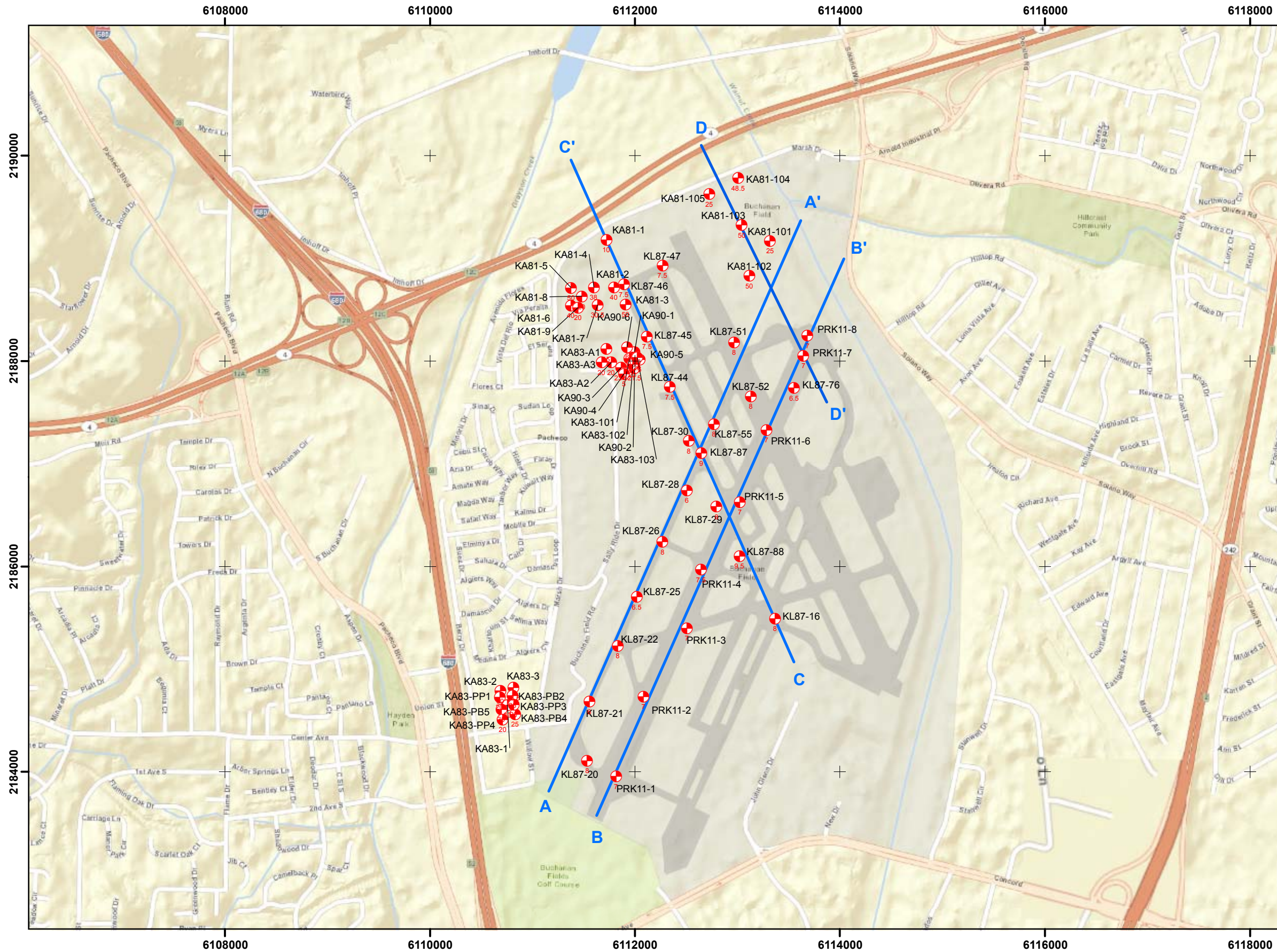


Note: Magnitude= 6.7; P. G. A. = 0.73 g

**LIQUEFACTION CROSS SECTION B-B'**  
 2% Probability of Exceedance  
 in 50-Years Scenario  
 Oakland International Airport  
 Oakland, California

10 ft  
 1000 ft  
 Vertical Exaggeration = 100

N:\Projects\04\_2012\04\_7922\_1200\_CaltransAirportRecov\Outputs\2013\_03\_05\_Report\mxd\Fig\_DC08b\_OAK\_ProfileB\_M6\_70\_a073\_2475Yr.mxd, 03/21/13, dpollard



**Legend**

- Existing Borings
- KA = Kaldveer Associates
- KL = Kleinfelder Associates
- PRK = Parikh Consultants
- Cross Section Location

Coordinates System: CA State Plane, Zone 3, NAD83, Feet

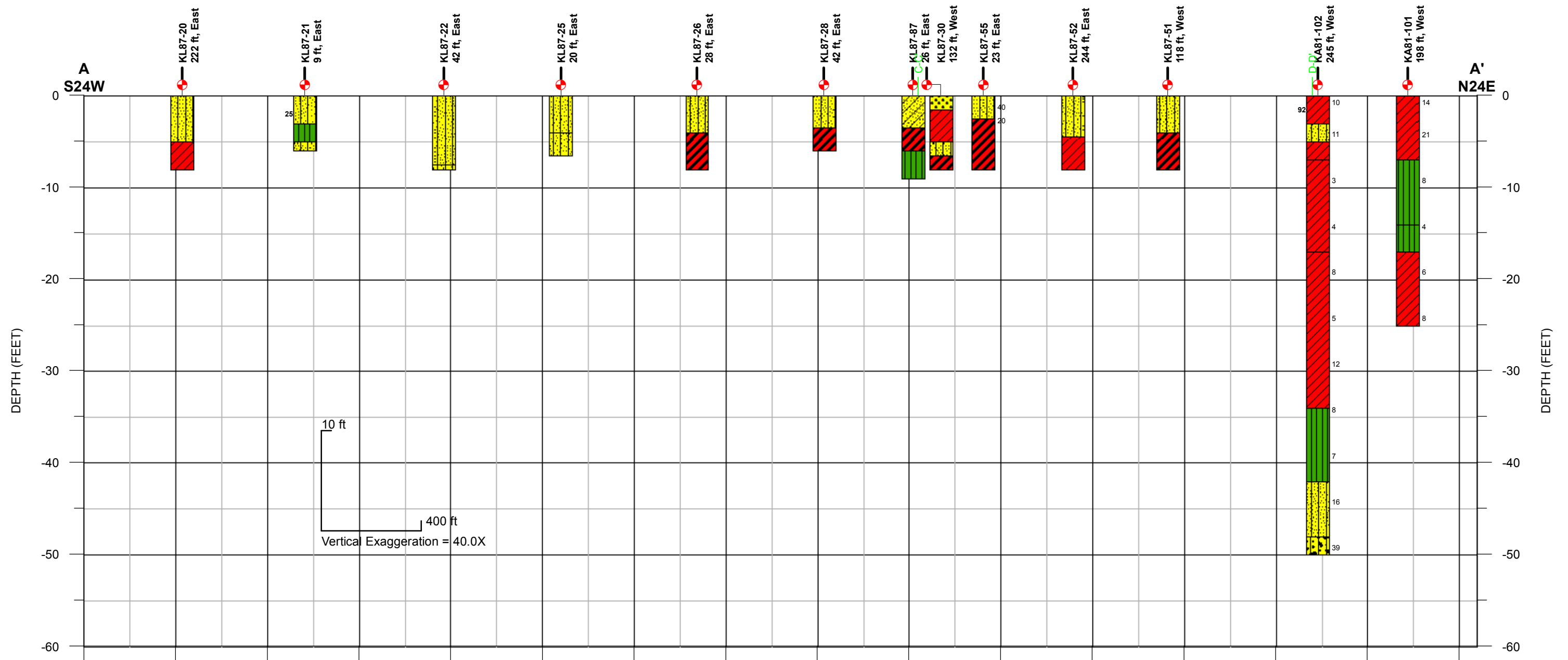


1:12,003



**PLAN VIEW**  
Buchanan Airport  
Concord, California

FIGURE DD-1

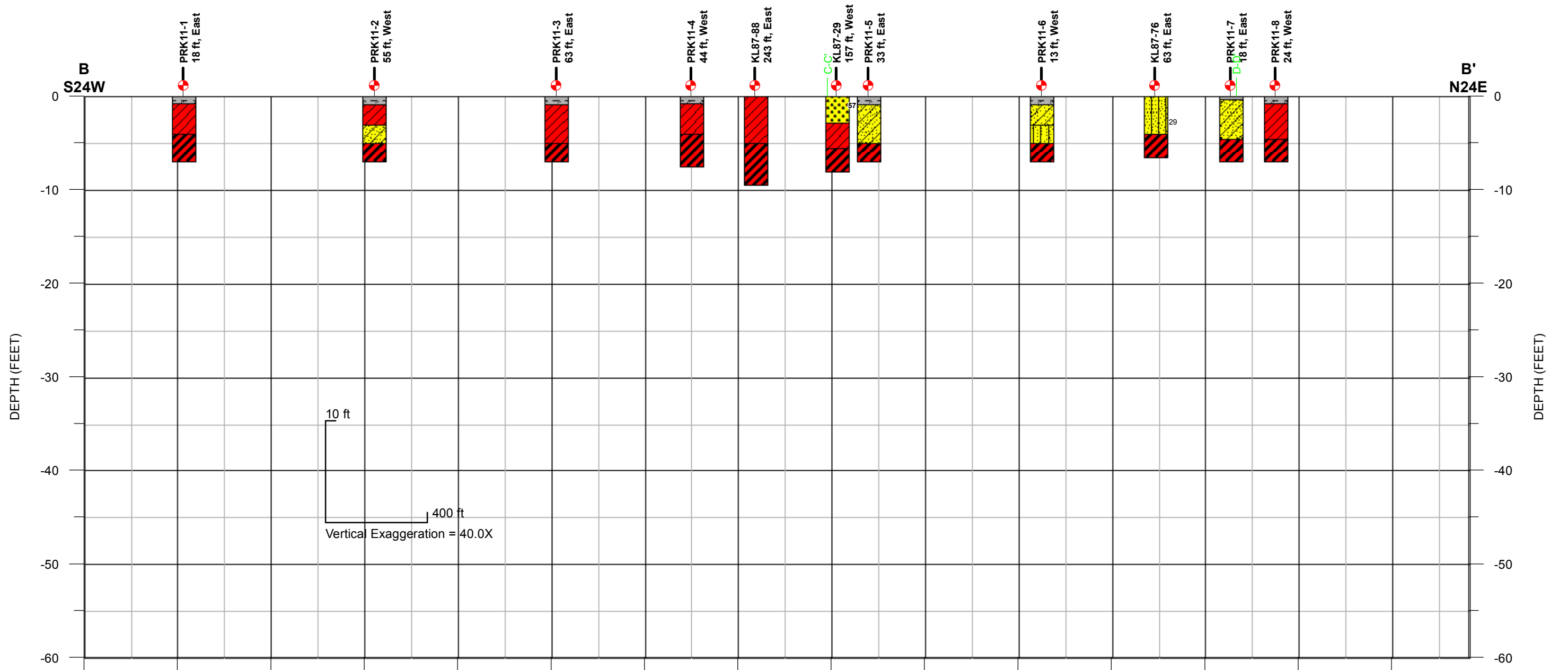


**Legend**

- |                          |                           |                             |   |
|--------------------------|---------------------------|-----------------------------|---|
| Lean CLAY (CL)           | Well-Graded SAND (SW)     | Silty Gravel (GM)           | 10 SPT Blow Count                                 |
| Lean to Fat CLAY (CL-CH) | Clayey SAND (SC)          | Low-Plasticity Organic (OL) | <20> Modified California Liner Sampler Blow Count |
| Fat CLAY (CH)            | Silty SAND (SM)           | Asphaltic Concrete          | 75 Fines Content (% - plotted on left of boring)  |
| Silt (ML)                | Poorly-Graded GRAVEL (GP) |                             |   |

**GEOTECHNICAL CROSS SECTION A-A'**  
Buchanan Airport  
Concord, California

FIGURE DD-2a

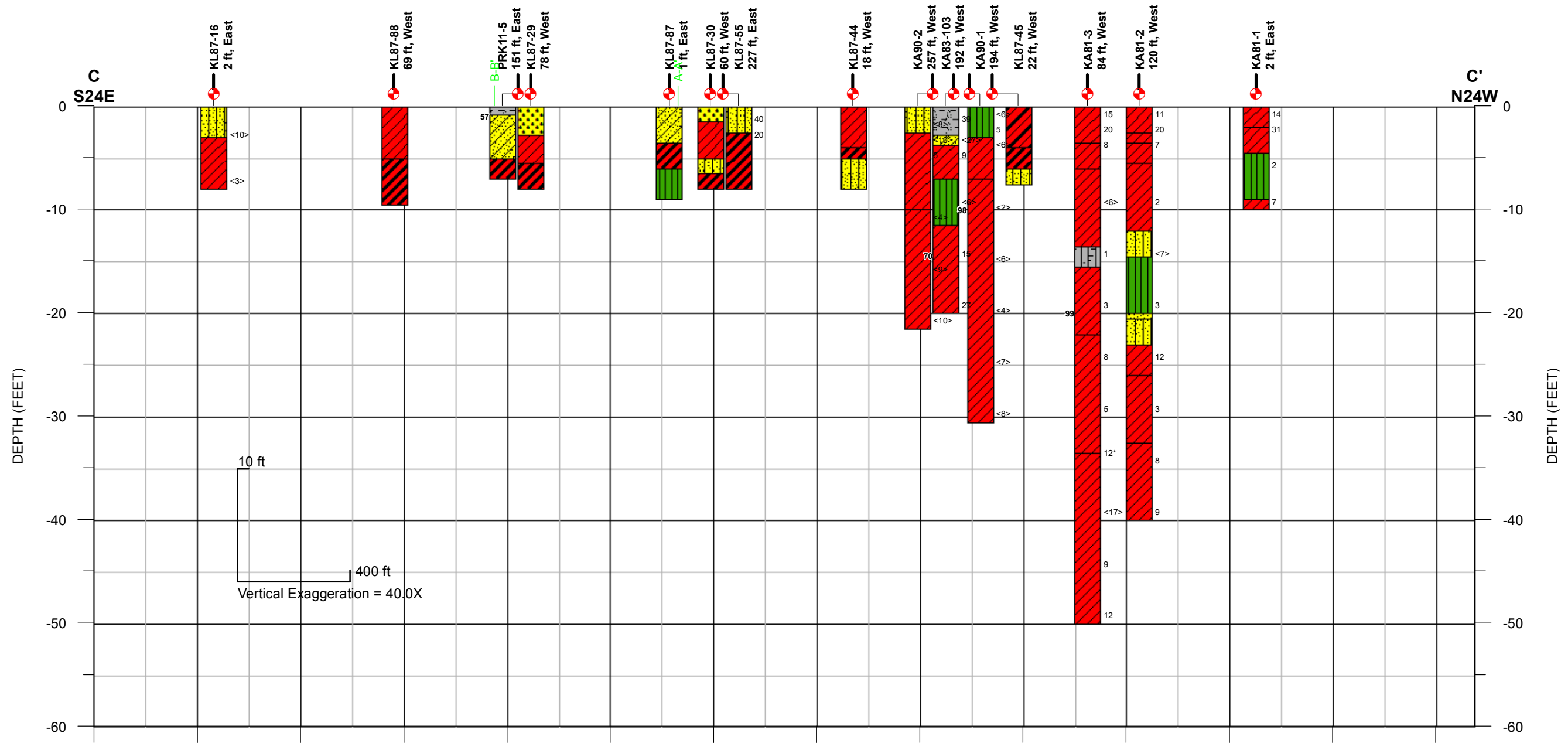


**Legend**

- |                          |                           |                             |   |
|--------------------------|---------------------------|-----------------------------|---|
| Lean CLAY (CL)           | Well-Graded SAND (SW)     | Silty Gravel (GM)           | 10 SPT Blow Count                                 |
| Lean to Fat CLAY (CL-CH) | Clayey SAND (SC)          | Low-Plasticity Organic (OL) | <20> Modified California Liner Sampler Blow Count |
| Fat CLAY (CH)            | Silty SAND (SM)           | Asphaltic Concrete          | 75 Fines Content (% - plotted on left of boring)  |
| Silt (ML)                | Poorly-Graded GRAVEL (GP) |                             |   |

**GEOTECHNICAL CROSS SECTION B-B'**  
Buchanan Airport  
Concord, California

FIGURE DD-2b

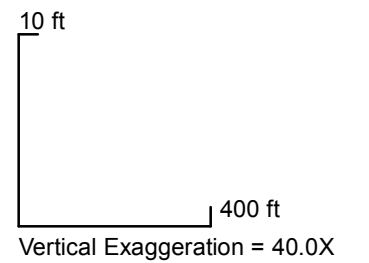
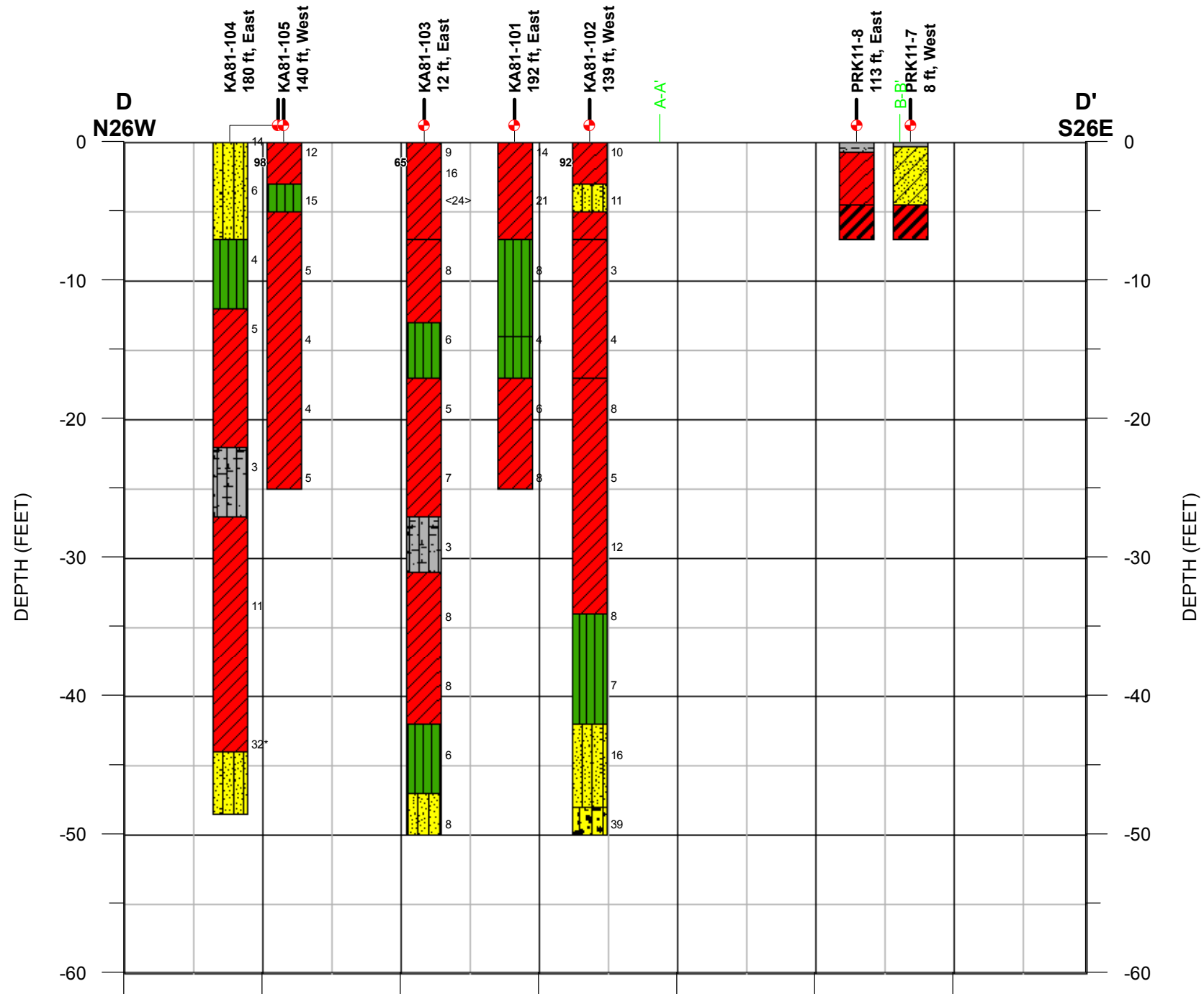


**Legend**

- |  |                          |  |                           |  |                             |      |   |
|--|--------------------------|--|---------------------------|--|-----------------------------|------|---|
|  | Lean CLAY (CL)           |  | Well-Graded SAND (SW)     |  | Silty Gravel (GM)           | 10   | SPT Blow Count                                |
|  | Lean to Fat CLAY (CL-CH) |  | Clayey SAND (SC)          |  | Low-Plasticity Organic (OL) | <20> | Modified California Liner Sampler Blow Count  |
|  | Fat CLAY (CH)            |  | Silty SAND (SM)           |  | Asphaltic Concrete          | 75   | Fines Content (% - plotted on left of boring) |
|  | Silt (ML)                |  | Poorly-Graded GRAVEL (GP) |  |                             |      |   |

**GEOTECHNICAL CROSS SECTION C-C'**  
Buchanan Airport  
Concord, California

FIGURE DD-2c

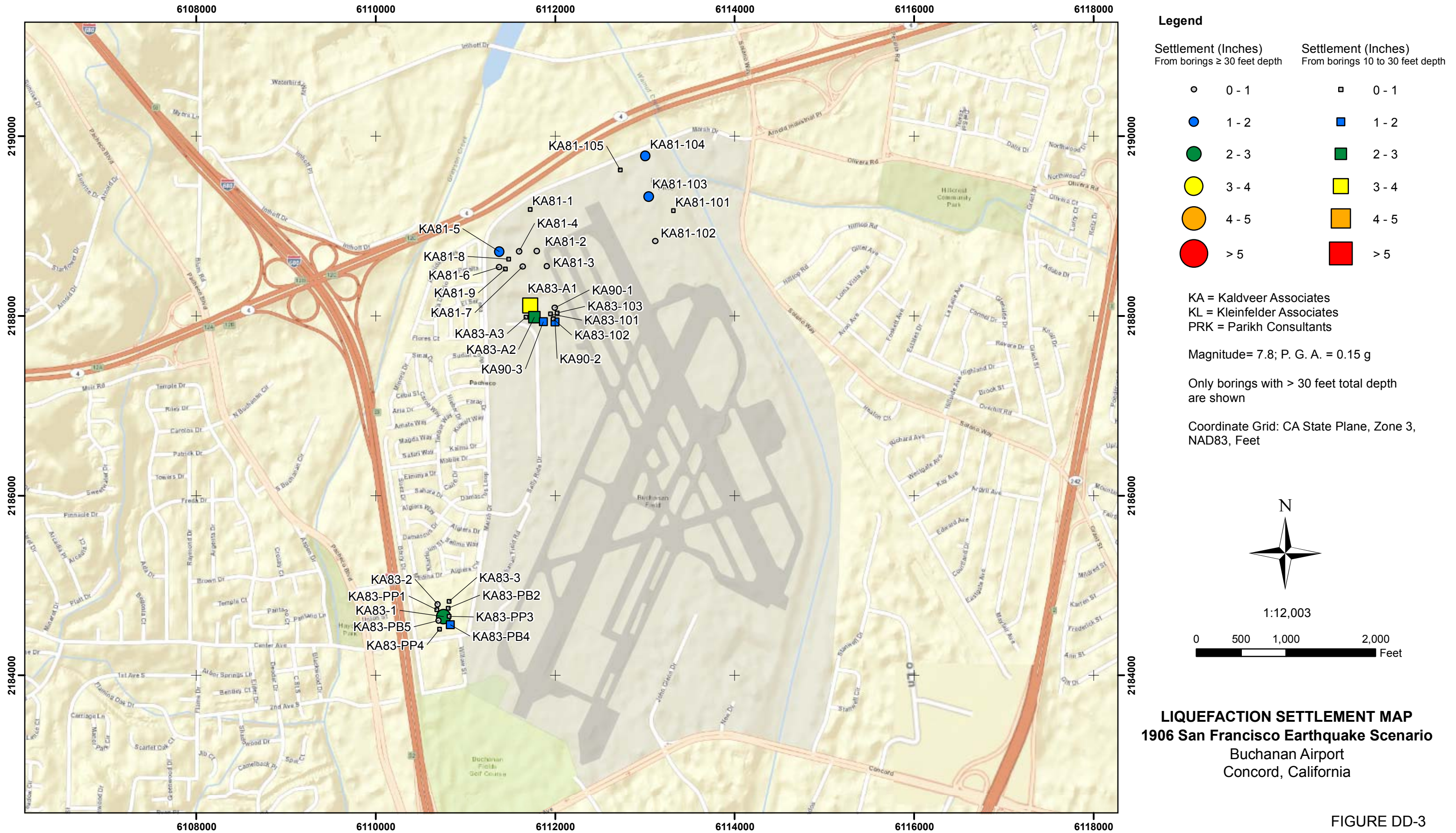


**Legend**

- |                          |                           |                             |   |
|--------------------------|---------------------------|-----------------------------|---|
| Lean CLAY (CL)           | Well-Graded SAND (SW)     | Silty Gravel (GM)           | 10 SPT Blow Count                                 |
| Lean to Fat CLAY (CL-CH) | Clayey SAND (SC)          | Low-Plasticity Organic (OL) | <20> Modified California Liner Sampler Blow Count |
| Fat CLAY (CH)            | Silty SAND (SM)           | Asphaltic Concrete          | 75 Fines Content (% - plotted on left of boring)  |
| Silt (ML)                | Poorly-Graded GRAVEL (GP) |                             |   |

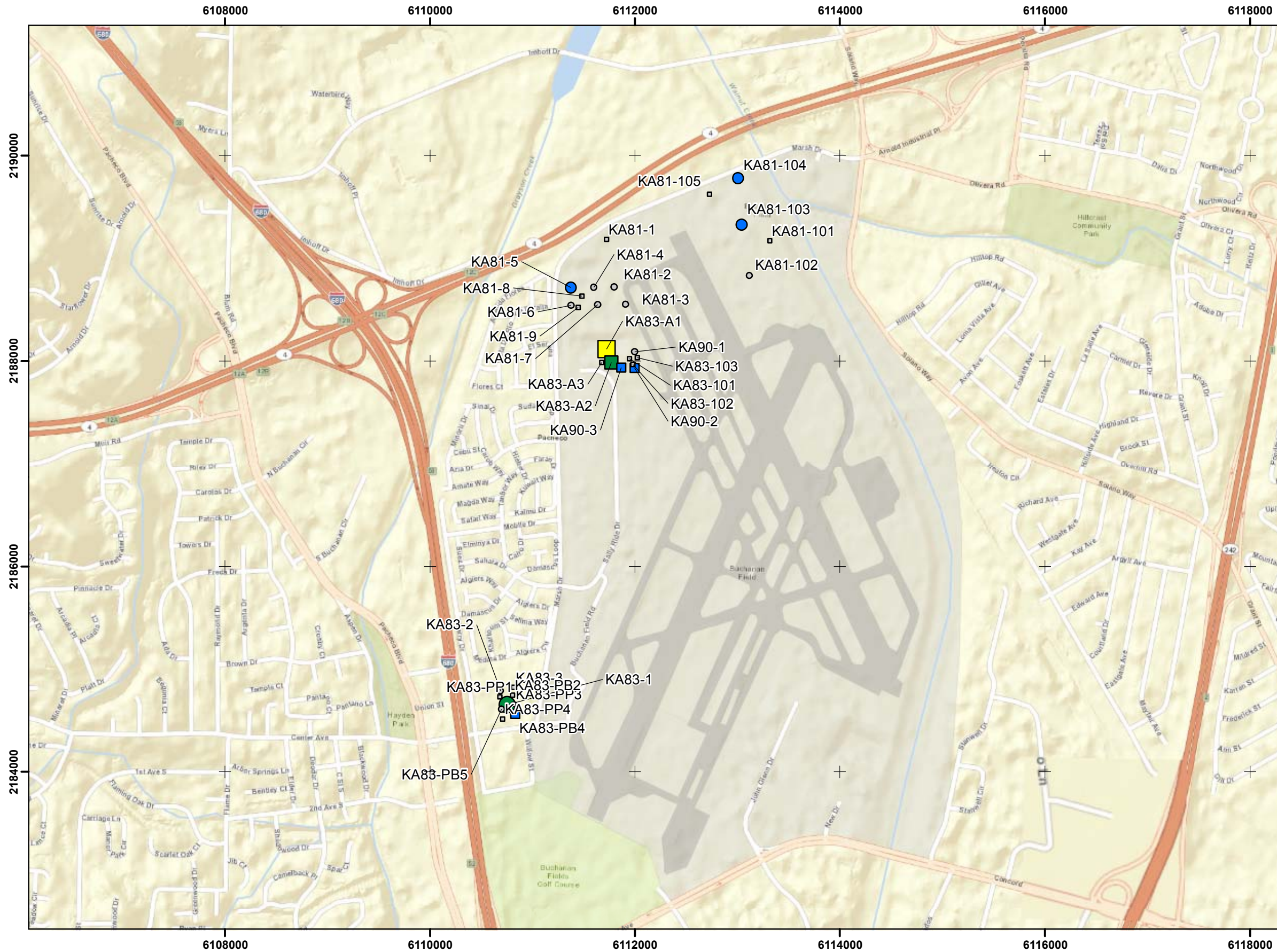
**GEOTECHNICAL CROSS SECTION D-D'**  
Buchanan Airport  
Concord, California

FIGURE DD-2d



N:\Projects\04\_2012\04\_7922\_1200\_CaltransAirportRecon\Outputs\2013\_03\_05\_Report\mxd\Fig\_DD03\_BUC\_LiquSettl\_M7\_80\_a015\_1906SF.mxd, 03/21/13, dpollard

FIGURE DD-3



**Legend**

Settlement (Inches) From borings ≥ 30 feet depth		Settlement (Inches) From borings 10 to 30 feet depth	
○	0 - 1	□	0 - 1
●	1 - 2	■	1 - 2
●	2 - 3	■	2 - 3
●	3 - 4	■	3 - 4
●	4 - 5	■	4 - 5
●	> 5	■	> 5

KA = Kaldveer Associates  
KL = Kleinfelder Associates  
PRK = Parikh Consultants

Magnitude= 7.26; P. G. A. = 0.24 g

Only borings with > 30 feet total depth are shown

Coordinate Grid: CA State Plane, Zone 3, NAD83, Feet

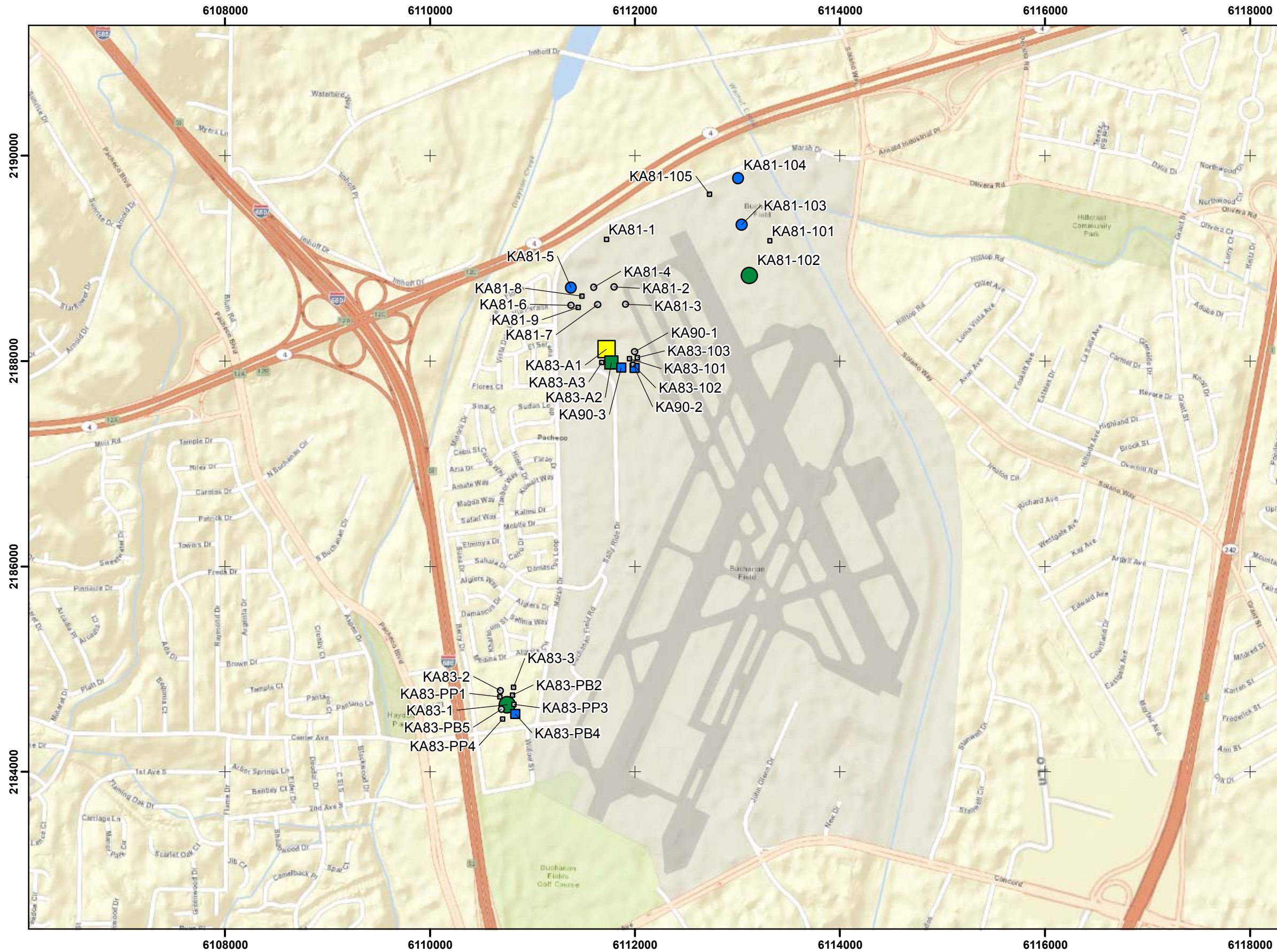


1:12,003



**LIQUEFACTION SETTLEMENT MAP**  
**Hayward-Rodgers Creek Scenario**  
Buchanan Airport  
Concord, California

FIGURE DD-4



**Legend**

Settlement (Inches) From borings ≥ 30 feet depth		Settlement (Inches) From borings 10 to 30 feet depth	
○	0 - 1	◻	0 - 1
●	1 - 2	■	1 - 2
●	2 - 3	■	2 - 3
●	3 - 4	■	3 - 4
●	4 - 5	■	4 - 5
●	> 5	■	> 5

KA = Kaldveer Associates  
KL = Kleinfelder Associates  
PRK = Parikh Consultants

Magnitude= 6.71; P. G. A. = 0.53 g

Only borings with > 30 feet total depth  
are shown

Coordinate Grid: CA State Plane, Zone 3,  
NAD83, Feet

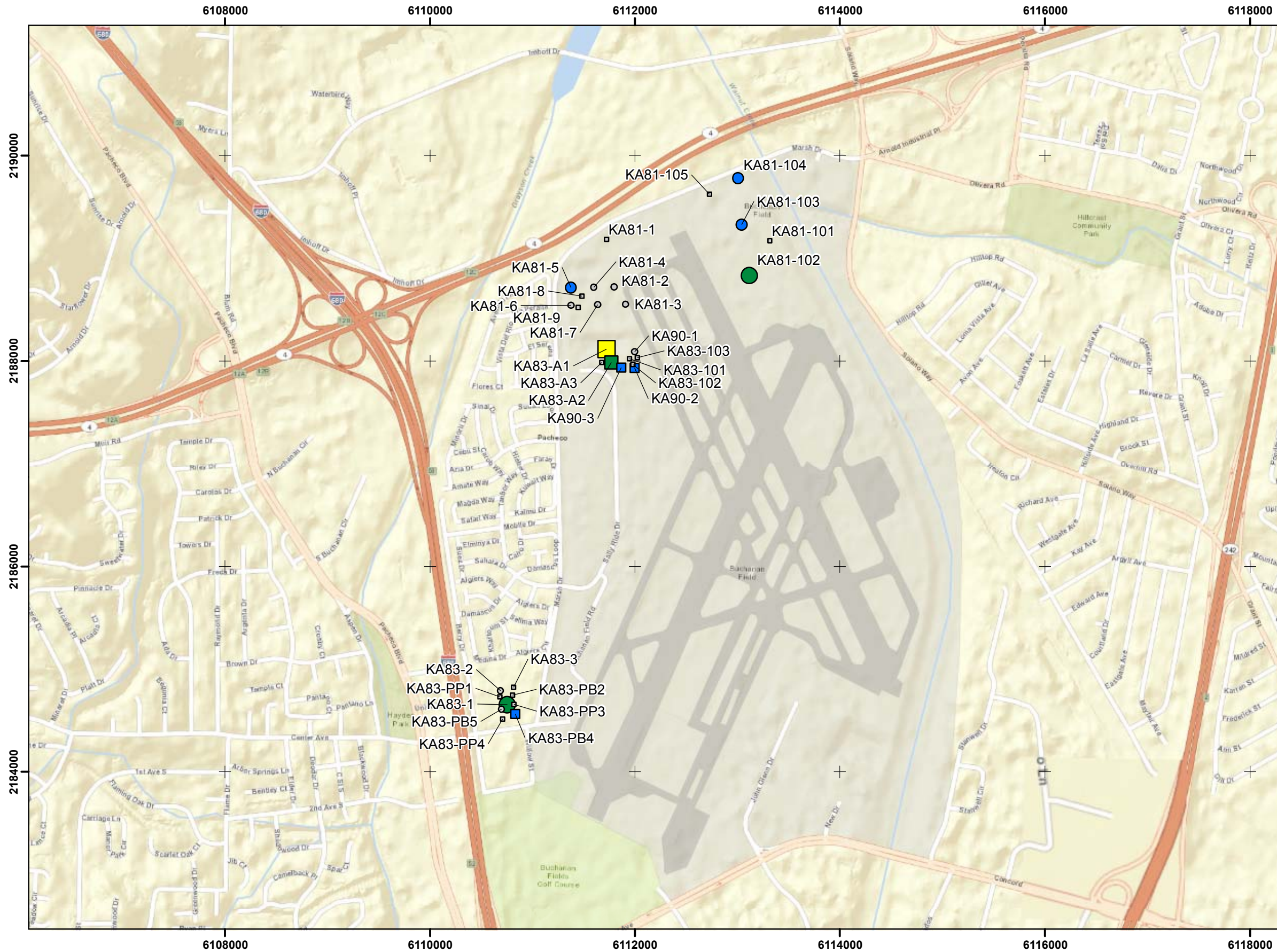


1:12,003



**LIQUEFACTION SETTLEMENT MAP**  
**Concord-Green Valley Scenario**  
Buchanan Airport  
Concord, California

FIGURE DD-5



**Legend**

Settlement (Inches) From borings ≥ 30 feet depth		Settlement (Inches) From borings 10 to 30 feet depth	
○	0 - 1	◻	0 - 1
●	1 - 2	■	1 - 2
●	2 - 3	■	2 - 3
●	3 - 4	■	3 - 4
●	4 - 5	■	4 - 5
●	> 5	■	> 5

KA = Kaldveer Associates  
KL = Kleinfelder Associates  
PRK = Parikh Consultants

Magnitude= 6.6; P. G. A. = 0.54 g

Only borings with > 30 feet total depth are shown

Coordinate Grid: CA State Plane, Zone 3, NAD83, Feet

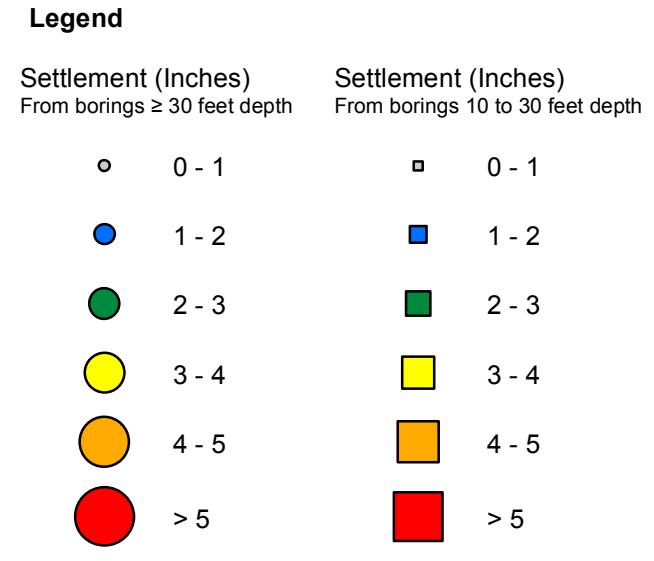
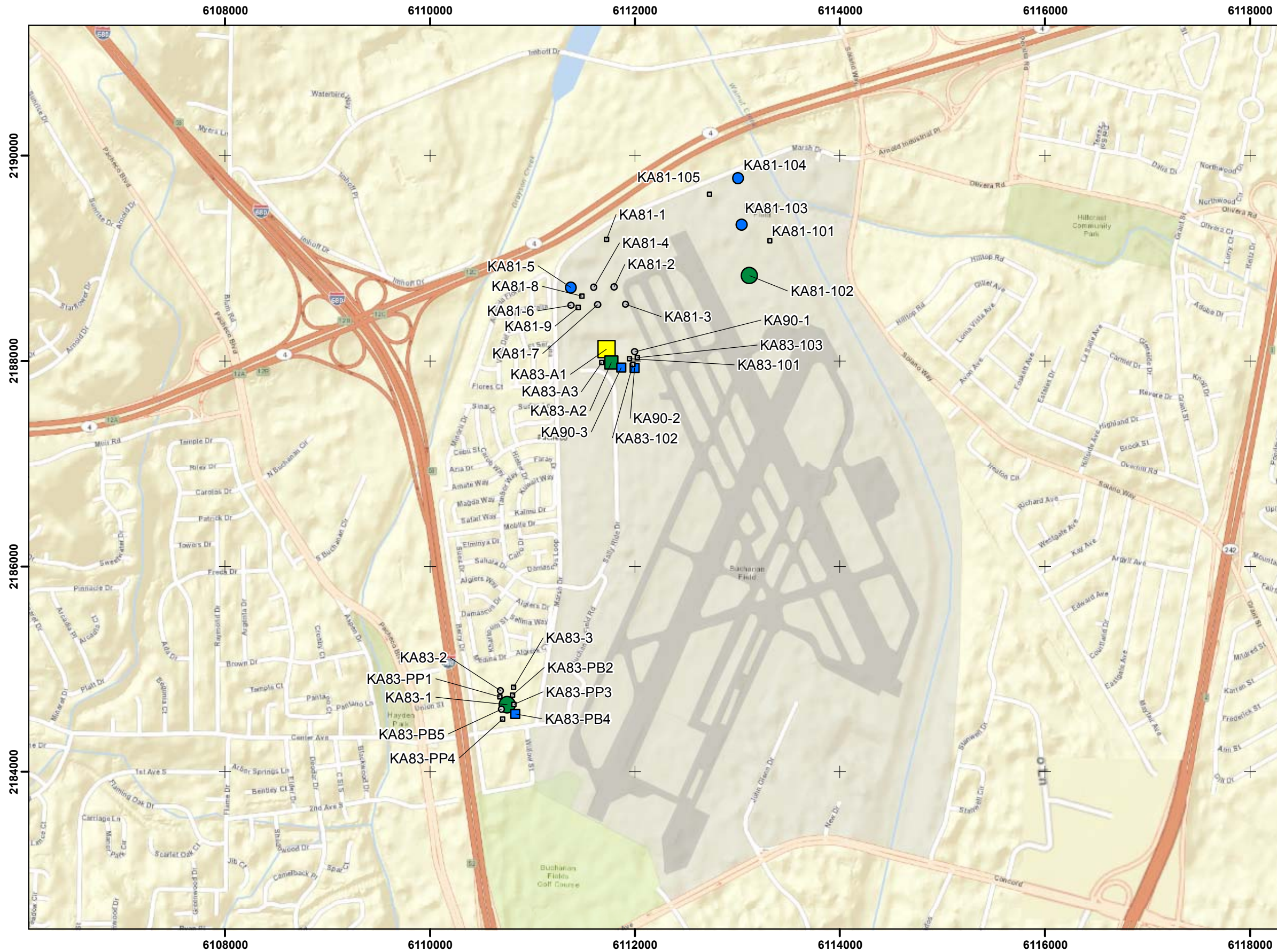


1:12,003



**LIQUEFACTION SETTLEMENT MAP**  
**10% Probability of Exceedance**  
**in 50-Years Scenario**  
Buchanan Airport  
Concord, California

FIGURE DD-6



KA = Kaldveer Associates  
KL = Kleinfelder Associates  
PRK = Parikh Consultants

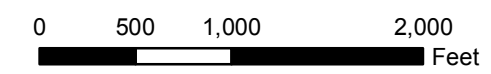
Magnitude= 6.6; P. G. A. = 0.87 g

Only borings with > 30 feet total depth are shown

Coordinate Grid: CA State Plane, Zone 3, NAD83, Feet



1:12,003

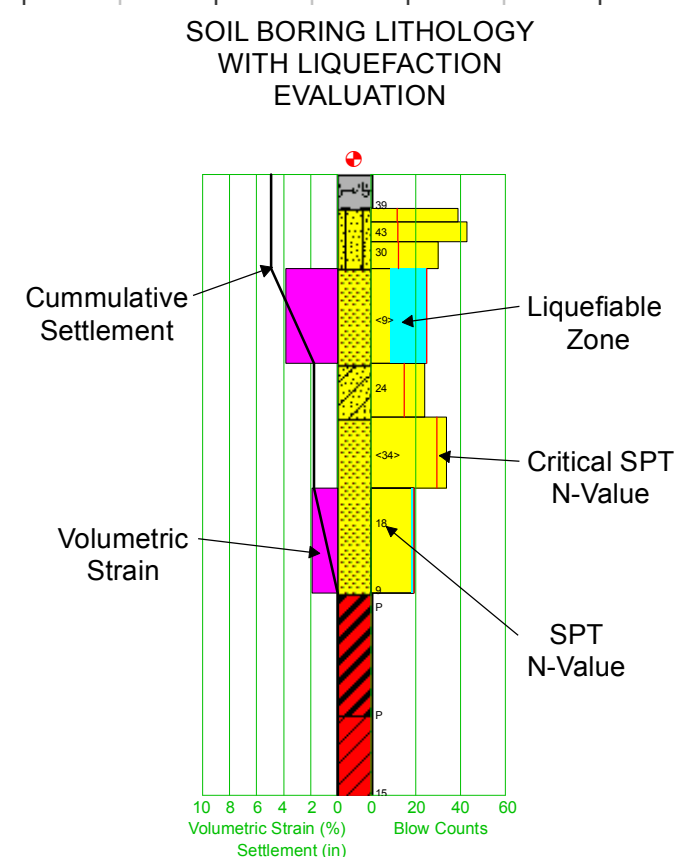
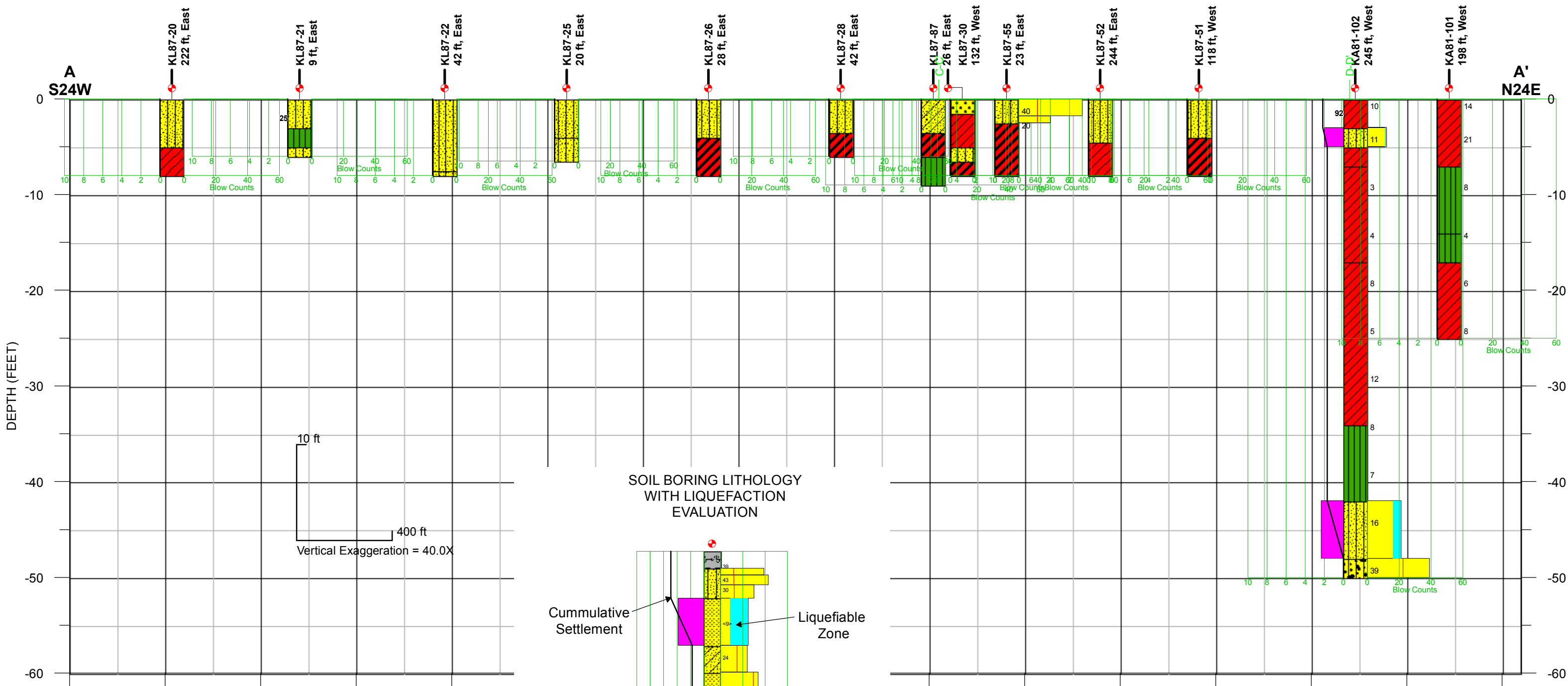


**LIQUEFACTION SETTLEMENT MAP**  
**2% Probability of Exceedance**  
**in 50-Years Scenario**  
Buchanan Airport  
Concord, California

FIGURE DD-7

N:\Projects\04\_2012\04\_7922\_1200\_CaltransAirportRecov\Outputs\2013\_03\_05\_Report\mxd\Fig\_DD07\_BUC\_LiquSettl\_M6\_60\_a087\_2475Yr.mxd, 03/21/13, dpollard

N:\Projects\04\_2012\04\_7922\_1200\_CaltransAirportRecov\Outputs\2013\_03\_05\_Report\mxd\Fig\_DD08a\_BUC\_ProfileA\_M6\_a087\_2475Yr.mxd, 03/21/13, dpollard

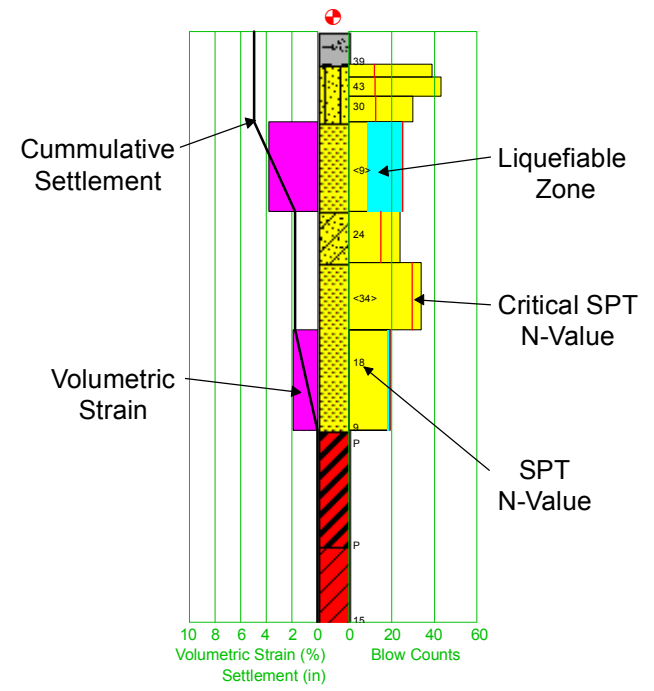
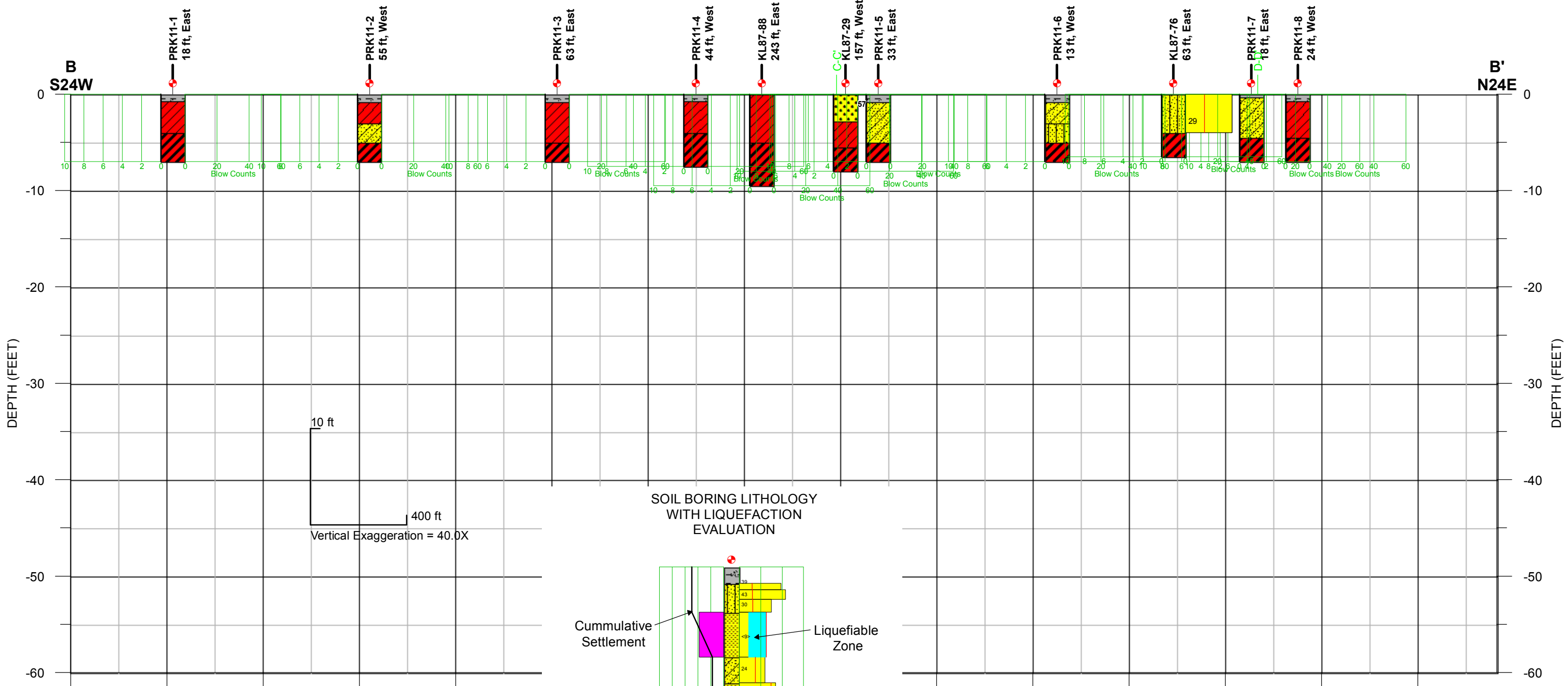


Note: Magnitude= 6.6; P. G. A. = 0.87 g

**LIQUEFACTION CROSS SECTION A-A'**  
 2% Probability of Exceedance  
 in 50-Years Scenario  
 Buchanan Airport  
 Concord, California

FIGURE DD-8a

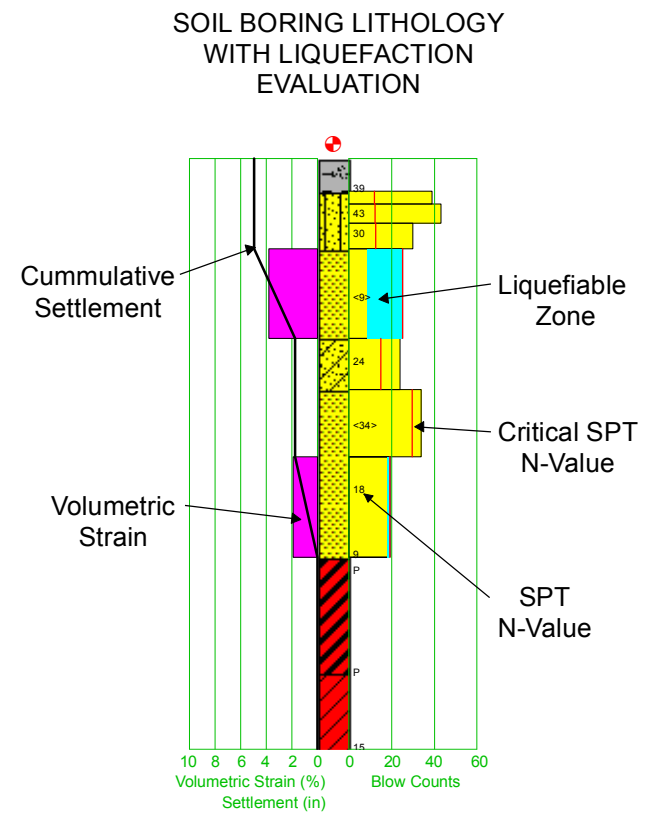
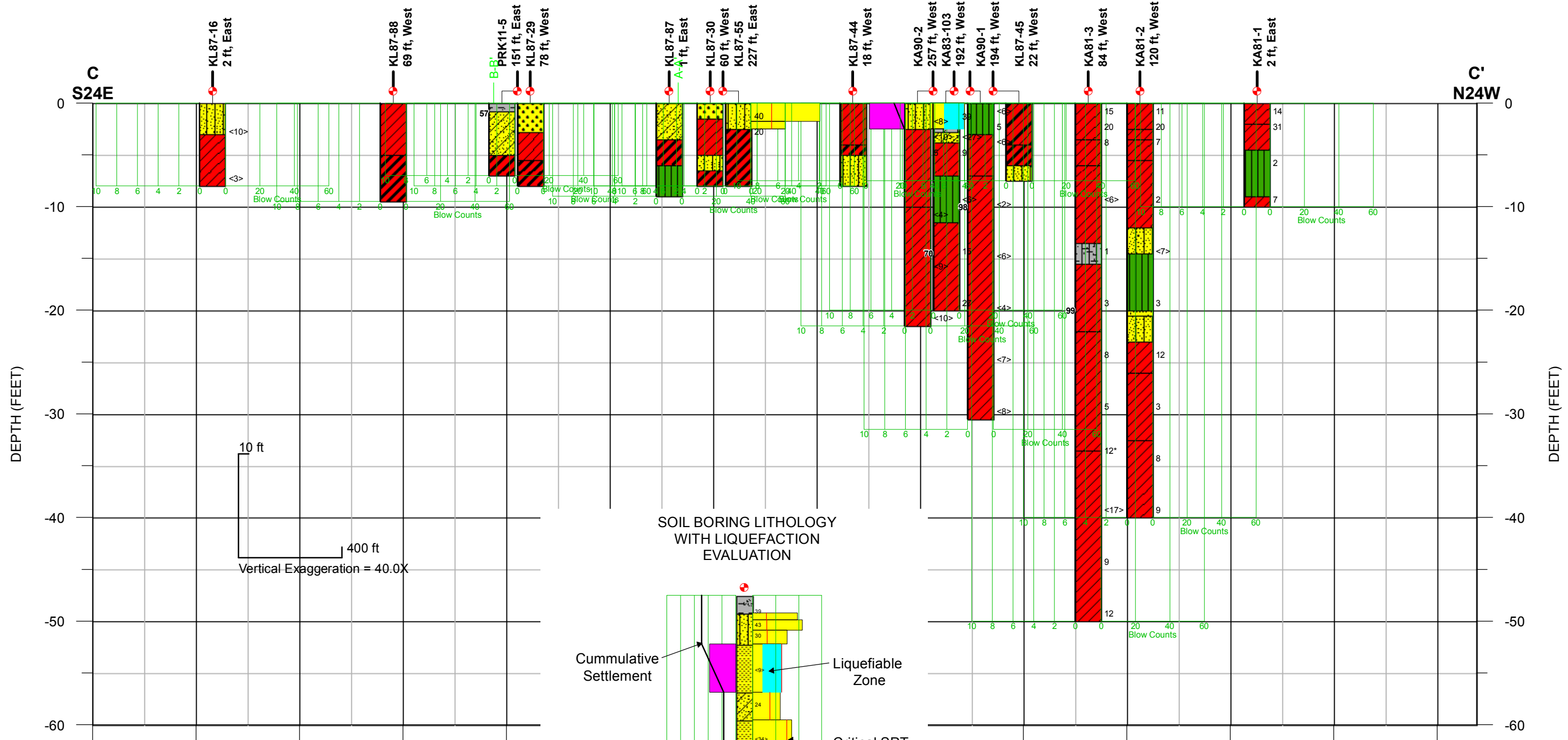
N:\Projects\04\_2012\04\_7922\_1200\_CaltransAirportRecov\Outputs\2013\_03\_05\_Report\mxd\Fig\_DD08b\_BUC\_ProfileB\_M6\_a087\_2475Yr.mxd, 03/21/13, dpollard



Note: Magnitude= 6.6; P. G. A. = 0.87 g

**LIQUEFACTION CROSS SECTION B-B'**  
 2% Probability of Exceedance  
 in 50-Years Scenario  
 Buchanan Airport  
 Concord, California

FIGURE DD-8b



Note: Magnitude= 6.6; P. G. A. = 0.87 g

**LIQUEFACTION CROSS SECTION C-C'**  
 2% Probability of Exceedance  
 in 50-Years Scenario  
 Buchanan Airport  
 Concord, California

FIGURE DD-8c

N:\Projects\04\_2012\04\_7922\_1200\_CaltransAirportRecon\Outputs\2013\_03\_05\_Report\mxd\Fig\_DD08c\_BUC\_ProfileC\_M6\_60\_a087\_2475Yr.mxd, 03/21/13, dpollard





**Legend**

- Existing Borings
- Cross Section Location

Coordinates System: CA State Plane,  
Zone 3, NAD83, Feet



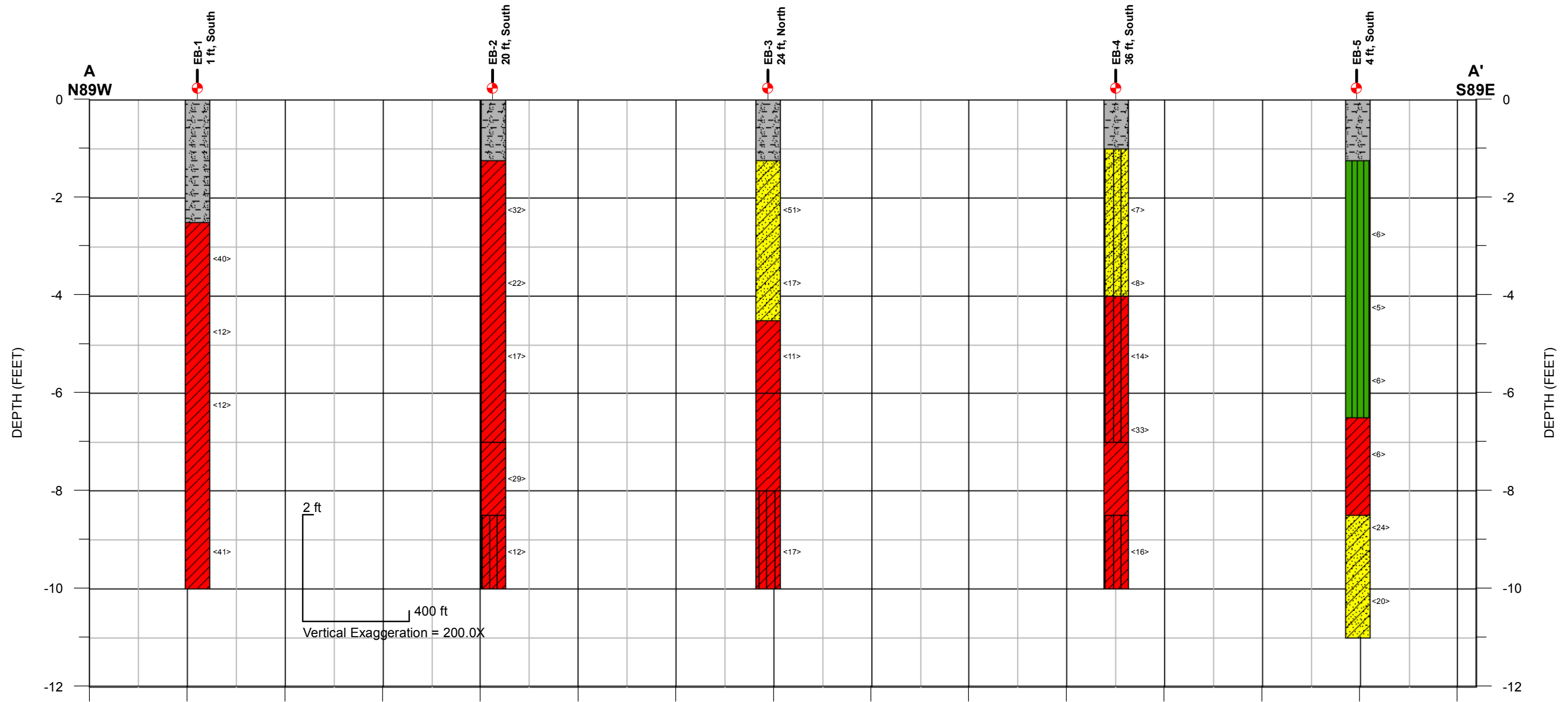
1:6,002



**PLAN VIEW**  
Livermore Airport  
Livermore, California

FIGURE DE-1

N:\Projects\04\_2012\04\_7922\_1200\_CaltransAirportRecov\Outputs\2013\_03\_05\_Report\mxd\Fig\_DE01\_LIV\_ExplorationLocationMap.mxd, 03/21/13, dpollard

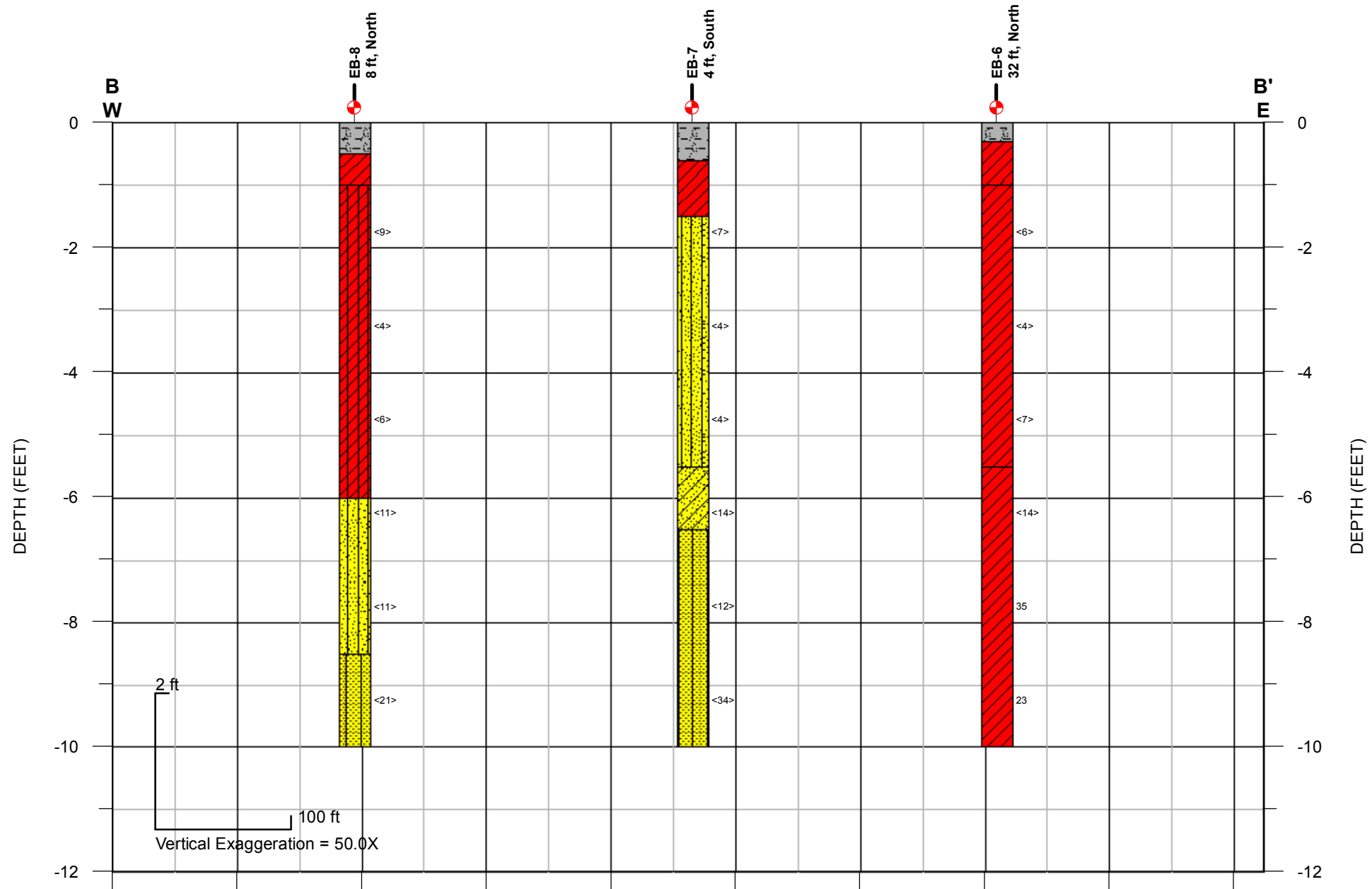


**Legend**

- |                                      |                              |   |
|--------------------------------------|------------------------------|---|
| Lean CLAY (CL)                       | Clayey SAND (SC)             | 10 SPT Blow Count                                 |
| Silty CLAY (CL-ML)                   | Clayey to Silty SAND (SC-SM) | <20> Modified California Liner Sampler Blow Count |
| Silt (ML)                            | Silty SAND (SM)              |   |
| Poorly-Graded SAND with Silt (SP-SM) | Asphaltic Concrete           |   |

**GEOTECHNICAL CROSS SECTION A-A'**  
Livermore Airport  
Livermore, California

FIGURE DE-2a

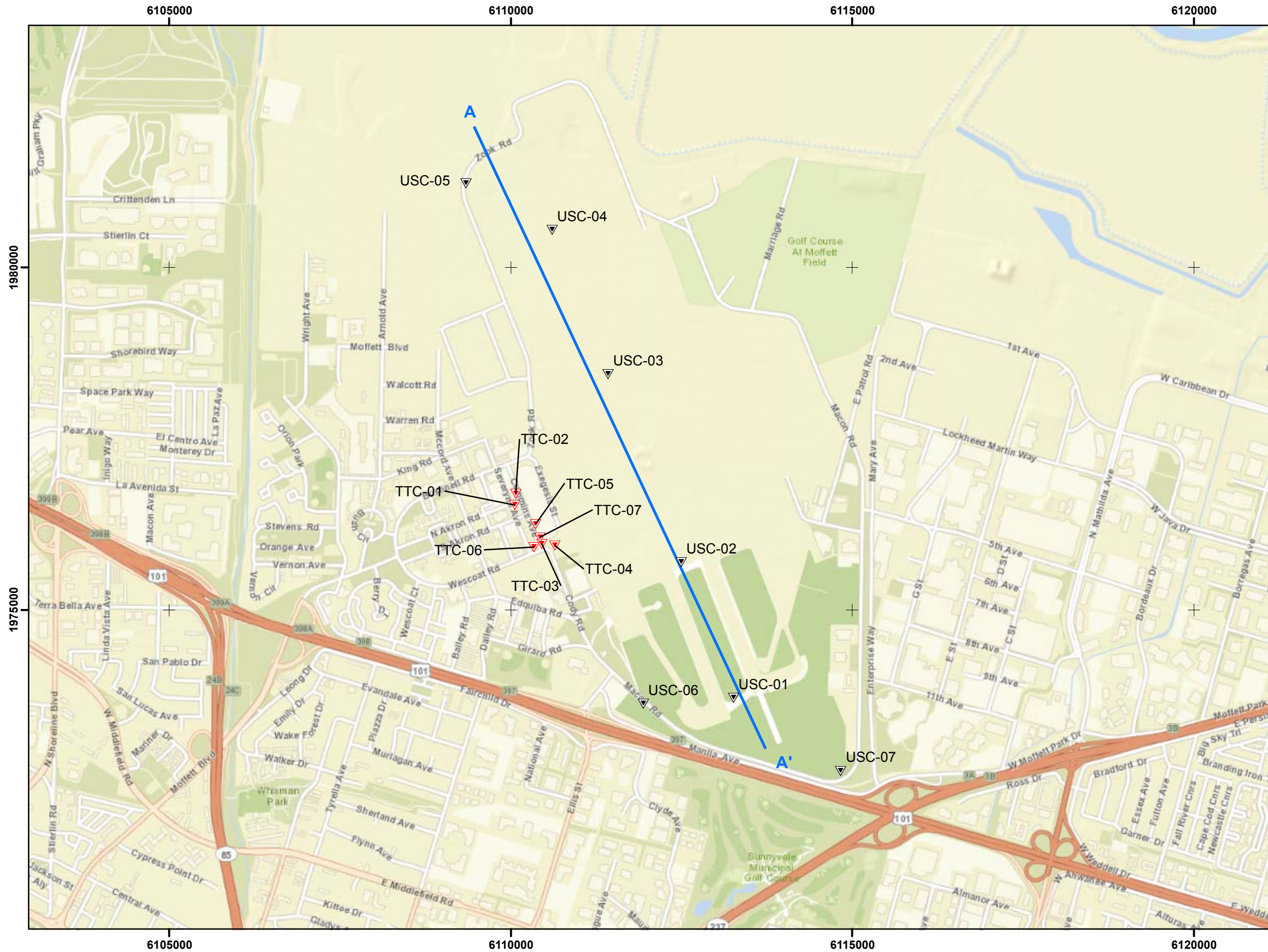


**Legend**

- |                                      |                              |   |
|--------------------------------------|------------------------------|---|
| Lean CLAY (CL)                       | Clayey SAND (SC)             | 10 SPT Blow Count                                 |
| Silty CLAY (CL-ML)                   | Clayey to Silty SAND (SC-SM) | <20> Modified California Liner Sampler Blow Count |
| Silt (ML)                            | Silty SAND (SM)              |   |
| Poorly-Graded SAND with Silt (SP-SM) | Asphaltic Concrete           |   |

**GEOTECHNICAL CROSS SECTION B-B'**  
 Livermore Airport  
 Livermore, California

FIGURE DE-2b



- Legend**
- ▼ USGS CPT, 2000
  - ▼ TetraTech CPT, 2005
  - Cross Section Location



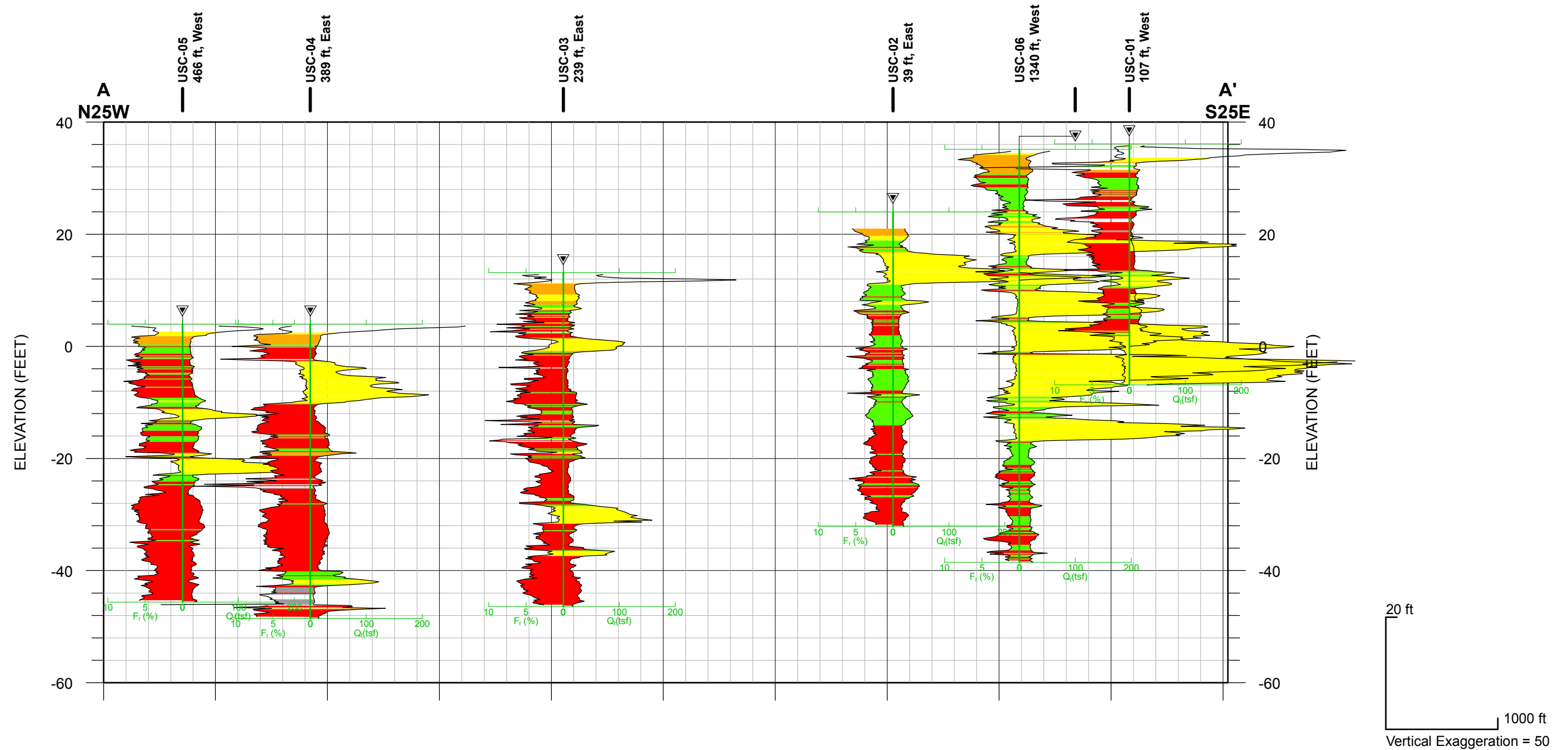
1:18,005



**PLAN VIEW**  
 Moffett Federal Airfield  
 Mountain View, California

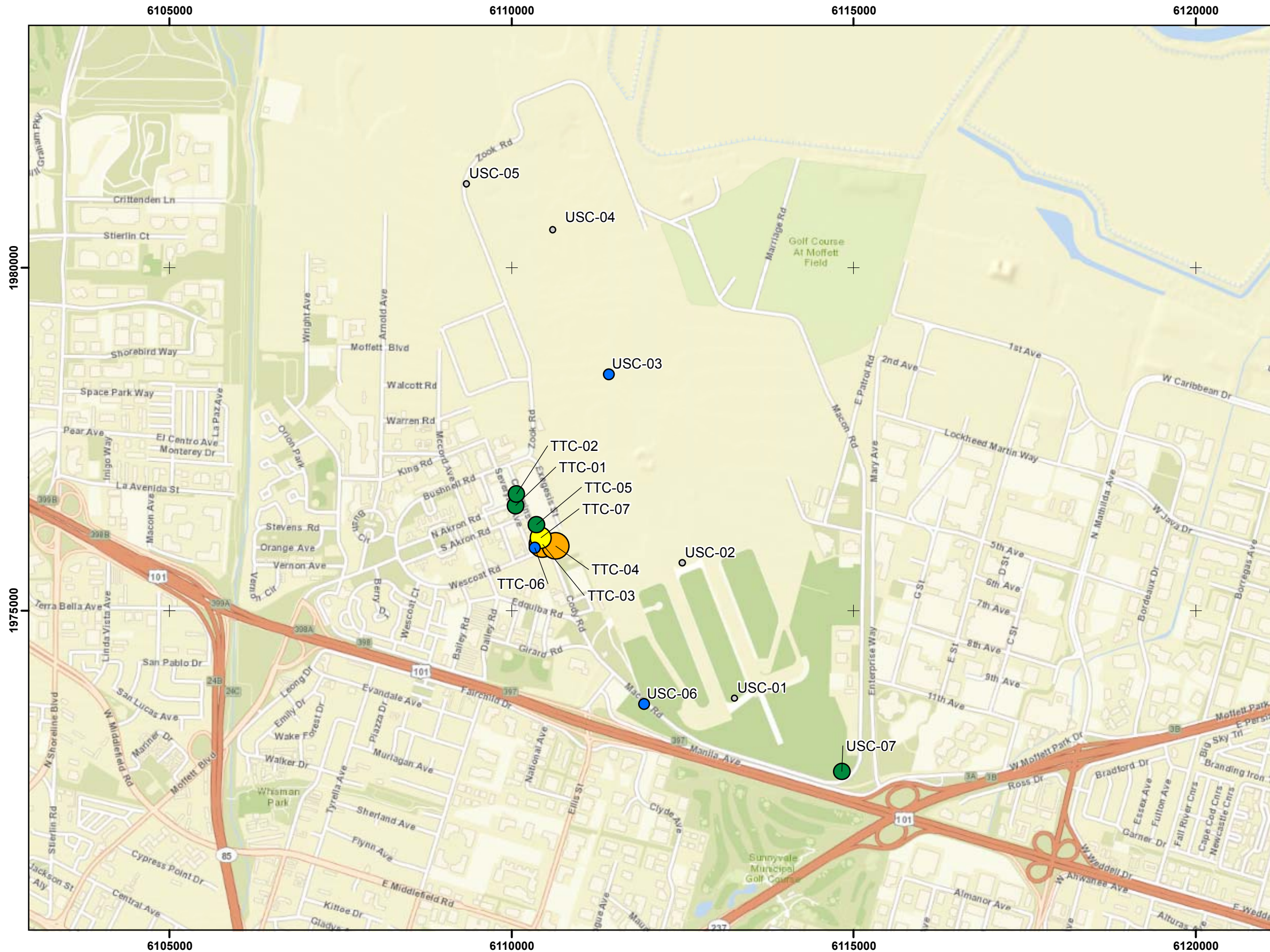
FIGURE DF-1

N:\Projects\04\_2012\04\_7922\_1200\_CaltransAirportRecon\Outputs\2013\_03\_05\_Report\mxd\Fig\_DF01\_MOF\_ExplorationLocationMap.mxd, 03/21/13, dpoliard



**GEOTECHNICAL CROSS SECTION A-A'**  
Moffett Federal Airfield  
Mountain View, California

FIGURE DF-2



**Legend**

Settlement (Inches)

- 0 - 1
- 1 - 2
- 2 - 3
- 3 - 4
- 4 - 5
- > 5

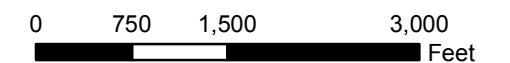
Magnitude= 7.8; P. G. A. = 0.31 g

Only borings with > 30 feet total depth are shown

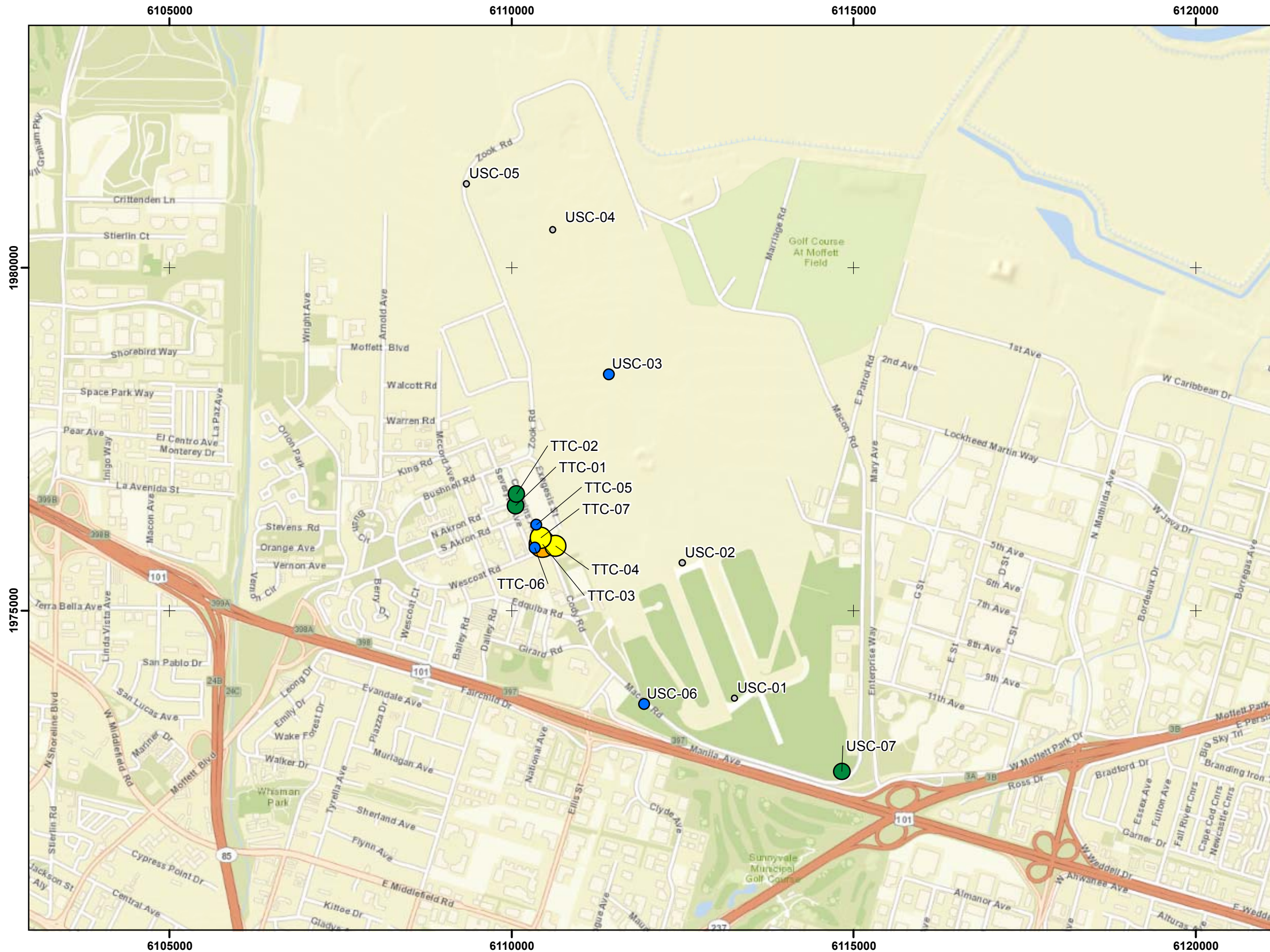
Coordinate Grid: CA State Plane, Zone 3, NAD83, Feet



1:18,005



**LIQUEFACTION SETTLEMENT MAP**  
 1906 San Francisco Earthquake Scenario  
 Moffett Federal Airfield  
 Mountain View, California



**Legend**

Settlement (Inches)

- 0 - 1
- 1 - 2
- 2 - 3
- 3 - 4
- 4 - 5
- > 5

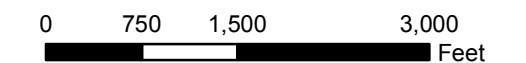
Magnitude= 7.26; P. G. A. = 0.32 g

Only borings with > 30 feet total depth are shown

Coordinate Grid: CA State Plane, Zone 3, NAD83, Feet



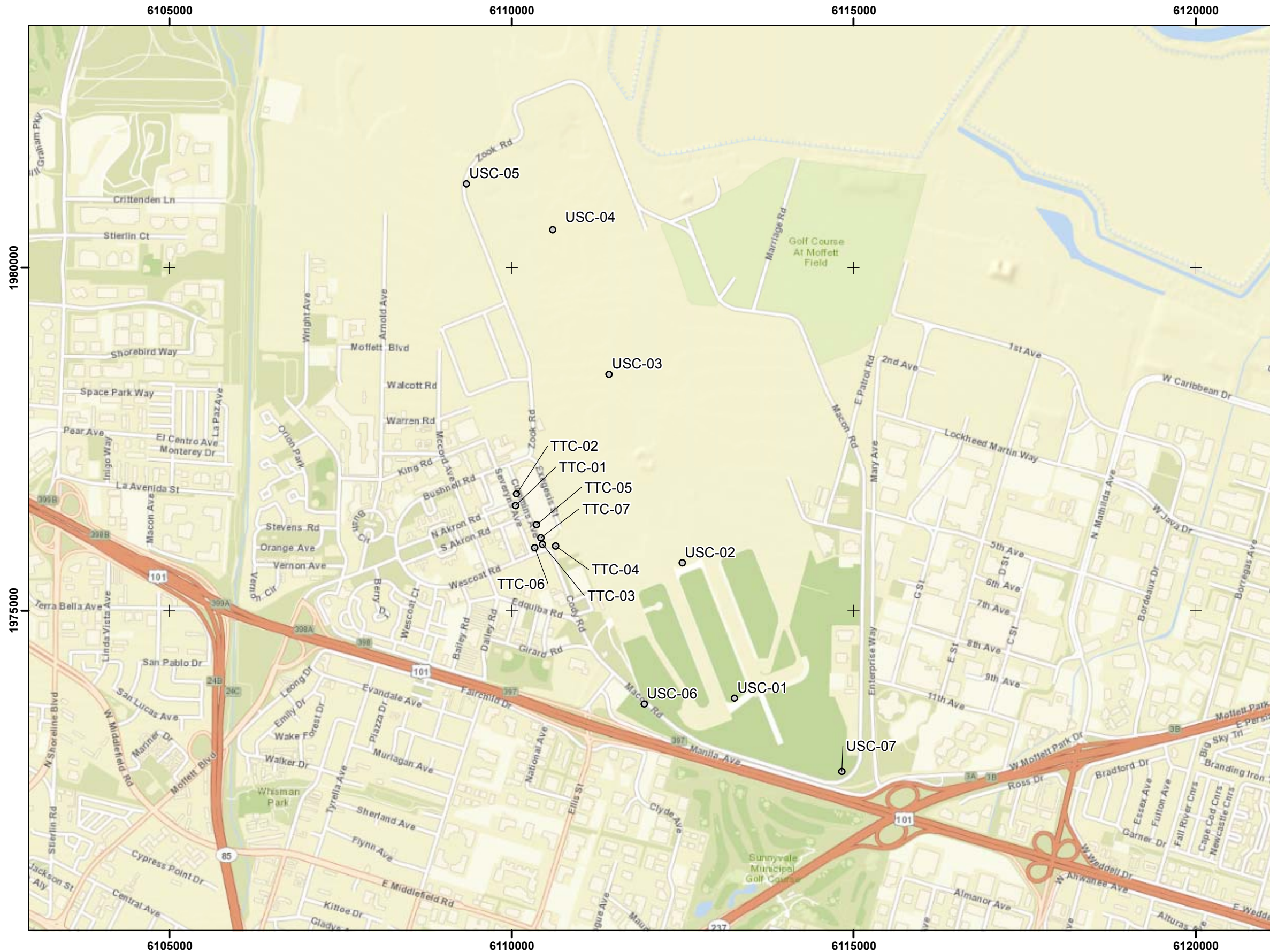
1:18,005



**LIQUEFACTION SETTLEMENT MAP**  
**Hayward-Rodgers Creek Scenario**  
 Moffett Federal Airfield  
 Mountain View, California

FIGURE DF-4

N:\Projects\04\_2012\04\_7922\_1200\_CaltransAirportRecon\Outputs\2013\_03\_05\_Report\mxd\Fig\_DF04\_MOF\_LiquSettl\_MT\_26\_a032\_HRC\_Fault.mxd, 03/21/13, dpollard



**Legend**

Settlement (Inches)

- 0 - 1
- 1 - 2
- 2 - 3
- 3 - 4
- 4 - 5
- > 5

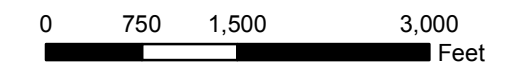
Magnitude= 6.71; P. G. A. = 0.10 g

Only borings with > 30 feet total depth are shown

Coordinate Grid: CA State Plane, Zone 3, NAD83, Feet



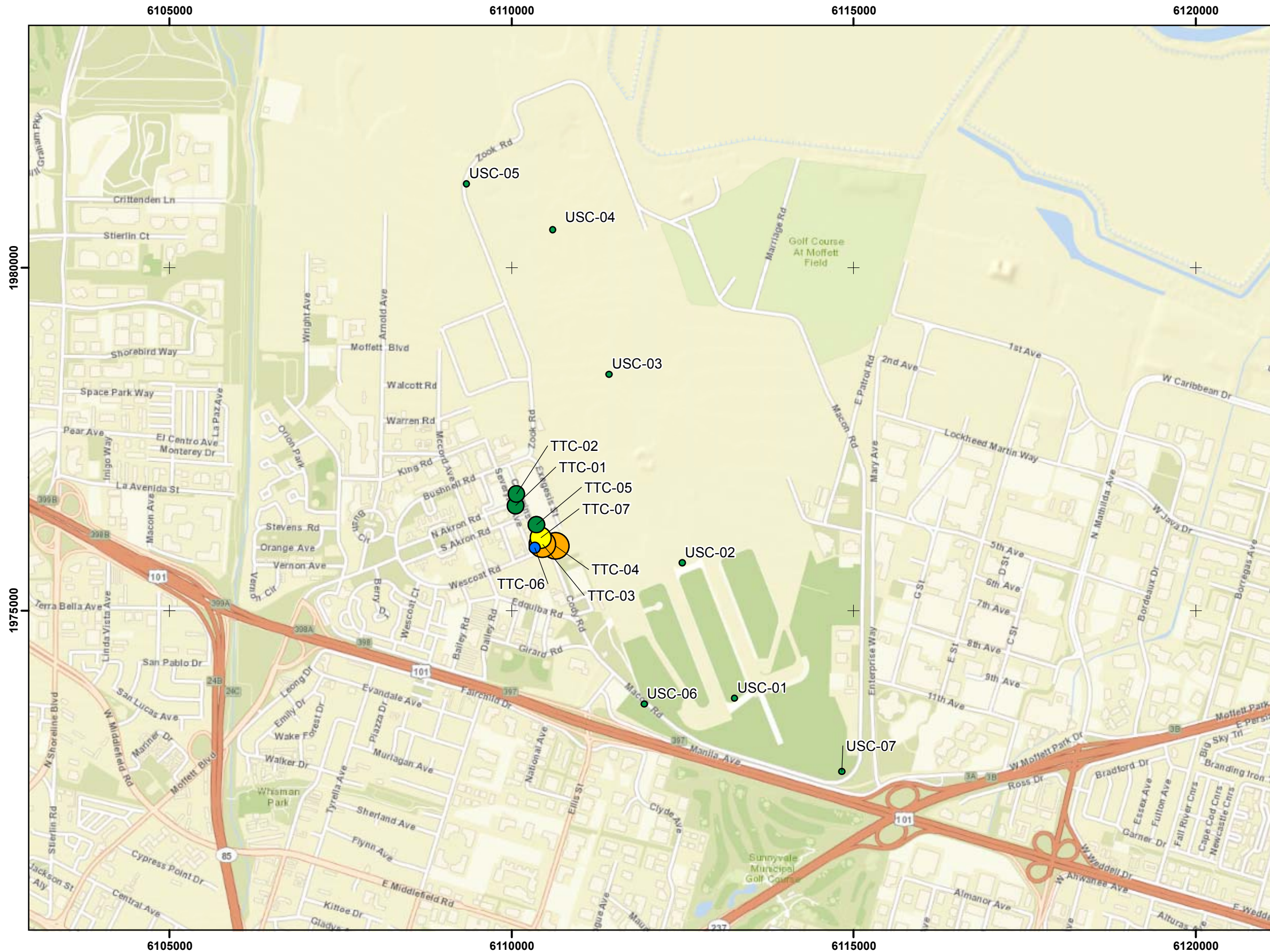
1:18,005



**LIQUEFACTION SETTLEMENT MAP**  
**Concord-Green Valley Scenario**  
 Moffett Federal Airfield  
 Mountain View, California

FIGURE DF-5

N:\Projects\04\_2012\04\_7922\_1200\_CaltransAirportRecon\Outputs\2013\_03\_05\_Report\mxd\Fig\_DF05\_MOF\_LiquSettl\_M6\_71\_a010\_CGV\_Fault.mxd\_03/21/13\_dpollard



**Legend**

Settlement (Inches)

- 0 - 1
- 1 - 2
- 2 - 3
- 3 - 4
- 4 - 5
- > 5

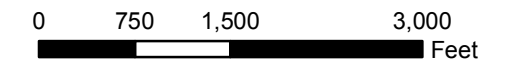
Magnitude= 6.7; P. G. A. = 0.49 g

Only borings with > 30 feet total depth are shown

Coordinate Grid: CA State Plane, Zone 3, NAD83, Feet

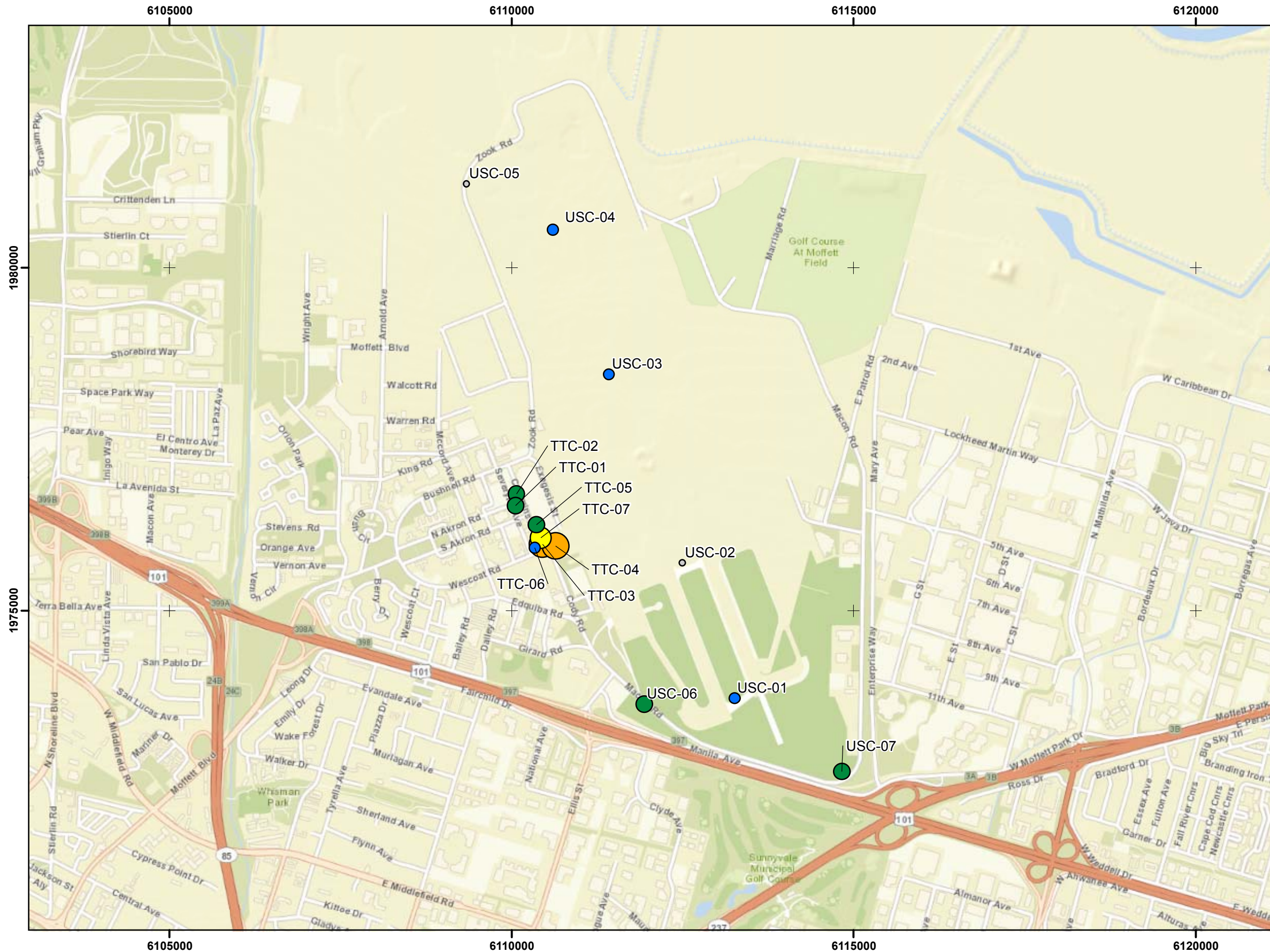


1:18,005



**LIQUEFACTION SETTLEMENT MAP**  
**10% Probability of Exceedance**  
**in 50-Years Scenario**  
 Moffett Federal Airfield  
 Mountain View, California

N:\Projects\04\_2012\04\_7922\_1200\_CaltransAirportRecon\Outputs\2013\_03\_05\_Report\mxd\Fig\_DF06\_MOF\_LiquSettl\_M6\_70\_a049\_475r.mxd, 03/21/13, dpollard



**Legend**

Settlement (Inches)

- 0 - 1
- 1 - 2
- 2 - 3
- 3 - 4
- 4 - 5
- > 5

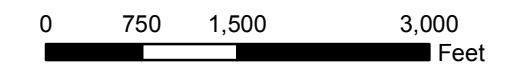
Magnitude= 6.7; P. G. A. = 0.75 g

Only borings with > 30 feet total depth are shown

Coordinate Grid: CA State Plane, Zone 3, NAD83, Feet

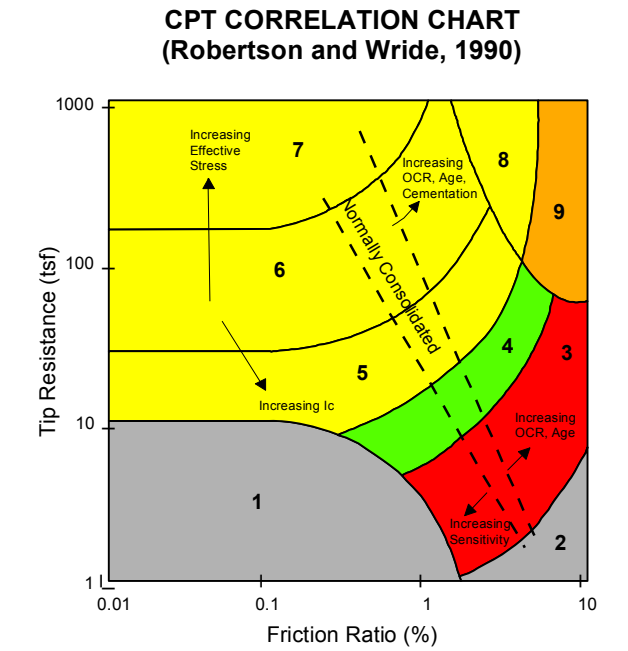
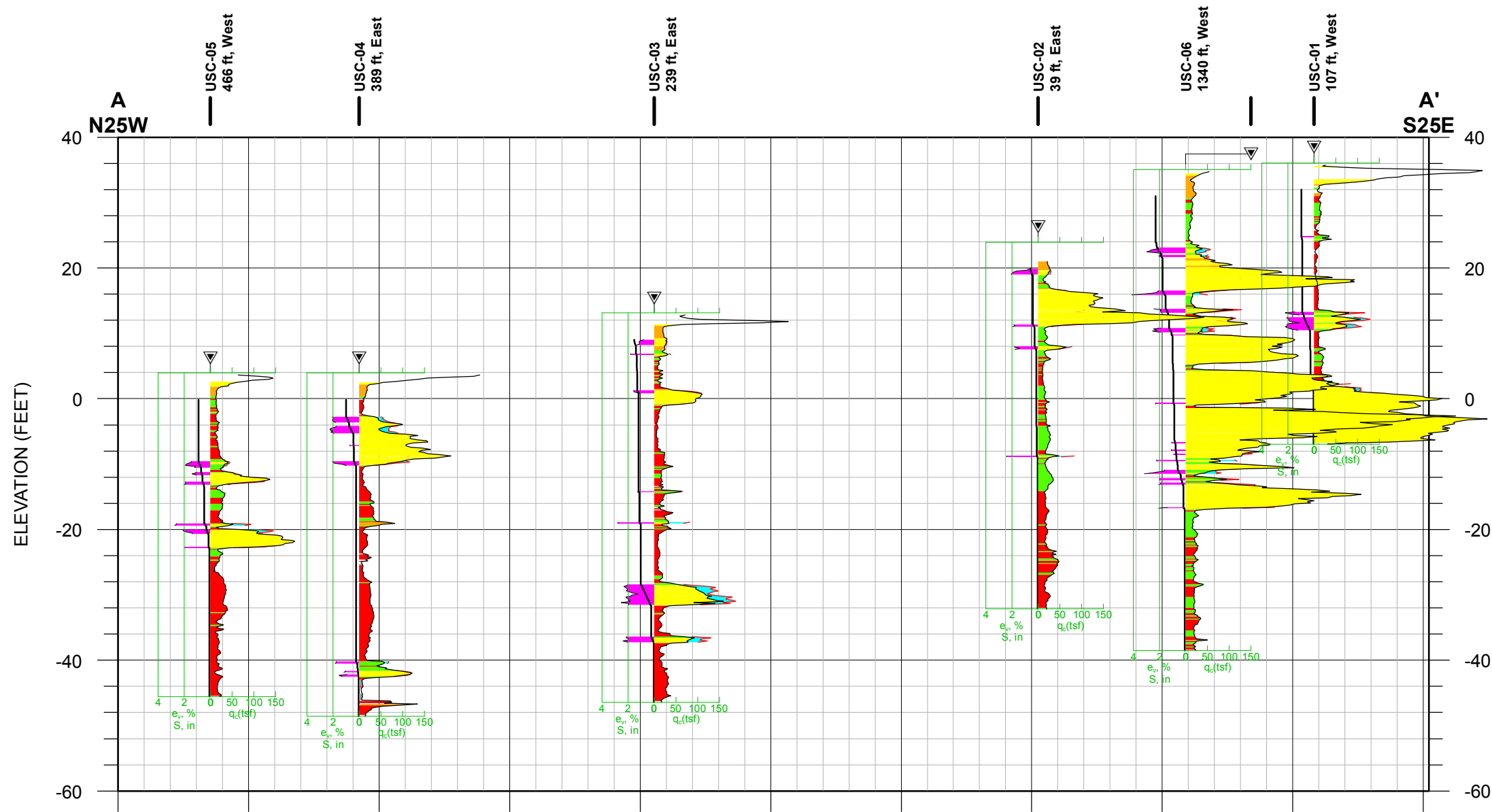


1:18,005



**LIQUEFACTION SETTLEMENT MAP**  
**2% Probability of Exceedance**  
**in 50-Years Scenario**  
 Moffett Federal Airfield  
 Mountain View, California

N:\Projects\04\_2012\04\_7922\_1200\_CaltransAirportRecon\Outputs\2013\_03\_05\_Report\mxd\Fig\_DF07\_MOF\_LiquSettl\_M6\_70\_a075\_2475Yr.mxd, 03/21/13, dpollard

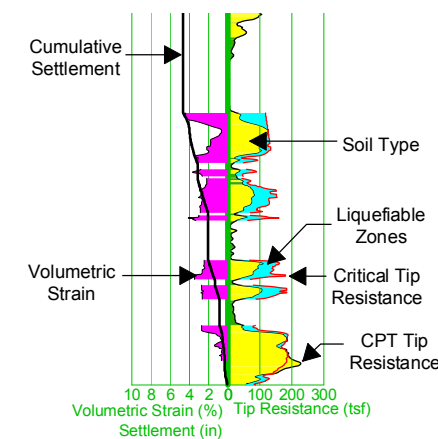


Zone	Soil Behavior Type
1	Sensitive Fine-grained
2	Peats
3	Silty Clay to Clay
4	Clayey Silt to Silty Clay
5	Silty Sand to Sandy Silt
6	Clean Sand to Silty Sand
7	Gravelly Sand to Dense Sand
8	Very Stiff Sand to Clayey Sand*
9	Very Stiff Fine-Grained*

\*heavily overconsolidated or cemented

Note: Magnitude= 6.7; P. G. A. = 0.75 g

**Liquefaction Legend**



**LIQUEFACTION CROSS SECTION A-A'**  
**2% Probability of Exceedance**  
**in 50-Years Scenario**  
Moffett Federal Airfield  
Mountain View, California